AD-A064 156 SYSTEMS TECHNOLOGY INC HAWTHORNE CALIF F/G 1/2
A STUDY OF THE EFFECTS OF AIRCRAFT DYNAMIC CHARACTERISTICS ON S--ETC(U)
NOV 78 R L STAPLEFORD, R J DIMARCO DOT-FA77WA-3936
UNCLASSIFIED STI-TR-1099-1 FAA-RD-78-155 NL

1 OF 3
AD
A064 156

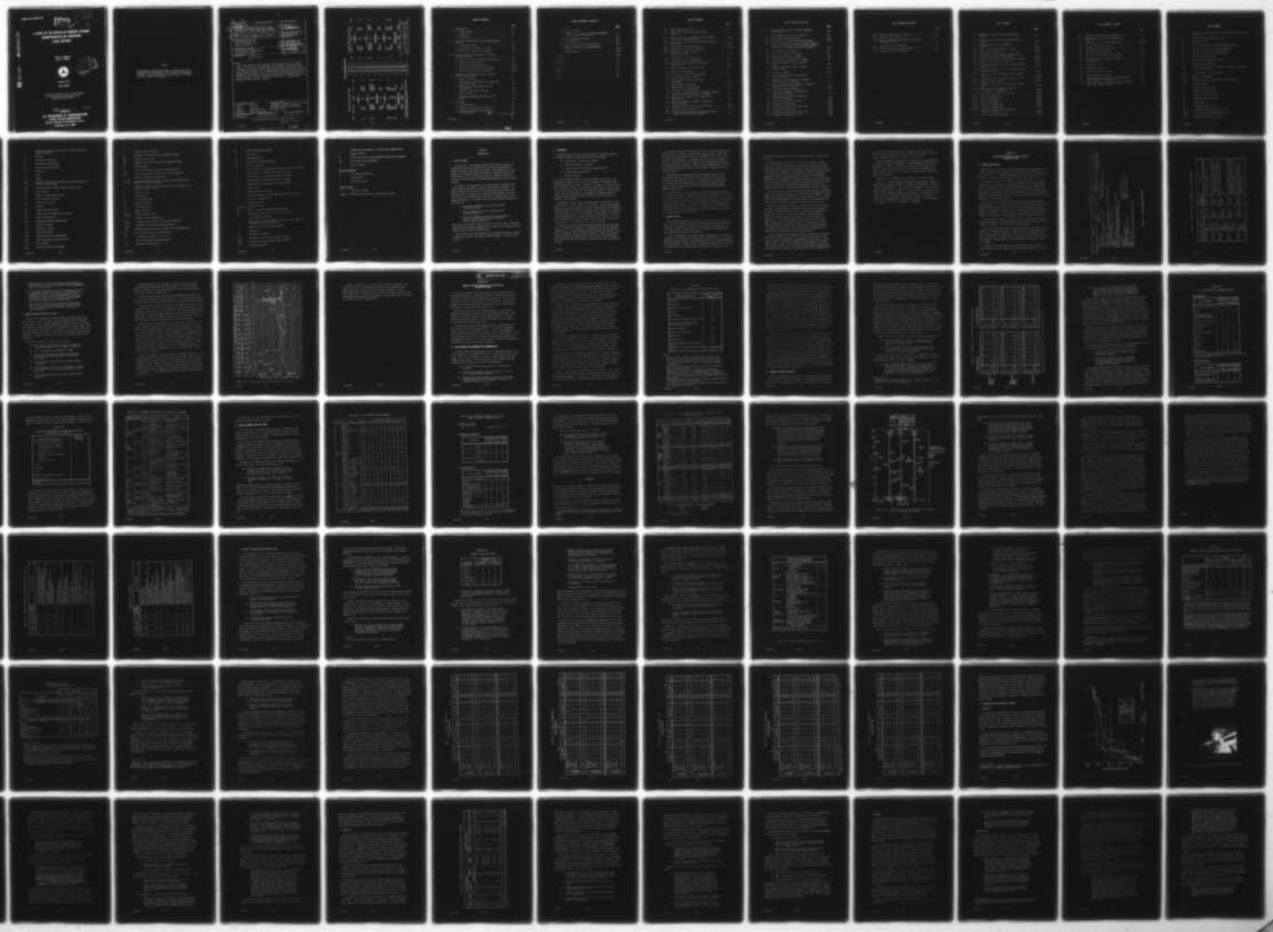

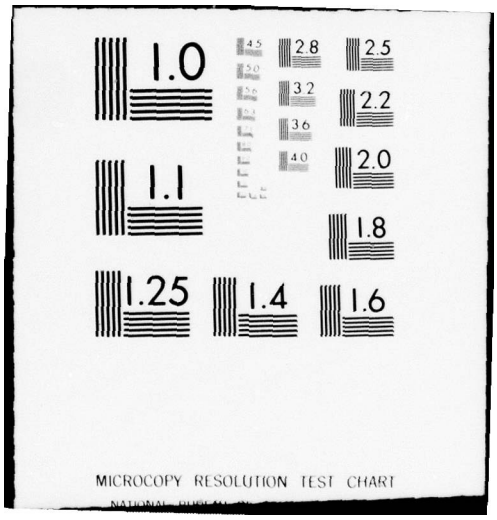
1.0
1.1
1.25
1.4
1.6
1.8
2.0
2.2
2.5
2.8
3.2
3.6
4.0
4.5
5.0
MICROCOPY RESOLUTION TEST CHART

REPORT NO. FAA-RD-78-155

A STUDY OF THE EFFECTS OF AIRCRAFT DY CHARACTERISTICS ON STRUCTURAL LOADS CRITERIA

Robert L. Stapleford
Richard J. DiMarco

November 1978

FINAL REPORT

Prepared for

U.S. DEPARTMENT OF TRANSPORTAT
FEDERAL AVIATION ADMINISTRATION
Systems Research & Development Servic
Washington, D.C. 20590

NOTICE

This document is disseminated under the sponsorship of the Department of Transportation in the interest of information exchange. The United States Government assumes no liability for its contents or use thereof.

(18) (19)

1. Report No.	2. Government Accession No.	3. Recipient's Catalog No.
FAA-RD-78-155		

(6) 4. Title and Subtitle: A STUDY OF THE EFFECTS OF AIRCRAFT DYNAMIC CHARACTERISTICS ON STRUCTURAL LOADS CRITERIA.

(11) 5. Report Date: November 1978

6. Performing Organization Code:

(10) 7. Author(s): Robert L. Stapleford and Richard J. DiMarco

(14) 8. Performing Organization Report No.: STI-TR-1099-1

10. Work Unit No.:

9. Performing Organization Name and Address:
Systems Technology, Inc.
13766 S. Hawthorne Blvd.
Hawthorne, CA. 90250

(15) 11. Contract or Grant No.: DOT-FA77WA-3936

(9) 13. Type of Report and Period Covered: Final Report. ~~1/77-11/78~~

12. Sponsoring Agency Name and Address:
Federal Aviation Administration
800 Independence Avenue, S.W.
Washington, D.C. 20591

14. Sponsoring Agency Code: Jan 77-Nov 78

15. Supplementary Notes

(12) 246p.

16. Abstract

The study reported herein examined the potential effects of aircraft dynamic characteristics on structural loads criteria. The study included an analysis of in-flight airframe failure accidents which occurred during a ten-year period, 1966-1975. A number of potentially contributing factors, including stability and control characteristics and handling qualities, were examined and correlated with the accident data. The study also covered a review of proposed criteria for continuous gusts and a comparison with existing discrete gust criteria. Problems in the selection of a turbulence penetration speed were also examined.

17. Key Words (Suggested by Author(s))		18. Distribution Statement
Aircraft	Statistics	Document is available to the U.S.public through the National Technical Information Service, Springfield, Virginia 22161.
Loads	Criteria	
Accidents	Causal Factors	
Dynamics	Handling Qualities	
Turbulence	Stability and Control	

19. Security Classif. (of this report)	20. Security Classif. (of this page)	21. No. of Pages	22. Price*
Unclassified	Unclassified	245	

*For sale by the National Technical Information Service, Springfield, Virginia 22161

340 425

METRIC CONVERSION FACTORS

Approximate Conversions to Metric Measures

Symbol	When You Know	Multiply by	To Find	Symbol
	LENGTH			
in	inches	*2.5	centimeters	cm
ft	feet	30	centimeters	cm
yd	yards	0.9	meters	m
mi	miles	1.6	kilometers	km
	AREA			
in^2	square inches	6.5	square centimeters	cm^2
ft^2	square feet	0.09	square meters	m^2
yd^2	square yards	0.8	square meters	m^2
mi^2	square miles	2.6	square kilometers	km^2
	acres	0.4	hectares	ha
	MASS (weight)			
oz	ounces	28	grams	g
lb	pounds	0.45	kilograms	kg
	short tons (2000 lb)	0.9	tonnes	t
	VOLUME			
tsp	teaspoons	5	milliliters	ml
Tbsp	tablespoons	15	milliliters	ml
fl oz	fluid ounces	30	milliliters	ml
c	cups	0.24	liters	l
pt	pints	0.47	liters	l
qt	quarts	0.95	liters	l
gal	gallons	3.8	liters	l
ft^3	cubic feet	0.03	cubic meters	m^3
yd^3	cubic yards	0.76	cubic meters	m^3
	TEMPERATURE (exact)			
°F	Fahrenheit temperature	5/9 (after subtracting 32)	Celsius temperature	°C

*1 in = 2.54 (exactly). For other exact conversions and more detailed tables, see NBS Misc. Publ. 286, Units of Weights and Measures, Price $2.25, SD Catalog No. C13.10:286.

Approximate Conversions from Metric Measures

Symbol	When You Know	Multiply by	To Find	Symbol
	LENGTH			
mm	millimeters	0.04	inches	in
cm	centimeters	0.4	inches	in
m	meters	3.3	feet	ft
m	meters	1.1	yards	yd
km	kilometers	0.6	miles	mi
	AREA			
cm^2	square centimeters	0.16	square inches	in^2
m^2	square meters	1.2	square yards	yd^2
km^2	square kilometers	0.4	square miles	mi^2
ha	hectares (10,000 m^2)	2.5	acres	
	MASS (weight)			
g	grams	0.035	ounces	oz
kg	kilograms	2.2	pounds	lb
t	tonnes (1000 kg)	1.1	short tons	
	VOLUME			
ml	milliliters	0.03	fluid ounces	fl oz
l	liters	2.1	pints	pt
l	liters	1.06	quarts	qt
l	liters	0.26	gallons	gal
m^3	cubic meters	35	cubic feet	ft^3
m^3	cubic meters	1.3	cubic yards	yd^3
	TEMPERATURE (exact)			
°C	Celsius temperature	9/5 (then add 32)	Fahrenheit temperature	°F

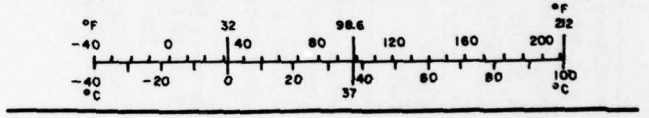

TABLE OF CONTENTS

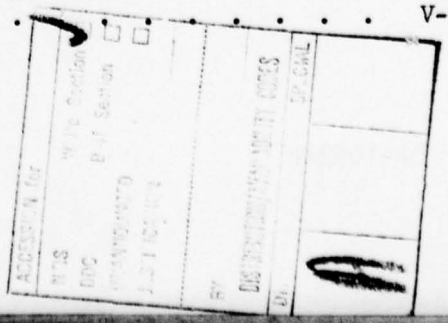

TABLE OF CONTENTS (Continued)

LIST OF FIGURES

LIST OF FIGURES (Continued)

LIST OF FIGURES (Concluded)

LIST OF TABLES

LIST OF TABLES (Concluded)

LIST OF SYMBOLS

a	Slope of the airplane normal force coefficient or of the wing lift curve
a_t	Inertial lateral acceleration of tail
A	Wing aspect ratio
$\bar{A}$	Ratio of rms incremental load to rms gust velocity
b_1	RMS value of σ_{gust} for non-storm turbulence
b_2	RMS value of σ_{gust} for storm turbulence
$\bar{c}$	Mean aerodynamic wing chord
C_D	Total aerodynamic drag coefficient
C_{D_o}	Parasitic drag coefficient
Ch_λ	Partial derivative of hinge moment with respect to λ, where $\lambda = \alpha, \dot{\alpha}, \delta, \dot{\delta}$, or q
C_L	Total aerodynamic lift coefficient
C_{L_α}	Wing lift curve slope
$C_{N_{max}}$	Maximum positive airplane normal force coefficient
D	Aerodynamic drag
e	Oswald's efficiency factor
e	Napierian logarithm base
F_e	Expected number of accidents
F_o	Observed number of accidents
F_s	Stick force
F_t	Aerodynamic force on tail
$F_{t_{max}}$	Time-maximum aerodynamic force on tail
$F_{t_{min}}$	Time-minimum aerodynamic force on tail
F_{t_s}	Structural (inertial) tail load

F_β	Derivative of F_t with respect to sideslip
F_δ	Derivative of F_t with respect to rudder deflection
g	Acceleration due to gravity
G	Stick-to-elevator gearing (ratio of stick force to hinge moment)
H	Hinge moment
H_e	Mass moment of elevator about hinge
H_e'	$H_e + rH_s$
H_s	Mass moment of stick about its pivot
H_λ	Partial derivative of hinge moment with respect to λ, where $\lambda = \alpha, \dot{\alpha}, q, \delta_e$, or $\dot{\delta}_e$
I_e	Moment of inertia of elevator about hinge
I_e'	$I_e + r^2 I_s$
I_e''	$I_e + H_e L_h - rI_s$
I_s	Moment of inertia of stick about its pivot
I_z	Aircraft yaw moment of inertia
k_{DF}	Normalized random input describing function gain
k_z	Aircraft yaw radius of gyration
K	Equivalent transfer function high-frequency gain
K_g	Discrete-gust alleviation factor
K_n, $K_{\int n}$	Pilot load factor control model gain
K_R	Yaw damper gain
K_θ	Pilot pitch attitude control model gain
K_φ	Continuous-gust alleviation factor
ℓ_p	Longitudinal distance from aircraft c.g. to cockpit
ℓ_s	Control stick length
ℓ_t	Longitudinal distance from aircraft c.g. to tail c.p.

L	Aerodynamic lift
L	Turbulence scale length
L_h	Distance from aircraft c.g. to elevator hinge
L_w	Vertical turbulence scale length
m	Aircraft mass
m_t	Tail mass
M_{TP}	Turbulence penetration Mach number
M_λ	Partial derivative of pitch acceleration with respect to λ, where $\lambda = \alpha, \dot{\alpha}, q, w, \dot{w}$, or δ
n, n_z	Load factor
n_g	Positive airplane gust load factor at V_c
n_{z_e}	Load factor error
n_{z_p}	Cockpit load factor
$n_{z_{pe}}$	Cockpit load factor error
N	Exceedance rate
N	Transfer function numerator or coupling numerator (when used with superscript and subscript or two superscript and subscript pairs, respectively, as in $N_{F_s}^{n_z}$, $N_{F_s}^{q}$, $N_{F_s}^{\alpha}$, $N_{\delta_e}^{q}$, $N_{\delta_e}^{\theta}$, and $N_{w_g}^{n_z\theta}$, where, e.g., $N_{F_s}^{n_z}$ is the numerator of the n_z/F_s transfer function
N_o	Upward axis crossing rate = $(1/2\pi)(\sigma_{\dot{x}}/\sigma_x)$ = radius of gyration, in Hz, of Δx power spectral density about zero frequency
p	Probability density
P	Engine power
P	Produce of four poles
P	Probability distribution
P_1	Probability of encountering non-storm turbulence
P_2	Probability of encountering storm turbulence
q	Pitch rate
$\bar{q}$	Dynamic pressure

r	Elevator control gear ratio, ratio of stick and elevator deflection angles
r	Yaw rate
r^2	Correlation coefficient
s	Gust penetration distance
s	Laplace transform operator
S	Wing area
t	Time
T	Thrust
$T_{\theta_2}^{-1}$	Higher of first-order pitch-angle-to-elevator-deflection transfer function zeros
U_{de}	Derived equivalent (design) discrete gust velocity
U_o	True airspeed
U_σ	Design continuous gust velocity
v	Lateral inertial velocity
v_g	Lateral gust velocity
V	Airspeed
V_A	Design maneuvering speed
V_B	Design speed for maximum gust intensity
V_C	Design cruising speed
V_{CR}	Maximum recommended cruising speed
V_D	Design dive speed
V_e	Equivalent airspeed
V_{NE}	Never exceed speed
V_{NO}	Maximum structural cruising speed
V_{s_1}	Stall airspeed with flaps retracted
V_T	True airspeed
V_{TP}	Turbulence penetration airspeed

w	Vertical inertial velocity
w_a	Unsteady lift transfer function parameter ($2U_o/\bar{c}$)
w_g	Vertical gust velocity
$\hat{w}_g$	Lagged vertical gust velocity in unsteady lift model
W	Airplane weight
Y_{p_n}	Pilot load-factor-control model transfer function
Y_{p_θ}	Pilot pitch-attitude-control model transfer function
z	Equivalent system first-order zero
Z_δ, $Z^*_{\delta_e}$	$1/U_o$ times partial derivative of vertical acceleration with respect to elevator deflection
Z_λ	Partial derivative of vertical acceleration with respect to λ, where λ = w, $\dot{w}$, α, or δ_e
α	Angle of attack
β	Sideslip angle
β_t	Tail sideslip angle
γ	Flight path angle
δ_e	Elevator deflection
δ_R	Rudder deflection
$\delta_{R_{limit}}$	Rudder authority limit
Δ	Transfer function denominator
Δn_{cont}	Incremental load factor for continuous turbulence
Δn_{dis}	Incremental load factor for discrete gusts
Δsp	Short-period approximation of transfer function denominator
Δx	Load or stress minus 1 g flight level
$\Delta\lambda$	The change in λ where λ = V, x, θ, α
ζ	Second-order system mode damping ratio
ζ_{sp}	Short-period damping ratio

η_p	Overall propulsion efficiency
θ	Pitch angle
θ_e	Pitch angle error
θ_s	Control stick angular deflection
μ_g	Airplane mass ratio
ν	Ratio of present or steady-state airspeed to initial airspeed
ν_1	First moment of a distribution about the origin
ν_2	Second moment of a distribution about the origin
ν_3	Third moment of a distribution about the origin
ν_4	Fourth moment of a distribution about the origin
ρ	Density of air
ρ_o	Density of air at sea level
σ	Ratio of air density at altitude to sea level value (ρ/ρ_o)
σ	Real part of complex root
σ	Standard deviation
σ_g, σ_{gust}	RMS gust velocity
$\hat{\sigma}_{v_g}$	Value of σ_{v_g} which maximizes $N(Ft/\sigma_{v_g})p(\sigma_{v_g})$
σ_λ	RMS value of λ where $\lambda = F_t, \dot{F}_t, u, w, x, \delta_R, \dot{\delta}_R$
τ	Control system time delay
τ	Time constant of speed buildup in nose over time constant for aerodynamic lag on force buildup
τ_i	Fraction of time in ith mission segment
φ	Bank angle
Φ	Power spectral density
Φ_{v_g}	Lateral gust velocity power spectral density
Φ_{w_g}	Vertical gust velocity power spectral density
χ^2	Chi-square statistic

ω	Undamped natural frequency of second-order frequency mode
ω	Angular frequency
ω_g	Lateral gust velocity power spectral density break frequency
ω_{sp}	Short-period natural frequency
Ω	Spatial frequency

Special Subscripts

dc	DC or steady-state value
o	Initial value
s	Steady-state value

Special Symbols

$(\dot{})$	Time rate of change
$(d/dv_g)(\ )$	Derivative with respect to lateral gust velocity

SECTION I

INTRODUCTION

A. PROJECT SUMMARY

The objective of the research reported herein was to explore the interactions among aircraft stability and control characteristics, handling qualities, and structural loading. The ultimate goal of such research is improved FAA loads criteria which adequately account for these factors. Such criteria would continue to provide a high level of safety without imposing unnecessary weight penalties on the aircraft designer.

The scope of this program was to include fixed-wing aircraft from large commercial transports to small general aviation aircraft. The project started with a review of those aircraft accidents over a ten-year period which involved an in-flight structural failure. The basic objective of this accident review was to put the whole project in the proper perspective. It was hoped that the accident data would provide an indication of:

- The relative importance of accidents involving structural failures.
- The circumstances which most commonly lead to structural failures.
- The role of handling qualities in these accidents and the identification of the most important handling quality parameters.

These hopes were largely realized except for the third item. Potentially important handling quality parameters were identified, but their importance cannot be proven from the available data.

The accident review was supported by a literature review and a number of analytical studies. The nature of these analyses is outlined in Subsection C.

B. BACKGROUND

The structural loads which an aircraft will be exposed to depend on the complex interactions among several factors, including:

- Environmental conditions encountered
- Aircraft utilization or mission
- Aircraft stability and control characteristics
- Aircraft handling qualities
- Pilot proficiency

An obviously important aspect of the environmental conditions is the atmospheric turbulence which will be encountered. The turbulence may have a natural source, such as a storm or the terrain, or may be from the wake of another aircraft. This turbulence could impose excessive loads on the aircraft and directly cause a structural failure. The structural loading resulting from a specific atmospheric disturbance depends on various aircraft characteristics and the reactions of the pilot or automatic control system.

Turbulence can also induce a structural failure indirectly. It can cause the pilot to lose control of the aircraft. During the attempted recovery a structural failure could result from exceeding the aircraft's design envelope, e.g., excessive airspeed or load factor. The likelihood of either loss of control or a successful recovery depends on various aircraft characteristics, aircraft loading, and the skill of the pilot. Other environmental conditions, such as poor visibility and icing, can also contribute to the possibility of a loss of control.

Aircraft utilization or mission affects loads in at least two ways. First, it affects the frequency of encountering various environmental conditions, e.g., transcontinental transports have less exposure to low altitude turbulence than short haul transports. Second, the aircraft mission affects the normal maneuver loads which will be experienced. High load factors are more common in a crop duster than in a commercial airliner.

The effects of aircraft stability and control characteristics, handling qualities, and pilot proficiency have been alluded to above. They affect the loads due to atmospheric turbulence, the probability of loss of control, and the probability of a structural failure during an attempted recovery. They also affect the probability of inadvertently oversteering the aircraft during a maneuver. Certain aircraft characteristics, e.g., low control forces, make it easier for the pilot to impose higher loads than he intended.

Structural loads criteria which provide adequate safety with no unnecessary weight penalties would have to properly account for all the factors discussed above. This is clearly beyond the current state of the art. Existing FAA certification requirements largely ignore many of these factors, because existing technology cannot adequately quantify their effects.

The above discussion has purposely not addressed the important subject of aircraft maintenance. Seemingly insignificant maintenance actions (e.g. painting or repairing a control surface without rebalancing it) can seriously alter the dynamic characteristics of an aircraft. Investigation of the contribution of maintenance to in-flight structural failures would be a major program by itself and was outside the scope of this project. Accidents which were identified as probably due to inadequate or improper maintenance were excluded from the data analyses.

C. REPORT OUTLINE

The accident review mentioned above is the subject of Sections II and III. Section II presents the data for accidents involving air carriers. Subsection A describes the data source, the general review process, and the overall results. Subsections B and C describe two accidents which were especially pertinent to this project.

Section III presents the accident data for general aviation aircraft. Subsection A discusses the data review and screening process. Subsection B presents overall statistics on environmental conditions, failed components, and flight purpose. Data by specific aircraft make and model are contained in Subsection C. These data include the number of accidents for each

aircraft and estimated accident rates (per flight hour) for many of the aircraft.

The remainder of Section III is devoted to an accident analysis conducted at the end of the project. The earlier analysis which used computerized summaries as raw data had identified a substantial number of accidents which appeared to be pertinent to project objectives. Late in the program it was decided that additional, useful data might be obtained by examining the complete files for some of the accidents. Subsequent to a corresponding contract modification, copies of the files for all accidents involving five selected aircraft were requested. Four of the five had higher than average accident rates. The fifth is a popular aircraft with a slightly lower-than-average rate for its group.

This review of the complete accident files was actually accomplished after the rough draft of most of this report had been completed. It was expedient to merely add the results to the end of Section III. We have tried to make the appropriate editorial changes to the manuscript for good flow and consistency. Hopefully the "add on" does not show.

The subject of Section IV is factors which may contribute to these accidents in general aviation aircraft. Subsection A is a general discussion of the many factors involved. Subsection B discusses airworthiness directives which might be related to these accidents. Subsection C examines possible correlations of accident rate with speed margins, e.g., margin between normal cruise and never exceed speed. The tendency of various aircraft to gain speed in two situations is analyzed in Subsection D. The subject of spiral stability is covered in Subsection E. The last subsection considers possible adverse effects of reversible control system dynamics.

Section V addresses the general problem of structural criteria for gust induced loads. Subsection A is a review of FAA criteria. Subsection B treats the problems in establishing criteria for continuous (random) gusts. Subsection C compares the requirements for discrete and continuous gusts. It is shown that several factors determine which is more critical. Subsection D tackles the difficult problem of what

to do about system nonlinearities in an analysis of continuous gust loads. An example problem (a limited authority yaw damper) is examined via a linearized analysis and a Monte Carlo simulation.

Section VI deals with the problems of selecting a turbulence penetration speed for commercial transports. FAA requirements are reviewed in Subsection A. Subsection B discusses current design and operational practice. Factors in the selection of a turbulence penetration speed are discussed in Subsection C. Subsection D presents some summarizing remarks on the subject.

Section VII is a summary of major results for the entire report.

Details of several analyses are presented in appendices. Appendix A deals with the analysis of speed increases in two maneuvers — lowering the nose and a spiral dive. The subject for Appendix B is longitudinal control system dynamics. Appendix C treats the effects of manual control on gust loads. Appendix D presents the details on the analysis of tail loads with a limited authority yaw damper (example to illustrate the effects of a nonlinearity on continuous gust loads). The last appendix, E, is simply a collection of sample V – n diagrams.

SECTION II

AIR CARRIER ACCIDENT DATA FOR IN-FLIGHT AIRFRAME FAILURES

A. INITIAL DATA REVIEW

The National Transportation Safety Board (NTSB) keeps a summary record on digital magnetic tape of every civil aviation accident that occurs in the United States. A standardized printout of most of these data is readily available. A sample of these accident briefs is shown in Fig. II-1.

An examination of all the briefs for one year was made. This showed that most of the accidents of interest here would have "in-flight airframe failure" listed as the first entry under "type of accident." However, a few of the accidents had "turbulence" listed as the first type of accident. Consequently, a printout of all accident briefs for which the first accident type was in-flight airframe failure or turbulence was requested for the latest available ten year period, 1966-1975.

This printout still included many accidents which are not pertinent to the investigation. A further screening of the data was accomplished by carefully examining each brief. Most of the air carrier accidents involved injuries to passengers or crew but not any significant in-flight structural damage to the aircraft. Five accidents were identified as potentially pertinent to the objectives of this program. These are listed in Table II-1.

Aircraft Accident Reports for all five were obtained from the NTSB and reviewed thoroughly. It was concluded that the last three accidents listed in Table II-1 were not really pertinent to this program.

The United DC-8 accident was not considered pertinent because there was no damage to load-carrying structure. Damage as cited in the accident report was: "Several exterior components of the aircraft were damaged by hail. Inside the aircraft, several seat tables and the ceiling of a rear lavatory were damaged. The performance of the aircraft was not affected by any of this damage."

The Wien F-27 accident was not considered pertinent because (Ref. 1) "The aircraft was not in compliance with existing airworthiness directives

BRIEFS OF ACCIDENTS

FILE	DATE	LOCATION	AIRCRAFT DATA	INJURIES F S M/N	FLIGHT PURPOSE	PILOT DATA
2-1134	9/11/66 NR.MITCHELL,OREG TIME - 0920	BEECH A35 N745R DAMAGE-DESTROYED	CR- 1 0 0 PX- 3 0 0	NONCOMMERCIAL PLEASURE/PERSONAL TRANSP	PRIVATE, AGE 29, 174 TOTAL HOURS, 28 IN TYPE, NOT INSTRUMENT RATED.

TYPE OF ACCIDENT
  AIRFRAME FAILURE IN FLIGHT
  COLLISION WITH GROUND/WATER UNCONTROLLED

PHASE OF OPERATION
  IN FLIGHT NORMAL CRUISE
  IN FLIGHT UNCONTROLLED DESCENT

PROBABLE CAUSE(S)
  PILOT IN COMMAND - CONTINUED VFR FLIGHT INTO ADVERSE WEATHER CONDITIONS
  PILOT IN COMMAND - SPATIAL DISORIENTATION
  AIRFRAME - WINGS SPARS
  MISCELLANEOUS ACTS,CONDITIONS - OVERLOAD FAILURE
FACTOR(S)
  WEATHER - LOW CEILING
  WEATHER - TURBULENCE, ASSOCIATED W/CLOUDS AND/OR THUNDERSTORMS
WEATHER BRIEFING - NO RECORD OF BRIEFING RECEIVED
WEATHER FORECAST - WEATHER SLIGHTLY WORSE THAN FORECAST

SKY CONDITION
  OVERCAST
CEILING AT ACCIDENT SITE
  300
VISIBILITY AT ACCIDENT SITE
  UNKNOWN/NOT REPORTED
PRECIPITATION AT ACCIDENT SITE
  NONE
OBSTRUCTIONS TO VISION AT ACCIDENT SITE
  NONE
TYPE OF WEATHER CONDITIONS
  IFR
TYPE OF FLIGHT PLAN
  NONE
REMARKS- RIGHT WING AND LEFT RUDDERVATOR FAILED IN FLIGHT

Figure II-1. Sample NTSB Accident Brief

TABLE II-1. SUMMARY OF POTENTIALLY PERTINENT AIR CARRIER ACCIDENTS

OPERATOR	AIRCRAFT DATA	LOCATION	DATA NTSB FILE NUMBER	REMARKS
Braniff	BAC 1-11 N1553 Destroyed	Falls City, Nebraska	8/6/66 1-0008	Right wing and empennage failed in extreme turbulence.
Braniff	Electra N9707C Destroyed	Dawson, Texas	5/3/68 1-0003	Right wing failed during attempted recovery from unusual attitude induced by thunderstorm turbulence
United	DC-8 N8010U Substantial Damage	New Richmond, Wisconsin	8/6/68 1-0066	Encountered severe turbulence and hail
Wien	F-27B N4905 Destroyed	Pedro Bay, Alaska	12/2/68 1-0038	Encountered severe to extreme clear air turbulence. Right outer wing, empennage, and portions of left wing separated in flight.
Saturn	L-382 (C-130) N14ST Destroyed	Springfield, Illinois	5/23/74 1-0008	Encountered moderate turbulence. Outboard section of left wing separated in flight.

at the time of takeoff from Anchorage on this flight and had not been, within the scope of the maintenance requirements, airworthy for a considerable period of time before the accident."

Pre-existing fatigue cracks had weakened the wing structure but the degree could not be determined. Fatigue cracks were evident on radiographs made more than a year before the accident. Radiographs of the failure area made 1-2 months before the accident showed nine or more cracks ranging from 1/8 to 5/16 in. in length. Calculations made by the manufacturer indicated that with these cracks the wing would fail at approximately 4.5 g. Metallurgical studies indicated that there might have been some substantial additional deterioration of the structure prior to the accident. Therefore, the strength of the wing at the time of the accident could not be determined.

The Saturn L-382 accident was also eliminated because of pre-existing fatigue cracks. A NTSB analysis showed that the fatigue cracks could have reduced the wing strength so that 60 percent of limit load would cause failure. The accelerometer trace from the flight data recorder ended approximately 50 sec before the wing failed. The last portion of the trace showed peak loads less than 1.4 g. The NTSB determined (Ref. 2) "that the probable cause of the accident was the undiscovered, preexisting fatigue cracks, which reduced the strength of the left wing to the degree that it failed as a result of positive aerodynamic loads created by moderate turbulence."

The remaining two accidents are discussed in greater detail in the next two subsections.

B. BRANIFF BAC 1-11 ACCIDENT ON 8/6/66

Flight 250 was a regularly scheduled passenger/cargo flight enroute from Kansas City, Missouri, to Omaha, Nebraska. During the flight the crew attempted to penetrate a severe squall line oriented across their intended route, using the airborne weather radar to select a light area. The aircraft was flying at 5,000 ft and approximately at the recommended penetration speed of 270 kt. (V_c = 320 kt indicated airspeed). The autopilot was probably engaged. There was no upset.

The estimated sequence of events is as follows:

- A sudden gust caused an airspeed increase of 45-50 kt
- Simultaneously, or very shortly thereafter, a very large gust from below and the right was encountered
- This caused a nearly simultaneous failure of the right tailplane and the vertical fin (aircraft has T tail)
- Aircraft pitched nose down until the right wing failed in downward direction

The flight data recorder was damaged and data could not be recovered. Cockpit voice recorder was recovered and data were usable. Airspeed estimates were based on recorded cockpit sounds.

A computer study was made to determine the smallest gust which would cause only the fin and tailplane failures. For the aircraft at 300 kt equivalent airspeed, the gust was 140 ft/sec (equivalent airspeed) with a time to peak of 1/8 sec and applied from the right and angled upward 45 deg. If the aircraft were at 270 kt, the required gust was increased to 158 ft/sec.

Other studies indicated that control deflections within the authority limits of the autopilot would have a rather small effect (approximately 5-10 percent reduction in the required gust).

The FARs at that time did not require the consideration of simultaneous vertical and horizontal gusts. Analysis of the BAC 1-11 empennage indicated that an angled gust at the worst possible direction would give a tailplane loading approximately 10 percent more severe than if applied vertically.

The NTSB concluded that the structural failure was directly caused by an extremely severe gust. The aircraft manufacturer, the British Aircraft Corporation, agreed but a different conclusion was reached by two other parties. Braniff Airways and the Air Line Pilots Association concluded that the accident was caused by a complete loss of the rudder feel system which permitted the pilot to inadvertently apply full rudder.

The pertinence of this accident to this project can be summarized as follows:

a. Handling qualities, stability and control characteristics, and the flight control system apparently were not significant factors in this accident.

b. The accident investigation did show the worst gust direction for empennage loads was not vertical or lateral, but an intermediate direction. The recent amendment to FAR 25.341 recognizes this and requires consideration of gusts from any direction normal to the flight path. That amendment was probably motivated by this accident report.

c. The accident investigation also indicated a rather small effect of the autopilot (approximately 5-10 percent reduction in the gust required for failure) because of its limited authority.

C. BRANIFF ELECTRA ACCIDENT ON 5/3/68

Flight 352 was a regularly scheduled passenger flight enroute from Houston, Texas, to Dallas, Texas. During the flight the crew attempted to go around an area of severe thunderstorms which was astride the airway. They apparently encountered turbulence and decided to reverse course. While in a right turn, the aircraft was upset and went into a steep, spiral dive. During the attempted recovery, the aircraft was overstressed and the right wing failed. Autopilot status at the time of the accident could not be determined.

The estimated sequence of events is as follows:

- While flying at approximately 10,000 ft and 200 kt indicated airspeed, the pilot commenced a right turn
- Initial bank angle was estimated at 24 deg
- The aircraft was apparently upset by a gust which greatly increased the bank angle (estimated peak of 115 deg)
- Aircraft started rapid descent and airspeed started to increase
- Pilot attempted to recover by rolling back to left and pulling back on controls (peak accelerometer reading was 4.3 g)
- Recovery maneuver caused a structural failure of the right wing

The NTSB determined "that the probable cause of this accident was the stressing of the aircraft structure beyond its ultimate strength during an attempted recovery from an unusual attitude induced by turbulence associated with a thunderstorm."

A copy of the traces from the flight data recorder was obtained. The last portion of that data is shown in Fig. II-2. It was carefully reviewed for any evidence of handling quality problems during the attempted recovery.

At 36:42 we see the start of the turn to the right (the pilot was going to reverse course). At 37:00 altitude begins to decrease rapidly. A rapid airspeed increase begins at 37:05 indicating the spiral dive had developed. From 37:08 on there are apparent reversals in the time scale. The accident report concluded that despite the distortions in the time scale there were no reasons to doubt the magnitudes of the recorded signals.

The vertical acceleration trace is the one of most concern here. What we are looking for is any indication of a stability and control problem which may have contributed to the overload. A rapid increase in load factor to 3.8 g's starts at 37:07. This is apparently pilot-induced and the start of the recovery attempt. Within the next "2" sec (remember the time scale is probably distorted) there are wild fluctuations (3.8 to 0.5 to 1.9 to 0.7 to 3.0 g's). These may reflect the pilot's attempt to stabilize at 2-3 g's while making large roll inputs and being subjected to large cockpit accelerations. For the next 2 sec, the load factor seems to be stabilizing at about 2.5 g's which would be a reasonable level for the pilot to try to maintain.

The crucial question is why the load factor suddenly increases to 4.3 g's (the wing probably failed about this time). The change seems too large to have been caused by a gust alone. It was probably pilot-induced but any explanation would be merely conjecture. By this time the situation was extremely critical. The pilot was faced with an extremely high airspeed and sink rate, and the cockpit was probably being subjected to high acceleration levels. A near lightning strike also occurred at approximately this time.

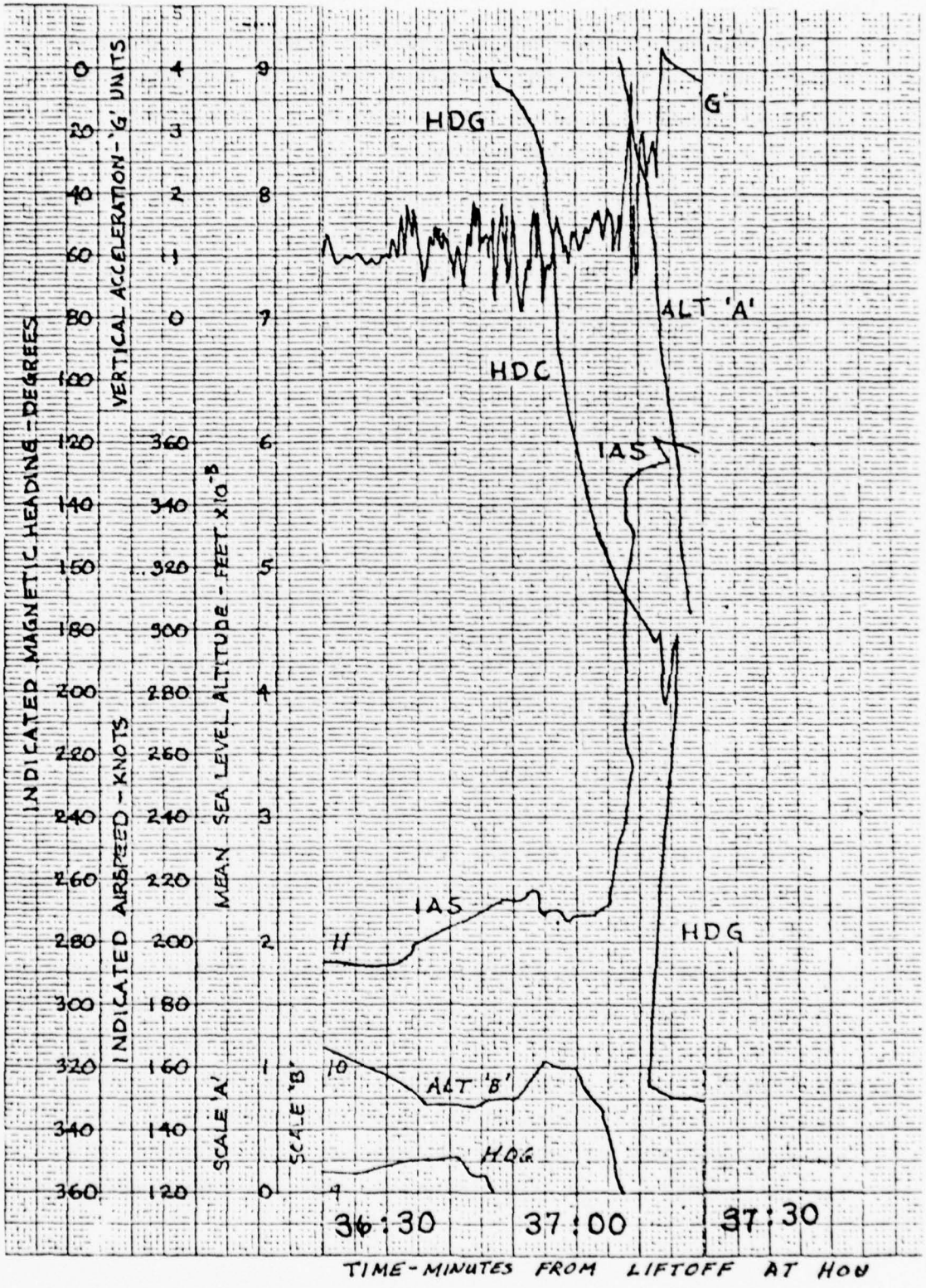

Figure II-2. Flight Recorder Data for Braniff Electra Accident

Overall, the data do not allow a firm conclusion with regard to the possibility of any contributing stability and control problems which might have been encountered by the pilot while attempting to maintain a high load factor. Time histories of the pilot's cockpit controls would have helped explain exactly what happened, but these data were not available on the type of flight recorder used.

SECTION III

GENERAL AVIATION ACCIDENT DATA FOR IN-FLIGHT AIRFRAME FAILURES

Section II discussed In-Flight Airframe Failure (IFAF) accidents involving Air Carriers. These constituted only a small portion of the 1966-1975 accidents for which NTSB briefs were obtained. The majority of these accidents involved general aviation aircraft. This section presents a statistical analysis of the general aviation IFAF accidents during that ten-year period from 1966 to 1975.

The analysis proceeds in the following sequence. The first subsection describes the screening of the raw accident data. This is followed by a discussion of the overall accident statistics. The next portions present the statistics — most importantly accident rates — by individual aircraft make and model.

The last part of this section presents a more in-depth analysis of the accidents of a few specific aircraft. This study was undertaken after the analysis of the accident briefs. Based on the findings of that analysis, five aircraft were selected for this investigation. Copies of the complete files for the accidents involving these aircraft were requested from the NTSB. These were reviewed and important circumstances and features of these accidents were tabulated.

A. RAW ACCIDENT DATA SCREENING AND INTERPRETATION

As with the Air Carrier accidents, many of the general aviation accidents summarized in the NTSB printout were not pertinent to project objectives. Most of the "turbulence" accidents did not involve structural damage prior to impact. Of the remaining accidents, almost half were excluded. These involved one or more of the following:

- A sailplane, helicopter, home-built, or ex-military aircraft.
- Intrinsically hazardous flying activities, i.e., acrobatics and agricultural operation.
- Pre-existing airframe damage or weakness, e.g., fatigue, improper maintenance (but not improper operation, e.g., exceeding weight or c.g. limits).

A breakdown by reason for exclusion is given in Table III-1 for the eliminated accidents. This table provides some perspective on the analysis. The 281 excluded accidents indicated in Table III-1 almost equal the number of accidents retained in the analysis. Of particular interest is the large number of accidents excluded because of a "pre-existing structural deficiency." This raises a question as to the prior structural soundness of aircraft whose accidents were not excluded.

A number of the "excluded" briefs indicated that an annual inspection had failed to disclose existing substandard conditions. It appears quite possible that structural deficiencies could occasionally go undetected in the accident investigation: most of the IFAF accidents end as fatal crashes and, in a number of cases general disintegration occurs in the air, leaving some — perhaps critical — components strewn a distance from the wreckage. It is perhaps not coincidental, then, that more than 50 percent of the accidents in which "pre-existing structural damage" was identified were non-fatal. In a non-fatal accident the aircraft is recovered largely intact so that detection of pre-existing deficiencies is more likely.

A similar extenuating factor noted in the briefs of a few "excluded" accidents was the occurrence of flutter. Accidents where flutter occurred within an airplane's operational envelope are not relevant to project objectives, since such occurrences are already proscribed by the regulations. As in the case of structural pre-disposition to failure, such incidences might not always be identified in an accident investigation.

These concerns intensified the scrutiny given the candidate accidents. Further consideration of such mitigating factors is reserved for the analysis post-mortem later in this section and in Section IV, which discusses factors which may have contributed to the analyzed accidents. However, despite fairly restrictive criteria, a large number of general aviation accidents met the criteria for relevance to the program.

Various statistics were developed for these accidents. Most of the data used to compute these statistics were extracted from the briefs in a straightforward manner. An exception to this directly extracted data was the visibility conditions at the time of the accident. The determination

TABLE III-1

SUMMARY OF IFAF ACCIDENTS EXCLUDED FROM DATA ANALYSIS

REASON FOR EXCLUSION[a]	NUMBER OF ACCIDENTS FATAL/ALL
Sailplane	12/16
Helicopter	13/37
Home-built or ex-military	11/14
Balloon	0/1
Test flight	5/12
Pre-existing structural deficiency[b]	55/113
Failure did not involve primary load-carrying structure	1/23
Parachute jumping	1/6
Agricultural operations[c]	1/2
Aerobatics[d]	19/28
Miscellaneous[e]	11/24
Foreign jurisdiction (insufficient data)	2/5
Total	131/281

Notes:

[a]Each excluded accident is generally tallied under the first applicable reason from top to bottom; main exceptions are a few accidents which might have been counted under sailplane, helicopter, or home-built, had the aircraft type been readily identifiable.

[b]Missing, improper, loose, damaged (including fatigue damage), worn, or modified parts.

[c]Many other accidents which occurred during agricultural operations were contained in the NTSB printout. A number of these were turbulence accidents with no in-flight airframe failure. Of those remaining, most involved a "pre-existing structural deficiency."

[d]Many other accidents associated with acrobatic maneuvers involved a "pre-existing structural deficiency."

[e]For example: ice not removed prior to takeoff; pilot incapacitation; improperly secured door.

of whether the pilot had sufficient visual reference or had to rely on instruments required careful examination and interpretation of each brief.

The "type of weather conditions," characterized as either VFR (Visual Flight Rules) or IFR (Instrument Flight Rules), was not always listed. Even when prevailing weather conditions were characterized as VFR, other report details sometimes indicated that the pilot's visibility was impaired by local conditions when the accident occurred. For this reason the designations "Visual Meteorological Conditions" (VMC) and "Instrument Meteorological Conditions (IMC) rather than VFR and IFR are used to categorize visibility conditions. Conditions counted as IMC conditions included those listed as IFR and/or described by such remarks as: "... at night over unlighted terrain ..."; "... flew into clouds, entered spin . . ."; "pilot knew IFR weather conditions existed entire route"; "descent from 7 to 5000 ft on inst." Conditions listed as VFR but accompanied by less specific indications of visual impairment, such as the citation "continued VFR flight into adverse weather conditions," were classified as questionable.

A primary objective of the analysis was to catalog the direct causes of airframe failures and to assess their relative importance. For the three most recent years (1973-1975) an attempt was made to determine the sequence of events for each structural failure and to identify the immediate cause, e.g., turbulence per se, pilot maneuver during upset recovery, flutter. The data in the NTSB briefs were insufficient to do this in almost every instance. The lack of complete documentation of the causal sequence is not surprising since few of the IFAF accidents left any survivors to give first-hand accounts and there are no requirements for any kind of data recording in general aviation aircraft. The efforts to identify the immediate cause were therefore limited to a survey of the non-fatal accident briefs. The documentation on these did prove somewhat more complete than that for the fatals.

B. OVERALL ACCIDENT STATISTICS

For the 10-year period of interest 283 IFAF accidents met the previously discussed criteria. Of these, 247 (87 percent) were fatal and not one of these left <u>any</u> survivors. In the same timespan, the hours flown

for general aviation powered, fixed wing aircraft were 2.57×10^8, based on annual FAA estimates. This results in IFAF accident rates (per 10^5 hours) of 0.110 for all accidents and 0.096 for fatal accidents. These rates can be contrasted with the overall general aviation* rates for the same period of 17.9 for all accidents and 2.48 for fatal accidents (Ref. 3). Thus IFAF accounted for only 0.6 percent of all accidents and for 3.9 percent of fatal accidents.

Statistics which have particular relevance to the causal chain of events of IFAF accidents relate to the atmospheric conditions at the time of the accidents. Two aspects are of particular interest as potential causal factors — visibility and aerodynamic disturbance. Visibility conditions were classified as VMC, IMC, or unknown, as previously described. The citing of turbulence and/or thunderstorm activity as a factor was tabulated as an indication of an atmospheric disturbance. One additional factor was taken into account in summarizing the influence of these atmospheric conditions on IFAF accidents — whether or not the pilot was instrument rated. The resulting three-dimensional breakdown is given separately for fatal and for non-fatal accidents in Table III-2.

Overall, the data show a high incidence of the atmospheric phenomena:

- Seventy-six percent of the fatal accidents and 78 percent of the non-fatal accidents involved IMC and/or turbulence/thunderstorm (T/T).
- Only six accidents, all fatal, were definitely identified with VMC and no T/T (four of these involved icing conditions and two, pilot impairment).

The two conditions were each identified in a roughly equal number of all accidents (160 IMC, 140 T/T). However, their influence was substantially different within the various subgroups:

- IMC is the more important factor in fatal accidents, and T/T is more important in non-fatal accidents. Fatal accidents show a 62 percent IMC incidence compared with a 19 percent incidence for non-fatal accidents. On the other hand, T/T was cited in 69 percent of non-fatal accidents vs. 47 percent of fatal accidents.

---

*Includes rotorcraft, gliders and balloons. Figures for powered, fixed wing aircraft were not given separately.

TABLE III-2. SUMMARY OF IFAF ACCIDENT ATMOSPHERIC CONDITIONS

a) Fatal Accidents

	T/T	No T/T	Unknown	Sum
IMC	26	12	—	38
VMC	7	5	—	12
Unknown	6	6	9	21
Sum	39	23	9	71

Instrument Rated Pilots

	T/T	No T/T	Unknown	Summary
IMC	55	56	3	114
VMC	3	1	—	4
Unknown	18	24	14	56
Sum	76	81	17	174

Non-Instrument Rated Pilots

	T/T	No T/T	Unknown	Summary
IMC	81	69	3	153
VMC	10	6	—	16
Unknown	24	30	24	78
Sum	115	105	27	247

All Pilots*

b) Non-Fatal Accidents

	T/T	No T/T	Unknown	Sum
IMC	3	—	—	3
VMC	5	—	—	5
Unknown	2	1	2	5
Sum	10	1	2	13

	T/T	No T/T	Unknown	Summary
IMC	1	2	1	4
VMC	9	—	—	9
Unknown	5	2	3	10
Sum	15	4	4	23

	T/T	No T/T	Unknown	Summary
IMC	4	2	1	7
VMC	14	—	—	14
Unknown	7	3	5	15
Sum	25	5	6	36

*Includes 2 accidents for which pilot's instrument rating is unknown.

- Fatal accidents involving instrument-rated pilots show substantially less influence of IMC relative to T/T than do those involving non-instrument-rated pilots. This is most evident from a comparison of IMC-only vs. T/T-only for the two pilot subgroups.

These findings clearly indicate that most general-aviation IFAF accidents are generally triggered by atmospheric phenomena. The accident briefs do not allow assessment of the degree to which direct gust loads and maneuvering loads contribute to any individual overload, much less to overall IFAF incidence. The high incidence of IMC and the differences in the statistics for instrument-rated and non-instrument-rated pilots and for fatal and non-fatal accidents suggest that loss of control is a more important causal mechanism than direct gust overload. A detailed examination of the non-fatal accidents presented later in this section seems to bear out this conclusion (see Tables III-5, 6).

Another overall statistic developed is the relative failure frequencies of the various aircraft component parts. These data are tabulated in Table III-3 for fatal and non-fatal accidents. Note that percentages in each column of Table III-3a add up to more than 100 percent because more than one failed component was cited in some accident briefs with no indication of which part failed first.

For the most common component failures, the failed-component statistics for fatal and non-fatal accidents were in agreement:

- The wing was by far the most commonly cited component (63 percent of fatal and 67 percent of non-fatal accidents).

- The horizontal stabilizer took second place at about one-third the incidence of the wing. No other component was cited in more than 11 percent of the accidents.

Noticeable differences between the fatal and the non-fatal accident data are probably related to the dichotomy of outcomes which they represent. Failures of the empennage, are more likely to result in an uncontrollable instability, with fatal results; damage to the fuselage, flaps or (single surface of) ailerons, on the other hand, is not nearly as critical. Also, as noted previously, the data for non-fatal accidents were more complete. Thus, one or more failed components were reported in

TABLE III-3

IFAF ACCIDENT FAILED-COMPONENT INCIDENCE

a) All Components

FAILED COMPONENT	PERCENTAGE OF ACCIDENTS	
	FATAL	NON-FATAL
General disintegration	9.7	0
Wing	63	67
Wing appurtenances (wing-mounted tips, engines, fuel tanks)	2.0	0
Horizontal stabilizer	17	22
Empennage or tail*	11	5.6
Elevator	7.9	8.3
Vertical stabilizer	5.7	0
Rudder	2.0	0
Aileron	1.6	8.3
Fuselage	1.6	8.3
Flaps	0	2.8
None Given	15	2.8

*Does not necessarily mean the entire tail failed but that this term was used in the brief.

b) Wing Involvement

FAILED COMPONENT	PERCENTAGE OF ACCIDENTS	
	FATAL	NON-FATAL
Wing and/or wing appurtenances cited	64	67
Specific component(s) excluding wing, cited	11	31

all but one (2.8 percent) of these accidents, compared with 15 percent for fatal accidents. Finally, the incidence of failures of only components other than the wing is three times higher for non-fatal accidents than for fatal accidents, probably because: 1) less damage is more likely to result in a non-fatal accident; and 2) fatal accidents generally end in an uncontrolled descent which results in secondary (possibly wing) failures, as evidenced by the 9.7 percent incidence of "general disintegration" in fatal accidents.

A breakdown was also made of the type of flying for which each aircraft was being used when an accident occurred. The use categories by which the data are summarized are defined by the FAA as:

1) Personal: Any use of an aircraft for personal purposes not associated with a business or profession, and not for hire. This includes maintenance of pilot proficiency.

2) Business, combines:

   — Business transportation: Any use of an aircraft not for compensation or hire by an individual for the purposes of transportation required by a business in which he is engaged.

   — Executive transportation: Any use of an aircraft by a corporation, company or other organization for the purposes of transporting its employees and/or property not for compensation or hire and employing professional pilots for the operation of the aircraft.

3) Instruction: Any use of an aircraft for the purpose of formal instruction with flight instructor aboard, or with the maneuvers on the particular flight(s) specified by the flight instructor.

4) Other: All other uses including air taxi, ferry flight, demonstration, research and development, and "industrial/special."

These statistics are summarized in Table III-4.

TABLE III-4

IFAF ACCIDENT AIRCRAFT USE

USE	PERCENTAGE OF ACCIDENTS	
	FATAL	NON-FATAL
Personal	70.4	69.4
Business	23.5	19.4
Instruction	2.0	8.3
Other	3.6	2.8
Unknown	0.4	0

FAA data (Ref. 3) for the same 10-year period, 1966-1975, yield this breakdown of percent of hours flown for general aviation aircraft: personal, 25%; business, 29%; instruction, 26%; and other, 20%. Thus, personal use accounts for nearly three times the proportion of accidents expected on the basis of hours flown. The proportion for business use is fairly close to the corresponding exposure. Instruction and other flying produce only a small fraction of the proportion expected on this basis. The large differential effects are probably related to such factors as pilot proficiency and rating, presence of an instructor, operational conditions (e.g., IMC/VMC), and adherence to good operational practices. A greater likelihood of flying in favorable weather conditions is a factor which might be expected to reduce the number of IFAF accidents during instructional use. This effect is also suggested by the difference in the percentage of fatal vs. non-fatal accidents for this use. This difference is the only substantial one for these two accident subgroups.

The differential effects of type of flying on IFAF accident incidence are quite substantial and should be considered in comparing accident rates among individual aircraft.

In order to gain further insight into the mechanisms of IFAF accidents, the data for the 36 non-fatal accidents were examined in greater detail. A "primary causal factor" was determined in each case, if possible, based on

the listed "probable causes," "factors," and "remarks." These factors are summarized in Table III-5. This table again emphasizes the importance of adverse atmospheric phenomena, particularly turbulence, on these accidents.

TABLE III-5

DISTRIBUTION OF IDENTIFIABLE "PRIMARY CAUSAL FACTORS" FOR NON-FATAL IFAF ACCIDENTS

Primary Causal Factors	Number of Accidents	
Adverse atmospheric phenomena		23
Turbulence only (including 3 vortex, 2 lost control, and 1 upset)	17	
Turbulence and IMC	2	
Turbulence and thunderstorms	2	
IMC only	1	
"Adverse weather"	1	
Spin		3
Overspeed		3
Spiral		2
Unique miscellaneous occurrences		4
None identified		1
TOTAL		36

The non-fatal accident data were also sorted by aircraft model for those with two or more accidents, in hopes of finding some commonalities for a given make and model. These data are reported in Table III-6 along with a composite accident description for each aircraft. There is a sufficient degree of consistency among the individual accident descriptions for some of the aircraft to suggest the existence of an underlying causal mechanism. However, the smaller number of accidents for each specific aircraft prevents any firm conclusions.

TABLE III-6. THUMBNAIL DESCRIPTIONS OF IFAF NON-FATAL ACCIDENTS

AIRCRAFT MAKE/MODEL	NUMBER OF ACCIDENTS	BASIC DATA*	PRIMARY CAUSAL FACTOR	FAILURE†
Beech 35	5	N, N, Y, N	Turbulence	Rudder separated
		N, N, Y, N	Severe turbulence upset	Wing damaged
		Y, N, Y, N	Turbulence	Improper c.g. (wings skin)
		Y, ?, Y, N	Vortex turbulence	Wing damaged
		Y, N, Y, N	Clear air turbulence	Wing and fuselage overstressed
	Composite	_, N, Y, N	Turbulence	Wing damaged
Piper PA-24 (Comanche)	4	Y, ?, ?, ?	Pilot struck head preflight	(Wings skin)
		Y, N, Y, N	Lost control, spiral	Wings wrinkled
		N, N†, Y, N		Tail surface damaged
		N, ?, Y, N	Vortex turbulence (upset?)	(Horizontal stabilizer)
	Composite	_, N, Y, N	Turbulence, possible control loss	Wings deformed or stabilizer damaged
Piper PA-30 (Twin Commanche)	4	N, N, Y, N	Clear air turbulence	Wing skin wrinkled, rivets popped
		Y, N, Y, N	Turbulence, uncontrolled descent	Wings buckled
		Y, Y, Y, N	Exceeded V_{NE}	Bent stabilizer
		Y, N, Y, N	Turbulence	Horizontal stabilizer bent
	Composite	Y, N, Y, N	Turbulence	Wings deformed, or stabilizer bent
Cessna 182	3	N, Y†, Y, N	Lost control, spin after entering cloud	Wing, stabilizer damaged
		N, Y†, Y, ?	Ice, lost flying speed and control	Wings buckled
		N, ?†, Y, Y	Penetrated thunderstorm	Wing and horizontal stabilizer overstressed
	Composite	N, Y†, Y, ?	Turbulence, control loss	Wing, stabilizer
Cessna 210	3	N, N, Y, N	Severe turbulence	Wings damaged
		N, N, Y, N		Wings damaged
		N, N, Y, Y		Wings damaged
	Composite	N, N, Y, ?	Turbulence	Wings damaged
Bellanca Viking Series	2	N, N, Y, N	Lost control in turbulence	Right wing skin separated
		Y, ?, Y, N	Vortex turbulence	Wing skin ruptured
	Composite	_, N, Y, N	Turbulence	Wing skin
Cessna 150	2	Y, ?, N, N	Stall maneuver recovery	(Elevator, stabilizer)
		N, Y, N, N	Flew into clouds, spin	Fuselage wrinkled
	Composite	_, ?, N, N	—	—
Cessna 205, 206	2	N, ?†, N, N		Permanent set in wings
		Y, Y, N, N		Wrinkled both wings
	Composite	_, Y, ?, N	Adverse weather	Wings deformed
Piper PA-28 (Cherokee)	2	N, ?, ?, ?	Student exceeded V_{NE} by 9 kt	(Elevator, aileron, flap assembly)
		N, Y†, N, N	Recovery from high speed dive	Bent wing spar
	Composite	N, ?, N, N	Excessive speed	—

*Answer Yes (Y), No (N), Unknown or Questionable (?) to 4 questions: 1) Was pilot instrument rated? 2) Did IMC contribute to the accident? 3) Was turbulence a factor? 4) Were thunderstorms a factor?

†Components in parentheses were listed under probable causes...airframe "(component)".

†"Continued VFR flight into adverse weather conditions" was listed as a probable cause.

The remainder of the accident statistics are discussed in connection with the individual aircraft involved.

C. DATA BY AIRCRAFT MAKE AND MODEL

The accident count is broken down by individual aircraft make and model in Table III-7. Data for very similar model variants have been combined under one heading. Aircraft are otherwise classified only as single-engine or twin engine models.

The accident count breakdown lacks the measure of exposure needed for making comparisons between aircraft. Nonetheless, the Beech 35 (76 accidents) and the Piper PA-24 (39 accidents) stand out in Table III-7 against the backdrop of the other aircraft, many of which had only one accident. Because the Beech 35 accounted for 27 percent of all the IFAF accidents, incidences of adverse atmospheric conditions and of component failures in its accidents were compared with those for the other aircraft.

In general, the compared statistics were similarly distributed, as shown in Table III-8. The major differences were:

- IMC was cited somewhat more often in Beech 35 accidents; however if the "unknowns" are excluded, the percentages are very close — 85 percent IMC for Beech 35 and 83 percent for all others.
- The Beech had almost 2-1/2 times the incidence of "general disintegration" for the rest of the aircraft.

Comparison of tail failures is difficult because of the Beech 35 "vee" tail. The two fixed surfaces provide the combined functions of the vertical and horizontal stabilizers. The movable surfaces (called ruddevators) combine the functions of the elevators and rudder.

To determine the importance of differences in the number of accidents over a broad segment of the general aviation population of interest, the raw accident count for individual aircraft was normalized by estimates of the hours flown by the aircraft over the 10-year period. These exposure estimates were based on flying hours data published annually by the FAA.

TABLE III-7. IFAF ACCIDENT COUNT BY AIRCRAFT

CLASS	AIRCRAFT	FATAL ACCIDENTS/ALL ACCIDENTS										
		TOTAL	1966	1967	1968	1969	1970	1971	1972	1973	1974	1975
Single Engine	Beech 19, 23, 24 (Musketeer)	4/4		1/1		2/2			1/1			
	Beech 24R	2/2								1/1		1/1
	Beech 33, 36	1/1					1/1					
	Beech 35 (Bonanza)	71/76	10/10	7/7	7/8	4/5	3/4	5/5	3/3	10/12	13/13	9/9
	Bellanca 14-19, 17-30, 17-31	7/9	1/1						3/4		1/2	2/2
	Cessna 120, 140	2/2				1/1			1/1			
	Cessna 150	3/5		0/1	1/2	2/2						
	Cessna 170	1/1		1/1								
	Cessna 177	2/3			1/1	0/1			1/1			
	Cessna 177RG	1/1								1/1		
	Cessna 182	2/5					0/1		1/2	0/1		1/1
	Cessna 190	1/1									1/1	
	Cessna 195	2/2		1/1	1/1							
	Cessna 205, 206	1/3	0/1				0/1				1/1	
	Cessna 210	11/14	2/2	2/2	0/2		2/2		2/2	2/2	1/1	0/1
	Ercoupe	3/3	1/1	1/1							1/1	
	Helio 391	1/1			1/1							
	Luscombe 8	2/3	1/1	1/1		0/1						
	Maule M-4	1/1								1/1		
	Navion	9/9	1/1		2/2			1/1		3/3		2/2
	Piper PA-12 (Super Cruiser)	1/1		1/1								
	Piper PA-17 (Vagabond)	0/1								0/1		
	Piper PA-18, L-21 (Super Cub)	1/1		1/1								
	Piper PA-20 (Pacer)	0/1	0/1									
	Piper PA-22 (Tri-Pacer)	1/2				0/1			1/1			
	Piper PA-24 (Comanche)	35/39	11/11	3/4	4/5	3/4	1/1	7/7	4/4	2/3		
	Piper PA-28 (Cherokee)	15/17	1/1	1/1	2/2		1/1	1/1	3/4	2/2	4/5	
	Piper PA-28R (Cherokee)	10/10				1/1			3/3	2/2	2/2	2/2
	Piper PA-32 (Cherokee Six)	7/8			2/3	1/1			1/1	1/1	2/2	
	Rockwell Commander 112	1/1								1/1		
	SIAI-Marchetti S205	1/1						1/1				
	Stinson 108	1/1	1/1									
	Temco GC-1B (Swift)	1/1										1/1
	Travel Air 6000	1/1	1/1									
	SUBTOTAL	202/231	30/32	20/22	31/37	14/19	8/11	15/15	24/27	26/31	26/28	18/19
Twin Engine	Beech 18 (Twin Beech)	0/1				0/1						
	Beech 50 (Twin Bonanza)	1/1									1/1	
	Beech 65-80 (Queen Air)	2/2						1/1		1/1		
	Beech 65-90 (King Air)	1/1								1/1		
	Beech 95 (Travel Air)	3/3		1/1			1/1	1/1				
	Cessna 310, 320	3/4	1/2	1/1			1/1					
	Cessna 337 (Super Skymaster)	2/2						1/1	1/1			
	Cessna 401, 414, 421	4/4			1/1						2/2	1/1
	Piper PA-23 (Apache Aztec)	8/9			1/1	1/1	0/1		2/2	2/2	2/2	
	Piper PA-30 (Twin Comanche)	11/15	1/1	4/4	1/1	0/1	1/1	1/1	1/2		0/1	2/3
	Piper PA-34 (Seneca)	1/1										1/1
	Rockwell Aero Commander	9/9	2/2	1/1	1/1		2/2			1/1	1/1	1/1
	SUBTOTAL	45/52	4/5	7/7	4/4	1/3	5/6	4/4	4/5	5/5	6/7	5/5
TOTAL		247/283	34/37	27/29	35/41	15/22	13/17	19/19	28/32	31/36	32/35	23/24

TABLE III-8. COMPARISON OF BEECH 35 VS. REST OF GENERAL AVIATION ACCIDENT STATISTICS

a) Number of Accidents

Beech 35: 76 All other aircraft: 207

b) Atmospheric Conditions

CONDITION		PERCENTAGE OF ACCIDENTS	
		BEECH 35	ALL OTHER
Visibility	IMC	63	54
	VMC	11	11
	Unknown	26	35
Disturbance	T/T	49	50
	No T/T	41	38
	Unknown	10	12

c) Failed Components

FAILED COMPONENT	PERCENTAGE OF ACCIDENTS	
	BEECH 35	ALL OTHER
General disintegration	14	6.3
Wing	59	65
Wing appurtenances	1.3	1.4
Specific component(s), excluding wing	9.2	16
Horizontal stabilizer	18	18.
Empennage (or tail)	11	10
Elevator	13	6.3
Vertical stabilizer	*	5.8
Aileron	1.3	2.9
Fuselage	1.3	2.9
Rudder	*	2.4
Flaps	0	0.5
None given	17	12

*The Beech 35 has a "vee" tail. Failures of the ruddevators are listed under elevator. Failures of the stabilizer are listed under horizontal stabilizer.

In assessing the relative magnitudes of these individual accident rates general aviation aircraft were further subdivided by sorting the single engine aircraft into two groups: those with fixed landing gear, and those with retractable landing gear. The accident rate data were compiled for aircraft:

- With a substantial number of accidents.
- With substantial flying hours relative to other group members, including one aircraft typical of each group but with no accidents.
- Which were closely related to, but differed primarily in one aspect from, an aircraft in one of the above categories. These included the Beech 33 and 36, conventional-tail successors of the Beech 35, and the following retractable-landing-gear variants of a model line: Beech 24R, Cessna 177RG, and Piper PA-28R.

The computed fatal/all accident rates are presented in Table III-9 along with other related data. Within each group the aircraft are listed in the order of increasing all-accident rate. The columns following each of the accident rates indicate the statistical significance, if any, of the difference between each aircraft's accident rate and that of the whole group (of selected aircraft) to which it belongs. The significance is based on the two-tailed test of the chi-square statistic which is computed as:

$$\chi^2 = \frac{(F_o - F_e)^2}{F_e}$$

where F_o is the observed number of accidents for a given aircraft and F_e is the number expected, based on the group accident rate and the individual aircraft's exposure. Individual accident counts and hours flown are also provided in the table, making it easier to interpret the variation of significance with accident rate.*

Table III-9 also lists the number of accidents excluded for the reasons discussed earlier. It is perhaps interesting that all three of the

---

*Note in several cases a relatively high (or low) accident rate is not statistically significant because the number of hours flown is not large enough.

TABLE III-9. IFAF ACCIDENT RATE STATISTICS FOR GENERAL AVIATION AIRCRAFT (1966-1975)

GROUP	MANUFACTURER/MODEL	FATAL/ALL ACCIDENTS	ACCIDENT RATES				10^5 HOURS FLOWN	USE BREAKDOWN (PERCENTAGE)				EXCLUDED FATAL/ALL ACCIDENTS
			ALL	SIGNIFICANCE*	FATAL	SIGNIFICANCE*		PERSONAL	BUSINESS	INSTRUCTION	OTHER	
Single Engine, Fixed Landing Gear	Cessna 172	0	0	L	0	L	245.1	46.5	11.7	31.9	9.9	0/3
	Cessna 150	3/5	.0139	L	.0083	L	359.4	19.4	2.8	71.9	5.9	0/4
	Piper PA-22 (Tripacer)	1/2	.0372		.0186		53.8	62.1	7.2	27.3	3.4	3/8
	Cessna 182	2/5	.0386		.0154		129.5	44.4	35.1	5.5	15.0	0/4
	Cessna 170	1/1	.0432		.0432		23.2	81.2	11.9	2.4	4.5	2/3
	Piper PA-28 (Cherokee)	15/17	.0695	H	.0613	H	244.5	35.2	14.2	43.4	7.2	0/1
	Cessna 120, 140(A)	2/2	.0778		.0778		25.7	79.9	3.8	10.4	5.9	0/2
	Cessna 205, 206	1/3	.0880		.0293		34.1	16.3	36.2	1.9	45.6	2/4
	Beech 19, 23, 24 (Musketeer)	4/4	.130	H	.130	H	30.7	34.0	15.6	44.5	5.9	1/3
	Cessna 177 (Cardinal)	2/3	.155	H	.103		19.4	41.3	21.9	22.9	13.9	0
	Piper PA-32 (Cherokee Six)	7/8	.243	VH	.213	VH	32.9	23.1	33.7	5.4	37.8	0/1
	GROUP*	38/50	.0417		.0317		1198.3	36.8	13.0	40.5	9.7	8/33
Single Engine, Retractable Landing Gear	Mooney M20	0	0	VL	0	VL	65.6	49.9	36.6	4.8	8.7	7/12
	Beech 33, 36	1/1	.0386	L	.0386	L	25.9	See Beech 35 (combined)				0
	Cessna 177RG (Cardinal RG)	1/1	.256		.256		3.9					0
	Cessna 210	11/14	.385		.303		36.3	33.2	51.8	1.8	13.2	1/4
	Piper PA-28R (Cherokee Arrow)	10/10	.401		.401		25.0					0
	Piper PA-24 (Comanche)	35/39	.719	H	.645	H	54.2	44.7	39.1	4.8	11.4	2/4
	Beech 35 (Bonanza)	71/76	.779	VH	.728	VH	97.5	38.8	49.4	2.0	9.8	2/2
	Navion	9/9	.812		.812		11.1	72.0	22.9	1.9	3.2	1/1
	Bellanca 14-19, 17-30, 17-31	7/9	.914		.711		9.8	42.5	49.3	1.6	6.6	0
	Beech 24R	2/2	1.157		1.157		1.7					0
	GROUP*	147/161	.486		.444		331.1	43.0	44.0	3.0	9.9	18/23
	ALL SINGLE ENGINE	202/231	.115		.101		2003.1					—
Twin Engine	Piper PA-31 (Navajo)	0	0		0		18.4					0/2
	Beech 18 (Twin Beech)	0/1	.0243		0	L	41.2	32.1*		1.0*	66.9*	4/5
	Beech 99 (Travel Air)	3/3	.0601		.0601		49.9	77.1*		1.6*	21.3*	1/3
	Cessna 310, 320	3/4	.0669		.0502		59.8	56.5*		2.1*	31.4*	1/3
	Beech 65-80, -90 (King, Queen Air)	3/3	.0778		.0778		38.5					0/3
	Beech 50 (Twin Bonanza)	1/1	.103		.103		9.7					0
	Cessna 336, 337 (Skymaster)	2/2	.108		.108		18.5	69.2*		1.9*	28.9*	0
	Cessna 401, 402, 411, 414, 421	4/4	.115		.115		34.9					0
	Piper PA-23 (Apache)	8/9	.119		.106		75.4	56.4*		10.0*	33.6*	0/3
	Rockwell Aero Commander	9/9	.278	H	.278	H	32.4	55.6*		1.5*	42.9*	2/3
	Piper PA-30 (Twin Comanche)	11/15	.536	VH	.393	VH	28.0	69.1*		6.6*	24.3*	0/2
	GROUP*	44/51	.125		.108		406.8	57.6*		4.2*	38.2*	8/24
	ALL TWIN ENGINE	46/52	.0914		.0791		568.8					
	ALL AIRCRAFT	247/283	.1100		.0960		2571.9					

Letters	Mean Relative to That of Group	Probability of Chance Occurrence
	Not significantly different	Greater than 5%
L	Low	Less than 5%
H	High	Less than 5%
VL	Very low	Less than 0.1%
VH	Very high	Less than 0.1%

*For all group members specifically listed.

*Based on 1967-1969 data given in Ref. 4

"zero-accident" aircraft had some excluded accidents. In particular, one of these — the Mooney M20 — had more excluded accidents (12) than any other aircraft in Table III-9. For this reason, the Mooney's accidents were examined in more detail with the following findings:

- Ten of the aircraft were older models made of pressure bonded laminated spruce. Deterioration of the wooden structure was found in 9 of the 10 aircraft; the vertical fin was cited 8 times and the wing once. The tenth accident was caused by pilot incapacitation due to intoxication and CO poisoning. Of the two "metal" Mooneys, one lost the vertical fin because of missing bolts and the other lost its nose gear.

- Atmospheric conditions were specified in only two of the twelve accidents; turbulence/thunderstorm was cited as a factor in one case and clear air turbulence in the other. Apparently it was felt that the structural deficiencies cited in most cases were the prime causes of those accidents.

- Only one of the pilots was instrument-rated and only five had more than 500 hours previous flight time.

- Only one of the accidents occurred prior to 1968.

Two of the accident briefs for the wooden Mooneys mentioned Airworthiness Directive (AD) 69-5-3, in one case noting compliance and in the other, non-compliance. The stated object of this directive, which superceded AD 68-25-6, was "to detect wood and glue joint deterioration in wood wing and wood empennage structures." The earlier AD was issued in mid-1968. Two accidents in late 1968 may have prompted the revision.

This review for the Mooney justified the exclusion of these 12 accidents. Those accidents were largely due to a recognized problem with the wood structure and none are relevant to the scope of this project. Further examination of the excluded accidents was not done. We now turn back to the data for the included IFAF accidents.

The all-accident rate data are also presented graphically vs. their statistical significance in Fig. III-1. This plot provides a composite summary of the distribution of accident rates for the selected aircraft and gives some indication of the importance of inter-aircraft differences.

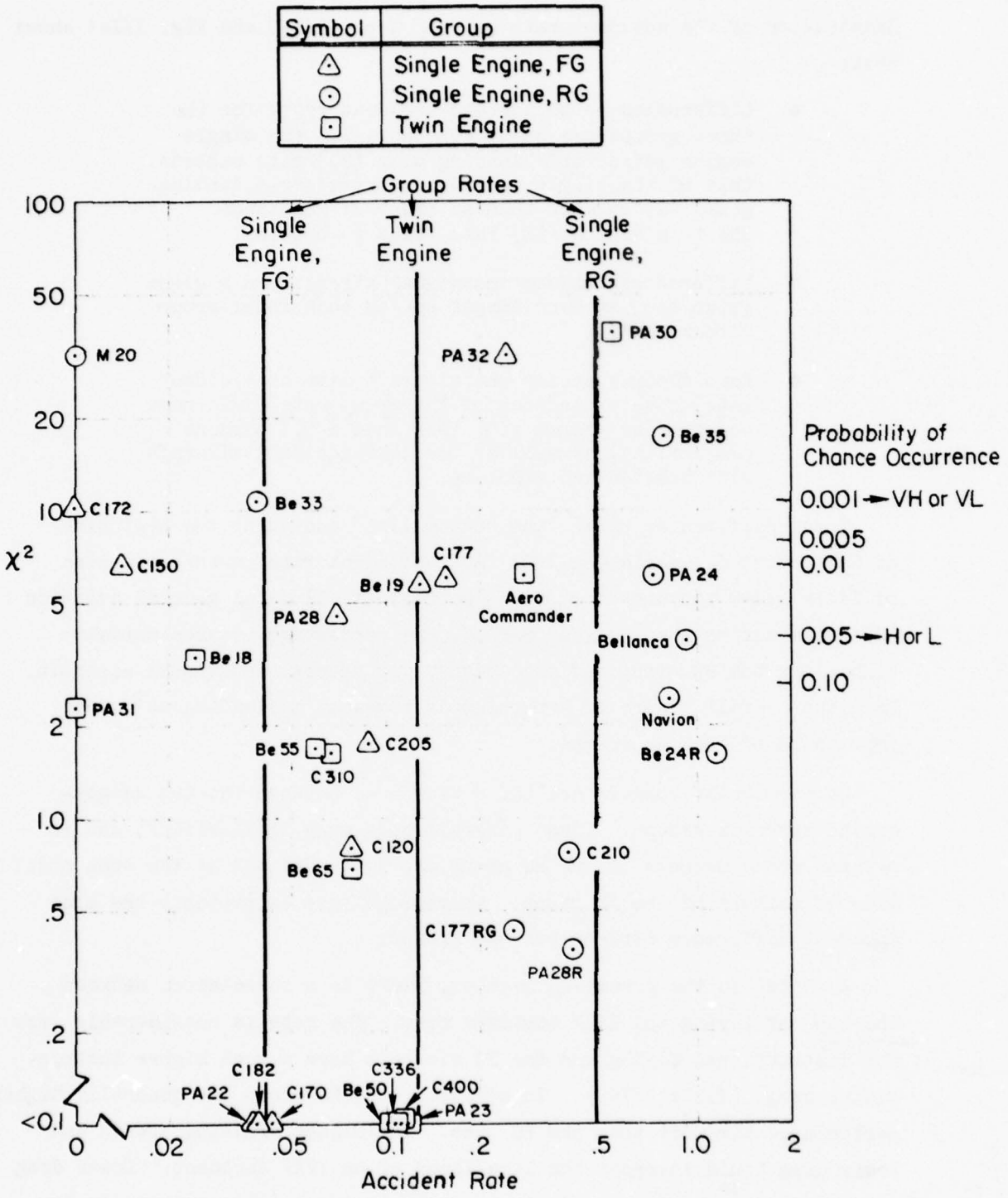

Figure III-1. IFAF Accident Rate vs. Group Relative Chi-Square Statistic for Selected Aircraft

Examination of the accident rate data in Table III-9 and Fig. III-1 shows that:

- Differences between group accident rates for the three groups are quite substantial. The single engine retractable landing gear (RG) rate exceeds that of the single engine non-retractable landing gear (FG) by more than an order of magnitude. The twin engine (TE) rate falls in between.

- Differences between individual aircraft in a given group show an even larger spread than inter-group differences.

- Each group contains one aircraft with an accident rate whose exceedance of the group rate could have occurred by chance with less than a 0.1 percent probability, as well as one zero-accident aircraft with substantial exposure.

These differences alter "the bottom line" quoted at the beginning of Subsection B. While the IFAF fatal accident rate on the last line of Table III-9 accounts for only 4 percent of all fatal general aviation accidents during the ten year period, the percentage is substantially higher for the RG group and even higher for several individual aircraft. Thus the overall figure of 4 percent is somewhat misleading as to the importance of IFAF accidents.

Of particular concern are the differences between the two single-engine aircraft groups. These aircraft have many similarities, and in several cases members of the RG group are just variants of the same model line of members of the FG group. Operational use is probably the most coherent difference between the two groups.

As noted in the preceding section, there is a correlation between the type of flying and IFAF accident rate. The rate is considerably less for instructional flying and the FG aircraft have a much higher instructional usage (Table III-9). In addition, the RG group are generally higher performance aircraft than the FG ones. The higher cruising speeds and lower drag could increase the likelihood of an IFAF accident. Lower drag aircraft accelerate more quickly to V_{NE} when upset (see analysis in Section IV-D).

One would also expect RG aircraft to have a higher exposure to adverse weather conditions, e.g., IMC, turbulence, and icing. On the other hand, the pilots of these aircraft should have more experience and be better qualified, e.g., one would expect a higher percentage of instrument ratings.

While operational usage undoubtedly contributes to FG/RG differences, correlation of this factor with IFAF accident rate is rather poor for individual aircraft. Some members of both the FG and RG groups with very little instructional time still have very low accident rates.

Operational usage (e.g., IFR flying) alone would suggest a higher accident rate for twins than even the single-engine RG group. That the exact opposite is true may be due to a higher level of training and proficiency for the crews of twins.

Differences between individual aircraft within each group are even more intriguing. Operational usage should not be much of a factor in such differences. The use breakdown and exposure time for the Mooney M20 and the Piper Comanche, for example, are very similar, yet their IFAF accident rates are at opposite ends of the distribution. An even more puzzling contrast is offered by the Beech 35 and its derivative, the Beech 33, 36 line. As noted earlier, the Beech 35 has a vee-tail whose fixed and movable surfaces provide both longitudinal and directional stability and control. The Beech 33, 36 is nearly identical structurally, the notable exception being its conventional tail configuration. Yet the Beech 35's IFAF accident rate at $0.779/10^5$ hrs, is 20 times that of its straight-tailed companion, and in fact, is exceeded only by a few aircraft with substantially less exposure (less than 12 percent of the Beech 35's flying hours during the 10 years).

One possible explanation for the dichotomy in IFAF accident involvement of the two Beech aircraft lay in the longevity of the model line. The Beech 35 was one of the early post-World War II aircraft; its first production version — the Model 35 — originated in 1947. The Beech 33, 36 line is a more recent offshoot of the 35 line; it was first produced in 1960. Both aircraft are still being manufactured; they come off essentially the same assembly line. Many of the pre-1960 aircraft are still

active. Possibly, the age and/or the earlier structural design of these aircraft could make them more susceptible to IFAF than the later models of both lines. To check out this possibility the Beech 35 accident count and exposure data were broken out by individual model. These are summarized in Table III-10 with the resulting accident rates, which are also plotted on Fig. III-2. Because of its potential correlation with these rates, the Beech 35's history of structural and corresponding performance changes was reviewed, as is summarized in Table III-11.

The trend of the accident rates with model is not clear. Because of the small number of accidents for any one model, one can expect the rather large, random fluctuations shown in the Fig. III-2 accident rates. By combining models, gross differences between older and newer models can be more reliably identified. In the Beech 35 series, the most substantial structural change was made in Model H35, see Table III-11. Comparison of the IFAF accident rate for earlier models with that of the H35 and subsequent models, as shown in Fig. III-3, indicates a substantial difference. The accident rate for the older models is considerably higher than for the newer ones. With the rather large number of accidents involved, this outcome is unlikely to be the result of chance.

However, this reduced accident rate for the later models is still far greater than that for Beech 33, 36. Since the H35 precedes the Beech 33, 36 line by only 3 years, and its accident rates and those of intervening models (J35, K35) are actually lower than the later model average, the disparity in the IFAF accident rates of the two Beech aircraft is not explained by these data.

TABLE III-10. IFAF ACCIDENT DATA FOR VARIOUS MODELS OF BEECH 35 (1966-1975)

MODEL	PRODUCTION YEAR	NUMBER BUILT	NUMBER OF IFAF ACCIDENTS; FATAL/ALL	EXPOSURE (10^5 HR)	ACCIDENT RATE (PER 10^5 HR)	
					FATAL	ALL
35	1947-48	1500	10/12	6.63	1.51	1.81
A35	1949	701	5/5	3.88	1.29	1.29
B35	1950	480	2/2	3.60	0.56	0.56
C35	1951-52	719	6/6	6.74	0.89	0.89
D35	1953	298	1/1	3.17	0.32	0.32
E35	1954	301	4/5	3.09	1.29	1.62
F35	1955	392	3/3	4.12	0.73	0.73
G35	1956	476	6/6	5.17	1.16	1.16
H35	1957	464	2/2	5.37	0.37	0.37
J35	1958	396	1/1	5.00	0.20	0.20
K35	1959	436	2/2	5.63	0.36	0.36
M35	1960	400	4/4	5.14	0.78	0.78
N35	1961	280	2/2	3.46	0.58	0.58
P35	1962-63	467	7/7	6.73	1.04	1.04
S35	1964-65	667	5/5	10.57	0.47	0.47
V35	1966-67	662	5/6	9.35	0.53	0.64
V35A	1968-69	470	4/5	5.97	0.67	0.84
V35B	1970-	*	2/2	3.78	0.53	0.53
35R†	—	(13)	0/0	0.12	0	0
ALL			71/76	97.5	0.73	0.78

*218 built in 1970-71; 116 built in 1972; still in production.
†Modified Model 35 incorporating various A35 and B35 features.

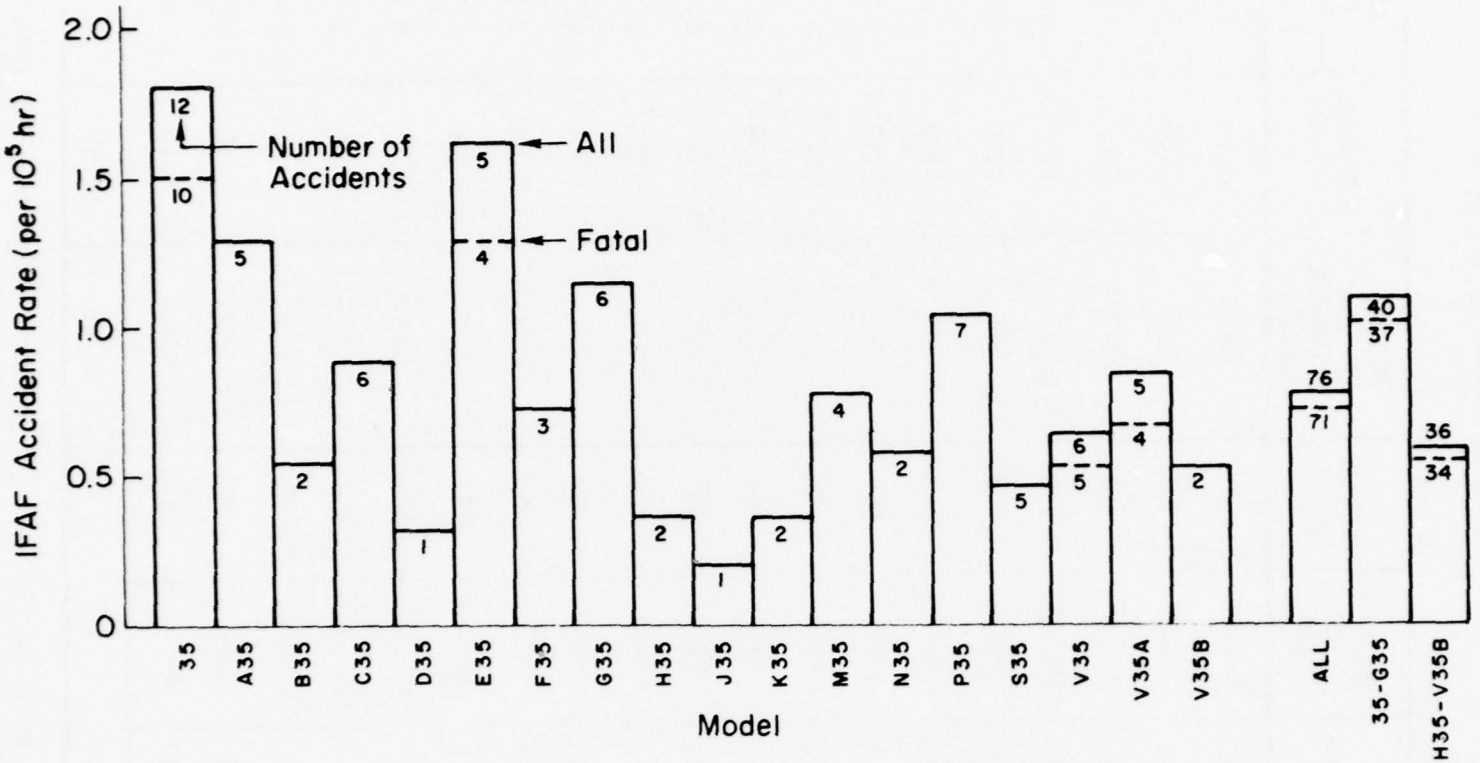

Figure III-2. IFAF Accident Rates for Various Models of Beech 35 (1966-1975)

TABLE III-11. SUMMARY OF BEECH 35 STRUCTURAL HISTORY (REF. 37)

MODEL	GROSS WEIGHT (lb)	HORSE-POWER	V_{NE} (mph, CAS)	MAXIMUM RECOMMENDED CRUISE SPEED (mph, CAS)	MAJOR DESIGN CHANGES
35	2550	185	202	151	
A35	2650	185	202	149	Increased wing strength, incorporated conventional sheet metal center section wing carry through structure. Certified in utility category at max. gross weight. Increased baggage compartment load capacity. Plastic-covered propeller replaced metal-edged one.
B35	2650	185	202	149	New control wheel (flat to absorb crash landing impact loads).
C35	2700	185	202	153	All metal propeller. 20 percent increase in tail chord. V-tail dihedral angle increased from 30 to 33 deg. Local wing structural beef-ups. Stall-warning horn added.
D35	2725	185	202	166	
E35	2725	185/225	202	166/161	Aileron trim control. Strengthened rear spar upper cap. V_{NO} increased from 160 to 175 mph.
F35	2750	185/225	202	166/161	Wing strengthened by extension of spar web and thickening of leading edge skin. Stabilizer spar cap area increased. Third side window in baggage compartment. Optional pair of 10 gallon wing fuel tanks.
G35	2775	225	202	177	Wing structural beef-up.
H35	2900	240	210	183	"O-470" series Continental engine. New 84 inch propeller. Wing main spar strengthened by enlarging spar cap and extending spar web outboard to wing tip. Stronger wing leading edge assembly and rear spar. General structural beef-up in the nose section, center wing carry-through, and fuselage. Very substantial strengthening of stabilizer/ruddevator assembly. Heavier downspring. V_A increased from 130 to 142 mph. Many H35's retrofitted with fuel injection system.
J35	2900	250	225	181	Fuel injection system. Optional autopilot. V_{NO} increased from 175 to 185 mph.

(Continued on following page)

TABLE III-11. (Concluded)

MODEL	GROSS WEIGHT (lb)	HORSE-POWER	V_{NE} (mph, CAS)	MAXIMUM RECOMMENDED CRUISE SPEED (mph, CAS)	MAJOR DESIGN CHANGES
K35	2950	250	225	181	Rudder travel increased. Baggage door strengthened.
M35	2950	250	225	181	New high stability wing tip.
N35	3125	260	225	176	Area of third window more than doubled. Number of fuel tanks reduced from 4 to 2 so gauges are "full time" (no switching). New "ram's horn" control wheel. V_A increased from 142 to 148 rph. Bobweight added (increased stick force/g)
P35	3125	260	225	176	Redesigned instrument panel. Stall warning horn and light replaced with buzzer. Propeller changed twice during production run.
S35	3300	285	225	187	"O-520" series engine. Aft bulkhead moved back 19 inches. Engine canted 2.5 deg right and 2 deg down to reduce rudder trim required during takeoff and climb, and to improve longitudinal stability. Stall warning buzzer replaced with horn. Streamlined max-stability wing tips. Model-33 type pointed ruddevator balance horn. Longer and more streamlined propeller spinner and tail cone. V_{NO} increased from 185 to 190 mph. V_A increased from 148 to 152 mph.
V35	3400	285	225	185	Optional turbo-charged engine (installed in 79 of 622 units). Needle and ball instrument replaced with turn coordinator. Optional full time lateral stability augmentation. Cast aluminum control wheel introduced during production run.
V35A	3400	285	225	185	"Swept" windshield for less obstructed forward vision. Pressure driven gyros replaced vacuum type. Turbo-charged engine in 46 of 470 units.
V35B	3400	285	225	185	Turbo-charged engine option discontinued during production run (11 made). In 1972, structural changes in cabin to accommodate redesigned interior.

D. REVIEW OF SELECTED NTSB ACCIDENT FILES

The foregoing analysis of the NTSB accident briefs identified a substantial number of IFAF accidents which were potentially very relevant to the objectives of this project. It also revealed large differences in the rates of these accidents between the three aircraft groups, and even larger differences in rates between individual aircraft in the same group. As indicated by the chi-square statistic, the differences between aircraft were very unlikely to have occurred by chance. Thus they would appear to reflect actual differences in pilot-aircraft factors. It was important to try to identify those factors pertinent to this program and to determine their relative contribution to the accidents.

The data gathered from the accident briefs provided some clues as to the importance of some of these factors. However, the briefs are very compact distillations of the information gathered in the accident investigation. They were a good screening device but left many questions unanswered, such as:

- How much weight should be put on the listed "Probable Cause(s)" and "Factor(s)"?
- What was the specific basis for such general categorizations as "Continued VFR flight into adverse weather conditions" or "Spatial disorientation"?
- How proximate in time and place was the weather "at the accident site" and what was the significance of its omission?
- What possibly mitigating circumstances were not included in the brief?

A review of some of the complete accident report files in Washington, D.C. showed that they would provide some answers to these kinds of questions. Moreover, besides more complete factual accounts, the files also contained photographs of the accidents which might give some clue to structural failure modes in these accidents. All this detail might allow a more accurate assessment of likely immediate cause of some accidents. More importantly, it could give a better idea of how similar the accidents

were for individual aircraft models and between models. Therefore, a thorough examination of the accident files of several of the aircraft was done.

Five aircraft were selected for this "in-depth" analysis: Beech 35, Piper PA-24, Cessna 210, Navion and Piper PA-30. The first four aircraft are members of the single-engine, retractable gear group, which had the highest IFAF accident rate. Among these aircraft:

- The Beech 35 and the Piper PA-24 had more IFAF accidents than any of the other general aviation aircraft and statistically-significant higher accident rates than the rest of the group.
- The Cessna 210 had an accident rate of roughly half that of the two above and somewhat below that of the group, though substantial nonetheless.
- The Navion was another high accident rate aircraft of modern (metal) construction.

The twin-engine Piper PA-30 was also selected for further analysis because it had the highest accident rate for its group — roughly four times the group average.

Copies of the NTSB files were ordered for the accidents of these aircraft, and — because of its previously discussed similarity to the Beech 35 — for the one Beech 33, 36 accident. These totalled 154 files, representing 53 percent of all the IFAF accidents. One-hundred-thirty-eight of these (90 percent) were actually received,* as summarized in Table III-12.

These 138 files were all carefully reviewed with the following objectives in mind:

- Minimally, to fill in the gaps and to expand the data base of circumstantial evidence built from the NTSB accident briefs, and to increase our insight into the meaning and importance to be given to the tersely coded data in the briefs.

---

*The others could not be located in the NTSB archives.

TABLE III-12

SUMMARY OF NTSB FILE ORDER

AIRCRAFT	NUMBER OF FILES	
	REQUESTED	RECEIVED
Beech 33	1	0
Beech 35	76	64
Cessna 210	14	14
Navion	9	9
Piper PA-24	39	38
Piper PA-30	15	13
Total	154	138

- Ultimately, to identify the immediate cause or causes of any in-flight failures common to a large number of accidents, particularly, peculiar to a specific aircraft model.

The contents of these accident files can include any factual information which the accident investigator feels is relevant to a particular accident. These data usually include the following:

- Pilot/operator aircraft accident report (NTSB Form 6120.1 or equivalent), which provides factual background information on the aircraft, pilot and passengers, and a brief account of the accident ["mandatory" except in accident occurring in the jurisdiction of another (non-U.S.) Government; generally useful only for non-fatal accidents, to provide pilot's (operator) personal account of the accident].

- Factual Aircraft Accident Report (NTSB Form 6120.4 or equivalent) in which the investigator gives the factual background, as above, but in greater detail: catalogues the damage sustained by the aircraft, and provides a narrative of the accident including all relevant factual details (mandatory for accidents occurring in U.S. jurisdiction).

- Summary of Meteorological factors, including Area Weather Forecasts, Sigmets and Airmets, weather observations, pilot reports, etc., relevant to the time and place of the accident.

- Statements of Witnesses to the accident itself or to other possibly relevant circumstances.

- FAA Air Traffic Report Package, including statements of Air Traffic Control Personnel as to weather briefings and/or in-flight communications with the pilot, often including transcripts of the latter.

- Wreckage Chart showing the locations of the aircraft wreckage (scaled sheet provided as part of Form 6120.4, but often simply separately attached to report).

- Photographs of the general area of the crash and of the wreckage.

- Newspaper reports of the crash.

The files sometimes also include detailed technical evaluations of selected damaged components, original toxicology reports, and miscellaneous documentation of the pilot's certification status and the aircraft's ownership and maintenance and repair records.

There was a considerable variation in documentation from file to file. The files reviewed ranged from 8 to more than 200 pages, with a typical file running 50-100 pages. The "eight-page" files were generally for non-fatal accidents, and did not extend beyond the pilot/operator aircraft accident form and an abbreviated investigator's report. The files for fatal accidents were generally much more detailed and lengthy.

Though the files give a considerably more complete picture of what is known about the accidents than do the briefs, allowing a more accurate assessment of the importance of the various factors involved, they do not permit reconstruction of the sequence of events leading up to in-flight failure in most accidents. Excepting non-fatal accidents, this determination must be made primarily from the log of radio contacts with the pilot prior to the accident, from the eye-witness accounts of the accidents, from the characteristics of the structural damage, and from the distribution of the wreckage.

The reviewed files indicate that radio contact with the pilot just prior to the accident is rare. Where found, it usually gives no more indication of the causal sequence of the problem than the circumstantial evidence provides, although it does occasionally offer positive verification of this evidence.

The next best source of information on causal sequence is the eyewitness accounts. With a few notable exceptions, these generally begin after the initial events leading to the accident. This is understandable since:

- It is typically the unusual sounds of an aircraft in trouble, e.g., engine revving or explosion, that first draws the witnesses' attention.
- Often the aircraft cannot be seen until it comes out of the clouds which typically are present in these accidents.
- The accident sequence is initiated from a high altitude (cruise condition) where the aircraft would be difficult to see, even in clear skies.

This generally leaves the interpretation of the structural damage and wreckage pattern as a last resort for reconstructing the accident. This has been found to be a difficult proposition because with few exceptions:

- The aircraft involved suffer multiple failures making it difficult to pinpoint a structural weakness, if one exists.
- In-flight structural damage is compounded by subsequent damage sustained on impact and/or occasionally by fire damage.

Thus for most of the accidents the data is essentially circumstantial, like that extracted from the briefs, though more detailed and accurate.

Figure III-3 identifies the basic data which was routinely extracted from each file. This Check List and Summary Data list was developed based on our previous exposure to the NTSB accident data base via the briefs and a comprehensive review of several of the accident files. Basic data were summarized on this sheet in compactly coded form to simplify gross inter-accident comparison.

NTSB ACCIDENT FILES REVIEW: CHECK LIST AND SUMMARY DATA		
ACCIDENT DATE		
NTSB FILE NO.		
Aircraft Data	Model No. Serial No. Non-Standard Condition GW < GW_{max}? c.g. OK? Total Time on Airframe (hr) Last Inspection Date Hrs Since Last Inspection Operative Autopilot Onboard?	
Pilot Data	Total Hours Hours in Type Hours in Last 90 Days Instrument Rating? Simulated/Actual Inst. Hours	
Weather	Day/Night VMC/IMC Winds (kt) Thunderstorm Activity Precipitation Icing Lightning	
Flight Condition	Altitude (ft) Indicated Airspeed (mph) Maneuvers	
Structure Failure Data	Gear up? Flaps up? Cowl Flaps? Likeliest First Separation Other In-Flight Failures Length of Wreckage Trail Fatigue Check Indicated? Parts Inspected:	
Other Factors	Pilot Incapacitation?	

Figure III-3. Routinely Kept Accident File Data

The meaning of most of the basic data items in the Fig. III-3 list is obvious. Occasionally, however, even seemingly straightforward items required some interpretation, e.g., a pilot who had years of experience as an instructor and was instrument-rated in the Navy but not FAA rated was counted as instrument rated. The only items which require some explanation, except for "weather," are:

- Aircraft Data, Non-standard condition: catch-all for all structural and control system abnormalities, e.g., improper repairs or maintenance, missing or modified parts, airworthiness directives not complied with.

- Flight Condition, Altitude and Indicated Airspeed: last reported by pilot.

- Flight Condition, Maneuvers: those in progress at time of accident, e.g., turn, descent, pullout (recovery).

- Structure Failure Data, Likeliest first separation: inability to find a structural component after impact or finding it near the beginning of the wreckage trail was taken as indication that it may have been the first to separate. More than one component may be so identified for one accident.

The items which characterize the weather must be taken in proper perspective. In rare instances, these conditions were described by the pilot in radio communications prior to the accident. In some cases they were reported by pilots somewhere in the vicinity of the accident close to the time of its occurrence. Precipitation and thunderstorm data were also occasionally obtained from radar observations. For the most part, however, weather conditions were identified from accounts given by ground witnesses, who could only report on the actual conditions in which they saw or heard the aircraft after the accident sequence had begun.

Ground rules for establishing weather conditions were as follows:

- Lighting Conditions: as indicated on Form NTSB 6120.4 and verified by the time of day of the accident.

- Instrument Meteorological Conditions: in essence the same as previously defined for the NTSB briefs, namely, evidence of pilot visual impairment; the most common evidence found in the in-depth analysis were:

- pilot reporting IFR or in clouds, soup, etc.
- aircraft observed coming from clouds
- accident occurred on a dark night over sparsely populated (and therefore dimly lit) area
- conditions at accident site included: low overcast or broken ceiling or heavy precipitation.

- Turbulence: positive indications taken as
  - pilot report of moderate or worse turbulence
  - witness reports of heavy wind activity, e.g., "very gusty," "strong winds."

- Thunderstorm: identified either by name, or by description, e.g., thunder, lightning, storm cell, in an area in which forecasted. Failure of all witnesses to specify taken as evidence of absence from immediate vicinity.

- Precipitation: anything from drizzle to driving rain or snow showers. Failure of witnesses to specify taken as evidence of non-involvement.

- Icing: icing was presumed to have occurred only when the pilot reported it. In those instances, the accident was excluded. Icing was indicated to not have occurred if the freezing level was substantially above the pilot's last reported altitude, or the service ceiling of the aircraft if no indication of aircraft's altitude was given. Otherwise icing was counted as questionable.

- Lightning: specifically cited by at least one witness.

Conditions for which insufficient or conflicting information was found were counted as questionable. If the presence of thunderstorm in the immediate vicinity or the general area was indicated, turbulence was counted as yes or "?". A yes was counted only if there was a positive indication of turbulence.

Statistical comparisons of the weather conditions and some of the other data in the Fig. III-3 list appear later in this subsection. Other possibly relevant details unique to individual accidents were also noted. Some of these are described in the next subsection.

Not all of the accidents whose files were examined were included in the statistical comparisons. Non-fatal accidents were excluded because, as previously observed in the analysis of the NTSB briefs and verified by the examination of the files, they appear to differ from the fatal accidents as a class in various key respects, most notable among which are:

- The attendant atmospheric conditions: non-fatal accidents are more likely to be identified with VMC and with an atmospheric disturbance.
- Structural damage is inevitably much less severe in non-fatal accidents, possibly reflecting different modes of failure.
- The non-fatal accidents are not nearly as thoroughly investigated, as previously noted; hence, key details are often missing, e.g., no photographs of structural damage were found in any of these files and descriptions of the damage were brief.*

However, because they do include presumably accurate first-hand accounts of in-flight structural failures which may give some clue to the immediate causes of fatal accidents — e.g., non-fatal VMC accident might very well have been fatal in IMC — thumbnail descriptions of these accidents are given in the next subsection in which individual aircraft data are summarized. The summary given in Subsection III-C adequately represents the non-fatal accidents statistically since the files in these cases are not much more detailed than the briefs, and both simply reflect the direct statements of the pilots.

Also excluded from the summary were accidents in which mitigrating circumstances which would put the accident outside the interests of the investigation were identified as contributing causes. Such determinations could not have been reliably made from the accident briefs.

Excluded accidents are tabulated by reason for exclusion in Table III-13. As shown in the table, 13 accidents were non-fatal. Of the remaining 125 accidents, 22 were excluded for other reasons.

---

*The lack of a detailed description of the damage is not surprising, since the report could be filed after repairs were made and there is no requirement to document such damage; in fact, a number of such accidents may even go unreported.

TABLE III-13

SUMMARY OF IFAF ACCIDENTS EXCLUDED FROM IN-DEPTH ANALYSIS

	AIRCRAFT					TOTAL
	BEECH 35	CESSNA 210	NAVION	PIPER PA-24	PIPER PA-30	
NUMBER OF FILES REVIEWED	64	14	9	38	13	138
Number of Aircraft Excluded Because:						
Non-Fatal Accident	3	3		3	4	13
BAC $\geq$ 0.1%*	5		1	1	1	8
Hypoxia		1				1
Pilot-Reported Icing	1	1		1	1	4
Instrument Problems	3†					
No Attitude Gyros	1		1			2
Other	1†			3‡		4
Totals	14	5	2	8	6	35
NUMBER OF ACCIDENTS INCLUDED	50	9	7	30	7	103

*A Blood Alcohol Concentration (BAC) of 0.1 percent is the limit above which automobile drivers are presumed to be guilty of driving while intoxicated in most states. Some states and other countries prescribe even lower limits.

†These are described in greater detail in the subsection which gives Beech 35 specifics.

‡One of these accidents involved a witnessed tail flutter, apparently within the operating envelope of the aircraft. The second accident bore a marked resemblance to the first, and was unique in other respects. These two accidents are described in greater detail in the subsection describing PA-24 specifics. File data for the third accident did not yield proof that an in-flight airframe failure had occurred. The airplane crashed, unwitnessed, in the water, no wreckage chart was given nor could one be determined from the file data, and the main component apparently found at a distance from the main wreckage failed differently than in all the other accidents.

Elimination of the 22 excluded fatal accidents would reduce the fatal and all accident rates by 11-18 percent for the 5 selected aircraft. This would still leave each of them with substantial IFAF accident rates. In addition, the reduction appears to be quite uniform across these aircraft. Similar reductions could thus be expected for the other aircraft. Thus exclusion of these accidents should help focus on the objectives of this project without biasing the statistics.

Key data for the 103 included accidents is summarized in Table III-14a, 14b. Table III-14a details the statistics for the most relevant circumstances attending the accidents. The first 2 items are basically factual. Percentages listed for the items under "weather conditions at the time and place of the accident" can only be taken as very approximate indications of the likelihood that these conditions played a causal role in the accidents. The high percentage of "?" in the turbulence and icing data, in particular, attest to the uncertainty of this assessment. Wind conditions at the accident site were most often reported in highly qualitative terms, if at all. Icing could not be identified by ground witnesses.

The thunderstorm data also reflect some of this uncertainty. The "yes" category in this item was broken into two parts to reflect the possible far-reaching influence of thunderstorms in the form of turbulence which can occur in clear air, miles from the actual storm cells.

Some care must be taken in interpreting the data for the Cessna 210, the Navion and Piper PA-30. The data for these aircraft represent a very small number of accidents. Each accident represents 11-14 percentage points. With this in mind, the data in Table III-14a appear to indicate the following trends across all aircraft:

- The incidence of IMC is very high, with some indication of possible visual impairment in over 80 percent of all accidents. Probable VMC was very rare. Furthermore, the "questionable" accidents were mostly cases where conditions in the general area were known to include IMC, though it was not positively identified with the time and place of the accident.
- Precipitation also was a fairly common circumstance, occurring in nearly 60 percent of the 103 accidents, and outnumbering instances where no precipitation was noted by a significant factor for every aircraft.

TABLE III-14. SUMMARY OF IFAF ACCIDENT NTSB FILE DATA
a. CONCURRENT CIRCUMSTANCES

		AIRCRAFT				
		BEECH 35 (50)*	CESSNA 210 (9)*	NAVION (7)*	PIPER PA-24 (30)*	PIPER PA-30 (7)*
AIRCRAFT/PILOT DATA:		PERCENTAGE OF ACCIDENTS				
Did aircraft have operative autopilot?	Yes	28%	22%	14%	73%	71%
	No	30	33	29	7	—
	?	42	44	57	20	29
Was the pilot instrument-rated?	Yes	36	67	29	13†	29
	No	64	33	71	83	71
WEATHER CONDITIONS AT THE TIME AND PLACE OF ACCIDENT:		PERCENTAGE OF ACCIDENTS				
What were the lighting conditions?	Day	80	78	71	77	86
	Dawn	—	—	—	—	—
	Twilight	8	11	14	7	14
	Bright Night	—	—	—	—	—
	Dark Night	12	11	14	17	—
Did IMC exist?	Yes	86	100	100	80	57
	No	6	—	—	3	—
	?	8	—	—	17	43
Was there turbulence?	Yes	32	44	43	17	43
	No	10	22	29	23	29
	?	58	33	29	60	29
Was there thunderstorm..?	In immediate vicinity	28	56	29	3	14
	In the area?	8	11	—	20	43
	No	46	22	71	57	29
	?	18	11	—	20	14
Was there precipitation?	Yes	60	89	71	40	71
	No	18	—	—	23	14
	?	22	11	29	37	14
Did icing occur?	No	40	33	—	33	43
	?	60	67	100	67	57
Was there lightning?	Yes	24	33	43	7	29

* Number of accidents.

† Unknown for one accident. Either of two certificated pilots could have been at the controls at the time of one of the accidents. One was instrument-rated, one was not.

TABLE III-14. (Concluded)
b. STRUCTURAL FAILURE DATA

COMPONENT	AIRCRAFT				
	BEECH 35 (50)*	CESSNA 210 (9)*	NAVION (7)*	PIPER PA-24 (30)*	PIPER PA-30 (7)*
PERCENTAGE OF ACCIDENTS IN WHICH COMPONENT FAILED					
Wing	98%	100%	100%	97%	100%
Aileron	NOT TABULATED†				
Aft Fuselage†	34	56	71	33	14
Horizontal Stabilizer	80	78	86	60	71
Elevator	78	100	57	#	#
Vertical Stabilizer	§	67	57	37	—
Rudder	§	44	14	13	29
PERCENTAGE OF ACCIDENTS IN WHICH COMPONENT WAS LIKELY FIRST SEPARATION					
Wing	48	67	29	70	71
Aileron	4	22	14	23	29
Aft Fuselage†	—	—	—	—	—
Horizontal Stabilizer	32	22	14	43	—
Elevator	56	44	43	#	#
Vertical Stabilizer	§	11	—	10	—
Rudder	§	22	—	—	—
None Identified	12	22	43	10	14

* Number of Accidents

† Since wing failures — usually involving separation of at least one wing — occur in nearly all these accidents, and since aileron failures cannot usually be distinguished as independent of wing failure, the fact that the aileron was noted to have failed is not of interest.

† Forward of the stabilizer attach points

§ The Beech 35 has a "vee" tail. Failures of the stabilizer are listed under "horizontal stabilizer." Failures of the ruddevators are listed under "elevator."

The Piper PA-24 and the Piper PA-30 have an all-moving tail. Failures of this "stabilator" are listed under "horizontal stabilizer."

- Icing could be ruled out as a factor in at most, about 40 percent of an aircraft's accidents.

- About 80 percent of <u>each</u> aircraft's accidents occurred in daylight.

On the other side of the coin, these differences between aircraft appear noteworthy:

- More Beech 35, Cessna 210 and Navion aircraft were indicated <u>not</u> to have an autopilot than were to have one. In marked contrast, an autopilot was installed on at least 70 percent of both Piper aircraft.*

- Cessna 210 accidents involved a considerably higher percentage of instrument rated pilots than those of the other aircraft.

- Accidents of the Cessna 210 and, to a lesser extent, those of the Piper PA-30 show more evidence of thunderstorm involvement than the accidents of the other aircraft.

Table III-14b summarizes the structural failure data for the accidents of the 5 aircraft. The objective of this summary is to help identify the failure mechanism by finding out where the initial failure occurs.

The first item is simply a tabulation of how often each component failed in flight. This description bears some qualification. Structural damage which occurred after the initial failure was not of interest. Thus components which had been struck by other components or were damaged by other than aerodynamic overloads were not counted in this tabulation. High speed impact and sometimes fire usually did extensive damage. Distinguishing between these failure types from the data in the files was not always easy.

---

*Most of the accidents where the presence of an autopilot could not be established occurred after 1972. At the start of 1973, NTSB Form 6120.4 was changed; it no longer provided <u>explicitly</u> for an indication of "Installed Flight Instruments" which included the autopilot.

Unfortunately, as indicated in the table, most accidents involve multiple failures. Thus the tabulation of in-flight failures does not point strongly to any one component. It is not surprising that at least one wing almost invariably fails, since the wings are the main load carrying structure and the accidents usually terminate in gross over-speed conditions. The data also show:

- That the horizontal tail surfaces are more likely to fail than the vertical ones or the aft fuselage.
- That the aft fuselage failed more often on the Cessna 210 or the Navion than on the other three aircraft.

The other breakdown in Table III-14b attempts to identify the initial failure from the wreckage trail, based on the proposition that the part that fails first separates first. Parts found at the upstream end of the trail or not at all after an extensive search were listed as likely first separations. Note that more than one component sometimes met these qualifications in an accident. Thus the column totals may be greater than 100 percent.

The first-separation data point to the wing and, to a lesser extent, the elevator (or stabilizer) as the likely initial failure for all five aircraft:

- The wing was cited in roughly 70 percent of the accidents of the Cessna 210 and the Piper PA-24 and PA-30. This is substantially more often than any of the other components cited in these accidents.
- The elevator was cited slightly more often than the wing for the Beech 35 and the Navion (3 versus 2 instances).

The wing data is also considered more conclusive for another reason. The wing should have a lower surface-area-to-weight ratio than the tail surfaces. Therefore the tail surfaces should travel shorter distances from their point of separation and are more likely to be found at the upstream end of the wreckage trail. They are also more likely to go unrecovered because they are smaller.

As was done on the analysis of the accident briefs, a breakdown of the circumstantial evidence felt to be most directly related to the occurrence of the accidents was done for each aircraft. This breakdown had one more dimension than the previous one. In the earlier breakdown, turbulence and thunderstorm had been combined into one category as an indication of atmospheric disturbance. A separate breakdown for each did not appear warranted in that analysis, because it was not clear from the briefs that both conditions would consistently be cited if there was distinct evidence of both, e.g., if a witness saw the aircraft crash in a thunderstorm and he also reported violent wind gusting. Examination of the accident files allowed such distinction. Since a thunderstorm may include many adverse effects other than turbulence (e.g., poor visual conditions due to rain and dark clouds, or lightning which may strike an aircraft) thunderstorms and turbulence were counted separately.

The resulting four-dimensional breakdowns are given in Tables III-15 through III-19. It is difficult to draw meaningful conclusions from these tables; only the Beech 35 and the Piper PA-24 had enough accidents to justify such fine breakdowns. The data are presented here mainly in the hope that they will be useful to some future researcher.

These tables also provide a compact summary of the combined influence of the major pilot and atmospheric factors likely to contribute to the occurrence of an in-flight structural failure. With regard to the importance of these factors, note that the five tables reveal only one accident that is thought to have occurred in VMC in the absence of turbulence and/or thunderstorms. This accident occurred to a Piper PA-24 and is described in the subsection dealing specifically with that aircraft.

Up to this point, pilot-proficiency has been quantified only in terms of whether or not he was instrument rated. Other factors might significantly influence his ability to handle an aircraft in adverse conditions such as are associated with IFAF accidents, e.g., how experienced he is, how familiar he is with the aircraft, how much time he actually has flown on instruments. Total flying hours was the best indicator of pilot

TABLE III-15. BEECH 35 SUMMARY DATA

VISUAL CONDITIONS

		IMC				VMC				?				ALL			
		TURBULENCE				TURBULENCE				TURBULENCE				TURBULENCE			
		Yes	No	?	Sum	Yes	No	?	Sum	Yes	No	?	Sum	Yes	No	?	Sum
IR Pilot THUNDERSTORM	Immediate Vicinity	8%		4	12					2		2	4	10		6	16
	In the Area			2	2											2	2
	None Indicated	2	2	8	12			2	2					2	2	10	14
	?			2	2					2			2	2		2	4
	Sum	10	2	16	28			2	2	4		2	6	14	2	20	36
Non-IR Pilot THUNDERSTORM	Immediate Vicinity	6		6	12									6		6	12
	In the Area			4	4	2			2					2		4	6
	None Indicated	6	8	16	30	2			2					8	8	16	32
	?	2		10	12							2	2	2		12	14
	Sum	14	8	36	58	4			4			2	2	18	8	38	64
All Pilots THUNDERSTORM	Immediate Vicinity	14		10	24					2		2	4	16		12	28
	In the Area			6	6	2			2					2		6	8
	None Indicated	8	10	24	42	2		2	4					10	10	26	46
	?	2		12	14					2		2	4	4		14	18
	Sum	24	10	52	86	4		2	6	4		4	8	32	10	58	100

TABLE III-16. CESSNA 210 SUMMARY DATA

VISUAL CONDITIONS

		IMC				VMC				?				ALL			
		TURBULENCE				TURBULENCE				TURBULENCE				TURBULENCE			
		Yes	No	?	Sum	Yes	No	?	Sum	Yes	No	?	Sum	Yes	No	?	Sum
IR Pilot THUNDERSTORM	Immediate Vicinity	33%			33									33			33
	In the Area			11	11											11	11
	None Indicated			11	11											11	11
	?		11		11										11		11
	Sum	33	11	22	67									33	11	22	67
Non-IR Pilot THUNDERSTORM	Immediate Vicinity	11		11	22									11		11	33
	In the Area																
	None Indicated		11		11										11		11
	?																
	Sum	11	11	11	33									11	11	11	33
All Pilots THUNDERSTORM	Immediate Vicinity	44		11	56									44		11	56
	In the Area			11	11											11	11
	None Indicated		11	11	22										11	11	22
	?		11		11										11		11
	Sum	44	22	33	100									44	22	33	100

TABLE III-17. NAVION SUMMARY DATA

VISUAL CONDITIONS

		IMC				VMC				?				ALL			
		TURBULENCE				TURBULENCE				TURBULENCE				TURBULENCE			
		Yes	No	?	Sum	Yes	No	?	Sum	Yes	No	?	Sum	Yes	No	?	Sum
IR Pilot THUNDERSTORM	Immediate Vicinity	14			14									14			14
	In the Area																
	None Indicated	14			14									14			14
	?																
	Sum	29			29									29			29
Non-IR Pilot THUNDERSTORM	Immediate Vicinity	14			14									14			14
	In the Area																
	None Indicated		29	29	57										29	29	57
	?																
	Sum	14	29	29	71									14	29	29	71
All Pilots THUNDERSTORM	Immediate Vicinity	29			29									29			29
	In the Area																
	None Indicated	14	29	29	71									14	29	29	71
	?																
	Sum	43	29	29	100									43	29	29	100

TABLE III-18. PIPER PA-24 SUMMARY DATA

VISUAL CONDITIONS

		IMC				VMC				?				ALL			
		TURBULENCE				TURBULENCE				TURBULENCE				TURBULENCE			
		Yes	No	?	Sum	Yes	No	?	Sum	Yes	No	?	Sum	Yes	No	?	Sum
IR Pilot	Immediate Vicinity																
	In the Area	3			3									3			3
	None Indicated			7	7		3		3						3	7	10
	?																
	Sum	3		7	10		3		3					3	3	7	13
Non-IR Pilot	Immediate Vicinity	3			3									3			3
	In the Area			17	17											17	17
	None Indicated	3	17	17	37					3		3	7	7	17	20	43
	?			13	13					3		3	7	3		17	20
	Sum	6	17	47	70					7		7	13	13	17	53	83
All Pilots	Immediate Vicinity	3			3									3			3
	In the Area	3		17	20									3		17	20
	None Indicated	3	17	23	43		3		3	3	3*	3	10	7	23	27	57
	?			13	13					3		3	7	3		17	20
	Sum	10	17	53	80		3		3	7	3	7	17	17	23	60	100

*Either of two certificated pilots could have been at the controls in one of the accidents. One was instrument rated, one was not.

TABLE III-19. PIPER PA-30 SUMMARY DATA

VISUAL CONDITIONS

		IMC				VMC				?				ALL			
		TURBULENCE				TURBULENCE				TURBULENCE				TURBULENCE			
		Yes	No	?	Sum	Yes	No	?	Sum	Yes	No	?	Sum	Yes	No	?	Sum
IR Pilot THUNDERSTORM	Immediate Vicinity																
	In the Area									14%			14	14			14
	None Indicated																
	?			14	14											14	14
	Sum			14	14					14			14	14		14	29
Non-IR Pilot THUNDERSTORM	Immediate Vicinity			14	14											14	14
	In the Area									29			29	29			29
	None Indicated		29		29										29		29
	?																
	Sum		29	14	43					29			29	29	29	14	71
All Pilots THUNDERSTORM	Immediate Vicinity			14	14											14	14
	In the Area									43			43	43			43
	None Indicated		29		29										29		29
	?			14	14											14	14
	Sum		29	29	57					43			43	43	29	29	100

experience consistently given in the accident files. Figure III-4 compares the total flying hours of the involved pilots for the five aircraft. Piper PA-24 pilots who had IFAF accidents appear to be substantially less experienced than the pilots of the other aircraft. Since reliable data on the distribution of experience for all pilots of these aircraft were not found, it is not possible to determine whether this reflects differences in the pilot populations for these aircraft, or a tendency of low-time pilots to have more difficulty with a Piper PA-24 than with the other aircraft.

E. ADDITIONAL DATA ON SPECIFIC AIRCRAFT

1. Beech 35

The most common circumstance indicated in the Beech 35 accidents was IMC. Eighty-six percent of the accidents for which statistics were tabulated showed some definite evidence of IMC. Only three accidents seemed to have occurred in VMC. Substantial turbulence was indicated in two of the three. In one case there was roughly 30 mph winds gusting to about 50 mph; turbulence in the other case was associated with a nearby thunderstorm.

The third accident was more of a mystery. It happened on a Beech Aircraft Corporation test flight whose purpose was to check the operational performance of a replacement turbo supercharger unit. The pilot was quite experienced.* The only atmospheric condition not ruled out was turbulence; ground winds were 15 kt gusting to 25 kt.

The structural failure data previously summarized in Table III-14b did not give any strong indications of the likely first failure in Beech 35 accidents. The examination of the wreckage details did reveal <u>how</u> the structure typically failed:

*1026 hr, 187 in type, instrument rated with 113 hr on instruments, also certificated as an instructor and glider pilot.

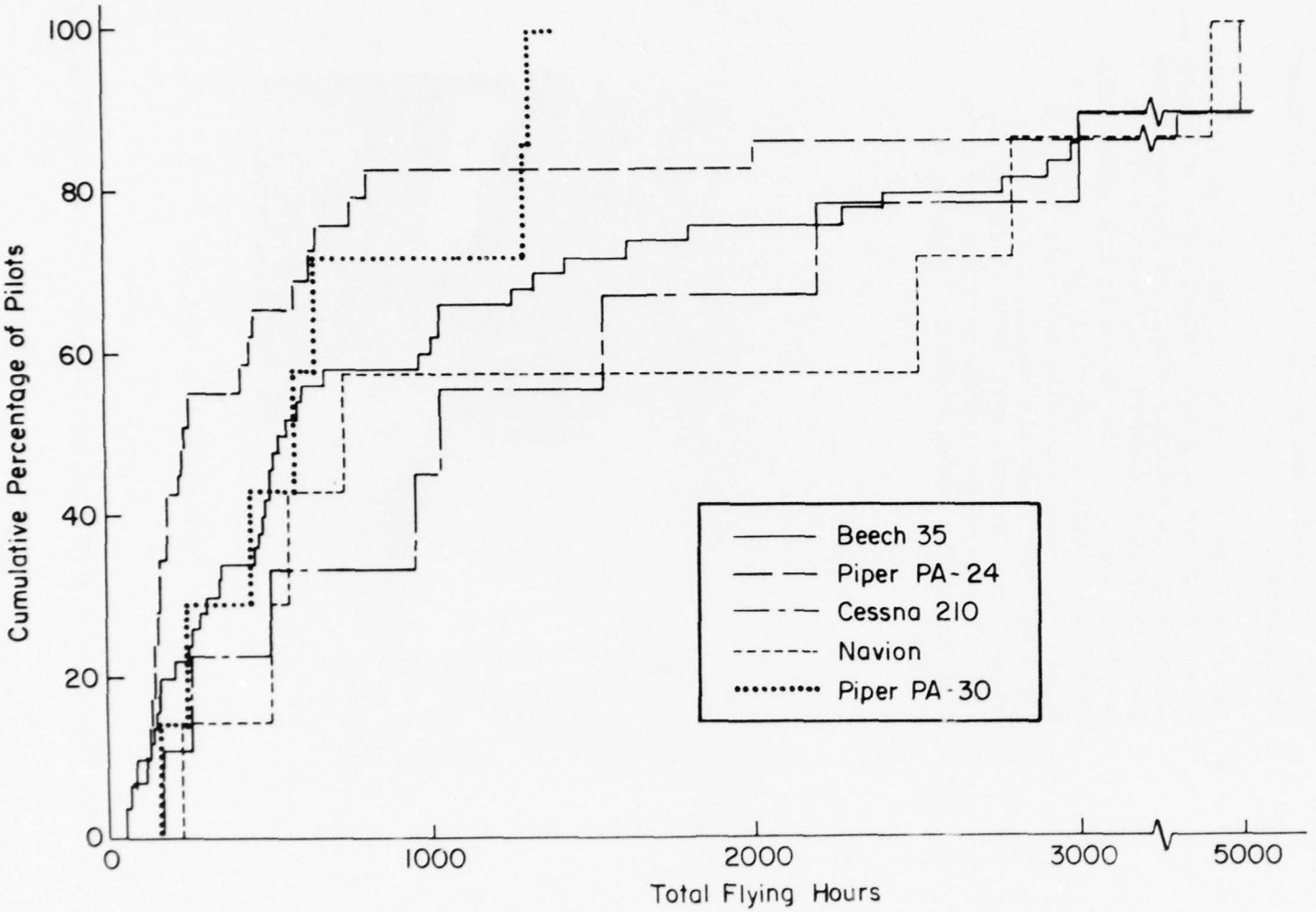

Figure III-4. Comparison of Pilot Total Flying Time

- The wing usually failed just outboard the fuselage attach points or in the center carry through structure. It often remained essentially intact after it separated.

- The stabilizer also tended to fail at the fuselage attach point and to remain intact after it separated. In addition, it commonly exhibited another characteristic failure pattern; in 56 percent of the accidents the butt ribs of one or both stabilizers were bent as much as 90° at the main spar attach point. In conjunction with this bent butt rib, the stabilizer's surface usually had a crease running from the main spar attach point to the trailing edge of the stabilizer somewhere in the vicinity of the center ruddevator hinge point, see Fig. III-5.

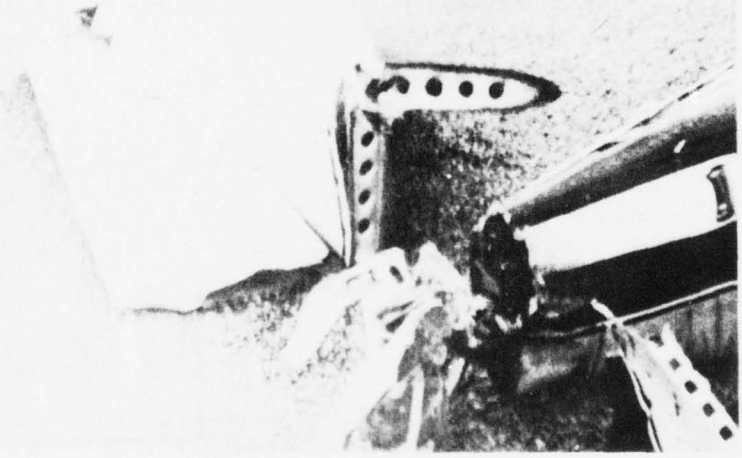

a. Left stabilizer butt rib

Figure III-5. Photographs of Typical Beech 35 Stabilizer Failure

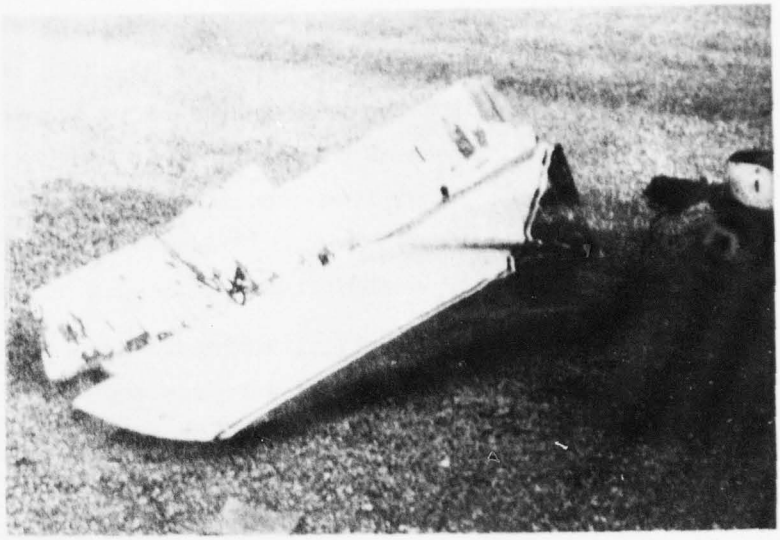

b. Right stabilizer.

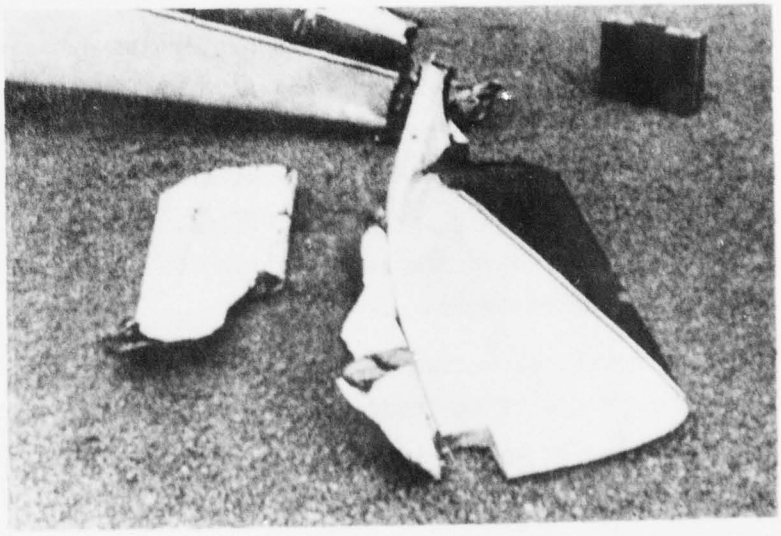

c. Underside left stabilizer.

Figure III-5. (Concluded)

There was some concern about possible pre-existing structural weakness for the straight model 35 — the first of the Beech 35 line. These aircraft had some problems with the wing center carry through structure (see Section IV, Table IV-2, Beech AD 63-25-1). This model was involved in 12 of the IFAF accidents identified from the briefs. Files for nine of these accidents were reviewed. There was no indication that the center carry through structure had a significant influence on these accidents.

Details of some of the individual accidents are worth noting. As previously noted, non-fatal accidents were not represented in the final IFAF statistics. These accidents were nonetheless carefully studied and compared to see if the first hand accounts given by the pilots might suggest a causal mechanism which might also apply to the fatal accidents.

There were 3 non-fatal Beech 35 accidents for which files were received. All three involved turbulence. Two were somewhat similar. One involved a wake turbulence upset of an instrument-rated and experienced pilot (1165 hr, 680 in type; commercial license). The upset resulted in loss of control. The left wing suffered substantial damage at some point between the turbulence encounter and subsequent recovery. The second happened to an inexperienced (270 hr, 65 in type) non-instrument rated pilot, who encountered atmospheric turbulence while he was making a turn in, at worst, intermittent IMC. In the latter case, the pilot mentioned going into a spiral, which suggests that the visual conditions may have played a part in the upset. Both wings were damaged in the recovery.

The third non-fatal accident involved a direct turbulence overload and separation of one of the ruddevators, according to the pilot. The aircraft subsequently became inverted and apparently the accident was non-fatal only because of a combination of fortuitous circumstances: the aircraft was close to the ground; the pilot's attempts at recovery slowed the aircraft somewhat; and the impact was broken by trees and cushioned by snow.

Some fatal accidents were also not counted in the Beech 35 statistics, for the reasons previously given in Table III-13. Most of these were excluded for reasons unrelated per se to the specific aircraft involved, e.g., pilot incapacitation, icing, absence of proper instrumentation. There is a general interest in these accidents as indicators of mitigating factors which may have gone undetected in the IFAF accidents of any of the aircraft. Other excluded accidents are more interesting because they may be more related to the Beech 35.

One of these accidents, listed under "Other" in Table III-13, involved an aircraft in a non-airworthy condition:

> "The trailing edge of the right ruddevator had been repaired after having been damaged while moving the aircraft into a hangar. This repair had been made by stop drilling the cracks, riveting re-enforcement plates along the trailing edge, and applying tape to the surface of the ruddevator."

This accident was of interest because it seems likely to have involved an imbalance of the ruddevator. Such an imbalance may result in flutter. The only evidence found in the file that might indicate flutter had occurred was the following (underlining ours):

> "The aft section of the fuselage with the left stabilizer and ruddervator still attached was located along the centerline of the wreckage distribution path and approximately one mile north of the main wreckage. Inspection of the separated area of the fuselage showed evidence of <u>severe torsional loads prior to failure</u>. The <u>right stabilizer and ruddevator had separated</u> from the aft fuselage. The separated edges of the main spar attach fitting showed <u>evidence of severe upward bending prior to failure</u>. All separated areas of the spars were bright and clean with no visual evidence of fatigue."

Three other excluded accidents involved instrument problems. The first was known to involve a sub-standard vacuum distribution system and loss of attitude and directional gyros. In the other two cases, the problem was not explicitly stated. Background information in both cases points to the vacuum system. If this were the problem, these cases could also have involved malfunctioning gyros. The circumstantial

evidence given by the Air Traffic Control records seems to support this possibility. Erratic flying was observed prior to these accidents. These excluded accidents raise the question of possible undetected problems with the instruments in the other Beech 35 accidents.

Details in two of the included accidents relate to the possibility of instrument malfunction. In both cases, rotational score marks were found on the directional gyro rotor and in one case on the attitude gyro rotor. No reference was made to the possible source of these marks or how they might have occurred. In one case, however, the pilot was observed on radar flying erratically in a manner which suggests spiral divergence (s-turns) a number of minutes before the crash. In the other case, the pilot was radar-observed in a turn for which no instruction had been issued. However, he may have been avoiding the "weather" in front of him. Perhaps a more important factor in this case was the pilot fatigue which was cited in the NTSB brief.

Three explanations for the score marks appear plausible:

- The rotors were scored on impact.
- The gyros tumbled in an extreme attitude and the rotors were scored as a result.
- The score marks were evidence of a gyro malfunction.

Unfortunately the available data provide no clues to the answer. Three other included accidents are of interest because

- Their reports included witnessed events close to the initiation of the accident sequence.
- These events seemed to be related to instrument and/or piloting problems other than those which might be associated with turbulence or thunderstorm.

Brief summaries of these three accidents are given below.

- Pilot was looking for VFR landing at original destination but area was fogged in so he wanted to return to the nearest airport. He appeared to be preoccupied with some problem just prior to this. He was instructed to turn left to 130° heading and acknowledged. When observed

on 190°, he was asked if he was heading 130°. He said not yet and was told to turn left to 120°. Immediately he was observed on radar to make a tight right turn. He crashed on a 360° heading.

- A minute or two before crash, pilot was in a holding pattern. He was requested to contact ground approach control on 134.1 M Hz (presumably a change in frequency required). Pilot's acknowledgement: "Ah, Rog, standby a second, oh, I've had my gyros tumble and I'm about to lose this thing."

- Witness observed aircraft fly overhead in direction of intended route then make half to full circle and dive. He reported not seeing lightning nor noting that the aircraft flew through the overcast, but it was night with overcast sky over an unpopulated area.

The first two pilots were instrument rated with 453 and 589 total flying hours. The last pilot was not instrument rated and had only 52 total flying hours.

These three accidents are exceptional in that they included witnessed events close to the initiation of the accident sequence. One other accident which is similar in that respect is also of interest because it is markedly different in another respect: it almost certainly was caused by a turbulence upset. The important details were:

> An inexperienced pilot (161 hr, 25 in type, no instrument rating or actual instrument hours) reported in hazy conditions and requested a DF steer. Twenty minutes later he reported that he was in a cloud and that it was "a little turbulent" and that he was going to slow down and descend. He was advised to make a 180° turn and get out of it. He failed to acknowledge and shortly thereafter reported in trouble...real turbulence...up and down drafts...and difficulty holding heading. Again a 180° turn was suggested. The last thing heard from the aircraft was a voice saying, "Hold her down! Hold her down!" The turbulence was associated with a thunderstorm which produced rain and lightning in the vicinity of the crash.

These accounts suggest that most Beech 35 IFAF accidents are the result of loss of control, rather than direct gust overloads. This

theory is supported by the statistical data — the high incidence of IMC and non-instrument rated pilots. The accidents involving instrument rated pilots show a higher incidence of thunderstorms and/or turbulence. The instrument rating may not prevent loss of control but only require more severe environmental conditions to trigger it.

2. Cessna 210

As with the Beech 35, the incidence of IMC in the Cessna 210 accidents is very substantial — some definite indication of it was present in all the accidents tabulated. The 89 percent incidence of precipitation, noticeably higher than for any of the other aircraft, also stands out in Table III-14a. Perhaps the more interesting statistics, however, were the proportion of instrument rated pilots, which was so much higher than for all the other aircraft, coupled with a higher thunderstorm involvement, which was shared only by the Piper PA-30. The possible connection between these two observations was previously noted — instrument rated pilots can be expected to encounter thunderstorms more frequently than non-instrument rated pilots.

Both the high thunderstorm incidence and low proportion of non-instrument rated pilots suggest that loss of control due only to IMC is not a major causal mechanism. To examine this proposition, pilot experience and weather conditions for the 9 included accidents are summarized in Table III-20.

The accidents are listed in order of decreasing pilot total hours. They exhibit a fairly consistent trend toward increasing severity of weather conditions with increasing pilot experience. The third and the last accidents are the only notable exceptions to this trend. The last accident involved an inexperienced (student) pilot. He very well might have had an IFAF accident in considerably less severe conditions.

The pilot in the third listed accident had a considerable number of total hours. Some of his time was in a Cessna 182 of which he was part owner; some was in a Bonanza owned by his employer. He claimed to the

TABLE III-20. SUMMARY OF PILOT AND WEATHER FACTORS IN CESSNA 210 ACCIDENTS

PILOT EXPERIENCE					WEATHER CONDITIONS*				
TOTAL HOURS	HOURS IN TYPE	INSTRUMENT RATED	INSTRUMENT HOURS SIMULATED/ACTUAL	OTHER RATINGS	THUNDER-STORMS	TURBULENCE	PRECIPI-TATION	LIGHTNING	ICING
5000+	~50	Yes	?/?	Commercial	@ Yes	Yes	Light	No	?
3000	~1061	Yes	83+/?		@ Yes	@ Severe	Heavy	Yes	No
2178+	~5-6	Yes	?/?	Commercial	No	?	?	No	?
1539	19	Yes	57/54	Commercial	@ Yes	Yes	Heavy	Yes	?
1028	26	No	15/0	Commercial	@ Yes	?	Heavy	No	?
950	150	Yes	65/?		Yes	?	@ Yes	No	No
500+	?	Yes	45/5.5	Commercial	?	No	Heavy	No	No
~250	150	No	3/0		No	No	Yes	No	?
~160	160	No	?/?	Student	@ Yes	Yes	Heavy	Yes	?

*All accidents were associated with IMC. "@" indicates that a condition existed in the immediate vicinity of the aircraft between the time immediately preceding the initiation of the accident sequence and ground impact.

operator who checked him out the morning of the fatal flight to have 20-25 hr in a Cessna 210. It was strictly a VFR checkout with no dual instrument instruction. The pilot crashed 10 minutes after takeoff on a dark overcast night. This accident suggests control loss due only to IMC. However, turbulence and icing cannot be ruled out. Precipitation was also not ruled out, and its presence in all the other Cessna 210 accidents suggests the possibility that it may have an appreciable influence on these accidents.

The seventh and eighth accidents in Table III-20 also seemingly suggest possible loss of control due only to IMC. It is possible that the heavy rain indicated by the seventh accident could have been associated with a thunderstorm. "Occasional heavy rain and possible thunderstorm activity" were forecasted throughout the period from approximately nine hours prior to three hours after the accident. However, there was no indication that the thunderstorm ever materialized.

The eighth accident may not even have been initiated in IMC. This accident involved a turbo-charged airplane, topping the clouds by flying at altitudes from 18,500 ft to 25,000 ft. The pilot turned back to his destination to avoid apparent IFR landing conditions. At 25,000 ft he last reported weather conditions improving in front of him. These other details were noted in the accident report:

- A week or two prior to accident pilot had had his son use oxygen on a flight in which he was forced to go to 18,000 ft to top the clouds. He did not use oxygen and did not indicate how long his son did.
- Last known oxygen system servicing was six months earlier.
- Oxygen system capacity was 2 hr 50 min for pilot plus 3 passengers (as there were).
- Pilot was apparently not well versed in need for and use of oxygen system.
- Oxygen tank was found with one line connected, valve open and zero pressure.

The report contained excerpts on hypoxia from a booklet which discussed the subject. In these, it was indicated that at 25,000 ft a person had two minutes "useful consciousness" before the absence of sufficient oxygen incapacitated him. It appears highly plausible that this accident could have been the result of hypoxia.

The excluded non-fatal accidents offer further evidence that factors other than IMC are more important in the Cessna 210 IFAF accidents. Two occurred in VMC and, in the other, visual conditions were not reported. None of the pilots were instrument rated.

One of the VMC accidents is especially relevant to the interesting circumstances noted earlier about the fatal accidents:

- The aircraft was turned upside down by clear air turbulence about five miles from a line of thunderstorms. Pilot lost 300-400 ft during the recovery. Upper surfaces of both wings were extensively damaged. Control system damage was indicated to be substantial but was not described.

- Pilot was very experienced (6,000 hr, 4,500 in type) but not instrument rated.

Another of these three accidents also involved a turbulence caused upset:

- Pilot encountered snow showers of increasing intensity and rerouted because it appeared a "safe VFR flight" to destination would not be possible on that route. Shortly thereafter he encountered severe turbulence (updraft followed by downdraft) which caused him to red-out and the aircraft to pitch violently. He found himself in 60° bank and immediately pulled power reducing speed from 160-165 mph to 100-110 mph. He noticed both wings were bent and he had little or no aileron control. He used the rudder to level the wings.

- The wings and ailerons suffered extensive damage; the flight control system was operating properly.

- Pilot was experienced (2,783 hr, 257 in type; 216 hr simulated but no actual instrument time) but not instrument rated; he did have a commercial rating.

In neither of these accidents was it clear whether the damage was due to direct turbulence overload or occurred during the recovery.

The third accident involved a considerably less experienced pilot (400 hr, 200 in type; no instrument time or rating) who encountered "severe turbulence and down drafts" which apparently wrinkled the skin on the tops of both wings at the strut attachment point.

The circumstantial evidence from the reviewed files strongly suggests that, for Cessna 210 IFAF accidents,

- Turbulence is a decisive factor.
- Precipitation and/or IMC are somewhat less important, though one and/or the other may be a necessary condition for a fatal accident.
- IFAF accidents resulting from loss of control due to IMC only is not an important causal mechanism.

As the structural failure data in Table III-14b indicate, the Cessna 210 tends to disintegrate in its IFAF accidents. A more detailed examination of the failure data emphasize this point. In the case of paired (right/left) components, i.e., wings, stabilizers and elevators, the Table III-14b data indicate in how many accidents either fails. In the Cessna 210 accidents:

- Both wings failed in six of the nine accidents.
- Both stabilizers failed in seven of the nine accidents.
- Both elevators failed in six of the nine accidents.

Moreover, more often than not the failed components came apart in two or more fragments which usually exhibited substantial deformation. There did not appear to be any distinct failure pattern over all the accidents, perhaps because of the extensive deformation and fragmentation of the components. As noted in their descriptions, even the non-fatal accidents generally involved fairly extensive damage.

3. Navion

The concurrent circumstances in the seven Navion accidents include a high proportion (five) of non-instrument rated pilots with IMC indicated in every accident. Precipitation also was indicated in five of the accidents and possibly was involved in the other two. Four of the five accidents of the non-instrument rated pilots indicated no thunderstorm involvement, and none of these showed any definite indication of turbulence. In three of these four, the crash occurred well off course, and ground witnesses reported a similar peculiarity in the aircraft's behavior prior to each.

In one instance a witness saw "the flashing light and the plane circling to the left", in "pretty heavy" snow on a dark night. In another case a witness reported hearing the aircraft for about five minutes prior to the accident and "he sounded like he was turning." In the third accident several witnesses heard the aircraft wandering around about 10 minutes prior to the accident; one said it sounded in trouble "like it was changing from one attitude (sic) to another very rapidly," then it stabilized for about 10 minutes then it again sounded "like it were doing aerobatics," then like in a dive.

The above descriptions fit the behavior of an aircraft when the pilot is having trouble maintaining control. The fact that the aircraft all crashed considerably off course tends to support this possibility. In any case, excluding the remote possibility of instrument malfunction in all three cases, these accidents suggest some form of control loss due only to IMC.

The two accidents involving instrument rated pilots, who were also the most experienced (4,905+ hr and 2800+ hr) of the seven accident pilots, were markedly different. Both involved turbulence, in one case associated with a thunderstorm in which the aircraft crashed.

The main features of the structural failure patterns in the Navion accidents were

- A large number of downward wing failures (all of the six left wing failures on which a direction of failure was indicated, and four of the six such right wing failures).

- A high degree of disintegration, usually involving separation of the skin from the various components. This made it difficult to distinguish structural components much less to identify failure modes.

4. Piper PA-24

The structural failure characteristics of the Piper PA-24 accidents are discussed first because of their relevance to the discussion of the accident circumstances. The failed component data in Table III-14b show some differences between the PA-24 and the aircraft of other maufacturers. With the exception of the wing, the failure rates of its components are no greater, and usually about 20 or more percent less, than those of the other aircraft.* When its components separated, the sections usually remained relatively intact. The following failure patterns were observed:

- With only one or two exceptions, the wing separated outboard at roughly the flap-aileron junction, and the failure usually occurred in the upward direction (21 of 23 wing failures in which "up" or "down" was indicated). The wing tip separated in at least half of the cases. In a few instances, the portion inboard of the initial separation separated near the main landing gear well.

- Again, with an exception or two, the stabilator (all-moving tail) always failed near midspan, outboard of the junction of the main and stub spars. Unlike the wing, this failure was usually downward (12 of 14 stabilator failures in which direction mentioned).

- With one exception, the vertical fin separated essentially intact with the upper two-thirds, or more, of the rudder attached to it.

---

*Differences between Beech 35 and Piper PA-24 failed component rates may simply reflect the dual role played by the Beech's "vee" tail.

Usually, both wings and/or both stabilators failed. An interesting variation in this trend marked the last four included fatal accidents, all of which occurred in 1972. A single wing was the only component to fail in each.

The statistics on the circumstances attending the PA-24 accidents are very interesting. The high (80 percent) percentage of IMC, with only one definite VMC accident, is of course not unusual. The PA-24 also shows by far the lowest (13 percent) percentage of instrument rated pilots. In the incidence of adverse weather conditions other than IMC, the statistics differ substantially from those of the other four aircraft: the PA-24 shows markedly lower incidences of turbulence, thunderstorm and precipitation than any of the four.

It shares another major difference from the other manufacturers' aircraft with the PA-30. Both indicate that better than 70 percent of these aircraft had autopilots, compared with 28 percent or less for the other three aircraft. In fact only two of the accidents definitely occurred to Piper aircraft without autopilots.

As noted, the high accident involvement of non-instrument rated and less experienced pilots in combination with a high incidence of IMC is not unusual. Two cases in which the pilot was in radio communication with an Air Traffic Control Center just prior to the accident are relevant to the connection of the two factors:

- Non-instrument rated pilot (162 hr, 26 in type) was on top of high overcast at 11,500 ft fifteen minutes prior to crash and wanted to know where he might find breaks in the overcast. Pilot reported 20 miles west of Marysville. When asked his position, he said he was "orbiting." ATCS asked him to tune to Marysville VOR at 110.8 M Hz and to center the omni needle by turning the Omni Bearing Selector. He did and said needle centered at 070 and that he had a "to" indication. He was told to head 070° magnetic and report on this heading. Ten minutes prior to crash, he reported on 070° and in the clear. He crashed at 60 nm W-SW of Marysville.

- Non-instrumented rated pilot (~180 hr, ~15 in type) reported on top at 7,000 ft with cloud tops at 6,500 ft. He was close to destination but had a problem navigating. When asked his heading, he reported 170° after a long pause, but DF strobe showed 290°. Air Traffic Control Specialist (ATCS) advised him to head 100° and report when on course. When he did, ATCS "fixed" him at 280°. (ATCS also mentioned suspecting pilot's uncertainty about his position based on earlier radio contacts he had overheard.) Before ATCS could advise course correction, pilot said he was starting down through the overcast. He crashed within minutes.

Both these accounts describe inexperienced non-instrument rated pilots having difficulty navigatin in VMC. The added workload of maintaining the aircraft flight path in IMC would certainly have increased their difficulty several fold. In none of the other PA-24 accidents were there similar indications of navigating difficulties for more experienced and instrument rated pilots.

Five accidents involved instrument rated pilots. One accident happened near a thunderstorm. Turbulence and IMC were also indicated. The other four accidents did not involve thunderstorms and turbulence was not definitely indicated in any of them. However, they all involved other interesting details.

In one of these, either of two certificated pilots could have been at the controls. One had 5,000 hr, including 200 in type, but was not instrument rated; the other had 321 hr, only 5 in type, and an instrument rating. The aircraft had operative dual controls.

The owner (non-instrument rated) of the aircraft was demonstrating the autopilot (Mitchell Altimatic II) to the other pilot. This autopilot had malfunctioned on previous occasions:

- Three and a half months prior to the accident the autopilot altitude hold unit was repaired. The altitude sensing unit was found defective and replaced. The autopilot was flight checked at this time.

AD-A064 156 SYSTEMS TECHNOLOGY INC HAWTHORNE CALIF F/G 1/2
A STUDY OF THE EFFECTS OF AIRCRAFT DYNAMIC CHARACTERISTICS ON S--ETC(U)
NOV 78 R L STAPLEFORD, R J DIMARCO DOT-FA77WA-3936
UNCLASSIFIED STI-TR-1099-1 FAA-RD-78-155 NL

2 OF 3
AD
A064 156


1.0
1.1
1.25
1.4
1.6
1.8
2.0
2.2
2.5
2.8
3.2
3.6
4.0
4.5
5.0
5.6
6.3
MICROCOPY RESOLUTION TEST CHART

- A month and a half before the accident, a pilot reported that he had the autopilot engaged (either on climb out or in level flight) and he turned his attention to a chart and seconds later found himself at a 45° left bank, heading 90° off the course set into the autopilot. Once the original course was re-established the autopilot was re-engaged and "performed satisfactorily" on the rest of the trip.

- The next day a pilot noted that: the autopilot would not respond to a manual change in the altitude indication and pilot could not overpower the autopilot to descend with altitude hold engaged. If altitude hold was engaged with other than the indicated altitude dialed in, the airplane would "change attitude abruptly," in the direction appropriate to the commanded altitude change.

This accident file also included the following details:

- Visual conditions were not definitely established, but were more likely VMC.

- It appeared that neither pitch nor roll servos were not engaged at impact.

- Newspaper account mentions a student pilot who saw an aircraft in the area "climbing when it made an abrupt level maneuver and appeared to stall."

- All three landing gears were down but flaps were up.

- Structural damage included typical outboard separations of the left wing and both stabilators. The vertical fin also separated with the upper half of the rudder attached after being struck by the separated wing section.

Another of the accidents of instrument rated pilots bears sc similarity to this one. It is the only PA-24 fatal accident whi definitely occurred in VMC. An experienced pilot (7,395 hr, in unknown, instrument rated with 200 hr of simulated and 110 hr o instrument time, with commercial and instructor ratings) was in craft but was identified as definitely not a crew member. The a friend (448 hr, 20 in type, instrument rated with 40 hr of si and 26 hr of actual instrument time). The purpose of the fligh

the passenger to familiarize himself with the operation of a "portable dilutor demand oxygen system."

The possibly relevant details are

- The aircraft had the same model autopilot as in the "two-pilot" accident.
- The autopilot was off at impact.
- The oxygen valves were in the off position.
- The aircraft was in the landing configuration.
- Witnesses observed the aircraft flying very low and fast, descending as if to land when it dove into the ground. One heard an aircraft occupant yelling something.
- Apparently only the stabilators were damaged. Both were folded when just outboard the main spar/stub spar junction. The left outboard stabilator separated.

The structural damage indicated above was unusual in that it was the only included accident in which neither wing failed. As indicated in Table III-14b, the wing was the most likely first separation in 70 percent of PA-24 accidents compared with only 43 percent for the stabilator.

The report on this accident noted that operating instructions for the autopilot warned "Never disengage the pitch servo without having a firm grip on the control wheel."

It cannot be definitely established in either of these cases that the autopilot was definitely a factor. However, the usual explanation for an IFAF accident does not appear appropriate. In both cases there were two experienced pilots on board and the weather conditions were not bad. One was definitely VMC and the other was probably VMC.

The other two accidents involving instrument rated pilots differed from the two just described in two key points:

- There was a mitigating circumstance — namely, IMC.

- One aircraft had a different autopilot (Piper autocontrol); whether the other had an autopilot is unknown.

Both aircraft were flown by very experienced pilots.

The pilot of the aircraft with the autopilot (7,000 hr, 125 in type, 150 hr on actual instruments, commercial and instructor ratings) was being observed on radar when he was instructed to turn right for identification and then left 360°. The pilot reported these maneuvers as they were being observed. Radar observer saw him initiate a left turn and, after turning through about 70°, to gradually disappear, suggesting a let down from 7,000 ft to a lower altitude.*

The pilot in the other accident had 3,300+ hr and there was a considerably less experienced pilot onboard. Nothing is known of the events immediately preceding the accident.

The most interesting feature of these two accidents is in the nature of the structural damage. The unusual characteristics in the former instance included these:

- The stabilators separated at the torque tube attachment fittings. The right one also separated outboard failing down and separating up.

- The vertical fin separated with the upper two-thirds portion of the rudder attached. The rudder control horn and lower portion of the rudder were found attached to the fuselage by the cables. Both ears of the lower rudder hinge had failed at the control horn. (The rudder horn assembly was the only component sent to Washington, D.C. for examination.)

In the latter case, these atypical characteristics were noted:

- The right stabilator separated intact at the torque tube attachment fitting. The upper skin inboard of the leading edge bays dished downward between the ribs. The upper skin was creased spanwise.

---

*Details of the flight suggest the possibility that the aircraft could have run out of fuel.

- The left stabilator inboard leading edge was displaced upward.

- The vertical fin with the rudder attached was twisted and bent, and folded aft.

The underlined portions in the above damage descriptions describe the gross characteristics of the damage in one of the excluded accidents. That accident was witnessed by a Cessna 172 pilot and his passengers — who were friends of the accident pilot. They had taken off earlier and were now being passed by the faster PA-24 on their way to have dinner together. They described what they saw as follows:

- The Cessna pilot said the aircraft "...passed us about 500 ft to our right and 50 ft above us. I would guess his speed at approximately 160 mph. While I was watching him, I noticed a vibration or side to side movement set up in his vertical fin. Almost immediately it gave several side to side movements, broke loose and flew clear of the aircraft. I am positive about the early vibration or apparent vibration as I thought at first it was a trick of the light. After flying straight for a few seconds, the plane fell away into a slight right hand spiral descent, made approximately five or six complete turns and crashed. The first part to become detached was the fin and rudder assembly." He also reported flying "at 2,500 ft" at the time "in excellent flying weather with very little turbulence and perfect visibility."

- The passenger said the other aircraft "...passed us at about 150 mph, our Cessna at that time was indicating 110 mph. When the Comanche was in front and to the right of our plane 500 to 700 ft away...I saw the rudder and vertical fin floping right then left and then it came off going to the right, the tail then came up and the plane went into a 10° right bank a few seconds later the left part of the stabilator came off. The plane then went into a right spiral, made about five turns and crashed. The weather at that time was clear, very little wind and the turbulence was slight."

  He later reported that he had told the PA-24 pilot his altitude was 2,500 ft indicated. "On reply, to the best of my knowledge" after carefully thinking about it (the PA-24 pilot) reported that he was at 4,500 ft indicated. Diving from 4,500 ft to 2,500 ft the airspeed, as I originally estimated to be 180 mph (in above witness report he said 150), could have been considerably higher than 180 mph. How much I do not know.

The descriptions of the accident strongly suggest that the vertical fin and rudder failed due to flutter. It is not known exactly how fast the aircraft was actually going when the fin came off. If the pilot had been descending rapidly from 2,000 ft above the other aircraft, the estimates of his airspeed might be considerably low. There is also the possibility that there was a pre-existing structural deficiency.

One such possibility is mentioned in the accident file. A year earlier, just before the pilot bought the aircraft, the following repairs were accomplished during its annual inspection:

- A new right stabilator tip rib and fiberglass tip were installed using original attachment methods. A dent the size of a 3/32 in. diameter rivet countersink dimple, 12-18 in. inboard from the tip on the right stabilator leading edge, was filled and the spot was painted when the new tip was. Stabilator balance was considered but it was decided due to the very small amount of weight added there would be little change in the balance of the control surface. The damage was termed "hangar damage."

- The nose gear inner and outer strut housing was replaced because of damage to the nose gear turning limit stops due to overturning the nose gear. "The rudder control system is connected directly to the nose gear by cables and control rods...any time the nose gear turning stops are exceeded a load is imposed on the rudder control stops. This load could cause damage to the rudder control system." The system was checked and no damage was found. "This overturning damage could only be done by moving the aircraft with tug or tractor"

Several pages of detailed description of the structural damage are contained in the report. Some key details are

- The vertical fin separated just above front and rear spar attachment bolts with upper two-thirds of the rudder attached by upper two hinges. The lower third of the rudder remained attached to the aircraft by the right rudder cable.

- The left stabilator separated ~8 in. outboard from the torque tube attachment points, with portions of right stabilator skin and rear spar attached. The stabilator was bent up ~30° near midspan and again ~30° outboard of this point.

- The right stabilator had the above mentioned portion torn out the inboard end of the trim tab, which was still attached by the two outboard hinges, was bent 45° up 40 in. in from outboard end, then ~50° down ~11 in. further inboard.

- The fuselage skin was severely buckled and ripped just forward of the empennage.

Damaged tail section parts were sent to NTSB Washington office for detailed analysis. Hardness measurements were in normal range for fin forward and rear spar cross sections, and rudder horn and rudder lower attach bracket.

The accident file also includes the following (accident happened on October 10, 1971):

- Piper Service Bulletin No. 362, issued August 14, 1977, which states "Piper Aircraft Corporation is investigating the effects of improper maintenance and/or unauthorized repair procedures with respect to possible deterioration of the margin of safety when applied to flutter characteristics of the horizontal and vertical tail surfaces."

  "In order to provide additional margin and in the interest of safety, Piper has reduced the never exceed speed V_{NE} to 203 mph C.A.S. for the PA-24-250 and PA-24-260 aircraft."

- Piper Service Bulletin No. 362A, issued October 6, 1972, which states "Further investigation in the areas described in Piper Service Bulletin No. 362, dated August 14, 1972 has shown that installing rudder balanced weights on PA-24-180, PA-24-250 and PA-24-260 models will prevent possible adverse airplane vibration effects, thus providing a greater margin of safety at higher speeds. For this reason we strongly urge the installation of these balance weights."

  "Until more information becomes available, the present V_{NE} speeds — 202 mph C.A.S. for the PA-24-180 and 203 mph C.A.S. for the PA-24-250 and PA-24-260 — will be retained."

- Airworthiness Directive 72-22-5 which re-placards V_{NE} on PA-24 models and V_{NO} and V_{NE} on the PA-24-250 and -260, as summarized in Section IV, Table IV-2.

One other accident with damage characteristics very similar to this one was excluded for a variety of other extenuating circumstances.

One of the three non-fatal Piper PA-24 accidents of which the files were reviewed also shows damage similar to the apparent flutter case. In that accident,

- The pilot (210 hr, 24 in type, non-instrument rated and no instrument time) claimed he encountered precipitation area, and was executing 180° turn when he encountered severe turbulence that "turned him past the vertical position." He lost 1800-2000 ft before regaining control.

- Prior to upset, pilot was in contact with approach control. He said he was approaching precipitation and wanted to know how heavy it was. Radar did not show any. Seven minutes later radar contact was lost. Pilot acknowledged (this message apparently).

- Investigator noted that there was no mention of turbulence on the tape of the radio communications.

The vertical fin was broken at its attachment points, with only the fairing attached; the rudder skin was bent half way up; there were no cracks. The other damage included:

- Wing tops wrinkled by compression loads.

- Stabilator leading edge skins bent down from midspan out.

Another of the non-fatal accidents involved a turbulence upset. In that case the pilot (389 hr, 117 in type, instrument rated with 53 total hours of simulated time plus actual instrument time) entered cloud and was making 180° turn when he encountered severe turbulence. He lost control and entered a spiral at "excessive speed." After recovery he descended to VFR conditions. The wing panels "sustained major damage."

The third non-fatal accident would have been excluded on the grounds of pilot incapacitation; the pilot had struck his head prior to takeoff.

It appears that a majority of the Piper PA-24 accidents occur when a non-instrument rated pilot encounters IMC. However, a few of the accidents do not fit this mold, nor can they be accounted for by weather

conditions. Two of these accidents in particular suggest other causal mechanisms, namely, autopilot malfunction and flutter of the vertical fin. Others that do not fit the mold bear some similarities to one or both of these accidents.

These apparently atypical accidents must be considered in light of the fact that:

- At least 73 percent of the involved PA-24 aircraft had autopilots, a far higher proportion than for the other three single-engine aircraft.
- Thirty-seven percent of the accidents involved failure of the vertical fin, most of these in a manner similar to the "flutter" accident.

While autopilot malfunctions and vertical fin flutter might be responsible for some PA-24 accidents, any estimate of the relative percentages at this time would be sheer speculation.

5. Piper PA-30

The summary of concurrent circumstances in Table III-14a shows the following key features for the PA-30:

- Like the PA-24, most of the involved aircraft had an autopilot.
- No incidence of definite VMC and a high proportion of non-instrument rated pilots.
- A high incidence of thunderstorm involvement, like the Cessna 210.

The high involvement of non-instrument rated pilots was somewhat of a surprise. One might expect a relatively high percentage of instrument ratings among pilots of a twin-engine aircraft.

The matrix of atmospheric conditions in Table III-19 show that there were two accidents in which there was neither turbulence nor thunderstorms. Both of these occurred to non-instrument rated pilots flying in IMC. There were also two accidents involving instrument rated pilots. One occurred near a thunderstorm and turbulence was indicated; the other occurred in heavy rain which might have been associated with a thunderstorm.

The non-fatal accidents give similar evidence of the relationship between instrument rating, IMC and IFAF accidents. All involved turbulence and

- Three involved instrument rated pilots in IMC. In only one instance was there loss of control, in extreme turbulence.
- One involved a non-instrument rated pilot in VMC. There was no loss of control.

Overall, the PA-30 IFAF accidents seem typical of the majority of those of the other aircraft.

The structural failure data summarized in Table III-14b show the wing to be most likely component to have failed first:

- At least one of the PA-30 wings failed in all cases.
- The wing was cited as a component likely to have separated first in 5 (71 percent) of the accidents; the aileron, the only other component so identified was only cited in 2 (29 percent) of the accidents.

The wing failure characteristics are markedly similar to those of the PA-24:

- Both wings failed in six of the seven accidents.
- The wing(s) failed upwards in six of the seven accidents.
- The wing always failed outboard of the engine. Typically a roughly six-foot section, from the wing tip to the trailing-edge flap-aileron junction, separated.

This is very interesting because the PA-30 is basically a single-engine PA-24 with "...the obvious changes necessary to adapt a single-engine design to twin configuration, and the attendant structural strengthening dictated by a higher gross weight and speed range" (Ref. 38). The planform of the two aircraft, in fact, appears to be identical except for the obvious differences related to engine placement (Ref. 39).

The stabilator failed in 71 percent of the PA-30 accidents. It did not seem to exhibit any regular failure mode. However, the non-fatal accidents also give some indications that the stabilator could be a critical component in PA-30 in-flight breakups:

- Three of the four accidents involved gust-induced loads with no loss of control. Two resulted in damage to only the stabilator and one resulted in damage to only the wings.

- The fourth accident involved loss of control from severe turbulence with damage to both the stabilator and the wings. The aircraft entered a vertical dive and the airspeed exceeded 250 mph. To recover from the dive, the pilot required the assistance of a passenger to pull back on the yoke.

The difficulty in recovering from the vertical dive may have been due to damage to the stabilator prior to the pullout. Likewise, some of the fatal accidents may have resulted from damage to the stabilator which then led to loss of control and separation of the wings.

Further evidence of a common structural weakness or other significant design detail was sought in the aircraft serial numbers. If all the involved aircraft were members of a distinct PA-30 subgroup, then characteristics peculiar to that subgroup might be significant. The production history of the Twin Commanche is given in Table III-21.

As the table indicates, in 1970 the PA-30 was superseded by the PA-39 which was essentially a PA-30 with counter-rotating (C/R) propellers. The entire line was discontinued in 1972 after a flood at the factory destroyed the dies used in its manufacture.

The serial numbers for all 13 PA-30s for which files were received were checked against the table. These numbers all belong to PA-30s produced prior to 1968; in fact, with one exception the aircraft came off the line prior to early 1966. The PA-39 C/R Twin Commanche, whose statistics were kept separately from those of the PA-30, did not have any in-flight-airframe failure (IFAF) accidents included in the count in the 1966-1975 period. A detailed structural history of the PA-30 could not be obtained, so the serial numbers in Table III-21 cannot be correlated with structural changes.

TABLE III-21

PIPER PA-30 PRODUCTION HISTORY

MODEL	YEAR	SERIAL NUMBERS	DESIGN HISTORY
A	1963 1964 1965	1-142 143-627 628-901	Basically a twin engine version of the Piper PA-24 Commanche, with structural modifications required to accommodate the engine reconfiguration and the higher performance characteristics and gross weight. A version with 290 HP engine was flight tested in early 1965 (never put into production).
B	1966 1967 1968	902-1422 1423-1679 1680-1744	Optional 5th and 6th seat, extra cabin windows, three basic equipment/instrumentation options; turbo-charged version, with standard wing tip tanks, first offered in 1966.
C	1969	1745-2000	Cabin refinements.
(PA-39)	1970 1971 1972	1-83 and 1-83 turbo- charged 84-132 133-152	Major design modification (along with change of model designation): reversal of direction of the starboard engine shaft provided counter-rotating propellers.

Also of considerable interest is the fact that C/R aircraft did not have any IFAF accidents. The unbalanced airflow over the airframe due to the PA-30's asymmetric power plant configuration compromised its handling qualities. The adverse characteristics included these:

- Aircraft would roll inverted when stalled at climb power setting, because one wing stalled before the other.
- An abrupt increase in trim rudder was required with decreasing speed.

According to Ref. 9, the use of C/R propellers "improved flight characteristics in all flight conditions due to balanced airflow over each side of the aircraft." These kinds of handling qualities differences could reasonably be expected to be important in the IFAF accidents of interest, in light of their apparent association with IMC and the attendant likelihood that the accident sequence involved loss of control in a high workload situation. Unfortunately, the limited exposure of the PA-39 in the decade surveyed does not provide a strong enough foundation for making the assertion that the C/R configuration is less susceptible to this kind of accident.

The PA-30 IFAF accidents do not indicate any major differences from the typical pattern — non-instrument rated pilots having trouble in IMC only, with more experienced and/or instrument rated pilots likely to have problems in IMC if there are other adverse conditions.

SECTION IV

DISCUSSION OF POTENTIALLY CONTRIBUTING FACTORS IN GENERAL AVIATION IFAF ACCIDENTS

A. GENERAL DISCUSSION

The previous section has presented statistical data on IFAF accidents for general aviation aircraft. Those data show significant variations in accident rates among the various aircraft. The objective of this section is to explore the many factors which potentially could account for the differences or might be significant in future aircraft. While the analyses presented here provide some useful insights, none of the factors considered can positively be correlated with the IFAF accident statistics. This is due to a number of problems which are discussed below.

The factors of interest regarding IFAF accidents can be divided into four broad categories:

- Aircraft utilization
- Pilot proficiency
- Structural characteristics
- Handling qualities.

Each of these categories is discussed in the following paragraphs.

Aircraft utilization is an important factor because it reflects the relative exposure to adverse weather conditions. Aircraft used primarily for training and short-distance VFR flights could be expected to have lower IFAF accident rates because of lower exposure to adverse weather conditions. This is reflected in the IFAF accident data by the low accident rate for the single-engine, fixed-gear group of aircraft. These aircraft have a much higher utilization for instruction (40 percent) than either of the other 2 groups (3 and 4 percent).

Pilot proficiency would also seem to be an important factor in that many IFAF accidents are apparently the result of loss of control in IMC and/or turbulence. This can lead to excessive airspeed or structural loads during the recovery. Overspeed problems are analyzed in Subsection D.

Low pilot proficiency suggests higher IFAF accident rates for trainer-type aircraft but this is apparently more than offset by the lower exposure to adverse weather conditions. Furthermore, many training flights involve an instructor in the airplane so even if the pilot has low proficiency, the instructor's presumably high proficiency should help prevent accidents.

The effects of pilot proficiency may be the explanation for the lower accident rate for twin-engine aircraft than for single-engine, retractable-gear aircraft. Twin engine aircraft show substantially more utilization in "Other" category (see table). A large portion of this usage presumably reflects passenger-carrying service, such as air taxi. In addition, the business usage of these aircraft is more likely to involve full time pilots in the service of the larger companies who can afford these aircraft. Thus the bulk of twin-engine hours are likely to be flown by professional company pilots who should be much better qualified than the average general aviation pilot.

Structural differences between aircraft are potentially an important factor. Some aircraft are simply structurally stronger than other aircraft because of either a deliberate design philosophy or the accuracy limitations in the structural design process. Some aircraft may have a structural design deficiency which was undetected in the certification process but which could become the objective of an Airworthiness Directive (AD), e.g., a flutter problem in a corner of the aircraft flight envelope. Finally, some designs impose stricter maintenance standards to maintain the structural integrity, such as strict mass balancing requirements to prevent control surface flutter.

Clearly the above features can significantly affect the susceptibility of a particular aircraft to an IFAF. The problem we face is a paucity of hard data to support solid recommendations. Under what conditions would Aircraft X have a structural failure and not Aircraft Y? Even if that data were available, there is still the problem of determining the conditions at the time of an IFAF. General aviation aircraft do not carry flight recorders and most IFAF accidents leave no survivors to report the circumstances.

There are, however, a few sources of relevant data on structural characteristics and these are examined later in this section. Subsection B reviews possibly relevant ADs and possible correlations with the accident data from Section III. Subsection C examines the correlation between the accident data and speed margins (differences between typical cruise speed and design limit speeds).

The final category of potentially contributing factors is the aircraft handling qualities. Handling qualities can influence the IFAF accident rates in several ways. They can

- Affect the probability of the pilot losing control.
- Affect the aircraft response after loss of control.
- Affect the possibility of the pilot inadvertently overstressing the airplane.
- Affect the overall loads and load distribution due to pilot control actions and turbulence.

A number of important handling quality characteristics are listed in Table IV-1. Typical values of these parameters for general aviation aircraft and additional discussion can be found in Ref. 5.

Since these handling quality characteristics could have important effects on IFAFs, it is desirable to correlate these parameters with the accident data. There are, however, several problems which make this impractical. The most serious problem is the general unavailability of reliable data on the handling quality parameters. These parameters are seldom measured and even if measured the data are usually manufacturer proprietary.

Since a direct correlation with the accident data was impractical, the only recourse was an analytical investigation of some of the potentially more important parameters. These analyses are described in the last 3 subsections of this section. Subsection D presents an analysis of overspeed tendencies. Key aircraft parameters which affect the speed increases due to pitching over or in a spiral dive are identified. Subsection E is a discussion of spiral stability. It reviews data on the problem of spiral divergence with an inexperienced pilot in IMC.

TABLE IV-1. IMPORTANT HANDLING QUALITY CHARACTERISTICS

HANDLING QUALITY CHARACTERISTICS	POTENTIAL EFFECTS RELEVANT TO IFAFs
Overspeed tendency	Large speed increases due to pitching over or in a spiral dive make it easier to exceed the design speed limits.
Spiral stability	Poor spiral stability makes it easier to enter a spiral dive.
Control system dynamics	Control system lags (pilot force to surface deflection) can cause PIOs (pilot induced oscillations) and make it easy to inadvertently overstress the airplane.
Stick force per g	Low maneuvering control force gradients make it easy to inadvertently overstress the airplane.
Stick force per knot	Poor speed stability makes it easier to develop large speed errors.
Short period damping and frequency	Poor short period characteristics can lead to PIO, overcontrol, or loss of control.
Dutch roll damping and frequency	Poor dutch roll characteristics can cause large tail loads; pilot may not be able to damp the oscillations.
Power effects on longitudinal and lateral/directional trim	Large trim changes can cause loss of control, imprecise control due to trim forces, or excessive pilot workload (which can contribute to loss of control).
Gear and flap effects on trim	Imprecise control or excessive workload.
Trim system features	Poor features (e.g., low sensitivity, bad location, lack of lateral or directional trim) can cause excessive workload.
Control system friction	Excessive friction can cause PIO and make it difficult to trim the airplane (which increases workload).
Control power	Inadequate control power to regulate against turbulence disturbances can cause loss of control.
Stall characteristics	Poor stall characteristics can cause loss of control or spin (e.g., inadvertent stall in severe turbulence).

It also discusses the factors which contribute to an aircraft's apparent spiral stability. Subsection F deals with the potential effects of longitudinal control system dynamics. It uses a hypothetical example to investigate conditions under which the control system dynamics could present a serious problem.

B. CORRELATION OF AIRWORTHINESS DIRECTIVES WITH IFAF ACCIDENT DATA

Airworthiness Directives (AD) for all aircraft with more than five IFAF accidents were reviewed to see if there were any correlations between the ADs and the accidents. Eleven aircraft were in this category: Beech 35; Bellanca; Cessna 210; Navion; Piper PA-23, PA-24, PA-28, PA-28R, PA-30, PA-32; Rockwell Aero Commander. The results are summarized in Table IV-2.

Several of the ADs seem to be correlated with IFAF accidents and these accidents may have been the motivation for the ADs. AD 72-22-5 (issued in late 1972) is especially interesting as it seems to be correlated with a reduction in the number of IFAF accidents for the PA-24, see Fig. IV-1.

These apparent correlations indicate some aircraft may have initially had some structural deficiencies which were corrected by the ADs. To reliably assess the impact of other factors, it would be necessary to

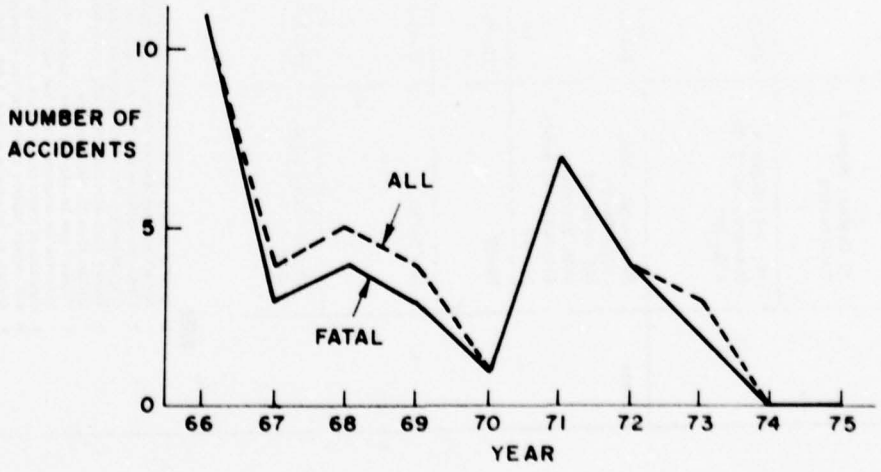

Figure IV-1. IFAF Accident History for PA-24

TABLE IV-2. SUMMARY OF POSSIBLY RELEVANT AIRWORTHINESS DIRECTIVES

MFR.	MODELS CITED[1]	AD NO.[2]	REASONS FOR AD[3]	REQUIREMENTS FOR COMPLIANCE	TIME TO COMPLY[4]	TIE-IN WITH IFAP DATA
Beech	35, including Super V Conversion	57-18-1	Fatigue of stabilizer front and rear spar attachment bulkheads and fuselage skin.	Inspect for cracks, buckles or distortion and repair or replace damaged structure.	100 hrs	NOT PERTINENT AD's ISSUED BEFORE 1966.
	35 Series; Super V Conversions		Possibility of static imbalance of ruddervator.	Check balance on model 35, and on all other aircraft whose ruddervators have been repaired or repainted.	100 hrs	
	35; 35R: Super V Conversions of 35, A35, B35	63-25-1	"Inspections required by AD 62-2-1 have not been adequate to detect all fatigue cracks in the steel center section front trusses prior to failure. To preclude these failures..."	Modify the fuselage and inspect the front and rear steel trusses.	25 hrs[6]	
Piper	PA-24-250, -260, -400; PA-30 (if equipped with Mitchell Altimatic II Autopilot)	65-11-4	"To prevent further jamming of the stabilator control system by the autopilot pitch servo breakaway ball link, ..."	Remount the pitch servo and install fairlead in fuselage per AD instructions.	25 hrs	
	PA-30	70-15-17	Not indicated.	"Attach ... to airspeed indicator in full view of pilot: 'DO NOT EXCEED 230 MPH CAS'"	Before further flight	None apparent.
	PA-23-250	72-21-7	"To improve the longitudinal stability characteristics and to prevent longitudinal stick force reversal during certain flight conditions, ..."	Accomplish alteration per Piper Service Bulletin (installation of stabilator bungee)	30 days	None apparent.
	PA-24(-180), -250, -260	72-22-5	"To prevent possible adverse airplane vibration effects ..."	Attach placard: "Do not exceed 188 mph cas (V_{ne})" [PA-24(-180)] or: "Max. structural cruising: 167 mph cas (V_{no}). Do not exceed 188 mph cas (V_{ne})" [PA-24-250, -260]	10 hrs	• Drop in accident rate from 4/yr (1967-73) to zero (1974-75)
				Alter airspeed instrument red line (and yellow cautionary arc) to reflect the limits above, or, with the stated modifications, the following limits: 1) With alteration of rudder with Piper kit: V_{ne} = 203, V_{no} = 180 [PA-24-250, -260], V_{ne} = 202 [PA-24(-180)] 2) With alteration of rudder and stabilator with Piper kits: V_{ne} = 247 [PA-24-250, -260] (the kits provided for the addition of counterweights)	3 mos	

NOTES

1 Usually models to which AD is applicable are further delimited by serial numbers and/or other qualifications
2 First two numbers are the year and the biweekly interval of issue, respectively; the third number uniquely identifies each AD
3 Quotes come directly from AD; non-quotes are interpretations deriving from AD requirements
4 "Hours" are in-service time; unless "total" is specified this interval is measured from the day the AD is issued
5 Compliance requires repeated action at no longer than this interval
6 And repeat within every 100 hrs thereafter
7 Repeat at intervals within 3 yrs /500 hrs in service, unless replacement with corrosion resistant bolts is made
8 Repeat at no longer than yearly intervals
9 Time to comply varies depending on in-service time
10 And at each annual inspection thereafter

TABLE IV-2 (CONCLUDED)

MFR.	MODELS CITED[1]	AD NO.[2]	REASONS FOR AD[3]	REQUIREMENTS FOR COMPLIANCE	TIME TO COMPLY[4]	TIE-IN WITH IFAP DATA
Piper (cont.)	PA-24(-180), -250, -260, -400: PA-30; PA-39	74-13-1	"To prevent possible hazards in flight associated with loose high shear rivets which attach the stabilator torque tube bearing support fittings ..."	Inspect per AD instructions and repair before further flight (except to place of repair per FAR 21.197) if looseness found.	25 hrs	• (2) Stabilator and (1) empennage failures in the three 1973 accidents [PA-24]
	PA-23-235, -250; PA-24(-180), -250, -260, -400; PA-30; PA-39	74-13-3	"To prevent possible hazards in flight associated with the corrosion of the stabilator attachment bolts, ..."	Remove bolts and inspect; replace if corrosion found	100 hrs[7]	• Drop in yearly accident rate from 2/yr (1972-74) to zero (1975) [PA-23] • (2) Stabilator and (1) empennage failures in the three 1973 accidents [PA-24]
	PA-28-235 PA-32-260 PA-34-200	74-19-1	"To detect improperly formed lightening holes in the outer wing spars ..."	Inspect per AD instructions and replace if cracks found and/or die stamping mark on wrong side.	10 hrs	• High incidence (76%) of wing failure [PA-28]
	PA-23; PA-24(-180); PA-28, -28R; PA-30; PA-32; et al.	77-3-8	"To detect and correct excessive corrosion of the wing lift struts ..."	Per AD instructions, • Perform the corrosion impedance measurement • Perform inspection: -for airplanes with wing lift struts installed 5 or more years -for airplanes with wing lift struts installed less than 5 years	30 days 30 days[8] 5 yrs[8] total	• High incidence of wing failure: 68% [PA-24]; 76% [PA-28]; 90% [PA-28R]; 73% [PA-30]
Rockwell (Aero-Commander)	500, A, B; 520; 560, A, E, F; 680, E, F, F(P), FL, FL(P); 720	65-6-1	"To prevent further failure of the wing lower front spar cap ..."	Per AD instructions: inspect, and repair if cracks found; reinforce if no cracks found	25-300 hrs[9]	• Two wing spar failures in 1966 [560E, 680F] • High incidence (83%) of wing failure [500, 500A, 560E, 680F, F(P), FL(P)]
	560E; 680, E; 720	67-28-1	"To detect cracks in the lower front spar cap between wing station 67 and 86 on each wing ..."	Per AD instructions, inspect, and repair if cracks found	25 hrs	• Wing spar failure in 1966 [560E] • High incidence (83%) of wing failures [500; 500A; 560E; 680F, F(P), FL(P)]
	500, A, B, S, U; 520; 560, A, E, F; 680, E, F, F(P); 720	75-12-9	"To prevent inadvertent pilot induced structural failures ..."	Install bob-weights per AD instructions	300 hrs	None apparent – AD issued very late in data time span
Bellanca	14-19, 14-19-2, -3, -3A; 17-30, A; 17-31 A, TC, ATC	76-8-4	"To detect deterioration in wood wing ..."	Per AD instructions, inspect, and repair if wood deterioration detected	10 hrs but ≤ 30 days	• High incidence (78%) of wing failures

separate out the effects of possible structural deficiencies. This was attempted in the review of the NTSB accident files for the in-depth analysis of IFAF accidents (Section III-D). However, the data in the files was never sufficient to preclude all such possible deficiencies.

C. CORRELATION OF SPEED MARGINS WITH IFAF ACCIDENT DATA

One factor which could be significant in IFAF accidents is the speed margins with which the aircraft is normally operated. This subsection describes an unsuccessful attempt to find a correlation between speed margins and IFAF accidents. Data were obtained for five retractable-gear, single-engine aircraft that span the accident rate range for this group. The aircraft were: Mooney M20; Beech 33, 36; Cessna 210; Piper PA-24; and Beech 35. The key parameters were:

- Never exceed speed, V_{NE}
- Maximum structural cruising speed, V_{NO}
- Design maneuvering speed, V_A
- Maximum recommended cruising speed (generally at 75 percent power), V_{CR}

Since these speeds can vary substantially for different models of the same aircraft, data were obtained for some different models. However, the accident rates are generally not available for individual models so in the subsequent plots, Fig. IV-2, the speed margins for specific models are plotted against the IFAF accident rate for all models of that aircraft. An exception is the Beech 35 data for which accident rates for four specific models were computed: 35*, G35, H35, and V35A. The H35 was the first model after a major structural revision, see Subsection III-C for details.

The margins between cruise speed and V_{NE}, V_{NO}, and V_A seem to have little correlation with the IFAF accident rates. With respect to the V_{NE} margins, the PA-24 data are difficult to interpret since AD 72-22-5 changed V_{NE}. Using the original values (prior to the AD) does not seem

*Cruise speed based on 62.5 percent power, all others are for 75 percent power.

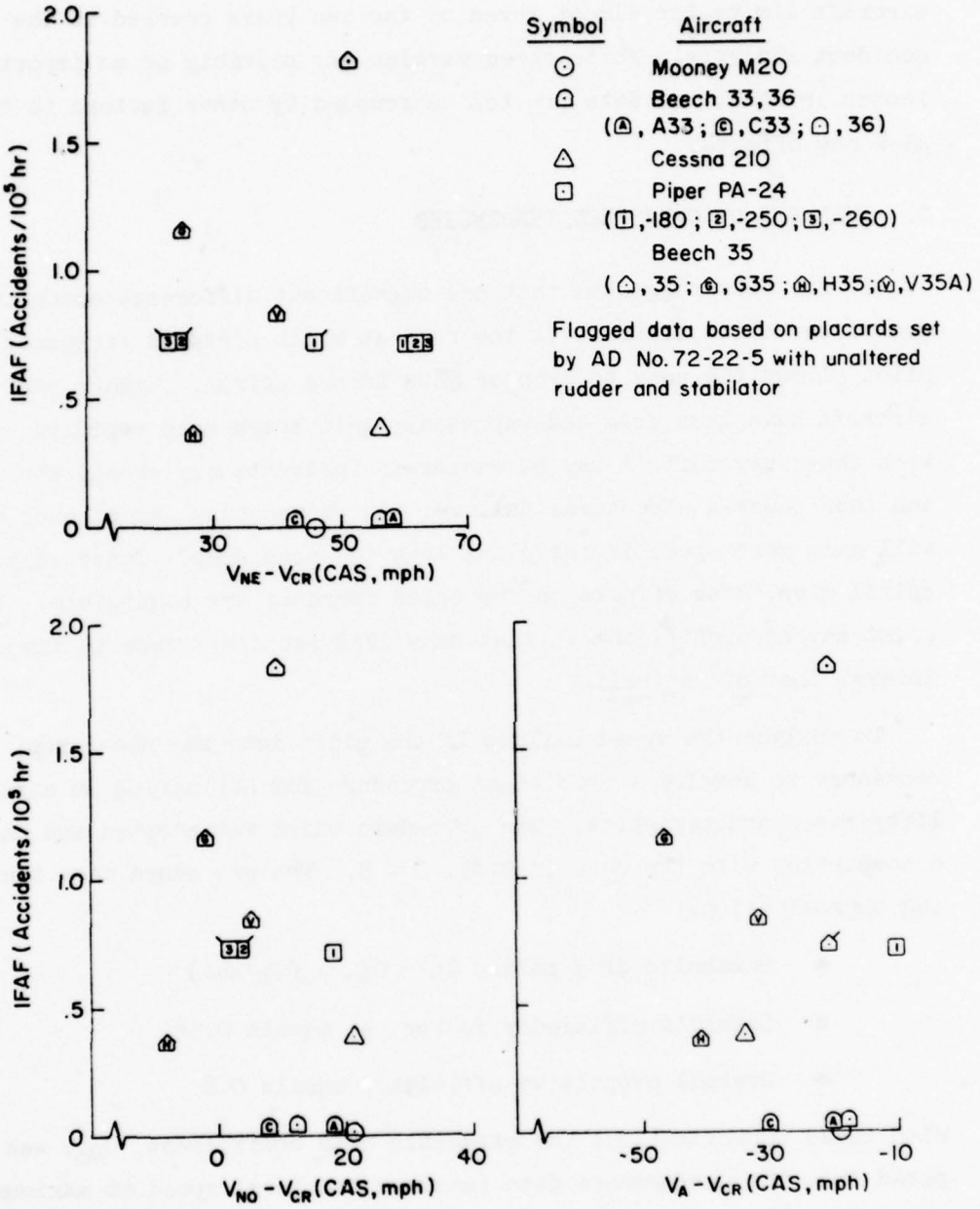

Figure IV-2. Accident Rates vs. Airspeed Margins

right since structurally V_{NE} should have been smaller. Using the AD values is also questionable since the pilots were unaware of the real aircraft limits for almost seven of the ten years covered in the IFAF accident analysis. While speed margins may possibly be an important factor in IFAF, the data are too confounded by other factors to clearly show any effects.

D. ANALYSIS OF OVERSPEED TENDENCIES

It has been suggested that one significant difference among the various general aviation aircraft is the rate at which airspeed increases if the pilot allows the nose to drop or gets into a spiral. Higher performance aircraft have less drag and supposedly gain speed more rapidly. Therefore, with these aircraft it may be easier to inadvertently exceed the red-line and thus cause a structural failure. As shown below the cleaner airplane will gain more speed if the pilot lets the nose drop. Conversely, in a spiral dive, drag effects on the speed increase are negligible. The latter point may be significant in that many IFAF accidents seem to involve a lateral loss of control.

To analyze the speed buildup if the pilot lets the nose drop, it was necessary to develop a consistent procedure for estimating an aircraft's lift/drag characteristics. The procedure which was adopted was based on a comparison with the data in Refs. 6 - 8. The procedure uses the following approximations:

- Parabolic drag polar, $C_D = C_{D_o} + (C_L^2/\pi eA)$
- Oswald's efficiency factor, e, equals 0.5*
- Overall propulsive efficiency equals 0.8

With these approximations the parasitic drag coefficient, C_{D_o}, was computed from the performance data (maximum sea level speed at maximum T.O. weight) given in Ref. 9 .

---

*This value is much less than that normally used (roughly 0.8) because we are dealing with trimmed lift/drag characteristics. Exact value is not critical because of the relatively low induced drag in the speed range of interest here.

These lift/drag characteristics were then used in a trajectory program to compute the maximum speed increase due to a pitch upset. The aircraft was initially trimmed in level flight at the maximum cruising speed (75 percent power) listed in Ref. 9 . Then the aircraft was pitched 15 deg nose down and this attitude was held for 8 sec. At the end of 8 sec, a constant 3 g recovery was initiated until the airspeed reached a peak.

The calculations were made for 5 aircraft and the results are summarized in Table IV-3 (the table includes two related parameters, $\Delta V/\Delta\theta$ and τ, which will be described shortly). Considering the wide range of performance of these aircraft, the differences in speed increase are suprisingly small. Examination of the time histories showed the following:

- The flight path angle, γ, very quickly (within 1-2 sec) reached a value of approximately −15 deg (same as pitch disturbance).
- Longitudinal acceleration was that due to gravity component, $g\gamma$, and decreased only slightly over 8 sec.
- Once recovery was initiated, additional speed increase was small, less than 1 kt.

Additional runs were made in which the recovery was delayed. These clearly showed that all aircraft initially accelerate at the same rate

TABLE IV-3

COMPARISON OF SPEED BUILDUP CHARACTERISTICS

	BEECH V35B	CESSNA 210	PA 24-260	CESSNA 177	CESSNA 150
Maximum speed increase (from trajectory program), KEAS	31.4	30.2	30.8	28.0	26.3
$\Delta V/\Delta\theta$, kt/deg	− 8.61	− 7.54	− 7.35	− 5.04	− 3.69
Time constant, τ, sec	25.9	22.7	22.1	15.1	11.1

and exponentially approach a constant airspeed condition. Thus, the difference between aircraft is not the initial acceleration but the steady-state condition (if the pitch angle is held).

An approximate relationship between the pitch input and the steady-state airspeed is given by (see Appendix A for derivation):

$$-\Delta\theta \doteq \frac{\bar{q}_o S}{W} C_{D_o}(\nu^2 - \nu^{-1}) + \frac{W}{\bar{q}_o S}\left[\frac{1}{C_{I_\alpha}}(1 - \nu^{-2}) - \frac{1}{\pi e A}(\nu^{-1} - \nu^{-2})\right]$$

where

$\bar{q}_o$ = Initial dynamic pressure

W/S = Wing loading

ν = V_s/V_o, steady-state to initial airspeed ratio

This equation is based on:

- Small angle approximation.
- Neglect of density gradient effects.
- Assumption that thrust is inversely proportional to airspeed.*

The above approximation agrees very well with the results from the trajectory program. The pitch/airspeed relationship is quite linear even for large airspeed changes. Consequently, a simpler linear approximation is:

$$\frac{\Delta V}{\Delta\theta} \doteq -V_o\left[3\frac{\bar{q}_o S}{W} C_{D_o} + \frac{W}{\bar{q}_o S}\left(\frac{2}{C_{I_\alpha}} - \frac{1}{\pi e A}\right)\right]^{-1}$$

Values of this derivative, $\Delta V/\Delta\theta$, for the 5 aircraft are also listed in Table IV-3. Here we see a much wider variation among the various aircraft. The higher performance aircraft have a much higher airspeed-to-pitch sensitivity. The value for a Beech Bonanza is 2.3 times that for a Cessna 150.

---

*This derives from the assumption of constant thrust horsepower, a common approximation for a constant speed propeller and piston engine, e.g., Ref. 40.

The sensitivity, $\Delta V/\Delta\theta$, can also be related to the exponential time constant for the speed increase, τ. For an exponential variation the initial acceleration and steady-state change are related by:

$$\dot{V}_o \tau = \Delta V$$

Since the initial acceleration is approximately $-g\Delta\theta$, the time constant is given by:

$$\tau \doteq -\frac{1}{g}\frac{\Delta V}{\Delta\theta}$$

$$\doteq -3\frac{\Delta V}{\Delta\theta} \qquad \text{for } \Delta V/\Delta\theta \text{ in kt/deg}$$

Values of the time constant are also listed in Table IV-3.

Even the shortest time constant (11.1 sec for Cessna 150) is greater than the 8 sec duration of the pitch down used in the trajectory program. This explains the small differences between aircraft obtained from the trajectory program. Over the duration of the maneuver, the acceleration does not change greatly and all aircraft initially accelerate at the same rate.

The results of this analysis can be summarized quite briefly. Higher performance (low drag) aircraft are more sensitive to pitch errors. While all aircraft initially accelerate at the same rate, the higher performance aircraft will maintain this acceleration longer. A sustained pitch error will cause a much larger speed increase for a high performance aircraft.

A similar analysis was done for a spiral dive. The spiral stability of a particular aircraft was not considered, instead, the analysis considered only the speed and flight path changes as functions of bank angle. The subject of spiral stability is treated separately in the next subsection.

The following assumptions were made:

- The spiral divergence is slow enough so that acceleration terms can be neglected, i.e.,

$$L \cos \varphi = W \cos \gamma$$

$$T - D = W \sin \gamma$$

where

L = lift

T = thrust

D = drag

φ = bank angle

γ = flight path angle

- There are no longitudinal control inputs, i.e., lift and drag coefficients are constant
- Thrust is inversely proportional to equivalent airspeed
- Maneuver starts from $\gamma = \varphi = 0$

From these assumptions one can find the equivalent airspeed and flight path angle as functions of the bank angle achieved during the spiral dive. The two simultaneous equations are:

$$\frac{V}{V_o} = \sqrt{\frac{\cos \gamma}{\cos \varphi}}$$

$$\sin \gamma = \left(\frac{T}{W}\right)_o \left[\frac{V_o}{V} - \left(\frac{V}{V_o}\right)^2\right]$$

$\left(\frac{T}{W}\right)_o$ = initial thrust/weight ratio, inverse of the initial lift/drag ratio

Plots of these functions are given in Fig. IV-3 for rather extreme variations in thrust/weight ratio. Note that the speed increase is nearly independent of the aircraft drag characteristics. Conversely, the flight path angle is nearly proportional to the thrust/weight ratio. The steeper flight paths for a higher drag (higher T/W) airplane were initially a surprising result but in hindsight are easily explained. Since for a given bank angle the airspeed change is nearly independent of the drag characteristics, the higher drag aircraft will have a larger drag increase. The larger drag increase can only be balanced by a steeper descent angle.

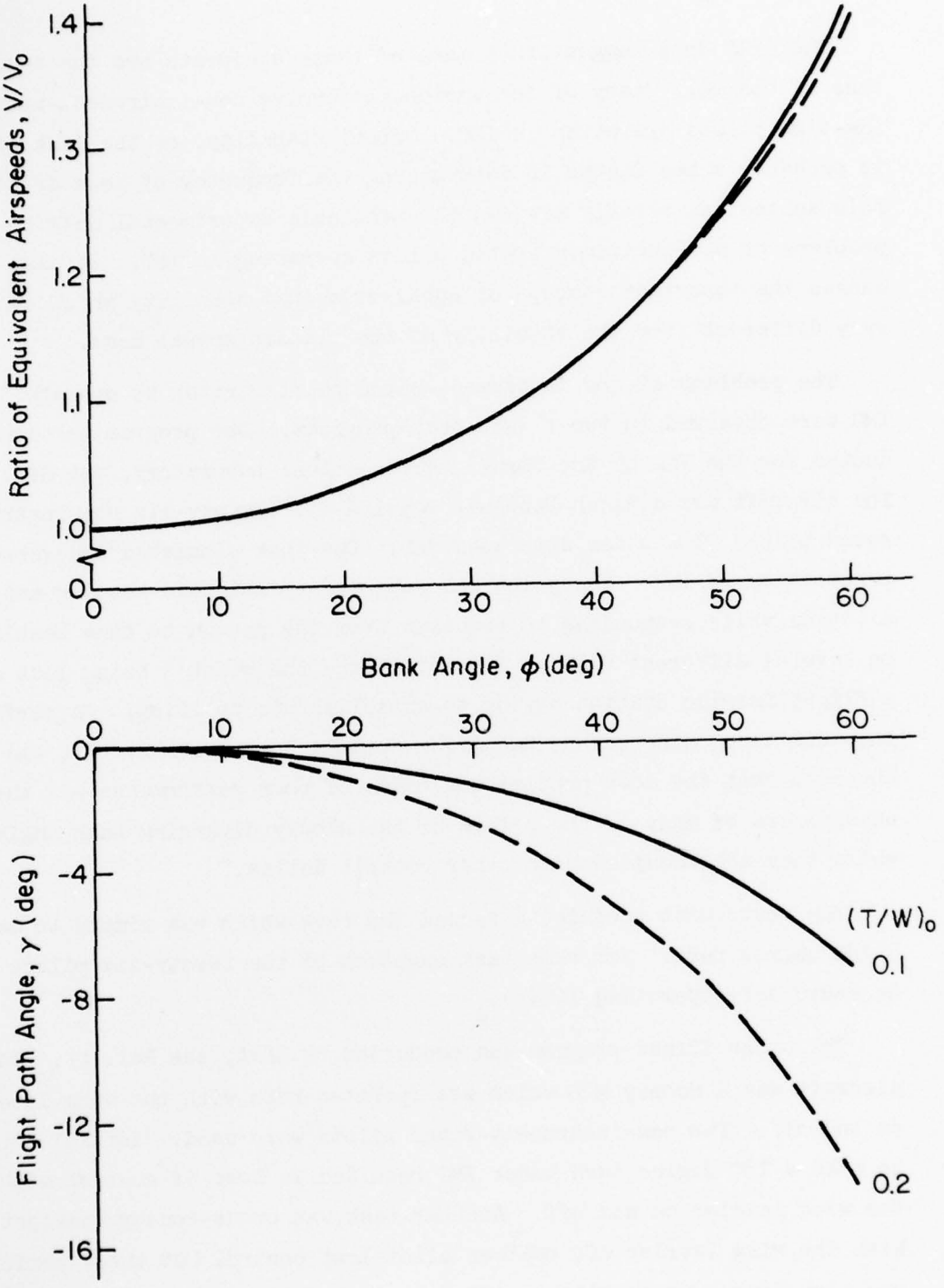

Figure IV-3. Speed and Flight Path Variations During a Spiral Dive

E. SPIRAL STABILITY

The IFAF data suggest that many of these accidents are the result of loss of control. Many of the accidents involve non-instrument-rated or low-time pilots operating in IMC. Spiral stability, or the lack of it, is probably a key factor in determining the frequency of loss of control. This subsection briefly reviews the available experimental data on the problems of non-instrument-rated pilots operating in IMC. It also discusses the important concept of apparent spiral stability which can be very different from the stability of the classic spiral mode.

The problems of non-instrument-rated pilots trying to operate in IMC were observed in two flight test programs. One program was conducted for the FAA by the Cornell Aeronautical Laboratory, see Ref. 10. The aircraft was a Beech Debonair Model A-33. Twenty-six non-instrument-rated pilots flew under simulated IMC. One task simulated inadvertent penetration of IMC. The pilot was supposed to maintain heading and altitude while responding to requests from the ground to take bearings on several different VOR's. This simulated the pilot's being lost and a Flight Service Station trying to establish his position. On performing this task, nine of the twenty-six pilots lost control. "It was observed that the most predominant cause of poor performance was the unawareness of many of the pilots of the slowly diverging bank angle while they are occupied with other cockpit duties."

The tests also included a second IMC task which was simply to make a 180 degree turn. For this task eighteen of the twenty-six pilots exceeded safe operating limits.

The other flight program was conducted by NASA, see Ref. 11. The aircraft was a Mooney M20 which was operated both with the wing leveler on and off. Two non-instrument-rated pilots were used. Initial attempts to make a 180 degree turn under IMC resulted in loss of control with both the wing leveler on and off. Another task was cross-country navigation. With the wing leveler off neither pilot lost control but their performance was very poor. Gross flight path deviations, both vertically and horizontally, resulted and pilot estimation of his position was very poor. Performance with the wing leveler on was greatly improved.

These two experiments clearly demonstrated the serious problem which results when a non-instrument-rated pilot gets into IMC. A key problem is the "apparent" spiral instability of many general aviation aircraft. An excellent discussion of this subject and example data are presented in Ref. 12. That report explains how an aircraft may have an apparent spiral instability although the spiral mode is actually stable. There are two reasons. The first is the lack of lateral and directional trim devices. The second is control system friction which prevents the control surfaces from centering. The problem is compounded by lateral and directional trim changes with airspeed. These cause asymmetric roll behavior, e.g., aircraft may diverge in a left turn but not a right one.

The importance of spiral stability is supported by the IFAF data for the Mooney M20. That aircraft had no IFAF accidents in over 6 million hours of flying. The unique feature of that aircraft is its wing leveler, which has been standard equipment since 1965. The wing leveler provides an extremely high level of apparent spiral stability.

From the above we conclude that:

- Apparent spiral stability may be an important factor in IFAF accidents.
- The distinction between apparent spiral stability and the spiral mode time constant is critically important for general aviation aircraft.

F. EFFECTS OF LONGITUDINAL CONTROL SYSTEM DYNAMICS

A generic study of longitudinal control for general aviation aircraft was performed. The objective was to determine the conditions which might cause problems in load factor control. Such problems could cause the pilot to inadvertently overstress the airplane, particularly during recovery from an upset. No problems which might exist on current aircraft were found but a potential problem for future designs was identified.

The analysis began with the formulation of a set of baseline dynamics which should be typical of single-engine, high-performance aircraft. (details of the model are given in Appendix B). The math model included

the short period (angle of attack and pitch rate) and elevator surface degrees of freedom. For the baseline case, the stick-fixed short-period mode had a frequency of 4.51 rad/sec and a damping ratio of 0.79. Stick free, the short-period mode was overdamped with roots at 1.64 and 3.71 sec^{-1}. The elevator surface mode had a frequency of 63 rad/sec with a damping ratio of 0.62. The force gradient was 14.4 lb/g.

A general comparison of stick-free and stick-fixed dynamics shows the following:

- The short-period mode may be significantly different in the two cases.
- Stick-free there are two additional poles (usually a quadratic pair) which represent the elevator surface mode.
- Numerator zeros are the same for control deflection (stick-fixed case) and control force (stick-free case) inputs.

Because of the last point, the analysis concentrated on potentially poor pole locations. Furthermore, the current FAR Part 23 regulations on short-period damping and stick force per g effectively restrict the short-period poles for both stick free and stick fixed. Therefore, the remainder of the analysis was devoted to investigating conditions which could cause undesirable locations of the elevator surface poles.

In the baseline case the surface poles are at much too high a frequency (63 rad/sec) to be of concern. Reasonable modifications to the hinge moment characteristics which would reduce the frequency to a troublesome level were sought. It was found that the stick force per g requirement effectively prevents this. From the basic equations of motion, it is shown in Appendix B that the product of the four poles (2 short period and 2 surface mode) must be equal to:

$$\frac{(Z_\alpha M_\delta - M_\alpha Z_\delta)}{gGI_e'} \frac{F_s}{n}$$

where

F_s/n = Stick force per g

Z_α, Z_δ = Partial derivatives of vertical acceleration with respect to angle of attack and elevator deflection

M_α, M_δ = Partial derivatives of pitch acceleration with respect to angle of attack and elevator deflection

g = Acceleration due to gravity

G = Elevator gearing, ratio of stick force to hinge moment

I_e' = Moment of inertia of elevator and control system about elevator hinge line

For the baseline dynamics the above is equal to 24,500 $(rad/sec)^4$. Moving the surface mode poles to low enough frequency to be troublesome would require some very large and impractical changes.

The other possibility is to overdamp the surface mode and have one relatively low-frequency pole and the other very large. This can be done by aerodynamically balancing the elevator to significantly reduce the hinge moment derivatives (Ch_δ, Ch_α, $Ch_{\dot{\alpha}}$, Ch_q) and adding a bobweight to maintain a reasonable stick force per g. One other required change is to increase the damping term, $Ch_{\dot{\delta}}$. The baseline case included only the aerodynamic component of this derivative, but there is also a component due to friction in the control system. Reference 13 examined flight test data and found that friction increased $Ch_{\dot{\delta}}$ to roughly 10 times the estimated aerodynamic component. Consequently, a large increase in $Ch_{\dot{\delta}}$ is not unrealistic.

A new set of dynamics was computed with the following changes from the baseline case:

- A 3.5:1 increase in $Ch_{\dot{\delta}}$
- A roughly 5:1 reduction in Ch_δ, Ch_α, $Ch_{\dot{\alpha}}$, and Ch_q
- Addition of a 5 lb bobweight

For this case, the stick-free short period has a frequency of 3.48 rad/sec with a damping ratio of 0.63. The surface mode roots are at 5.33 and 264 sec^{-1}. The force gradient is 10 lb/g.

The surface pole at 5.33 is low enough that it could cause pilot control problems. Unfortunately, there is not much data on aircraft dynamics of this type. The only known data source is Ref. 14. That report investigated the effects of control system lags on the flying qualities of fighter aircraft. Experimental evaluations were made in the variable-stability T-33.

Obviously there are serious problems in applying that data to the situation of interest here. The dynamics were evaluated for a fighter mission by two highly experienced pilots. While comparisons on an absolute basis are certainly questionable, the pilot rating trends with control system lag should be pertinent. Furthermore, one of the evaluation criteria was the ability to control load factor.

Of the many configurations tested in Ref. 14, two series are the most applicable (Configurations 1D, 1E, 1F, 1G, and 6C, 6D, 6E, 6F). Each series involved variations in a first-order flight control system (FCS) lag with all other FCS lags above 60 rad/sec. Key dynamic parameters for these configurations and our hypothetical example are given below:

Configuration	FCS Pole (Sec^{-1})	ω_{sp} (rad/sec)	ζ_{sp}	$1/T_{\theta_2}$ (sec^{-1})	IAS (kt)
General Aviation Example	5.3	3.5	0.63	2.5	150
1D, 1E, 1F, 1G	$0.5 \rightarrow \infty$	2.2	0.69	1.25	250
6C, 6D, 6E, 6F	$0.8 \rightarrow \infty$	3.4	0.67	2.4	350

The 6 series is an excellent match for our example except for the higher airspeed. The only significant effect of the higher airspeed is a higher sensitivity of load factor to pitch attitude.

The pilot ratings for these two series are shown in Fig. IV-4. The ratings for both series are very similar with a substantial degradation as the FCS pole is reduced. The main pilot problems were a tendency to pilot-induced oscillations (PIO) and a tendency to overshoot the desired load factor. The aircraft was OK for gentle maneuvers, but difficulties arose if aggressive maneuvering was attempted.

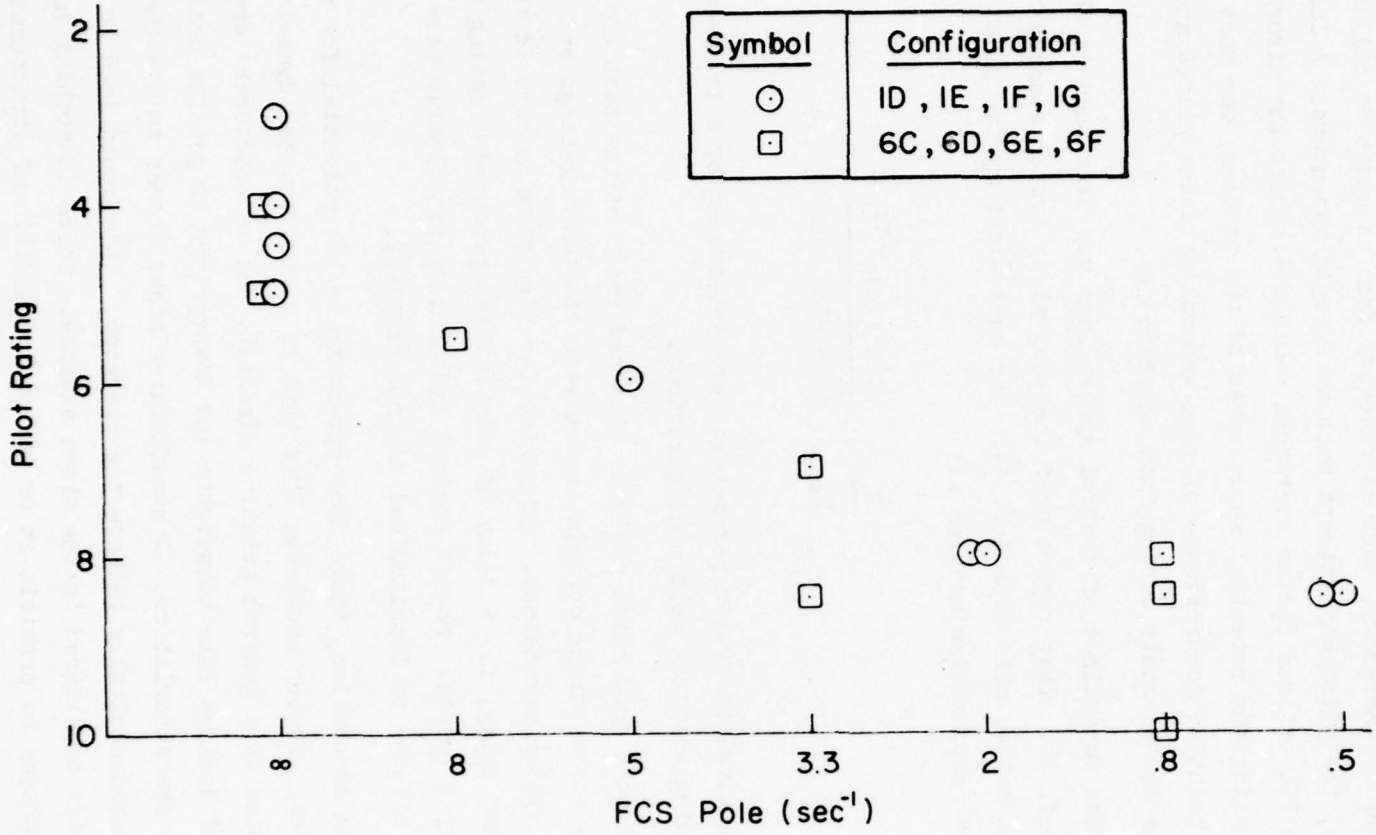

Figure IV-4. Effects of Flight Control System Lag

These results seem to be directly applicable to general aviation. Routine flying involves only rather gradual load factor control, so a low-frequency surface mode might not present any serious problems. During an emergency, such as recovery from an upset or collision avoidance, the pilot may attempt much more rapid maneuvers. A large-amplitude PIO or load factor overshoot could overstress the aircraft. In assessing the potential seriousness of the problem, one must consider the relative inexperience of many general aviation pilots and their possible mental state during such an emergency.

The importance of control system lags was also seen in the analysis of Ref. 15. That report used the equivalent system concept to fit the pilot rating data from Ref. 14. The equivalent system pitch rate/stick force response was modeled as:

$$\frac{q}{F_s} = \frac{K(s + Z)e^{-\tau s}}{s^2 + 2\zeta\omega s + \omega^2}$$

The equivalent system parameters were determined by a frequency response matching with the test configurations.

When a good match could be obtained (most of the test configurations) there was a strong correlation between the pilot ratings and the equivalent system parameters. Of particular significance here is the sensitivity to time delay, τ. A delay of only 0.1 sec produced a rating decrement of nearly 2 points. Modest control system loop can clearly have a significant effects on longitudinal control problems.

In conclusion, there does appear to be the potential for a serious problem. To our knowledge this type of control system dynamics has never happened in a general aviation aircraft, but manufacturers are making more use of devices like bobweights and downsprings to get the desired stick force characteristics. A manufacturer might choose to use these devices and aerodynamically balance the elevator. This could lead to the type of dynamics considered in the above example. There is nothing in the current regulations to prohibit it or to require additional structural strength to protect against higher load factors.

SECTION V

GUST LOADS

This section deals with structural loads due to gusts, for both large and small aircraft. As background information, the first subsection reviews FAR requirements for both discrete and continuous gusts. The reader who is familiar with these requirements can skip directly to Subsection B. That subsection reviews some of the problems, difficulties, and concerns with the continuous gust criteria. The next subsection discusses and compares the relative importance of the effects of the two gust characterizations on design strength. The last subsection presents an in-depth study of one of the problems encountered in the analysis of continuous gust loads.

A. FAR REQUIREMENTS

Gust loads requirements are contained in FAR Part 23 for small aircraft and in FAR Part 25 for large aircraft. These FAR's define the limit loads "which the airplane structure must be able to support...without detrimental permanent deformation." Discrete gust limit load requirements are similarly defined for both large and small aircraft. In addition, for large aircraft, consideration of "the dynamic response of the airplane to...turbulence" is also required, and its form is detailed in a recent addendum to Part 25.

Discrete gust requirements will be considered first. The design discrete vertical gust must be assumed to have the following shape.

$$w_g = \frac{U_{de}}{2}\left(1 - \cos\frac{2\pi s}{25\bar{c}}\right) \qquad (V\text{-}1)$$

where

U_{de} = Derived equivalent (design) gust velocity

s = Distance penetrated into gust

$\bar{c}$ = Mean geometric chord of wing

"In the absence of a more rational analysis," this gust must be assumed to produce load factors given by:

$$n = 1 \pm \frac{K_g U_{de} V_e a}{498(W/S)} \qquad \text{(V-2)}$$

where U_{de} and $\bar{c}$ are as previously defined and

$K_g = \frac{0.88\mu_g}{5.3 + \mu_g}$ = Gust alleviation factor

$\mu_g = \frac{2(W/S)}{\rho \bar{c} a g}$ = Airplane mass ratio

ρ = Density of air (slugs/cu ft)

W/S = Wing loading (psf)

g = acceleration due to gravity (ft/sec^2)

V_e = Airplane equivalent speed (kt)

a = Slope of the airplane normal force coefficient curve C_{N_A} per radian if the gust loads are applied to the wings and horizontal tail surfaces simultaneously by a rational method. The wing lift curve slope C_{L_α} per radian may be used when the gust load is applied to the wings only and the horizontal tail gust loads are treated as a separate condition.

For large aircraft the derived gust velocity is specified for 3 aircraft design speeds:

V_B Design speed for maximum gust intensity

V_C Design cruising speed

V_D Design dive speed

These design speeds are selected by the manufacturer, subject to certain constraints imposed by FAR Part 25. These constraints are discussed in Section VI. The derived gust velocities are listed in Table V-1. The same gust shape and magnitudes are used for small aircraft except there is no V_B design speed.

Between design speeds the limit load factor is assumed to vary linearly with airspeed. The result is a V-n envelope of the limit load factors for vertical gusts, as illustrated for large aircraft by Fig. V-1. Together with a similar "maneuvering envelope," this diagram defines the vertical

TABLE V-1

DESIGN DISCRETE GUST VELOCITIES

DESIGN SPEED	DESIGN GUST VELOCITY[a] (fps, EAS)	
	$h \leq 20{,}000$ ft	$h = 50{,}000$ ft
V_B	66	38
V_C	50	25
V_D	25	12.5

[a]Between 20,000 ft and 50,000 ft. gust velocity varies linearly with altitude.

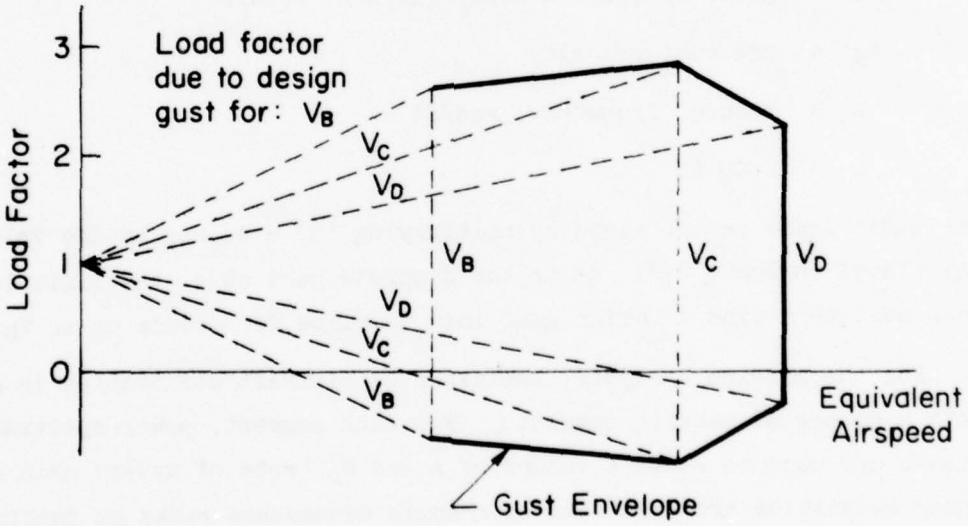

Figure V-1. Generic V-n Gust Diagram

limit loads for which the airplane must be designed. Similar load requirements are imposed for discrete unsymmetrical vertical gusts and for discrete lateral gusts.

For large aircraft, design criteria for vertical and lateral continuous gusts are defined by FAR Part 25. The designer is given the choice of using:

- Design envelope analysis, or
- Mission analysis and supplementary design envelope analysis.

In both the design envelope analysis and the supplementary design envelope analysis, power spectral techniques are used to establish values of $\bar{A}$, which is the ratio of rms incremental load to rms gust velocity. The gust power-spectral density is given by:

$$\Phi(\Omega) = \frac{\sigma_g^2 L}{\pi} \frac{1 + (8/3)(1.339L\Omega)^2}{[1 + (1.339L\Omega)^2]^{11/6}} \qquad \text{(V-3)}$$

where

Φ = power-spectral density $(ft/sec)^2/rad/ft$

σ_g = rms gust velocity

Ω = reduced frequency, rad/ft

L = 2500 ft

The limit loads are obtained by multiplying the $\bar{A}$ values by the velocities, U_σ, listed in Table V-2. As in the discrete gust case, the limit loads are then used to define a design gust load envelope for speeds up to V_D.

For the mission analysis, the expected aircraft utilization is divided into a number of mission segments. For each segment, power-spectral techniques are used to compute values of $\bar{A}$ and N_o (rate of upward axis crossings). These quantities are then used to compute exceedance rates as functions of load level, according to:

$$N(\Delta x) = \sum_i \tau_i N_o \left[P_1 \exp\left(-\frac{|\Delta x|}{b_1 A}\right) + P_2 \exp\left(-\frac{|\Delta x|}{b_2 A}\right)\right] \qquad \text{(V-4)}$$

where

τ_i = fraction of time in the i-th segment

Δx = net load or stress minus 1 g flight value

P_1, P_2 = probabilities of encountering non-storm and storm turbulence

b_1, b_2 = rms values of σ_{gust} for non-storm and storm turbulence

TABLE V-2

DESIGN CONTINUOUS GUST VELOCITIES

DESIGN METHOD	SPEED	U_σ (fps, TAS)[a]	
		$h \leq 30{,}000$ ft	$h = 80{,}000$ ft
Design envelope analysis	V_B	112.2	39.6
	V_C	85	30
	V_D	42.5	15
Supplementary design envelope analysis	V_B	79.2	33
	V_C	60	25
	V_D	30	12.5

[a]Between 30,000 and 80,000 ft, U_σ varies linearly with altitude.

The values of P_1, P_2, b_1, and b_2 given in FAR Part 25, proposed Appendix G, are copied in Figure V-2. The design limit loads are those for which the exceedance rate is 2×10^{-5}/hr.

To fully appreciate some of the discussions in the next two subsections, one needs to understand the derivation of Eq. (V-4). First, it is assumed that each patch of turbulence can be adequately modeled as a normally-distributed random process with a standard deviation, σ_g. This gust

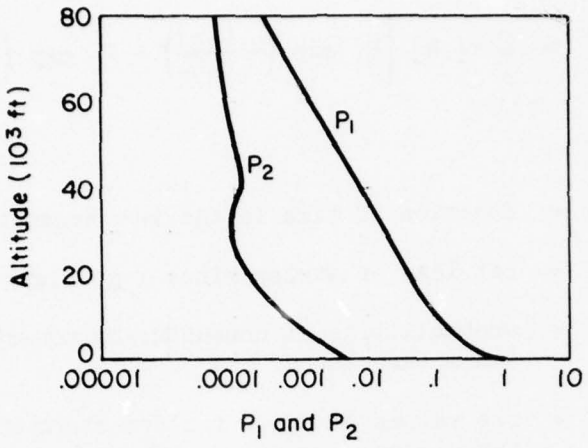

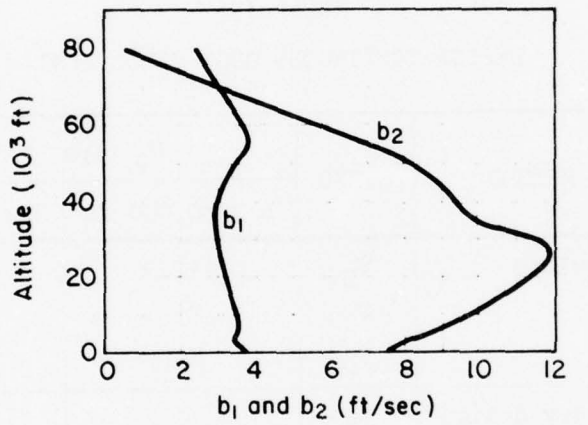

Figure V-2. Continuous Gust Statistical Parameters

intensity (σ_g) is a random variable with a probability density function, $p(\sigma_g)$. Then for any one flight segment the exceedance rate is given by:

$$N(\Delta x) = \int_0^\infty N(\Delta x|\sigma_g)\ p(\sigma_g)\ d\sigma_g \qquad \text{(V-5)}$$

where

$N(\Delta x|\sigma_g)$ = exceedance rate for Δx when the gust intensity is σ_g

For a linear system excited by a normally-distributed random process, the exceedance rate is:

$$N(\Delta x|\sigma_g) = N_o \exp\left[-\frac{1}{2}\left(\frac{\Delta x}{\bar{A}\sigma_g}\right)^2\right] \qquad (V\text{-}6)$$

where

$\bar{A}\,\sigma_g = \sigma_x$

N_o = upward axis crossing rate = $(1/2\pi)(\sigma_{\dot{x}}/\sigma_x)$ = radius of gyration, in Hz, of Δx power spectral density about zero frequency.

For the turbulence probability density function it is assumed that there are two kinds of turbulence, nonstorm and storm. The probabilities of encountering each are P_1 and P_2, respectively (probability of no turbulence is $1 - P_1 - P_2$). Given that turbulence has been encountered, the intensity, σ_g, is assumed to have a normal distribution with a rms value of b_1 or b_2. Thus, the probability density function for turbulence intensity can be written as:

$$p(\sigma_g) = \sqrt{\frac{2}{\pi}}\left\{\frac{P_1}{b_1}\exp\left[-\frac{1}{2}\left(\frac{\sigma_g}{b_1}\right)^2\right] + \frac{P_2}{b_2}\exp\left[-\frac{1}{2}\left(\frac{\sigma_g}{b_2}\right)^2\right]\right\} \qquad (V\text{-}7)$$

The final design equation, Eq. V-4 above, is obtained by:

i) Combining Eqs. V-5, -6, and -7

ii) Using the definite integral

$$\int_o^\infty \exp\left(-y^2 - \frac{a^2}{y^2}\right) dy = \frac{\sqrt{\pi}}{2} e^{-2|a|} \qquad (V\text{-}8)$$

iii) Weighting the exceedance rates for each mission segment by the fraction of time spent in the segment and summing over all segments.

B. REVIEW OF CONTINUOUS GUST CRITERIA

The addition of continuous gust loads criteria is certainly a significant step in aircraft design. While it is important to consider continuous

gust effects, there are potential problems and difficulties in applying the current criteria. These are discussed below.

1. Pilot Control Behavior

The effects of an automatic control system are relatively easy to include in an analysis because the system behavior is completely predictable and easily modeled. Pilot control behavior can also substantially affect the loads, as is demonstrated by the two examples in the next subsection. While models for a human pilot are quite well developed, their application to a specific situation is often not a straightforward process. The problems are especially serious for flight in severe turbulence as pilot modeling data are not available. The current inability to accurately predict the effects of likely pilot control behavior is a serious limitation in the analysis of continuous gust loads.

2. Nonlinearities

Significant nonlinearities can come from several sources, including the basic aerodynamic characteristics of the aircraft and various rate/position limits in the flight control system. Power-spectral analysis techniques are not mathematically valid for a nonlinear system. Some other, more costly, analysis procedure must be used.

An approximate technique common in servo analysis work is to model a nonlinear element by its random-input describing function. Since a describing function is directly dependent on the rms amplitude of the input to a nonlinearity, any aircraft response parameter becomes a function of the rms gust level. In terms of the earlier equations, this means $\bar{A}$ and N_o would be functions of σ_g rather than constants. As a result, Eq. V-4 is no longer appropriate for a mission analysis and exceedance rates would be computed by numerically evaluating the integral of Eq. V-5. This would greatly increase the cost of a mission analysis. It would be necessary to evaluate $\bar{A}$ and N_o for several, rather than one, values of σ_g and then do the integration of Eq. V-5.

The approach to be used in a design envelope analysis is less clear. The incremental design load is the product of $\bar{A}$ and a specified gust

velocity U_σ. The key question is what σ_g to use in computing $\bar{A}$. The intent of this requirement was probably to design for a load of several standard deviations in severe turbulence. If the design turbulence intensity is denoted as σ_{g_d} and the design load is η standard deviations, the design load for the linear case is $\eta\bar{A}\sigma_{g_d} = \bar{A}_{U\sigma}$ for $U_\sigma = \eta\sigma_{g_d}$. Thus in the linear case it is only necessary to specify the $\eta\sigma_{g_d}$ product. For a nonlinear system <u>both</u> η and σ_{g_d} must be specified.

The describing function approach is one way of coping with the effects of nonlinearities. While there are some difficulties in its application, the greatest concern is that it is an approximate solution. Furthermore, it is generally difficult to assess its accuracy and to determine if the results are conservative or unconservative. An alternative approach is to use a time domain, Monte Carlo simulation.

A Monte Carlo simulation could include an accurate model of all known system nonlinearities. The exceedance rates, $N(\Delta x|\sigma_g)$, could be measured for various load and rms gust levels. These data could then be used directly in the integration of Eq. V-5. The only inaccuracies would be those associated with the finite run lengths.

While the Monte Carlo approach may be theoretically attractive, it is very costly. Very long runs are required to get reliable data for the low exceedance rates associated with the design loads. Models which accurately reflect structural mode and unsteady aerodynamic effects could be extremely complex. A large number of runs could be required to cover the necessary combinations of weight, c.g., speed, altitude, rms gust level, etc. The cost could easily be prohibitive even with modern computers.

The above discussion was intended to point out the serious difficulties which can result if there are significant system nonlinearities. Furthermore, there is no clear-cut solution to the problems. For these reasons, a simplified example problem was analyzed as part of this project. The results, presented in Subsection D, demonstrate that the describing function analysis can be quite inaccurate and unconservative. The analysis did, however, lead to a procedure which can relatively easily determine the necessity for either describing function or Monte Carlo procedures.

3. Turbulence Model

Whatever the analysis procedure, the results are only valid if the turbulence model adequately reflects the characteristics of real turbulence. Despite a great deal of research on the subject, there are still serious questions as to a good turbulence model. There is a fundamental question of the validity of modeling turbulence as a normally-distributed random process. Some researchers have proposed models which are not normally-distributed but we are not aware of any loads calculations done with these models.

Among the advocates of normally-distributed turbulence, there is debate as to the proper value for the turbulence scale length, L. Appendix G of FAR Part 25 specifies a value of 2500 ft. Ref. 16 suggests a value of 800 ft. Variations in scale length of this magnitude can substantially alter the computed gust loads, as will be shown in the next subsection.

Another subject of debate is the probability density function for gust intensity, σ_g. Reference 17 recommends the same form as Eq. V-7 but recommends considerably different values for the parameters (P_1, P_2, b_1, and b_2) than specified in Appendix G of FAR Part 25. The effects of these parameter differences are clearly seen in the generalized exceedance curves of Fig. V-3. Reference 18 recommends even a different form (a Rayleigh distribution) for the probability density function.

The above abbreviated discussion has highlighted some of the key uncertainties in the modeling of atmospheric turbulence. These uncertainties detract from the value of continuous-gust analysis procedures but should not prevent their utilization. The real message is that more research is clearly required to better define a turbulence model for loads analysis.

C. COMPARISON OF DISCRETE AND CONTINUOUS GUST REQUIREMENTS

One common method of comparing discrete and continuous gust requirements is to compare the incremental load factor requirements. The incremental load factor for a discrete gust was given in Eq. V-2. That equation can also be written as:

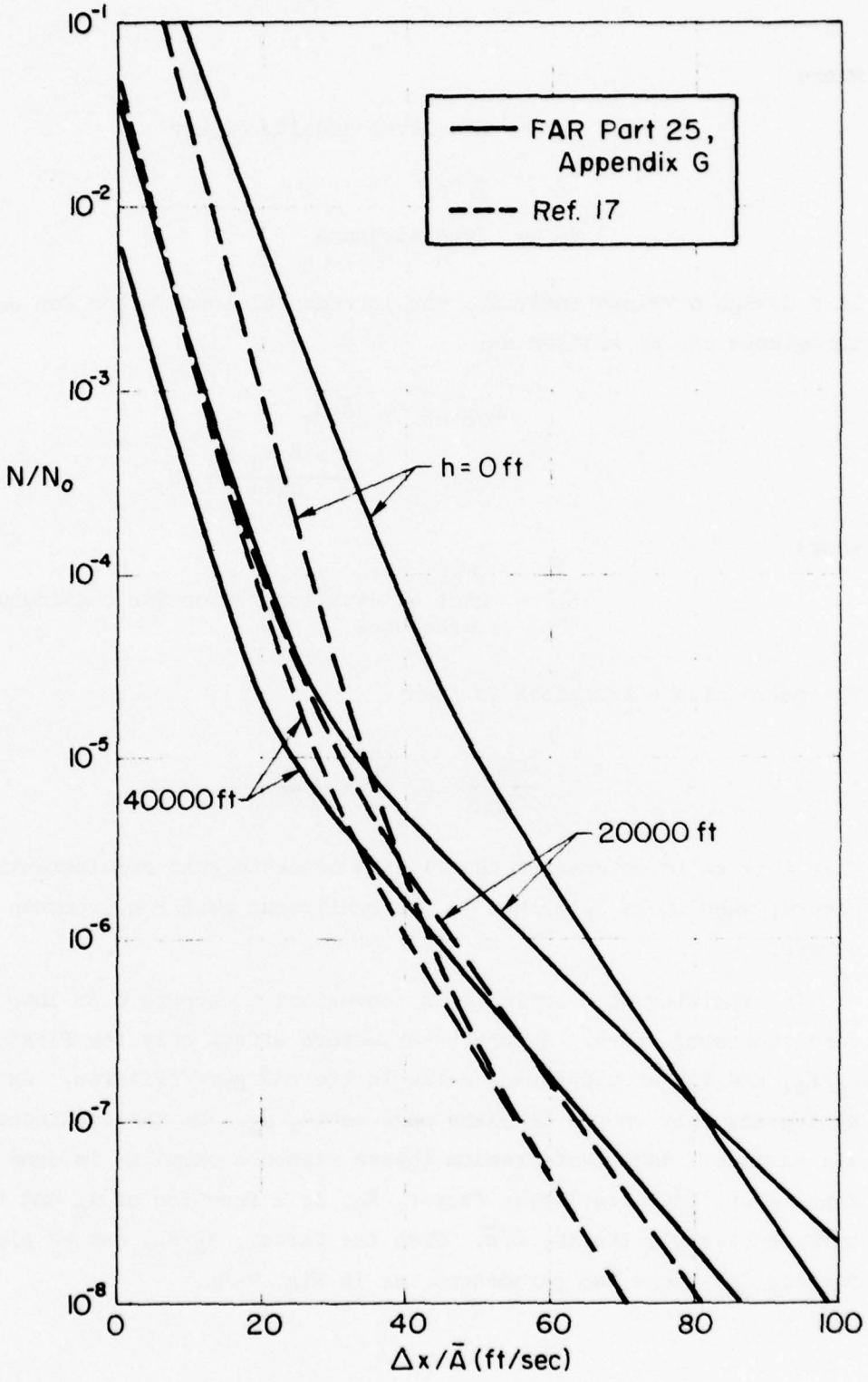

Figure V-3. Generalized Exceedance Curves

$$\Delta n_{dis} = \frac{a\rho_o \sqrt{\sigma}\, S\, V_T\, U_{de}\, K_g}{2W} \qquad (V\text{-}9)$$

where

ρ_o = Sea level density of air

$\sigma = \rho/\rho_o$

V_T = True airspeed

In a design envelope analysis, the incremental load factor for continuous turbulence can be written as:

$$\Delta n_{cont} = \bar{A}\, U_\sigma = \frac{a\, \rho\, S\, V_T\, K_\varphi}{2W}\, U_\sigma \qquad (V\text{-}10)$$

where

K_φ = Gust alleviation factor for continuous turbulence

The ratio of the two loads is then:

$$\frac{\Delta n_{dis}}{\Delta n_{cont}} = \frac{K_g}{K_\varphi} \times \frac{U_{de}}{\sqrt{\sigma}\, U_\sigma} \qquad (V\text{-}11)$$

When this ratio is greater than 1, the discrete gust requirements are more severe; when it is less than 1, the continuous gust requirements are more severe.

In examining this ratio it is convenient to separate it into the two factors indicated above. Aircraft parameters affect only the first factor, K_g/K_φ, and the second factor reflects the FAR gust criteria. As noted earlier, K_g depends only on the airplane mass ratio, μ_g. If the continuous gust analysis assumes 1 degree-of-freedom (heave response only) as is done for the discrete gust, the alleviation factor, K_φ, is a function of μ_g and the normalized turbulence scale length, $L/\bar{c}$. Then the factor, K_g/K_φ, can be plotted as a function of these two parameters, as in Fig. V-4a.

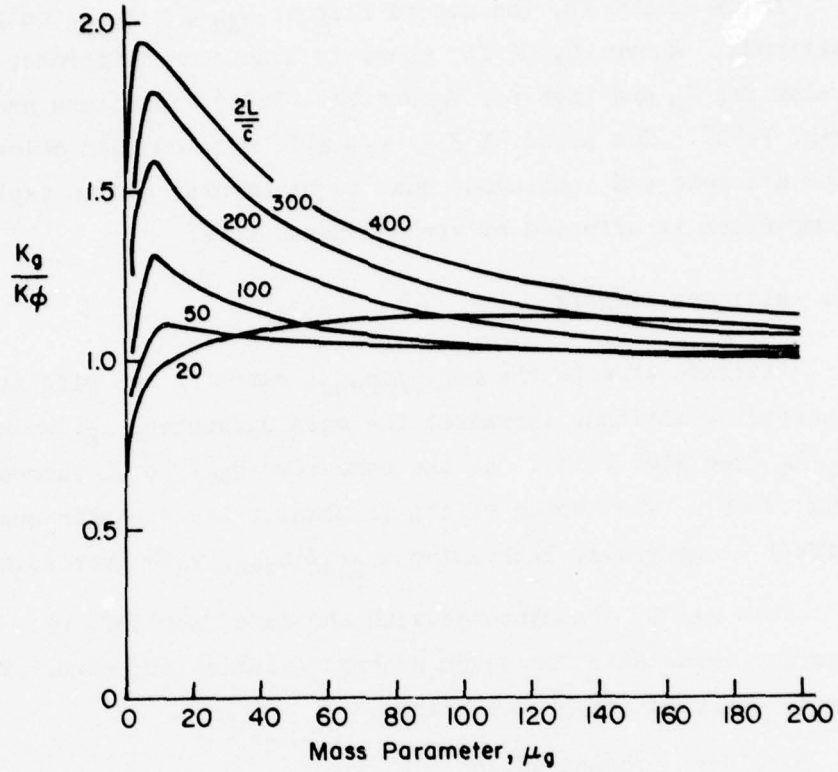

a) Ratio of Gust Alleviation Factors

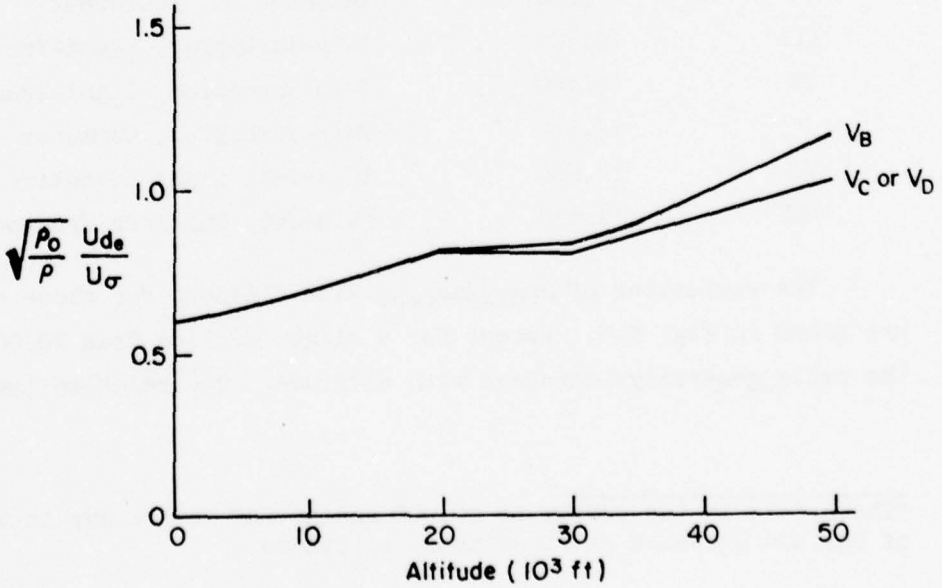

b) Ratio of Design Gust Levels

Figure V-4. Discrete/Continuous Gust Load Factor Requirements

Below 20,000 ft, the second factor, $U_{de}/\sqrt{\sigma}\, U_\sigma$, is only a function of altitude. Above 20,000 ft, there is also some difference between the value for V_B and that for V_C and V_D. These variations are shown in Fig. V-4b*. The plots of Fig. V-4 will also be used below to compare the discrete and continuous gust requirements, and to explore how the comparison is affected by various parameters.

1. Altitude Effects

Altitude affects the $\Delta n_{dis}/\Delta n_{cont}$ ratio in two offsetting ways. Increasing altitude increases the mass parameter, μ_g, which reduces K_g/K_ϕ (see Fig. V-4a). At the same time $U_{de}/\sqrt{\sigma}\, U_\sigma$ increases (see Fig. V-4b). The second effect is usually the stronger one so the net effect is generally increasing $\Delta n_{dis}/\Delta n_{cont}$ with increasing altitude.

This can be demonstrated with the data from Ref. 19. That report has similar loads data for seven general aviation aircraft. The types of aircraft analyzed are listed below:

Airplane	Gross Weight (lb)	
I	2,950	Single-Engine, Four-Seat, Fixed-Gear
II	3,600	Twin-Engine, Four-Seat
III	10,400	Twin-Turboprop, Light-Transport
IV	10,300	Twin-Turboprop, Light-Transport
V	12,560	Twin-Turboprop, Commuter
VI	12,800	Twin-Jet, Light Executive Transport
VII	18,650	Twin-Jet, Business Transport

The variations of $\Delta n_{dis}/\Delta n_{cont}$ with altitude for these seven airplanes are shown in Fig. V-5. Except for a slight decline from 20,000 to 30,000 ft, the ratio generally increases with altitude. The relative importance of the

*The breaks in the curves at 20,000 and 30,000 ft are due to variations of U_{de} and U_σ which start at those altitudes.

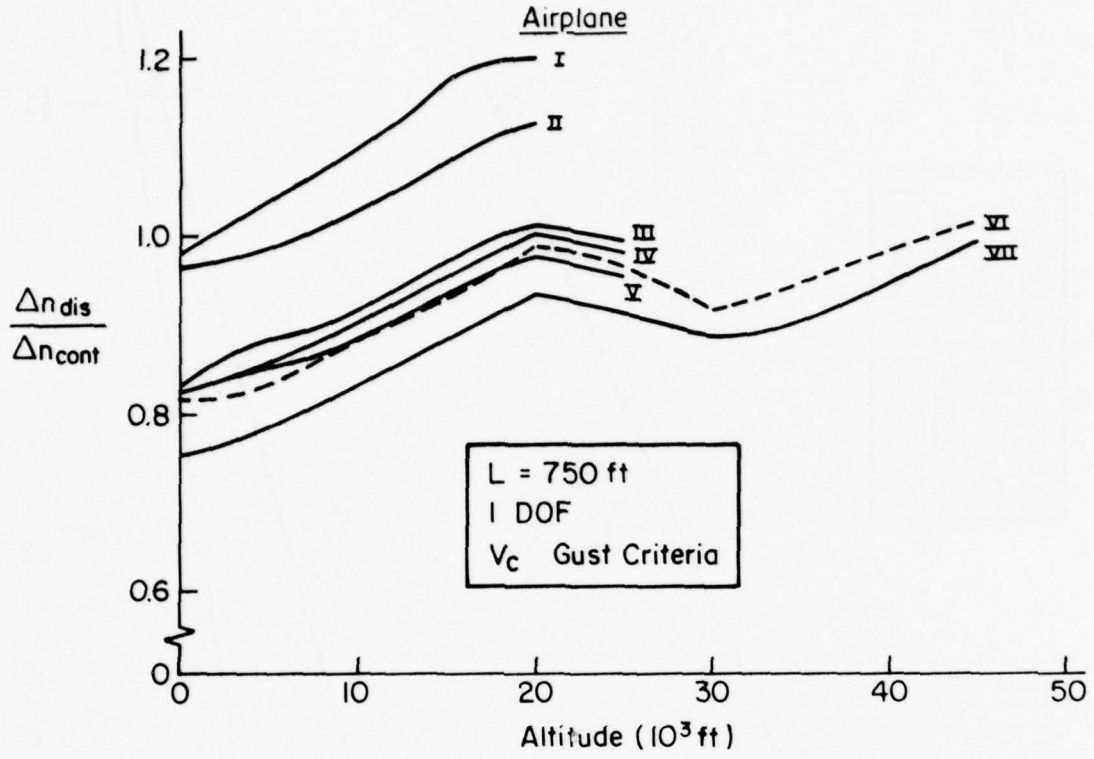

Figure V-5. Sample Effects of Altitude

discrete gust requirements is greatest at 20,000 ft and above roughly 40,000 ft.

2. Wing Loading Effects

Wing loading varies substantially between small, general-aviation aircraft and large commercial transports. Wing loading also has an important effect on the relative importance of discrete and continuous gusts. The mass parameter, μ_g, is proportional to wing loading; therefore, increasing wing loading decreases K_g/K_φ (Fig. V-4a) and decreases $\Delta n_{dis}/\Delta n_{cont}$.

This is confirmed by the seven airplane data from Ref. 19. A plot of the ratio, $\Delta n_{dis}/\Delta n_{cont}$, versus wing loading is shown in Fig. V-6. This

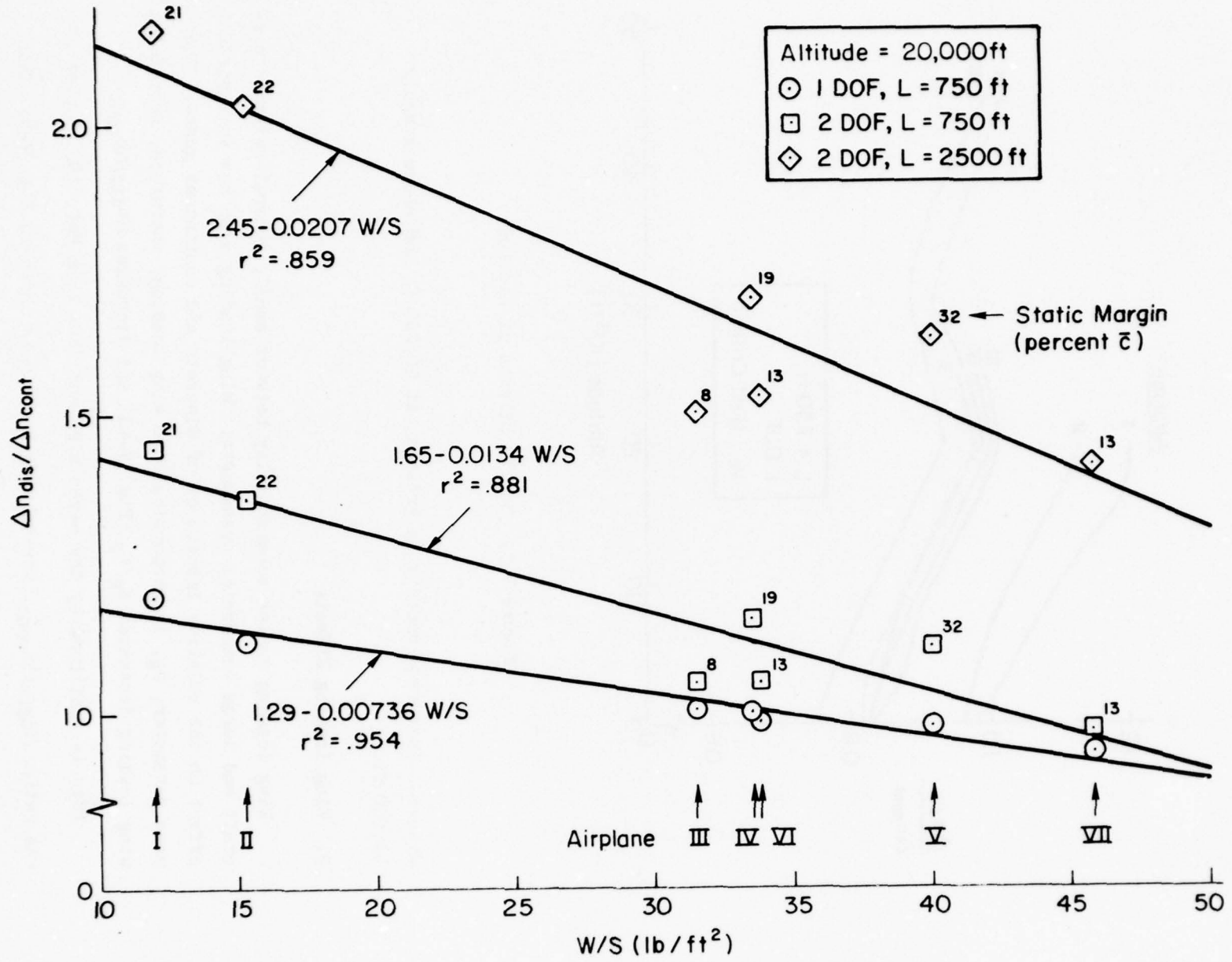

Figure V-6. Sample Effects of Wing Loading

clearly shows how discrete gust loads tend to be more critical for low wing loadings, and continuous gust loads tend to be critical for high wing loadings.

Figure V-6 also demonstrates the effects of other parameters and these will be discussed subsequently.

3. Effects of Turbulence Scale Length

Turbulence scale, L, has an important effect on the continuous gust loads. Increasing L, decreases K_φ which increases K_g/K_φ (Fig. V-4a) and $\Delta n_{dis}/\Delta n_{cont}$. The effect can also be seen in Fig. V-6 by comparing the two degree-of-freedom results for L = 750 and 2500 ft.

It is essential to remember that a larger L increases the relative importance of the discrete gust only because it generally reduces the continuous gust loads. A larger L concentrates more of the gust power at lower frequencies where there is less effect on the loads — the aircraft has more of a tendency to be convected with the gusts. Thus, the conservative approach would be to use the smallest value of L which is consistent with the research on atmospheric turbulence.

Reference 16 discusses the problems and uncertainties in trying to deduce turbulence scale length from measurements of atmospheric turbulence. As noted earlier, this reference suggests a scale length of 800 ft while FAR Part 25, Appendix G specifies 2500 ft. Computed gust loads will vary substantially depending on which value is used. It would appear more conservative to use the smaller value, at least until additional research can more precisely define an appropriate value.

4. Effects of Pitch Rotation

In the earlier discussion of continuous gust loads (e.g., Fig. V-4a), it was assumed that the aircraft was free only to heave. Another, and perhaps more rational, approach is to assume the aircraft can both pitch and heave, i.e., 2 degrees of freedom (DOF). Equation V-10 applies for both situations, but with 2 DOF the alleviation factor, K_φ, becomes a complex function of many parameters besides μ_g and $L/\bar{c}$.

Reference 19 includes corresponding continuous gust load calculations for both 1 and 2 DOF. The effects on the ratio, $\Delta n_{dis}/\Delta n_{cont}$, are shown in Fig. V-6. These results indicate significantly reduced continuous-gust loads when the aircraft is free to pitch into the relative wind. As shown in Fig. V-6, the scatter of the two DOF data about the mean square fit appears to be directly related to the variation of static margin for the different aircraft. This is, of course, to be expected since static margin is the primary determinant of weather-vaning tendency.

However, one must be very cautious about trying to generalize these results on the effects of pitch rotation. The 2 DOF continuous-gust load calculations reported in Ref. 19 were done using the formulae from Ref. 20. Those equations ignore gust gradient effects, i.e., the gust term in the pitch equation is merely $M_w w_g$. The inclusion of gust gradient terms can significantly affect the results.

Reference 21 recommends approximating gradient effects by using the term $[(M_q/U_o - M_{\dot{w}}) s - M_w]w_g$ in the pitch equation. The gradient effect (the s term) is significant because it causes the aircraft to initially pitch in the direction to increase the loads. Sample calculations for a light airplane (to be discussed shortly) showed a 19% increase in the design load factor when the above gradient term was added. A change of this magnitude would essentially eliminate or reverse the 1-2 DOF differences. In fact, in the two examples presented below, the 2 DOF loads are greater than those for 1 DOF.

5. Effects of Pilot Control

Discrete and continuous gust loads were calculated for two examples — a small general aviation airplane and a jumbo jet transport. The calculations were done for various assumptions as to the pilot's control behavior. The objectives were to:

- Investigate the effects on aircraft loads of likely variations in pilot control behavior
- Compare the design loads resulting from the discrete and continuous gusts.

Details of the calculations are given in Appendix C, but some features should be noted here:

- Gust gradient terms were included in the equations of motion
- For each condition the transfer function for load factor/vertical gust velocity was computed
- Δn_{dis} was the peak load factor when the transfer function was excited by the discrete gust of Eq. V-1.
- Design envelope analysis was used for continuous gusts (for computational convenience the Dryden form of the gust power-spectral density was used instead of the von Karman form of Eq. V-3).

The first example was a Boeing 747. Aircraft data for Mach 0.8 at 20,000 ft were obtained from Ref. 22. Five control situations were studied:

- Elevator fixed
- Elevator used to constrain pitch attitude ($\theta = 0$)
- Manual feedback of pitch attitude to elevator
- Manual feedback (pure gain) of cockpit load factor to elevator
- Manual feedback of integral of cockpit load factor to elevator

The second situation is a limiting case which is nearly identical to the 1 DOF analysis discussed earlier. The main difference is that we explicitly accounted for the elevator lift needed to balance the pitching moments. The last 3 cases were selected to include likely pilot control feedbacks.

The resulting design loads are summarized in Table V-3. There are several interesting aspects of these results. First is the relatively small variation of the discrete gust loads with control activity. This is because the discrete gust has such a short wave length, the aircraft has little time to pitch or respond to pilot inputs.

For the continuous-gusts there is a much greater variation. This is because most of the continuous-gust power is at frequencies below the short period or manual control frequencies. Therefore, manual control can significantly affect the rms response. Note that manual control of load factor actually increases the response. This is basically a poor feedback for manual control and mainly reduces the short-period damping. A stability augmentation system which would not have the human pilot limitations could obviously do much better.

TABLE V-3. LOAD FACTORS FOR 747 EXAMPLE

CONDITION	Δn_{dis}	Δn_{cont}	$\frac{\Delta n_{dis}}{\Delta n_{cont}}$
Elevator fixed	1.12	1.31	0.86
$\theta = 0$	1.04	1.14	0.91
$\theta \rightarrow \delta_e$ feedback	1.15	1.32	0.87
$n_{z_p} \rightarrow \delta_e$ feedback	1.21	1.83	0.66
$n_{z_p}/s \rightarrow \delta_e$ feedback	1.15	2.03	0.57

Note: Design gust velocities for V_c were used.

We also note that the discrete-gust loads are always less than those for the continuous gusts. This is apparently due largely to the very high wing loading (116 lb/ft^2) for this example. As discussed earlier, increasing wing loading tends to make $\Delta n_{dis}/\Delta n_{cont}$ less.

One final point on Table V-3 is worth noting. The 1 DOF ($\theta = 0$) loads are less than the 2 DOF (elevator fixed) loads. This result is attributed to the gust gradient effects mentioned earlier.

The second example was for a typical single-engine general aviation airplane. The aircraft dynamic model was the same one used to investigate longitudinal control system dynamics (Section IV-F and Appendix B). The flight condition was 150 kt IAS at 7000 ft. Because of the reversible control system, a stick free condition was analyzed in addition to the five conditions used in the 747 example.

The results are shown in Table V-4. The load variations with control activity follow the same general trends as for the 747 example, relatively small variations for the discrete gust and substantial variations for continuous gusts. This is again due to the differences in the frequency content of the two gust models. We also see the same adverse effect of manual control of load factor for the continuous-gust case.

TABLE V-4. LOAD FACTORS FOR GENERAL AVIATION EXAMPLE

CONDITION	Δn_{dis}	Δn_{cont}	$\frac{\Delta n_{dis}}{\Delta n_{cont}}$
Stick free	3.21	2.22	1.45
Stick fixed	3.27	1.90	1.72
$\theta = 0$	2.97	1.85	1.61
$\theta \rightarrow F_s$ feedback	3.21	2.28	1.41
$n_z/s \rightarrow F_s$ feedback	3.21	3.13	1.03
$n_z \rightarrow F_s$ feedback	3.19	2.53	1.26

Note: Design gust velocities for V_c were used.

The relative importance of the discrete and continuous gust loads is reversed from that for the 747. This is attributed to the low wing loading (16.7 lb/ft^2) for this example. It further substantiates the important effects of wing loading on $\Delta n_{dis}/\Delta n_{cont}$.

The explanation for the minimum loads in the 1 DOF ($\theta = 0$) condition is again the gust gradient. This was verified by redoing the stick-fixed continuous-gust calculation with the gust gradient terms removed. This lowered the load factor from 1.90 to 1.59. The same change would have negligible effect on the 1 DOF condition ($\Delta n_{cont} = 1.85$). Thus, with the gust gradient term removed the 2 DOF load would be less than the 1 DOF load.

D. AN EXAMPLE OF THE EFFECTS OF SYSTEM NONLINEARITY ON MISSION ANALYSIS CALCULATIONS

System nonlinearities preclude the direct application of the FAR mission analysis limit load definition based on Eq. V-4. The problem is basically that the aircraft response parameters are no longer normally-distributed random processes. Thus the simple expression, Eq. V-6, for conditional exceedance rate, $N(\Delta x|\sigma_g)$, is not applicable.

The purpose of this subsection is to assess the effects of a system nonlinearity on mission analysis calculations for a realistic example. Two methods of analysis are examined. The first approach uses the random-input describing function technique to approximate the nonlinearity as an effective gain which varies with rms gust velocity (σ_g). Power spectral techniques are then applied to the linearized system to calculate $\bar{A}$ and N_o as functions of σ_g. These are used in Eq. V-6 to approximate the conditional exceedance rates, which in turn are used to evaluate overall exceedance rates by numerically integrating Eq. V-5.

These conditional exceedance rates are compared with measurements taken in a time domain simulation. The Monte Carlo analysis treats the nonlinearity exactly; its accuracy depends only on the length of the simulation. The Monte Carlo results are also numerically integrated so that overall exceedance rates can be compared.

The rest of this subsection summarizes the example analysis. Essential details are documented in Appendix D.

1. Example Problem

The problem selected for study is the analysis of the lateral tail loads for an aircraft with a limited-authority yaw damper. This is a useful example since the yaw damper can greatly reduce the tail loads and therefore the damper limiting may have substantial effect. Reference 23 reports a 20 percent reduction in lateral gust design loads due to the L-1011 yaw damper. Such an effect is neither new nor uncommon among large jet aircraft. Increased lateral load levels due to yaw damper saturation in turbulence caused a serious problem for a first generation swept wing bomber in the early sixties (Ref. 24). Thus the example problem is both realistic and of practical concern.

The principal objective of this analysis is to determine the exceedance rates of limit level tail loads. It is at these load levels that the accuracy of a describing function analysis is of greatest concern. Accurate measurement of these very low rates in the time domain requires rather long time histories. To reduce the cost of these computations, the model used in the analysis was kept as simple as possible without sacrificing any of the

essential elements of the yaw damper problem. The key features of this model are:

- Roll motion is ignored
- Only aerodynamic forces and moments due to the vertical tail are included.
- Structural modes are not included.
- Yaw damper uses pure gain feedback of yaw rate.
- Unsteady lift effects are approximated by first order lag (this allows exact calculation of axis crossing rate for tail load).
- Gust spectrum is modeled as white noise passed through first order filter.

The resulting model has two degrees of freedom—side velocity and yaw—yielding equations of motion whose solution is only fourth order (including one for the gust filter). Model parameter values were selected to provide a good match to the dutch roll characteristics given in Ref. 22 for the 747 at 40,000 ft and Mach 0.8. As is typical of large jet aircraft, the unaugmented 747 exhibits very low dutch roll damping at high speed and altitude. As shown for this example in Fig. V-7, closure of the yaw damper loop substantially increases the damping of this mode. This reduces rms tail loads by nearly a factor of three. Thus, a damper authority limit has a potentially large effect on the tail loads in this example.

Though inertial loads have not been explicitly included in this model, the total structural load is generally well approximated by the aerodynamic component. In this simple example, in fact, structural and aerodynamic loads are exactly proportional. This is demonstrated in Appendix D, which also provides a detailed definition of the model.

2. Describing Function Analysis

The imposition of a rudder limit can reduce the effectiveness of the yaw damper loop closure shown in Fig. V-7. Whenever the rudder deflection commanded by yaw rate exceeds the authority limit, the damper, in effect, operates at less than the full yaw-rate-to-rudder gain. The effect of this

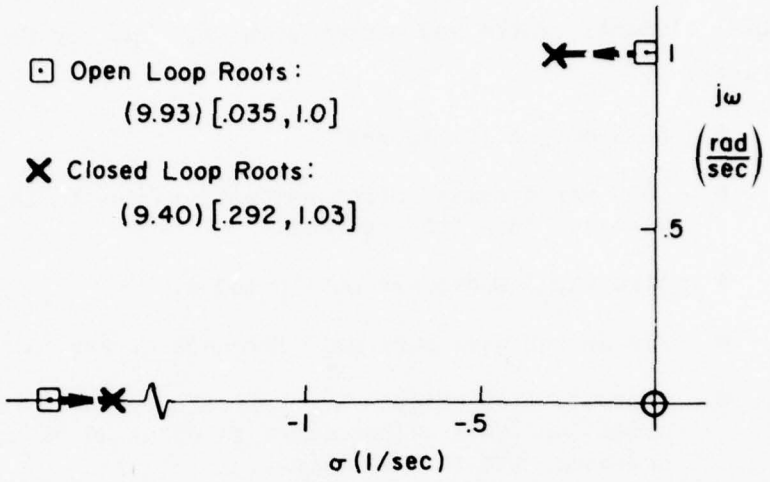

Figure V-7. Yaw Damper Loop Closure Effect

limiting over the course of time in turbulence can be linearized in terms of an "average" yaw-rate-to-rudder-gain. When normalized by the actual system gain, this "effective gain" takes on a value between 1, corresponding to damper operation with no limit, and 0, corresponding to unaugmented operation. Within these limits, the value depends on the characteristics of the patch of turbulence traversed and of the system response, and on the authority limit.

Transfer functions for the limited authority system can be calculated, based on closure of the damper loop with the effective gain. The resulting characteristic root locations for this closure lie on the locus between the open- and the closed-loop roots shown in Fig. V-7. With the "effective" transfer functions thus defined, values of $\overline{A}$ and N_o for the load on the vertical tail can be calculated for the given value of effective gain using standard analysis techniques.

One way of specifying the effective gain of a nonlinear element in this situation is to replace it with its random input describing function (Ref. 25). The value of this function is chosen to minimize the variance of the difference between the outputs of the nonlinearity and its linear approximation. This value is a function of the probability density of the input to the nonlinearity.

In the yaw damper example, this input, as well as all other response variables, is assumed to be a normally-distributed random variable, like the lateral gust velocity which is the system input. Then, the describing function approach quantizes the effective gain as a function only of the damper authority and the rms level of the input to the nonlinearity.

The calculation procedure which was used can be summarized as follows:

- Assume an effective yaw damper gain
- With this gain, compute various closed-loop transfer functions for a lateral gust input
- Compute N_o and $\bar{A}$ for the tail load
- Compute the ratio, (rms input to limiter)/(rms gust velocity)
- Use this ratio and the effective gain to compute those combinations of rms gust and rudder limit which would produce that effective gain.

Figure V-8 gives $\bar{A}$ and N_o as a function of rms gust velocity for a damper authority limit of 3.6 deg, which is approximately equivalent to the 747 limit. As Fig. V-8 shows, for this damper authority, it takes gust velocities somewhat greater than 25 ft/sec rms to change the value of these two parameters substantially. On the other end of the scale, as the gust velocity increases, $\bar{A}$ and N_o approach asymptotic values corresponding to unaugmented operation. These asymptotic values differ greatly from those for the unlimited yaw damper — by factors of, roughly, 3 and 0.5, respectively.

Based on the assumption that the tail load (F_t) is normally distributed, its exceedance rates for a given rms gust velocity are analytically defined as functions of $\bar{A}$ and N_o by Eq. V-6, just as for a linear system. In this case, however, $\bar{A}$ and N_o are functions of σ_{v_g}.

The final step in this analysis is to use these conditional exceedance rates to compute overall exceedance rates. This is done by numerically integrating Eq. V-5. For a full-scale mission analysis, this integration is done for each mission segment. The results are then combined into the final exceedance rates per Eq. V-4. For this example, the mission profile has been reduced to a single flight condition for simplicity.

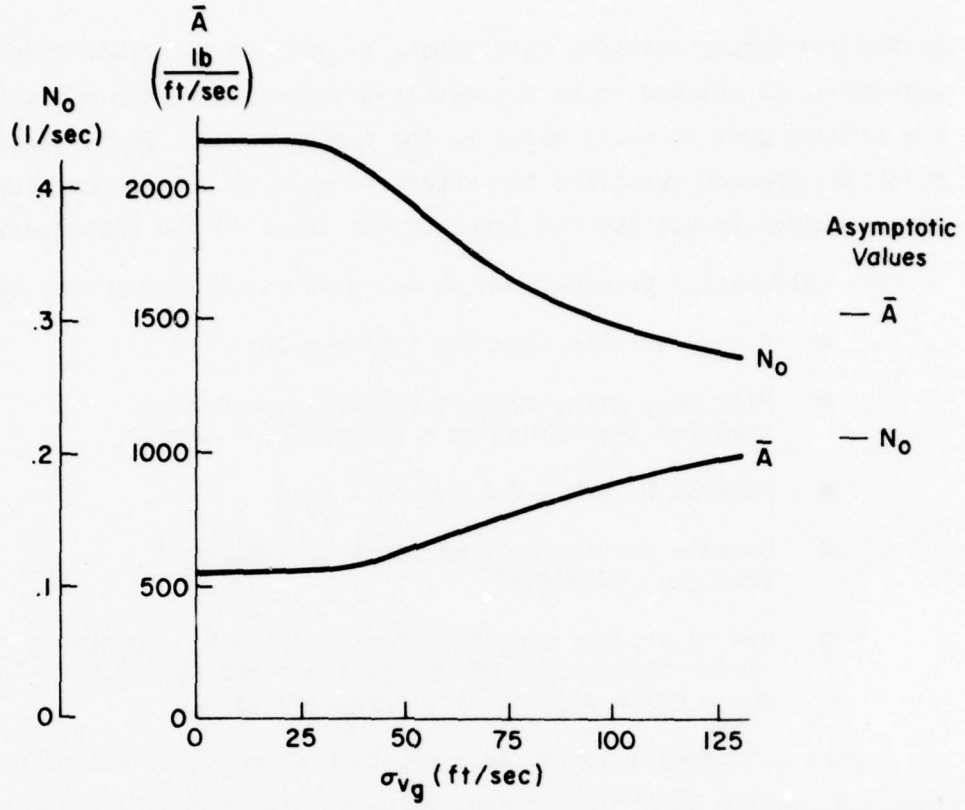

Figure V-8. Variations of Describing Function Analysis Parameters with Gust Velocity for $\delta_{R_{limit}} = 3.6$ deg

The gust velocity distribution of interest in this case is the one implicitly specified in the FAR mission analysis design criteria (Eq. V-7). At the 40,000 ft altitude of the example, the FAR gust distribution parameters P_1, P_2, b_1 and b_2 take on the values 0.007, 0.00011, 3.0 ft/sec and 9.36 ft/sec, respectively. This completes the definition of the terms in Eq. V-5.

Before presenting the results of that integration, it is instructive to try to predict the outcome. To do this consider the case of no yaw damper limit. Overall exceedance rates for this linear system can be computed using Eq. V-5, just as for the nonlinear case; of course, the computation is simpler since $\bar{A}$ and N_o are constant. Figure V-9 shows the variation of the integrand, $dN/d\sigma_{v_g}$, and its component factors, $N(F_t|\sigma_{v_g})$ and

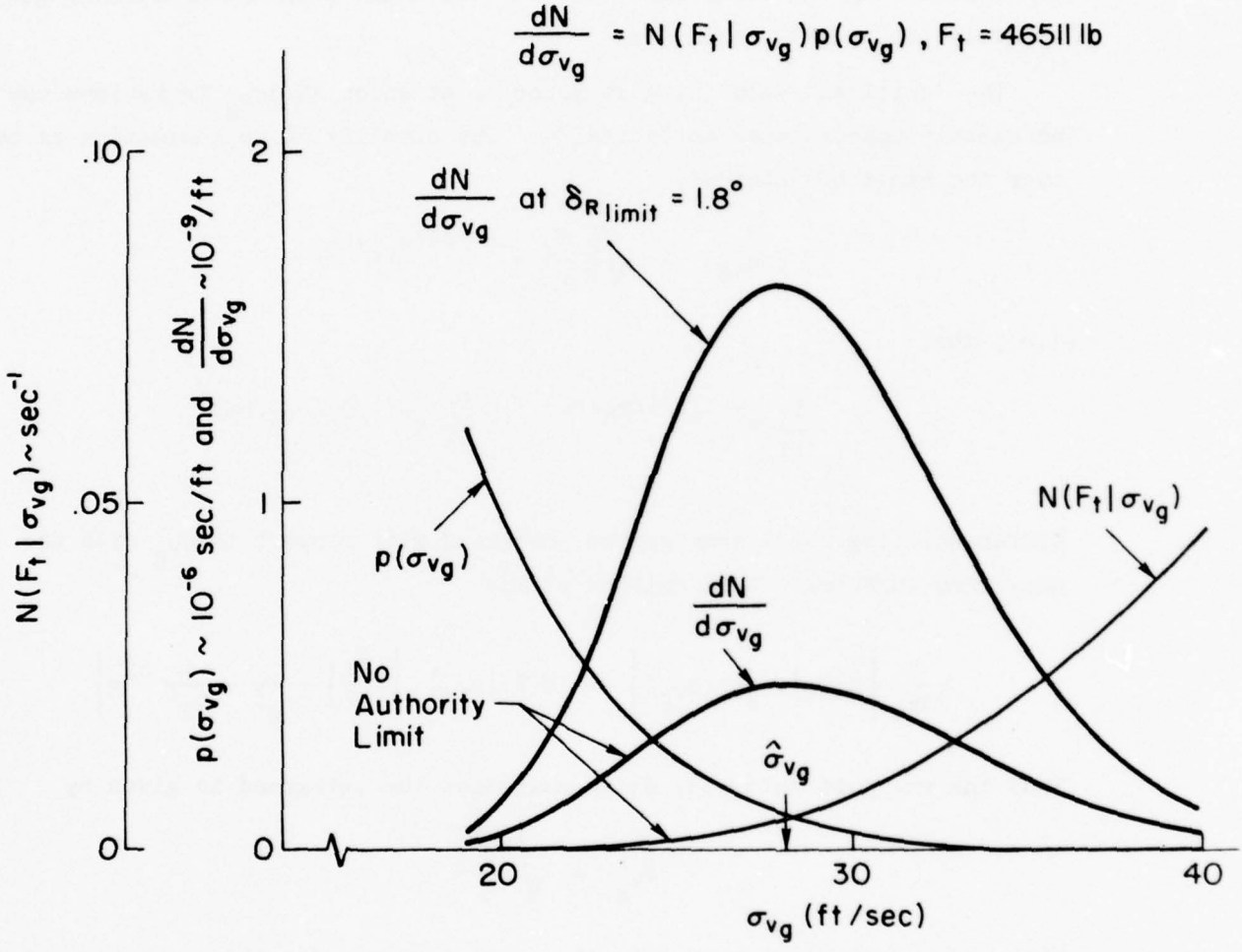

Figure V-9. Variations of Exceedance Rate Integrand with Gust Velocity

$p(\sigma_{v_g})$, with σ_{v_g}, for F_t = 46,511 lb. This value of tail load, is the design limit load with no damper limit, based on the mission analysis design criteria of 2×10^{-5} exceedances per hour (5.56×10^{-9}/sec).

Figure V-9 shows that the integrand has a well-defined peak. Below the peak, the integrand drops rapidly because the decrease in the conditional exceedance rate for F_t quickly outpaces the increased probability of encountering the lower gust levels. Above the peak the decreasing gust velocity probability dominates.

The "critical" value of gust velocity at which $dN/d\sigma_{v_g}$ is maximum can be closely approximated analytically. The simplifying approximation is that over the range of interest,

$$p(\sigma_{v_g}) \doteq \sqrt{\frac{2}{\pi}} \frac{P_2}{b_2} e^{-(1/2)(\sigma_{v_g}/b_2)^2}$$

i.e., that

$$\frac{P_1}{b_1} e^{-(1/2)(\sigma_{v_g}/b_1)^2} << \frac{P_2}{b_2} e^{-(1/2)(\sigma_{v_g}/b_2)^2}$$

Differentiating the linear system integrand with respect to σ_{v_g} with the non-storm turbulence term omitted yields

$$\frac{d}{d\sigma_{v_g}} \left[N(F_t|\sigma_{v_g}) p(\sigma_{v_g}) \right] \doteq N(F_t|\sigma_{v_g}) \left[\left(\frac{F_t}{\bar{A}} \right)^2 \frac{1}{\sigma_{v_g}^3} - \frac{1}{b_2^2} \sigma_{v_g} \right]$$

Thus the rms gust velocity, which maximizes the integrand is given by

$$\hat{\sigma}_{v_g} \doteq \sqrt{\frac{b_2 F_t}{\bar{A}}}$$

This gives a critical gust velocity of 28.2 ft/sec for the peak shown in Fig. V-9. This value lies close to the center of the interval from 20 ft/sec to 40 ft/sec for which the integrand has significant value.

The purpose of the above is to demonstrate that the critical gust range is easily predicted and is roughly 20-40 ft/sec for this example. Gust levels outside this range do not substantially change the design load overall exceedance rate.

Referring back to Fig. V-8 indicates that only as gust velocity approaches the high end of the 20-40 ft/sec range do the values of $\bar{A}$ and N_o begin to depart appreciably from their no-limit levels. At 40 ft/sec rms, $\bar{A}$ has increased from 548 to 583 lb/ft/sec and N_o has decreased from 0.436 to 0.414 sec^{-1}. These changes tend to offset each other in the calculation of the conditional exceedance rate. However, near and above the unlimited damper design limit tail load, $N(F_t|\sigma_{v_g})$ is much more sensitive to changes in $\bar{A}$, and the net effect at 40 ft/sec rms is a 23 percent increase in $N(F_t|\sigma_{v_g})$ over the unlimited damper value of 0.0460 sec^{-1}. Thus, for a 3.6 deg rudder limit, a small increase in the overall rate of exceedance of 46,511 lb is predicted.

A much larger increase would be predicted if the limit were halved to 1.8 deg. Gust velocity scales directly with authority limit for given values of $\bar{A}$ and N_o. Thus, to apply the Fig. V-8 curves to the 1.8 deg limit, the abscissa gust velocites in Fig. V-8 are halved. Gust velocities of 20 to 40 ft/sec rms then correspond to values of $\bar{A}$ and N_o substantially different from those for the unlimited damper. At $\hat{\sigma}_{v_g}$, these values are 657 lb-sec/ft and 0.375 sec^{-1} respectively, yielding more than a threefold increase in the conditional exceedance rate at this σ_{v_g} over the value for the unlimited yaw damper. This limit was therefore also analyzed, since the system was not very nonlinear at the higher limit, over the tail force range of interest.

The Eq. V-5 integrand for the 1.8 deg limit is included in Fig. V-9 to demonstrate how well it scales relative to the unlimited damper integrand. Note the virtual coincidence of the peak values. Thus the increase in $N(F_t|\hat{\sigma}_{v_g})$ provides a good estimate of the increase in overall exceedance rate for this limit.

Figure V-10 gives the overall exceedance rates as a function of tail load, for the yaw damper with no authority limit and with the 3.6 deg and 1.8 deg limits. The exceedance rate curve for the unaugmented system is also included in Fig. V-10, providing an upper bound for damper limiting effects. The figure verifies the predicted increases in the rate of exceedance of 46,511 lbs for the two finite-limit cases, and indicates further divergence of these curves

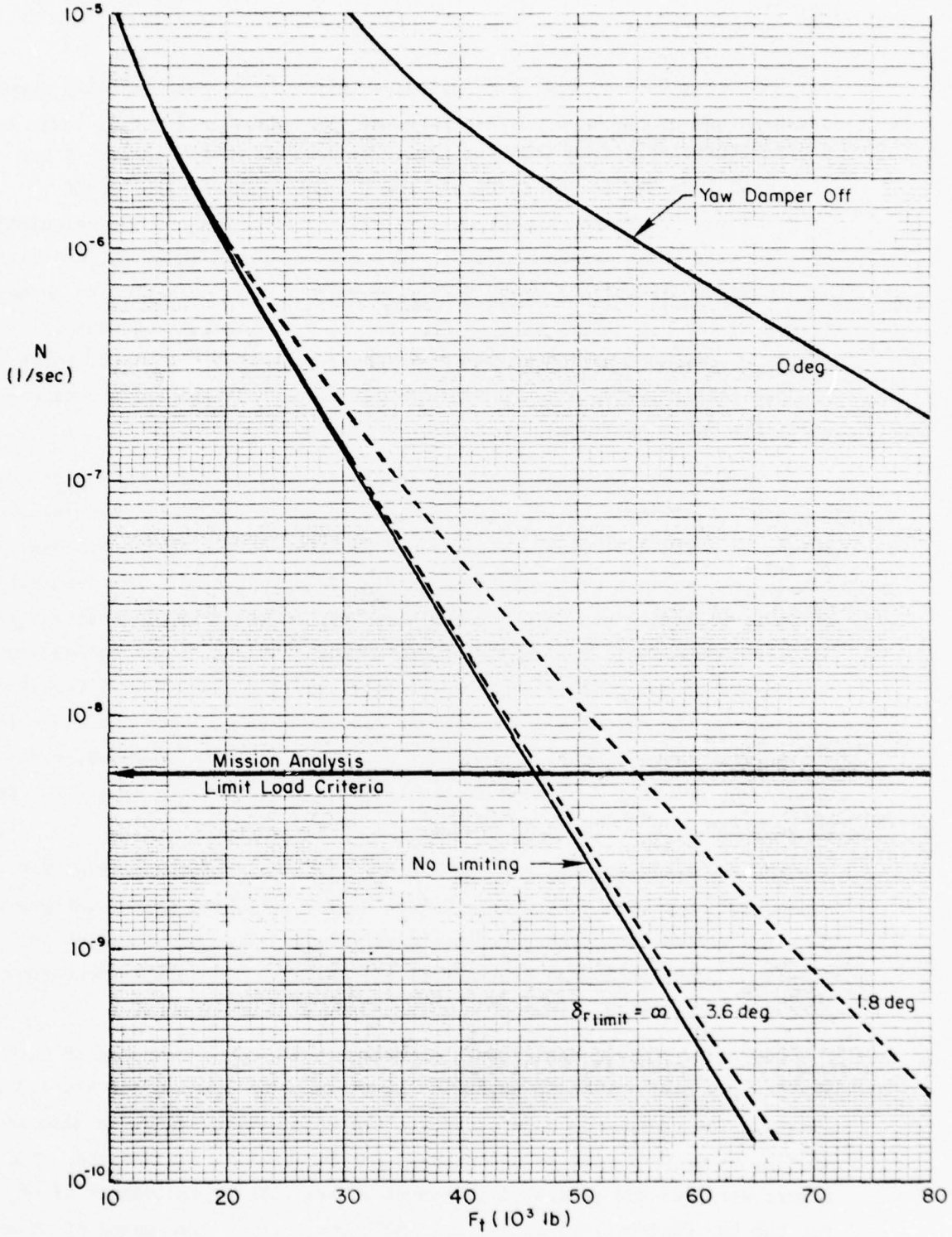

Figure V-10. Overall Exceedance Rates Based on Describing Function Analysis

from the unlimited damper curve with increasing tail load. This divergence is also predictable as a function of δ_{v_g} which, as noted, increases directly as the square root of tail load. In terms of mission analysis design limit tail load, Fig. V-10 shows that:

- Damper limiting can have a very large effect on the design limit load level, as indicated by the gap between the "damper-off" and "no-limiting" curves. This is, of course, the result of the marginally stable dutch roll characteristics of the unaugmented aircraft.
- At approximately the limit used on the 747 there is a negligible increase in limit load. However, halving this limit increases limit load by 20 percent.

Details of the describing function analysis are provided in Appendix D.

3. Time Domain Simulation

For the time-domain simulation, an existing digital computer program was modified. The modified program provides the time responses of the nonlinear system to random turbulence. The program produces time history plots of selected variables and measures both the probability distribution and exceedance rates of the tail load. To match the gust velocity distributional and spectral characteristics required by the mission analysis, a normal distribution of zero mean and unit variance is pseudo-randomly sampled and the result is appropriately scaled for a given rms level and filtered.

The simulation then amounts to a Monte Carlo analysis in which the tail load is treated as a random process for which we wish to measure exceedance rates. A run length of 30 minutes was selected to provide a reasonable tradeoff between the cost of running the simulation and the accuracy of the measurements. Based on the assumption that at least five exceedances are needed for reasonable accuracy, this time duration allows estimation of exceedance rates as low as 0.0014/sec, if the exceedances for positive and negative values of tail load are pooled. For the linear no limiting case, this rate occurs at roughly the 3σ level of F_t for any given σ_{v_g}. To extend the region of accuracy to the 4σ level would require roughly 30 times this run length, or 15 hours (see Appendix D, Fig. D-4).

After the start of each run, 15 seconds of "settling time" was allowed to pass before the initiation of on-line data reduction. This settling time is the equivalent of about 3 to 4 time constants at dutch roll damping ratios of 0.2 to 0.3. Since the turbulence time history always began with a patch of low amplitude gust velocities*, this interval was sufficient to insure that the system had reached steady state prior to the taking of data. Besides the accumulation of probability distribution and exceedance data, which were kept at roughly 0.25σ intervals of tail load, the program kept track of the minimum and the maximum tail force and calculated the first four moments of the distribution about the expected mean of zero.

Since the data generated for a given rms gust velocity and authority limit can readily be scaled to apply to another combination of gust velocity and authority limit with the same ratio, an rms gust velocity of 1 ft/sec was arbitrarily chosen as the input for all Monte Carlo runs. Runs were then made at authority limits corresponding to describing function effective gains (k_{DF}) of 0.8, 0.6 and 0.2. A run was also made with unlimited damper authority to validate the simulation. The validation data and other key program details are presented in Appendix D.

Figure V-11 compares sample time histories of tail load, yaw rate and gust velocity for the unlimited yaw damper with a corresponding segment from the run at $k_{DF} = 0.6$. The identical gust velocity traces provide a time reference for comparison of the system responses. The segment chosen for comparison features a very turbulent patch sandwiched between two lulls. It was selected to demonstrate the effects of the damper authority limit. For the 1 ft/sec rms gust input, the damper limit to produce an effective gain of 0.6 corresponds exactly to a yaw rate of 0.00104 rad/sec, as indicated in Fig. V-11b. Comparison of the traces shows that:

- During the lulls, when yaw rate remains within the authority-limit band for an extended period of time, differences in the tail force traces are negligible

---

* The runs for different authority limits used the identical gust time history.

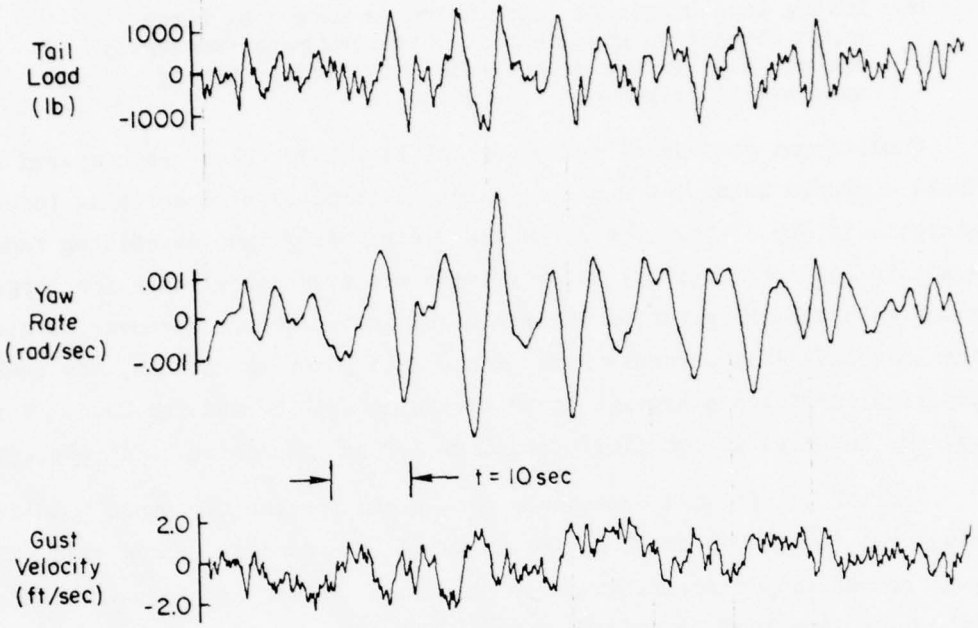

a) No Limiting: $k_{DF} = 1.0$

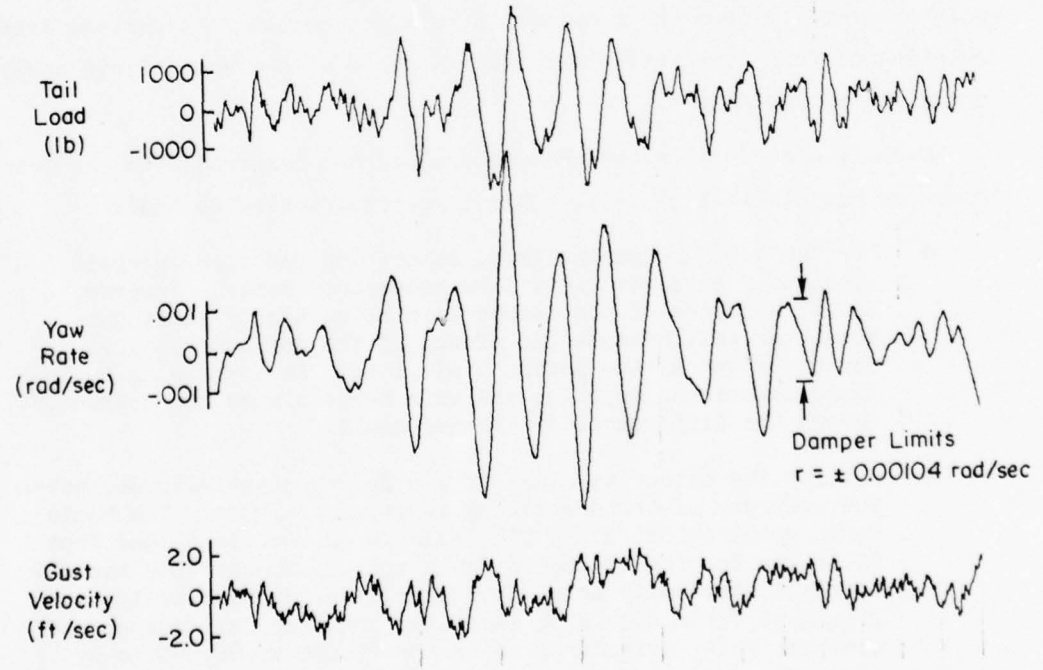

b) Limiting: $k_{DF} = .6$

Figure V-11. Sample Monte Carlo Simulation Time Histories

- During the turbulence patch which is marked by large rapid changes in gust velocity, the yaw rate frequently exceeds the limited damper authority producing very substantial increases in tail load.

Conditional exceedance rates for the Fig. V-11b case are compared with those computed using the $\bar{A}$ and N_o values determined by describing function analysis in Fig. V-12. These results clearly show that describing function analysis can substantially underestimate the exceedance rates for large tail loads when damper operation becomes highly non-linear. Moreover, neglecting the last and least accurate Monte Carlo data point at 2500 lb, the analytical/empirical difference appears to be diverging with increasing load. Unfortunately, the data is too limited to draw a firm conclusion on this point.

Similar conditional exceedance rate plots for the two other non-linear cases run (k_{DF} = 0.8 and 0.2) are included in Appendix D along with tail load probability distributions for each run. These conditional exceedance rate data were used to compute overall exceedance rates for comparison with those determined by describing function analysis. As in that approach, this computation is based on Eq. V-5. In the Monte Carlo case, however, the value of $N(F_t|\sigma_{v_g})$ is not analytically expressible. Instead this value is interpolated directly from the tabulated simulation results. Important details relating to this computation and other aspects of the Monte Carlo analysis are given in Appendix D.

Overall exceedance rates thus determined are compared with the describing function results in Fig. V-13. This comparison indicates that:

- For the 3.6 deg damper limit, describing function analysis adequately predicts limit load exceedance rates. However, linear analysis of the damper with no authority limit does almost as well because the effect of the non-linearity is not important at the design limit load. At increasing tail loads describing function analysis becomes more unconservative, though the differences are rather small.

- Halving the authority limit to 1.8 deg substantially decreases the accuracy of the describing function analysis. The Monte Carlo results indicate a 27% increase in the limit load from the value for the unlimited yaw damper, compared with the 20% increase previously noted for describing function analysis. The Monte Carlo data also indicates that the latter approach underestimates exceedance rates for 60,000 to 80,000 lb by roughly a factor of 2.

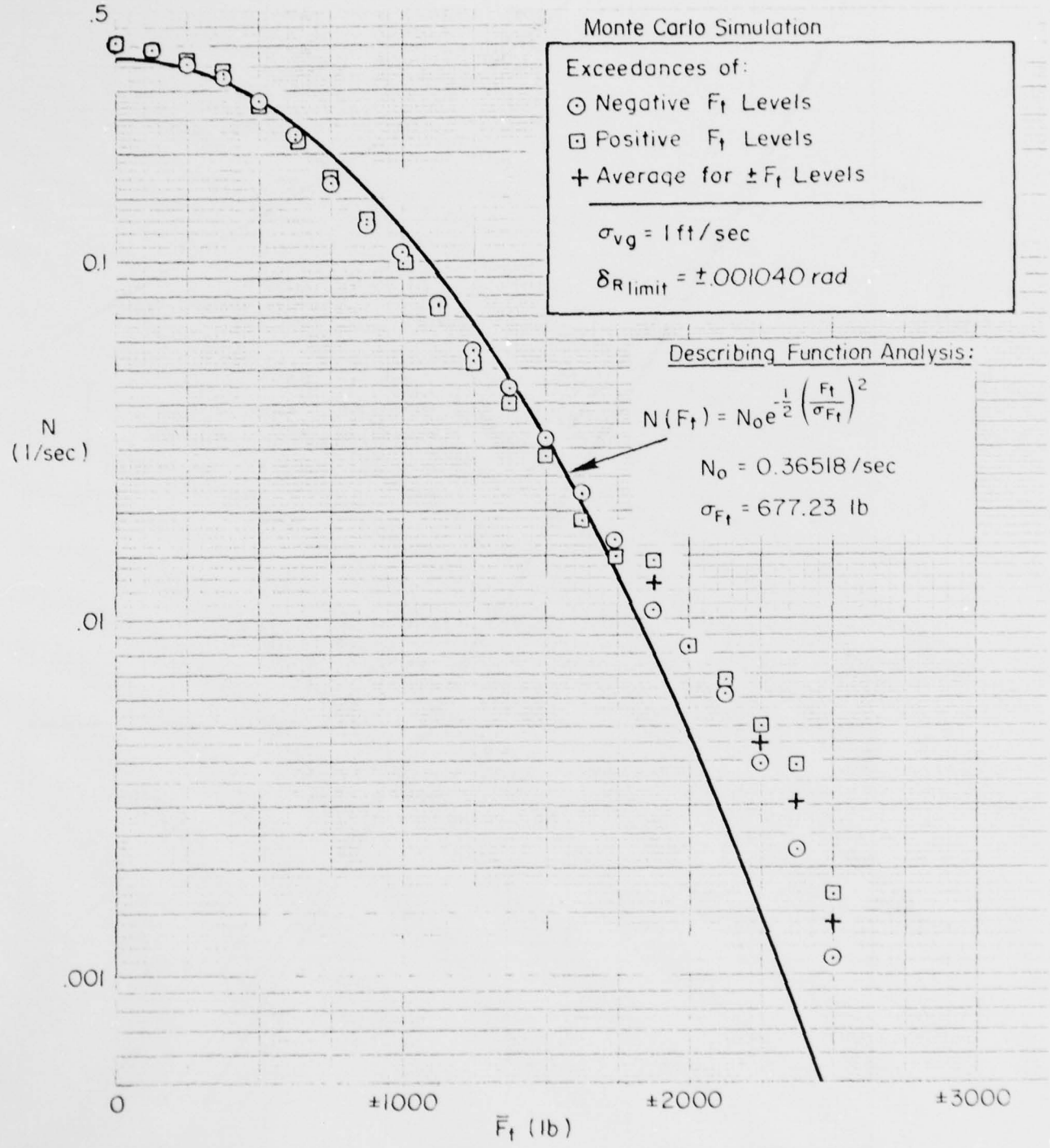

Figure V-12. Exceedance Rates for $k_{DF} = 0.6$

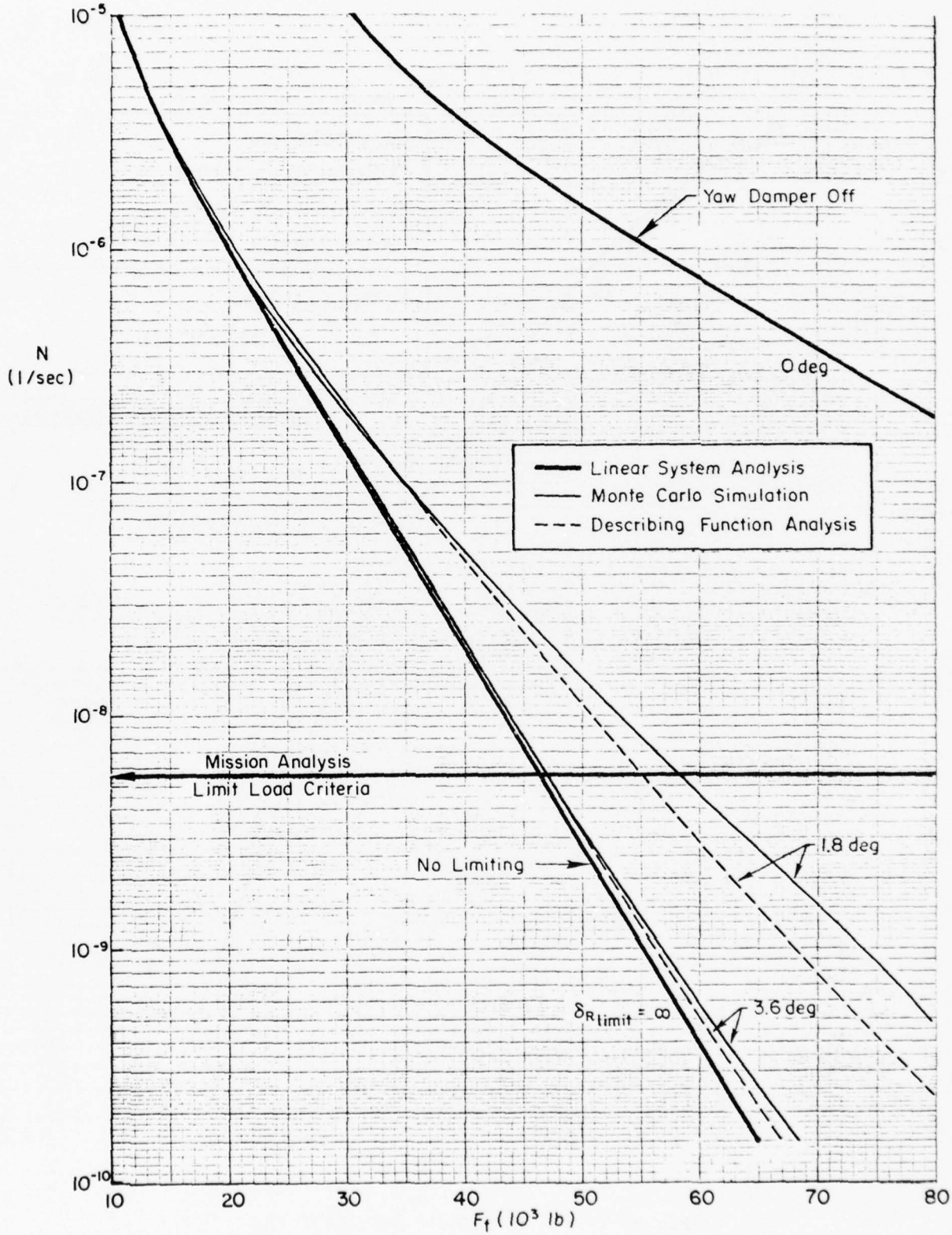

Figure V-13. Overall Exceedance Rates From Describing Function Analysis Versus Time Domain Simulation

Clearly, describing function analysis cannot be counted on to give a conservative estimate of design limit load.

As in comparing the linear (no limiting) vs. describing function results, differences between describing function and Monte Carlo overall results can be predicted from conditional exceedance rate data, though with considerably greater difficulty and less precision. Because a quantitative prediction could not be readily made in this case, it was not discussed previously. It is discussed here because the predictive process can be used to indicate the adequacy of describing function analysis.

The prediction focuses once again on the no-limiting design limit load. At the corresponding critical velocity previously determined (28.2 ft/sec), and a damper limit of 3.6 deg, the describing function gain, k_{DF}, is 0.98. Therefore, system behavior is nearly linear and either describing function or linear analysis is adequate. For a damper limit of 1.8 deg, k_{DF} is very close to 0.6. Thus conditional exceedance rates shown in Fig. V-12 apply, if F_t is scaled by $\hat{\sigma}_{v_g}$. At the scaled value of the design limit load, 1650 lb (46,511/28.2), differences between the describing function and Monte Carlo results are negligible. However, coincidence at this point can not be interpreted as verifying the describing function analysis.

Examination of the entire range of scaled tail loads in Fig. V-12 shows that the describing function results are not very accurate at other gust levels near $\hat{\sigma}_{v_g}$. The largest discrepancies occur at higher loads, or lower gust levels, where the Monte Carlo exceedance rates are considerably greater. The higher overall exceedance rates, and thus the higher design limit load, from the Monte Carlo analysis are therefore to be expected.

The Monte Carlo/describing function differences are shown clearly in Fig. V-14. The differences at the gust intensities below $\hat{\sigma}_{v_g}$ are obviously considerably more significant than the ones at higher gust levels. Furthermore, the magnitude of the difference could not be estimated by checking only one gust level. The two curves differ in shape and size.

The above discussion does not negate the importance of the $\hat{\sigma}_{v_g}$ gust level. It can still be used to evaluate a describing function analysis.

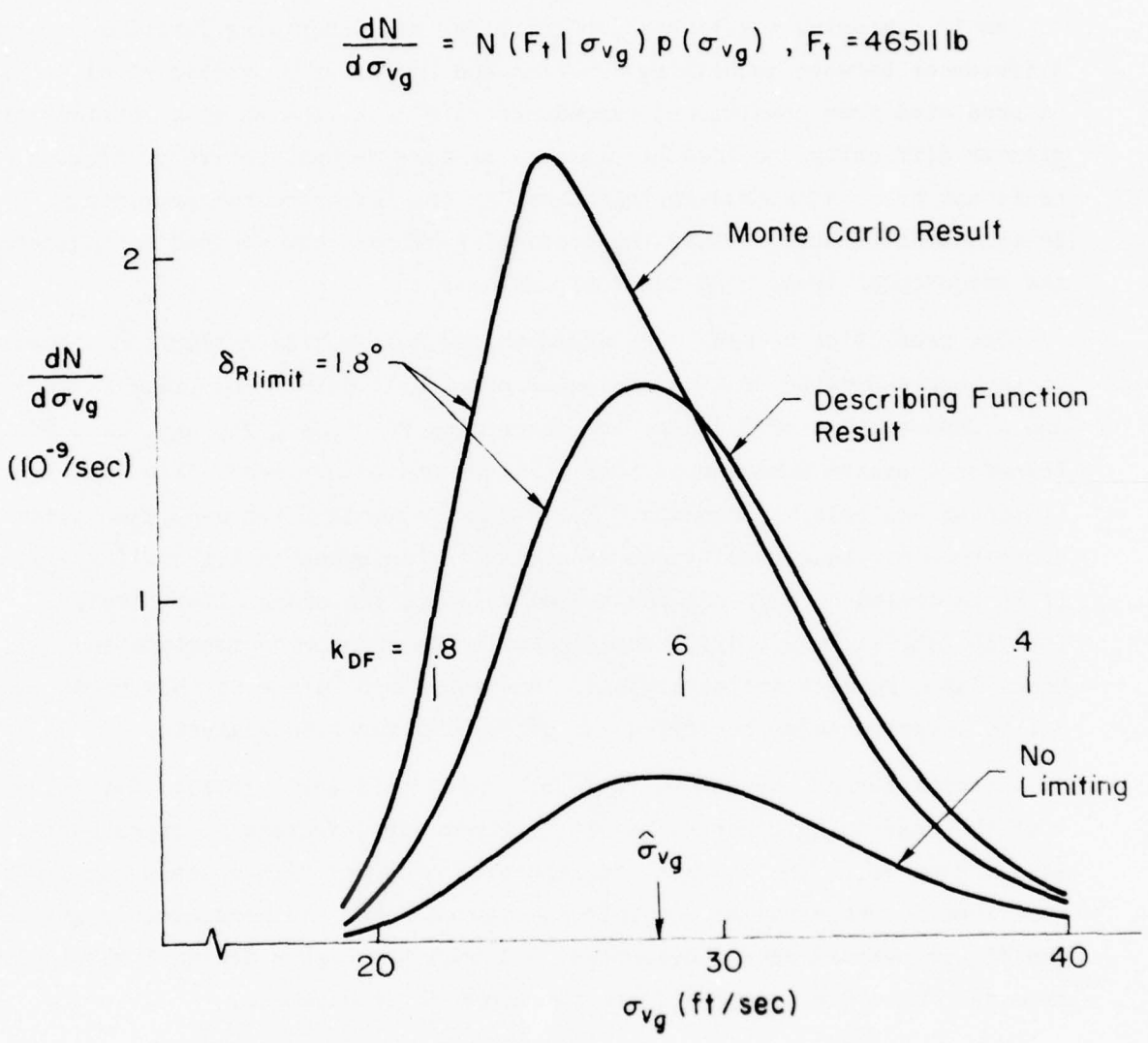

Figure V-14. Comparison of Variation of Overall Exceedance Rate Integrand

Comparison of Monte Carlo and describing function exceedance rates for that gust level will still indicate the validity of the describing function analysis; but, the comparison must include a broad range of loads about the design limit load.

4. Discussion

The effect of a simple, and not uncommon, control system nonlinearity on mission analysis calculations of design limit loads has been examined for a realistic aircraft design problem. Random input describing function analysis — a technique common in servo analysis work — was used to approximate the effect of the nonlinear element. This allows direct carryover of the standard power spectral techniques used for linear system analysis; however the computations must be repeated for various rms gust velocity levels, to define variations of $\bar{A}$ and N_o with gust level.

Through comparison with results obtained from a time domain simulation of the nonlinear system, it was shown that, for the example situation, the describing function approach tends to underestimate the frequency of large loads. For some levels of nonlinearity, it may provide a considerably unconservative estimate of design limit load. The basic problem is that describing function analysis can only approximate the loads as a normally-distributed random process. Within that constraint the describing function approach does a good job. However, as shown by the simulation, the loads in this case were not well represented by a normal distribution at gust levels at which system behavior was highly nonlinear.

It would be difficult to extrapolate this result to other situations involving, for example, different and/or multiple non-linearities. On the other hand, the routine use of a time domain simulation to establish design limit loads in every situation involving system nonlinearities is not an attractive alternative. A Monte Carlo analysis of such rare events as exceedances of design loads would be very costly, especially for large aircraft which require the inclusion of structural modes.

A simpler approach was adopted in the design of the L-1011 (Ref. 23):

> "The loads with yaw damper operative included a 5 percent increase to account for the slight degradation in yaw damper effectiveness at the limit load level due to saturation. This is a nonlinear effect and cannot, of course, be accounted for directly in the power spectral analysis. The percentage used was determined from analog computer simulations in which an appropriate continuous turbulence gust time history was used as an input, at several intensitites, and the airplane representation included the limiting rudder hinge moment."

Unfortunately, the reference doesn't detail the complexity of the simulation or the procedure used to estimate the design load increase from a few "appropriate" turbulence time histories.

The key to this approach lies in the selection of the appropriate gust intensities. As was shown for the example, the gust velocity which causes the greatest increment to the overall exceedance rate is easily determined for the linear system. It was also demonstrated that nonlinear effects do not change this critical gust velocity drastically; it is largely determined by the gust probability distribution and the load level of interest. The analysis also suggests a simple way of using this fact to minimize the costs of nonlinear analysis.

As noted, a critical gust level can be identified from the conventional linear analysis results. A describing function analysis for that gust level will indicate if the nonlinear effects are significant. If they are, a Monte Carlo simulation can be run at the critical gust level to determine the adequacy of the describing function analysis. The concept of a critical gust level is important because of the drastic cost increase in going from linear analysis to describing function analysis to Monte Carlo simulation. This concept provides a method for determining when either of the cheaper methods (linear or describing function analysis) is adequate.

As indicated in Refs. 23 and 26, determination of design loads by mission analysis requires a great deal of computational effort. The presence of significant nonlinearities, however, can greatly complicate the loads analysis, substantially increasing their cost. This example study has explored

some of the difficulties involved in such an analysis, examining the trade-offs between two likely approaches to the problem and offering a reasonable compromise between the two. There are, most certainly, other problems to be overcome before a general solution to the problem of including nonlinearities in mission analysis can be formulated.

SECTION VI

TURBULENCE PENETRATION AIRSPEED

The previous section reviewed and examined structural gust-load requirements. Whether or not those loads are reached in turbulence depends on many interactive elements, including the basic aircraft gust sensitivity, handling-qualities, stability and control characteristics, and pilot responses. A key factor in many of these elements is the airspeed at which the turbulence is penetrated. This section examines the relationship between the turbulence penetration airspeeds (V_{TP}) used by current jet transports and the Federal Aviation Regulations which provide the design and operational requirements which must be met by these aircraft. The purpose of this examination is to determine what might be done to better define turbulence penetration requirements.

The first subsection details the relevant FAR requirements. This is followed by a review of current design and operational practice with regard to V_{TP}. Subsection C discusses the factors involved in the selection of V_{TP} and new approaches to the selection process. The final subsection summarizes the present situation and offers some suggestions for possible improvements.

A. FAR REQUIREMENTS

To begin with, the regulations do not define turbulence penetration airspeed, explicitly. FAR Part 25, Airworthiness Standards, Transport Category Aircraft, requires only that, as part of the "Airplane Flight Manual... furnished with each aircraft" (§25.1581),

> "(a) Information and instructions...must be furnished, together with recommended procedures for — ....
>
> (8) Operation in turbulence for turbine powered airplanes (*including recommended* turbulence penetration airspeeds, flight peculiarities, and special control instruction)."

These procedures must be approved by the FAA. This is the only explicit reference to V_{TP} found in the regulations. However, as noted in Section V

the regulations do define V_B, the design speed for maximum gust intensity, in specifying the design gust V-n envelope for large aircraft.

As its definition implies, V_B is the airspeed at which the airplane is required to withstand the greatest discrete or continuous gust velocity. Note that this does not necessarily correspond to the highest load factor which may occur at a combination of higher airspeed and lower design gust velocity, e.g., V_C. In addition, load factor is not uniquely related to structural strength; load distribution may result in greater stresses in critical areas at lower values of load factor. What can be said is simply that the airplane is not required to be strong enough to withstand the maximum design gust velocity at a speed greater than V_B, without detrimental structural deformation.

Thus it would seem reasonable to expect that V_B structural requirements apply to the recommended airspeed for turbulence penetration. In effect, this would mean that V_{TP} must be chosen less than or equal to the selected V_B to provide adequate structural strength. On the other hand, the same considerations which dictate the lower limits on V_B also have relevance for V_{TP}. The various regulatory constraints on V_B selection are reviewed next, with Fig. VI-1 providing example V-n diagrams to illustrate key points.*

The minimum value of V_B is set by §25.335(d)(1):

> "(1) V_B may not be less than the speed determined by the intersection of the line representing the maximum positive lift $C_{N_{max}}$ and the line representing the rough air gust velocity on the gust V-n diagram, or $(\sqrt{n_g})V_{S_1}$, whichever is less, where —
>
> (i) n_g is the positive airplane gust load factor due to gust, at speed V_C (in accordance with §25.341), and at the particular weight under consideration; and
>
> (ii) V_{S_1} is the stalling speed with the flaps retracted at the particular weight under consideration."

The lower limit established by the intersection of the $C_{N_{max}}$ (stall) line and the V_B design gust load factor line is intended to provide a positive stall margin for gust velocities less than that of the V_B design gust.

---

*Other sample V-n diagrams are provided in Appendix E.

Figure V-10. Overall Exceedance Rates Based on Describing Function Analysis

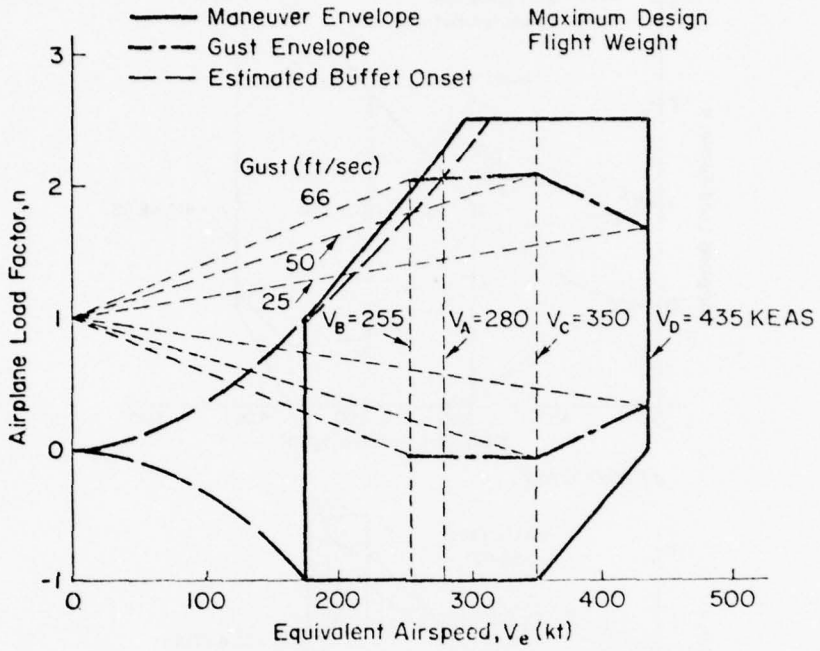

a) Sea Level

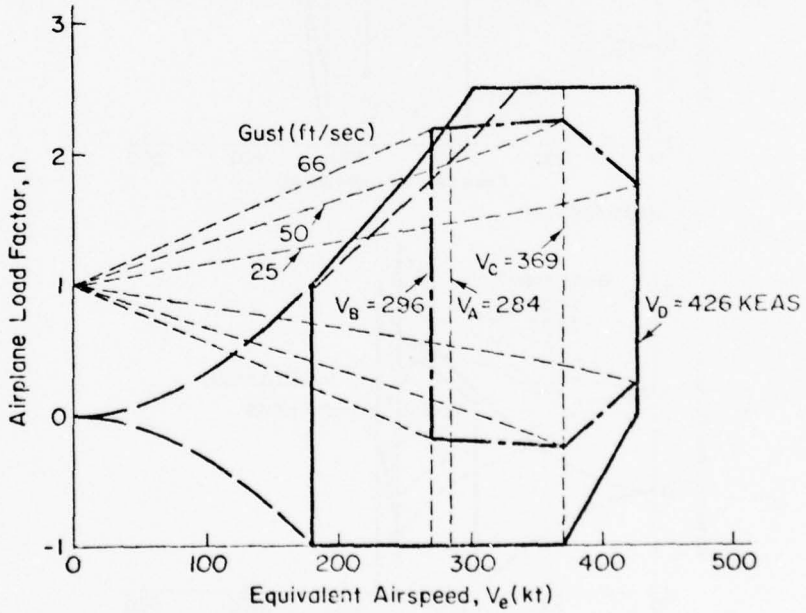

b) 10,000 feet

Figure VI-1. V-n Diagrams for Wide Body Jet Transport

Run length, of 15 hours (see Appendix

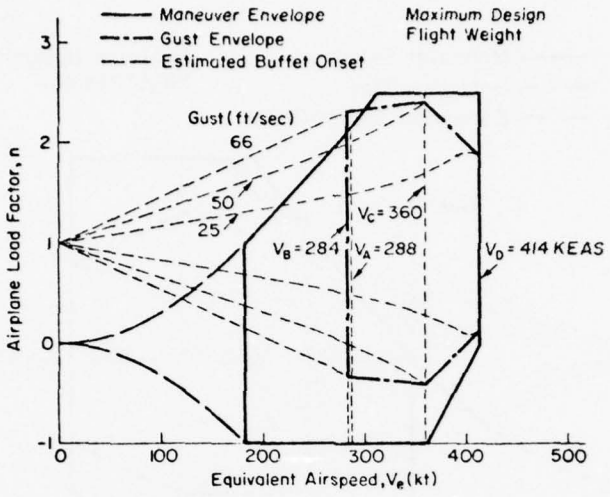

c) 20,000 feet

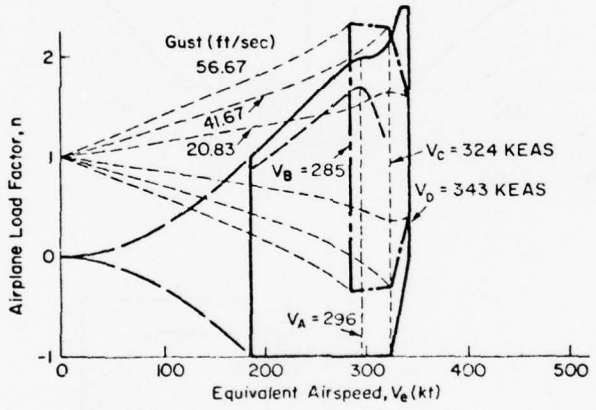

d) 30,000 feet

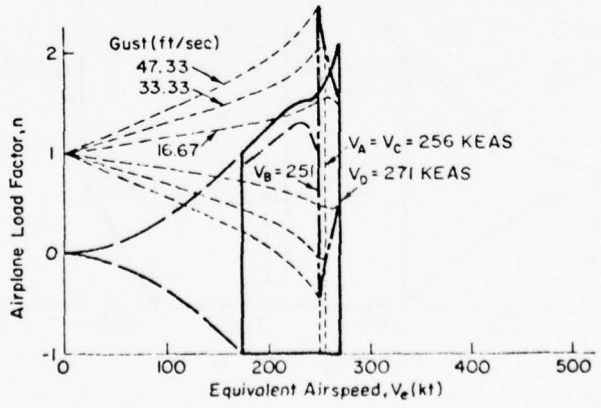

e) 40,000 feet

Figure VI-1. (Concluded)

However, the $C_{N_{max}}$ and V_B gust lines may not intersect. Mach number effects can cause a reduction in $C_{N_{max}}$ as speed increases. This phenomenon typically occurs at higher altitudes as shown in the example V-n diagrams of Fig. VI-1, particularly 1d and 1e.

The second V_B limit, $\sqrt{n_g}\, V_{s_1}$, provides an alternative when the intersection of the $C_{N_{max}}$ and V_B gust lines does not exist or is at very high speeds. Some appreciation for this second limit can be achieved by considering the case where there are no Mach effects on $C_{N_{max}}$. Then the second V_B limit would be defined by the intersection of the $C_{N_{max}}$ line* and load factor equal to n_g, see Fig. VI-2. It is interesting to note that in the example V-n diagrams of Fig. VI-1, V_B is actually set at the second limit, $\sqrt{n_g}\, V_{s_1}$.

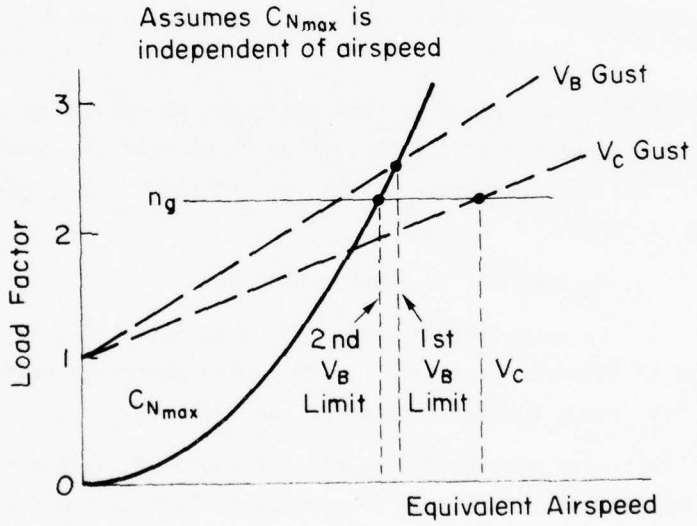

Figure VI-2. Illustration of V_B Lower Limits

Upper limits on V_B are imposed indirectly via explicit restrictions on the choice of V_C, as well as by the structural strength requirements resulting from that choice. The selection of V_C is based mainly on the consideration of operational requirements for performance/economy. The need to be competitive may dictate this selection.

*For $C_{N_{max}}$ invariant with speed, $n = (V/V_{s_1})^2$.

b) Limiting: $k_{DF} = .6$

Figure V-11. Sample Monte Carlo Simulation Time Histories

The explicit restrictions on V_C are given in §25.335(a):

> "(1) The minimum value of V_C must be sufficiently greater than V_B to provide for inadvertent speed increases likely to occur as a result of severe atmospheric turbulence.
>
> (2) In the absence of a rational investigation substantiating the use of other values, V_C may not be less than V_B + 43 knots. However, it need not exceed the maximum speed in level flight at maximum continuous power for the corresponding altitude.
>
> (3) At altitudes where V_D is limited by Mach number, V_C may be limited to a selected Mach number."

Because V_C is essentially predetermined by other requirements, these restrictions on minimum V_C may constitute upper limits on V_B. The basic intent of these limits is to provide a margin large enough to prevent the airplane from inadvertently reaching speeds at which severe turbulence would cause structural overload. The limits are not very restrictive.

At higher altitudes where V_C is limited by compressibility effects rather than structural considerations, there is no provision for a margin. In fact, the last paragraph of the V_B definition, §25.335(d), states that:

> "(2) V_B need not be greater than V_C."

implying that in the Mach-limited region V_B could exceed V_C. At lower altitudes the 43 kt margin required by §25.335(a) generally leaves an ample range from which V_B may be selected, see Fig. VI-1.

Maximum limits can also be indirectly imposed on V_B by the structural loads requirements of Part 25. As previously indicated, the design gust velocities for V_B are always greater than for V_C. Consequently, there is some value of V_B less than V_C for which the vertical gust load requirements for V_B exceed those for V_C. Selection of this value of V_B may require increased design structural strength which could mean an unacceptable increase in weight. Similar V_B loads requirements are imposed for discrete unsymmetrical vertical gusts (§25.351) and for lateral gusts (§25.349). These may also place upper limits on V_B to avoid adding more structural material.

B. CURRENT DESIGN AND OPERATIONAL PRACTICE

Prior to about 1963, the emphasis in selecting turbulence penetration airspeed was on maintaining large speed margins relative to structural limits. This was consistent with the performance capabilities of previous generation piston-engine transports, whose drag characteristics made it very difficult to exceed structural limit airspeeds (Ref. 27). However, concern caused by the upsets experienced by first generation jet transports shifted the emphasis to avoiding the control problems associated with low speeds (Refs. 28-30). For the most part, this emphasis is still reflected in current practice. At the lower altitudes, V_{TP} generally exceeds the minimum V_B prescribed by the regulation. At higher altitudes V_{TP} is set to a constant Mach number, the primary determinant of which is the peak of the buffet curve, see Fig. VI-3. This peak occurs at about the same Mach number independent of airplane weight and load factor. Besides providing the maximum load factor margin to buffet onset, this choice provides a reasonable balance between high and low speed margins. It appears that manufacturers generally meet Part 25 structural load requirements for V_B at V_{TP} at both high and low altitude.

Table VI-1 lists turbulence penetration airspeeds for common U.S. jet transports. The typical V_{TP} is an indicated airspeed in the vicinity of 280 KIAS at lower altitudes, changing to a Mach number close to 0.80 at higher altitudes. These numbers (280 KIAS and 0.80 M) were suggested as appropriate for most jet transports in Refs. 28 and 29, both of which were published in 1964. No explanation, save for the similarity of operational requirements, was found as a basis for this selection.

The preference for an altitude-independent V_{TP} is operationally motivated: it is easier for the pilot to remember. Trimming airspeed is a cut-and-try process in still air; its fluctuation in turbulence further complicates this adjustment (Ref. 31). Operating manuals generally warn against chasing airspeed (Refs. 32, 33, 34). The delay involved in looking up a reference airspeed can decrease the accuracy to which it can be established. In addition there is an increased chance for error in a tabular or graphical look-up.

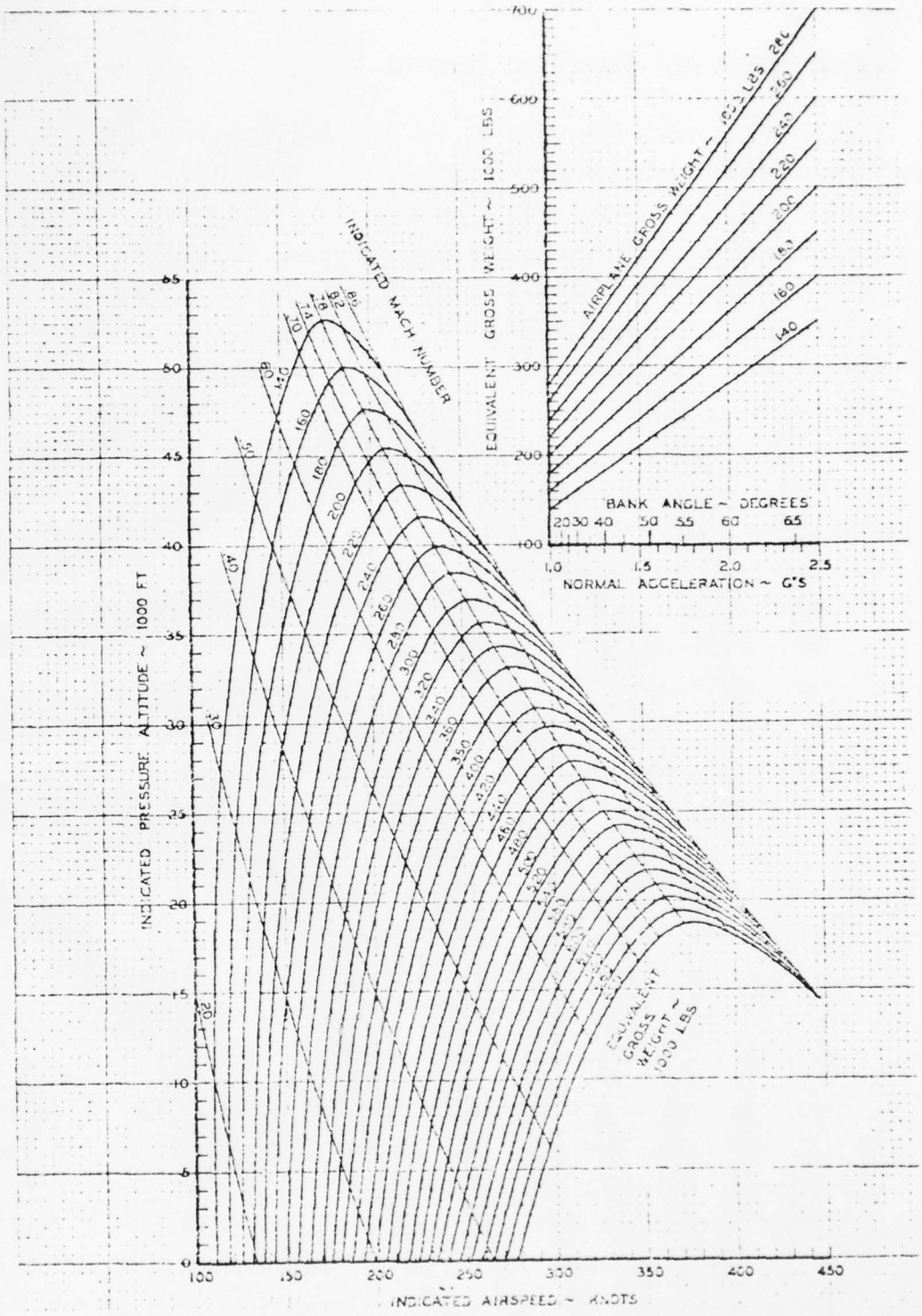

Figure VI-3. Typical Set of Jet Transport Buffet Boundaries

TABLE VI-1

TURBULENCE PENETRATION SPEEDS OF
COMMON U.S. JET TRANSPORTS[a]

AIRPLANE	V_{TP} (KIAS)	M_{TP}
Boeing 707	280	0.80
Boeing 720B	280	0.80
Boeing 727	280	0.80
Boeing 737	280	0.70
Boeing 747	280-290	0.82-0.85
Convair 880	280	0.80-0.84
Douglas DC-8	280[b]	0.80[b]
Douglas DC-9-10	265, 280	0.78
Douglas DC-9-30	285	0.79
Douglas DC-10	280-290	0.80-0.85
Lockheed L-1011	255-300[c]	0.80-0.84

[a]Speeds listed were extracted from manufacturer's or specific airline's manuals. Two values for DC-9-10 came from two different sources. In general, V_{TP} may vary with model variant. Approved alternatives may also exist for a given airplane.

[b]This single "rough air gust speed" was offered as alternative to a tabulated weight- and altitude-dependent "V_B" whose values were less than or equal to the former at all reference weights and altitudes.

[c]Scheduled from 255 KIAS at sea level, linearly increasing by 1.5 KIAS per 1000 ft to 300 KIAS at 30,000 ft where the Mach limit becomes dominant.

C. TURBULENCE PENETRATION AIRSPEED SELECTION FACTORS

Many factors should be considered in the selection of V_{TP}. Some of these factors tend to limit V_{TP} on the low side and others tend to limit it on the high side. Selection of V_{TP} is often then a compromise among these various considerations. Factors which tend to put lower bounds on V_{TP} are discussed below.

- V_{TP} must provide reasonable airspeed and angle-of-attack margins from both stall and low speed buffet.
- It is desirable to have V_{TP} high enough so the airplane is operating on the front side of the drag curve. When on the back side, any attempts to regulate altitude will cause a divergence if the throttles are left fixed. Since throttle manipulations in severe turbulence are discouraged, it is desirable to have the airplane on the front side.
- Aircraft responses tend to become sluggish as speed is decreased. Reducing speed reduces the frequencies of the short period, roll, and dutch roll modes.
- Reducing speed increases the size of control inputs required to balance the gust disturbances. For example, M_{δ_e} is proportional to speed squared but M_w is linear with speed. Therefore, the amount of elevator to balance the pitching moment from a unit vertical gust is inversely proportional to speed.

The above considerations tend to push V_{TP} up. The factors which provide upper bounds on V_{TP} are discussed next.

- V_{TP} must provide reasonable margins from the maximum design speed and from high speed buffet.
- Increasing speed generally increases the loads caused by a specified gust. This increases the probability of a structural failure and degrades the ride qualities of the airplane.
- Increasing Mach number can cause several adverse changes in the airplane handling qualities, e.g., an unstable spiral mode or a longitudinal tuck mode.

The best compromise among these conflicting considerations is often very difficult to establish. One reason is the inability to set up a uniform cost function for trading off the different factors. An initial step in this direction was taken by Ref. 35.

The approach used in that report was to define several constraints: maximum and minimum airspeed, maximum positive and negative load factors, and buffet. Power spectral analysis techniques were used to estimate the probability of exceeding any of the constraints. The calculations were repeated for variations in the trim altitude and airspeed. Optimum turbulence penetration speed was then selected on the basis of minimum probability of constraint exceedance, at each altitude, as shown in Fig. VI-4. For the results shown, airplane dynamics were augmented with a pure gain pitch angle feedback which provided a phugoid damping ratio of 0.7 for all flight conditions analyzed, simulating "loose" attitude control.

This concept appears to have considerable merit. However, the example computations were based on some important simplifications:

- No consideration was given to the relative risk associated with exceeding the different constraint boundaries.
- Analysis was confined to the three longitudinal degrees of freedom. Inclusion of the constraint boundaries associated with the lateral-directional axes could add considerable complexity to the computations.
- The structural boundary was defined by a single limit load factor. By contrast, in the L-1011 structural analysis exceedance curves for vertical gusts were calculated for 95 load quantities (shears, bending moments, torsions at different airframe locations) (Ref. 23).
- Rigid body airplane dynamics were used.
- The control law used to represent pilot inputs was overly simplified.

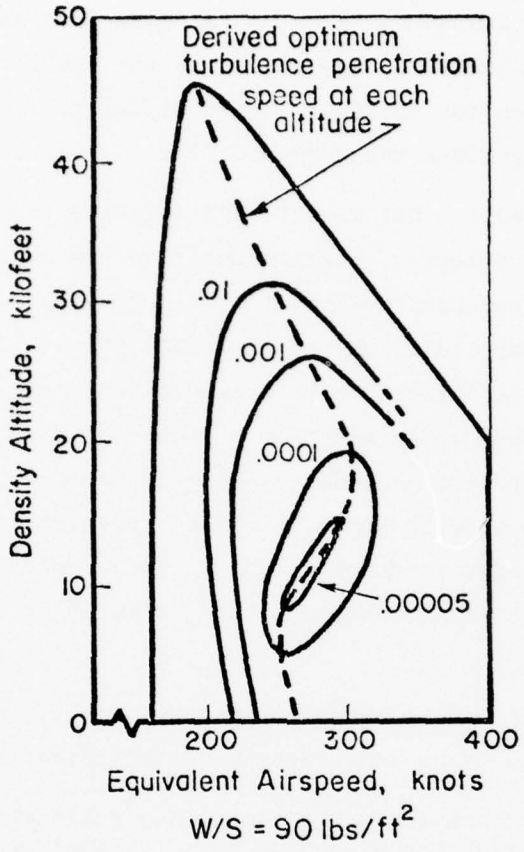

Figure VI-4. Probability Criterion Contours for Severe Turbulence, ($\sigma_w = \sigma_u = 30$ ft/sec), Loose Pitch Control, and 20 percent Static Margin (extracted from Ref. 35)

A comprehensive analysis including the above considerations does not, however, appear to be warranted, considering the complexity of such an analysis and in light of the imprecision with which key factors such as constraint boundary weighting could be set.

Figure VI-4 merits further consideration since it illustrates another important aspect of the V_{TP} definition — namely, the effects of altitude on constraint margins. Of particular interest is the rapid increase in constraint exceedance probability with altitude above roughly 20,000 ft at the optimum airspeed. This corresponds to the decreasing load factor margins indicated from the buffet boundaries, as shown earlier in Fig. VI-3.

Reference 32 recommends limiting turbulence penetration altitude to provide an incremental margin of 0.5 g. Similar advice given elsewhere (Refs. 29, 33, and 34) is less precise about how much margin to provide. From the typical buffet boundaries shown in Fig. VI-3, it appears that a margin of about 0.5 g would probably be reasonable. Much larger margins could require an undesirably large change in altitude when operating in a high weight condition.

In any analytical evaluation of turbulence penetration, an important problem is how to realistically account for likely pilot control actions. One solution proposed by the Air Force as part of its structural loads specifications (Ref. 36) is to provide for the possibility of using flight simulation to determine the effects of control inputs on structural loads when encountering extreme turbulence. A comprehensive simulation of this type would require a six-degree-of-freedom coupled nonlinear aircraft model with appropriate structural modes included. Load distribution calculations would not have to be made in real time. By recording data on the aircraft state (control deflections, angles of attack and sideslip, airspeed, etc.), load distribution calculations could be made off-line.

Such a simulation would obviously be a substantial undertaking, but it would provide an objective means of assessing structural loads in severe turbulence, including the effects of vehicle dynamics and pilot control actions. The simulation could also be used to refine turbulence penetration procedures and evaluate variations in turbulence penetration airspeed.

D. SUMMARY REMARKS

Selection of V_{TP} involves the consideration of many factors. One of the key considerations is the ability of the airplane to structurally withstand severe gust loads. While the most severe design gust requirements of Part 25 are imposed at V_B, the regulations do not impose an explicit relationship between V_B and V_{TP}. It appears that manufacturers generally elect to meet the V_B gust load requirements at the greater of V_B or V_{TP}. It would seem prudent to make this a requirement in the regulations.

Other factors in the selection of V_{TP} include the airplane handling qualities and margins from both stall and buffet. The current state of the art does not justify quantitative criteria for these factors. Perhaps the best that can reasonably be done is to require that these factors be carefully considered. On the other hand, use of a manned simulation to verify the choice of V_{TP} has much appeal. Since such a simulation is a substantial undertaking, it is not clear if it can reasonably be made a requirement. The idea does, however, merit further consideration.

The concept of a maximum turbulence penetration altitude should also be considered. Increasing altitude can substantially reduce margins* and increase the probability of exceeding airplane constraints. Definition of a maximum turbulence penetration altitude (as a function of weight) could be helpful to the pilot. Of course, the decision whether or not to descend when turbulence is anticipated would still be the pilot's. He would have to consider many factors including the possibility that the turbulence is worse at lower altitudes. The maximum turbulence penetration altitude would merely be a guide.

---

*For example, Fig. VI-3 illustrates the reduction in buffet margins with increasing altitude.

SECTION VII

SUMMARY

A significant portion of this project was spent on the analysis of data on accidents which involved aircraft structural failures in-flight. In reading this summary one should remember that the IFAF/in-flight airframe failure) statistics cited here do not include all recorded in-flight structural failures. Accidents were excluded for a number of reasons — the most common of which was a pre-existing structural deficiency. This includes fatigue damage and missing, improper, loose, damaged, or worn parts. Accidents involving aircraft which were not airworthy or were in violation of existing FAA regulations were outside the scope of the program.

The summary presented below is organized under several topics because of the number of distinct, but closely related, subjects covered in this report.

AIR CARRIER IFAF ACCIDENTS

- Although there are many turbulence accidents resulting in injuries to passengers or crew, there are few accidents involving fatalities or serious damage to the aircraft.
- There were only two IFAF accidents during the 10 year survey period, 1966-1975.
- One accident was probably the direct result of an extremely severe gust.
- The other was probably a structural overload in an attempted recovery from an upset induced by thunderstorm turbulence.

DATA FROM GENERAL AVIATION ACCIDENT BRIEFS

- IFAF accidents account for about 4 percent of the fatal general aviation accidents with an average IFAF rate of 0.1 per 10^5 flight hours.
- Seventy percent of the IFAF accidents involved pilots who were not instrument rated.

- Visibility was a major factor in the fatal IFAF accidents — probable IMC was nine times more frequent than probable VMC.

- Atmospheric turbulence was less of a factor in fatal accidents; the number of cases of turbulence or thunderstorm activity was only 10 percent greater than the number where there was no indication of turbulence.

- Most IFAF accidents would appear to result from loss of control rather than direct, gust-induced overloads.

- The IFAF accident rate of twin engine aircraft is slightly less than for single engine aircraft.

- Within the single engine category, retractable gear aircraft have a much greater IFAF accident rate (possibly a factor of 10) than fixed gear aircraft; this difference appears to be primarily a function of aircraft utilization.

- Within each of the three groups (single engine, fixed gear; single engine, retractable gear; twin engine) there is still a wide spread in IFAF accident rates for specific aircraft — from zero to several times the group average.

- In several cases these differences are statistically significant, some with a likelihood of less than 0.1 percent to have occurred by chance.

DATA FROM REVIEW OF SELECTED ACCIDENT FILES

- Statistics were compiled for 103 fatal accidents, involving 5 different aircraft.

- For all five aircraft, the incidence of probable IMC was very high (over 80 percent of the 103 accidents).

- For all aircraft, the incidence of precipitation was high (nearly 60 percent of the 103 accidents).

- The possibility of icing could only be eliminated in about 40 percent of the accidents.

- For the four aircraft with high accident rates for their group, only 13-36 percent of the pilots were instrument rated; for the Cessna 210, which had an accident rate slightly less than the group average, 67 percent of the pilots were instrument rated.

- Accidents of the Cessna 210 and, to a lesser extent, those of the PA-30 show more evidence of thunderstorm involvement than accidents for the other three aircraft.

- At least one wing failed in flight in all but 2 of the 103 accidents.

- From the data on the component which was the most likely to have separated from the aircraft first:
  - For the Cessna 210, the PA-24, and the PA-30, the wing was cited in 70 percent of the accidents — substantially more often than any other component.
  - For the Beech 35, the ruddevator was cited slightly more often than the wing.
  - For the Navion, the elevator was cited slightly more often than the wing, three versus two instances.

- Pilots involved in PA-24 accidents were generally less experienced (fewer flying hours) than pilots of the other four aircraft.

- Information from the Beech 35 accident files suggests that most of these accidents were due to loss of control in IMC rather than direct gust overloads.

- Most Cessna 210 IFAF accidents appear to result from: direct gust overloads; or loss of control in IMC and turbulence. The data are insufficient to distinguish between these two probable causes.

- Most Navion accidents appear to result from loss of control in IMC rather than direct gust overloads.

- Most Piper PA-24 accidents seem to fit the Beech 35 and Navion pattern — loss of control in IMC. There is, however, the definite possibility that some accidents were due to autopilot malfunctions or flutter of the vertical fin; but their relative importance cannot be estimated.

- PA-30 accidents seem to fit the typical pattern of mainly due to loss of control in IMC, although there is some evidence that thunderstorms were more of a factor than for the Beech 35, Navion, or PA-24.

CONTRIBUTING FACTORS IN GENERAL AVIATION IFAF ACCIDENTS

- There was insufficient data on the handling quality characteristics of specific aircraft to attempt a correlation between handling quality parameters and IFAF accident rates.

- No correlations were found between accident rates and margins between cruise and design limit speeds.

- All aircraft accelerate at approximately the same rate if the pilot lets the nose drop; however, high-performance aircraft maintain the acceleration longer. Equilibrium speed increase varies by more than 2:1 for different single engine aircraft.

- Speed increase in a spiral dive depends primarily on bank angle; aircraft characteristics have only secondary effects.

- In a spiral dive, high performance (higher L/D) aircraft reach smaller descent angles at the same bank angle.

- Apparent spiral stability is probably a significant factor in IFAF accidents.

- There can be significant differences between apparent spiral stability and the time constant of the classical spiral mode (differences are explained in subsection IV-E).

- Within current regulations it is possible to build an aircraft with control system lags large enough to cause problems in load factor control, although no known cases actually exist.

GUST LOADS

- For aircraft with high wing loading, proposed continuous gust criteria produce higher design load factors; for low wing loading, the existing discrete gust criteria produce higher loads.

- Proposed criteria for continuous gust loads do not account for effects of pilot control inputs which can substantially alter the loads.

- For the discrete gust criteria the effects of varying pitch response characteristics or control activity are rather minor; the effects are much greater for the continuous gust criteria.

- No validated model exists for pilot control behavior in severe turbulence; the range of likely pilot control behavior, based on our current knowledge, produces substantially different continuous gust loads.

- There is still substantial doubt as to the appropriate numerical values (and even the form) for a statistical model of continuous turbulence.

- With a lower value for gust scale length, as recommended by some researchers, the loads due to continuous gusts would be substantially increased.

EFFECTS OF NONLINEARITY ON CONTINUOUS GUST LOADS

- The example problem demonstrated that authority limits of an augmentation system can substantially increase design loads.

- A linearized analysis using the describing function approach can underestimate the design limit load.

- A relatively simple procedure has been developed to determine if a completely linear or describing function analysis is adequate, or if a Monte Carlo simulation is necessary.

TURBULENCE PENETRATION AIRSPEED

- Current regulations do not require the ability to withstand V_B gust loads at the turbulence penetration airspeed.

- A maximum turbulence penetration altitude might be advisable to provide adequate buffet margins.

- A manned simulation could be valuable in the selection of turbulence penetration airspeed and in the determination of gust induced loads including the effects of the pilot's control inputs.

REFERENCES

1. Wien Consolidated Airlines, Inc., Fairchild F-27B, N4905, Pedro Bay, Alaska, National Transportation Safety Board, AAR-70-16, July 1970.

2. Aircraft Accident Report, Saturn Airways, Inc., Lockheed L-382, N14ST, Springfield, Illinois, National Transportation Safety Board, AAR-75-5, Jan. 1975.

3. Cayce, Betty V., FAA Statistical Handbook of Aviation - Calendar Year 1975, 31 Dec. 1975.

4. Special Study — General Aviation Stall/Spin Accidents, 1967-1969, NTSB-ASS-72-8, Sept. 13, 1972.

5. Barber, Marvin R., Charles K. Jones, Thomas R. Sisk, and Fred W. Haise, An Evaluation of the Handling Qualities of Seven General-Aviation Aircraft, NASA TND-3726, Nov. 1966.

6. Greer, H. D., J. P. Shivers, M. P. Fink and C. R. Carter, Wind Tunnel Investigation of Static Longitudinal and Lateral Characteristics of a Full Scale Mockup of a Light Single Engine High Wing Airplane, NASA TN D-7149, May 1973.

7. Kohlman, D. L., Flight Test Data for a Cessna Cardinal, NASA CR-2337, Jan. 1974.

8. Roskam, J., Methods for Estimating Drag Polars of Subsonic Airplanes, copyright 1971 by the author.

9. Taylor, J. W. R., ed., Jane's All the World's Aircraft, 1973-74, London, Sampson Low, Marston and Co., Ltd., 1973.

10. Eckhart, Franklin F., et al., Flight Evaluation of a Stability Augmentation System for Light Airplanes, FAA-ADS-83, Nov. 1966.

11. Driscoll, Norman R., Effects of a Simple Stability Augmentation System on the Performance of Non-Instrument-Qualified Light-Aircraft Pilots During Instrument Flight, NASA TN D-3970, May 1967.

12. Campbell, John P., et al., Flight Investigation of the Effect of Control Centering Springs on the Apparent Spiral Stability of a Personal-Owner Airplane, NACA Rept. 1092, 1952.

13. Phillips, William H., A Flight Investigation of Short-Period Longitudinal Oscillations of an Airplane with Free Elevator, NACA Wartime Report L-444, May, 1942.

14. Neal, T. Peter, and R. E. Smith, An In-Flight Investigation to Develop Control System Design Criteria for Fighter Airplanes, AFFDL-TR-70-74, Dec. 1970.

15. Hodgkinson, J., W. J. La Manna and J. L. Heyde, "Handling Qualities of Aircraft with Stability and Control Augmentation Systems—A Fundamental Approach," The Aeronautical Journal, Vol. 80, No. 782, Feb. 1976, pp. 75-81.

16. Houbolt, John C., "Atmospheric Turbulence," AIAA Journal, Vol. 11, No. 4, April 1973, pp. 421-437.

17. Houbolt, John C., Updated Gust Design Values for Use With AFFDL-70-106, AFFDL-TR-73-148, Nov. 1973.

18. Clark, C. R., T. P. Neal, T. M. Harris, F. E. Pritchard, and R. J. Woodcock, Background Information and User Guide for MIL-F-8785B(ASG), Military Specification - Flying Qualities of Piloted Airplanes, AFFDL-TR-69-72, Aug. 1969.

19. Petrakis, John, and Nelson Miller, Responses of Small Rigid Aircraft to Discrete and Continuous Gust Analysis - Phase I, FAA-RD-74-160, Dec. 1975.

20. Peele, Ellwood L., A Method for Estimating Some Longitudinal and Lateral Rigid-Body Responses of Airplanes to Continuous Atmospheric Turbulence, NASA TN D-6273, Aug. 1971.

21. McRuer, Duane, Irving Ashkenas and Dunstan Graham, Aircraft Dynamics and Automatic Control, Princeton University Press, 1973.

22. Heffley, Robert K. and Wayne F. Jewell, Aircraft Handling Qualities Data, NASA CR-2144, Dec. 1972.

23. Stauffer, Warren A., and Frederic M. Hoblit, "Dynamic Gust, Landing, and Taxi Loads Determination in the Design of the L-1011," J. Aircraft, Vol. 10, No. 8, Aug. 1973, pp. 459-467.

24. Austin, William H., "The Effects of Atmospheric Turbulence on Handling Qualities and Structural Loads," presented at Royal Aeronautical Society, International Conference Atmospheric Turbulence, London, England, May 1971.

25. Graham, Dunstan and Duane McRuer, Analysis of Nonlinear Control Systems. New York, Dover, 1971.

26. Stauffer, Warren A., John G. Lewolt and Frederic M. Hoblit, "Application of Advanced Methods to Design Loads Determination for the L-1011 Transport," J. Aircraft, Vol. 10, No. 8, Aug. 1973, pp. 449-458.

AD-A064 156 SYSTEMS TECHNOLOGY INC HAWTHORNE CALIF F/G 1/2
A STUDY OF THE EFFECTS OF AIRCRAFT DYNAMIC CHARACTERISTICS ON S--ETC(U)
NOV 78 R L STAPLEFORD, R J DIMARCO DOT-FA77WA-3936
UNCLASSIFIED STI-TR-1099-1 FAA-RD-78-155 NL

3 OF 3
AD
A064156

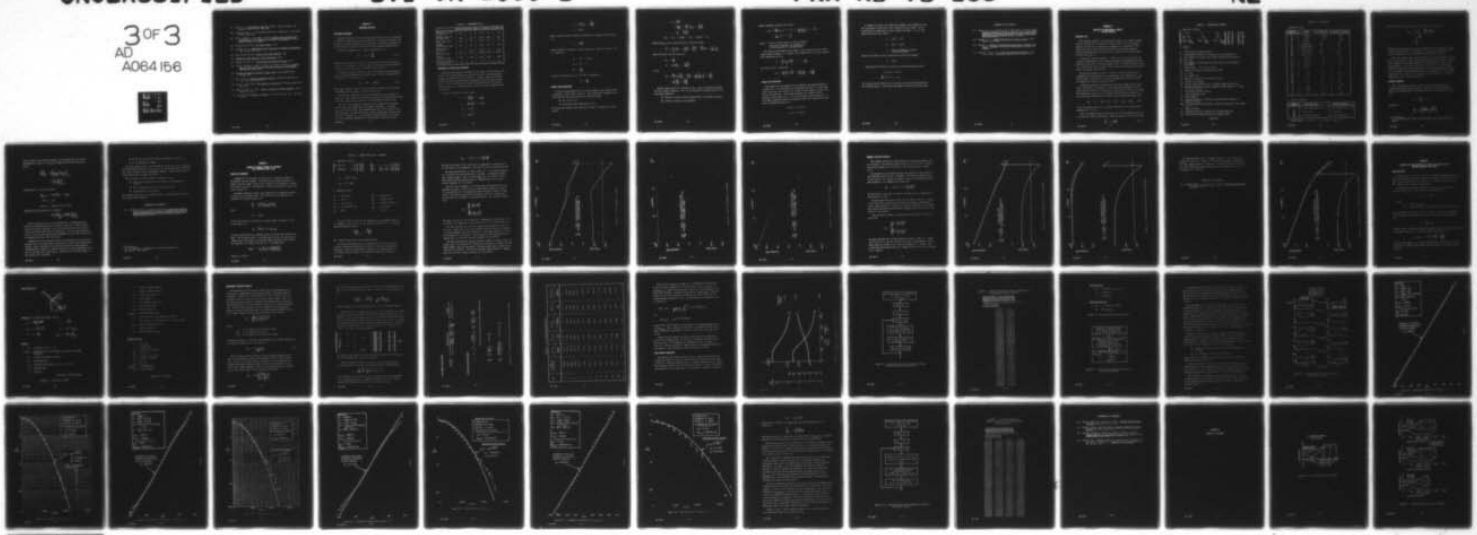

END
DATE
FILMED
3-79
DDC

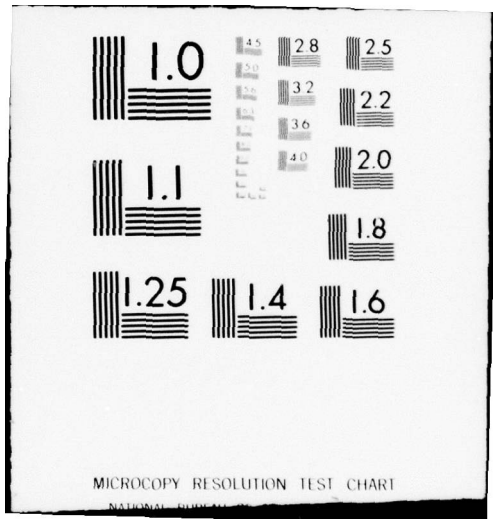
1.0
1.1
1.25
1.4
1.6
1.8
2.0
2.2
2.5
2.8
3.2
3.6
4.0
4.5
5.0
MICROCOPY RESOLUTION TEST CHART

27. Davies, D. P., Handling the Big Jets, Redhill, Surrey, England, ARB Brabazon House, 2nd ed., May 1968.

28. Soderlind, Paul A., "Jet Transport Operation in Turbulence," AIAA Paper 64-353, June 1964.

29. Sliff, Richard S., and James F. Rudolph, Operational and Design Considerations of the Sweptwing Jet Transport in Turbulence, Federal Aviation Admin., ca. 1963.

30. Continental Airlines, 727 Flight Manual, 1976.

31. Johnston, D. E., Fundamental Control Problems of Turbulence Penetration, STI, TR-1003, Dec. 1971.

32. Trans World Airlines, Convair 880 Flight Handbook, 1966.

33. Boeing 727 Flight Engineer's Training Manual, 1970.

34. Douglas Aircraft Co., DC-10 Flight Crew Operating Manual, 1976.

35. Porter, Richard F., James P. Loomis, and Alfred C. Robinson, A Procedure for Assessing Aircraft Turbulence-Penetration Performance, NASA CR-1510, Mar. 1970.

36. Airplane Strength and Rigidity Flight Loads, MIL-A-008861A(USAF), 31 Mar. 1971.

37. Ball, Larry A., Those Incomparable Bonanzas, McCormick-Armstrong Co., Inc., Wichita, Kansas, 1971.

38. Green, William, (Ed.), The Aircraft of the World, Doubleday, Garden City, NY, 1965.

39. Taylor, John W. R., (Ed.), Jane's Pocketbook of Light Aircraft, Collier Books, NY, 1976.

40. Etkin, Bernard, Dynamics of Flight, John Wiley and Sons, Inc., New York, 1959.

APPENDIX A

OVERSPEED ANALYSIS

LIFT/DRAG ESTIMATES

Reliable estimates of the lift/drag characteristics are not generally available for many general aviation aircraft. To evaluate overspeed tendencies of various airplanes it was necessary to develop a procedure for estimating the lift/drag characteristics from commonly available data.

The first assumption was a classic drag polar, i.e.,

$$C_D = C_{D_o} + \frac{C_L^2}{\pi e A} \qquad \text{(A-1)}$$

From the data of Ref. A-1 and A-2 it was found that Oswald's efficiency factor, e, was roughly 0.5 when dealing with trim (zero pitching moment) conditions. This value was then used for all aircraft.

The parasitic drag coefficient, C_{D_o}, was estimated from performance data. An overall propulsion efficiency, η_p, of 0.8 was assumed (based on data in Refs. A-1 to A-3), i.e.,

$$\eta_p P = DV = C_D \bar{q} VS \qquad \text{(A-2)}$$

The flight condition used for each aircraft was maximum sea level speed at maximum take-off weight, according to Ref. A-4.

The pertinent performance data and estimated C_{D_o} are summarized in Table A-1. Also listed are the cruise conditions (75 percent power) which were used as the initial conditions in the trajectory calculations.

The only other parameter required for the trajectory calculations was the lift curve slope, C_{L_α}, for trimmed conditions. A constant value of 4/rad was used. This parameter has very little effect on the speed increase. It only affects the initial flight path transient when the nose is lowered, i.e., the aircraft quickly returns to 1 g flight but with increasing airspeed due to the negative flight path angle.

TABLE A-1. PERFORMANCE DATA

	BEECH V35B	CESSNA 210	PA24-260	CESSNA 177	CESSNA 150
Maximum sea level speed (kt)	182	174	169	135	106
Maximum take-off weight (lb)	3400	3800	3200	2500	1600
Wing area (ft^2)	181	175	178	174	157
Engine horsepower (hp)	285	300	260	180	100
Wing aspect ratio	6.2	7.66	7.28	7.31	6.81
Estimated C_{D_o}	0.0172	0.0213	0.0203	0.0276	0.0345
Cruise altitude (ft)	6500	7500	6300	8000	7000
Cruise equivalent airspeed (kt)	160	146	147	110	92

EQUATIONS OF MOTION FOR PITCHOVER

Trajectory calculations were made for the speed increase which would result if the pilot pitched the aircraft nose down. The calculations assumed the aircraft started in level, 1 g flight. Then the aircraft pitched instantaneously through an angle $\Delta\theta$ and this attitude was held until t_1. At t_1 recovery is initiated by instantaneously increasing the load factor to n and holding that load factor until airspeed starts to decrease.

The basic equations of motion were:

$$\dot{V} = g\left(\frac{T-D}{W} - \sin\gamma\right)$$

$$\dot{\gamma} = \frac{g}{V}\left(\frac{L}{W} - \cos\gamma\right)$$

$$\dot{h} = V \sin\gamma$$

$$\bar{q} = \frac{1}{2}\rho V^2$$

$$D = \bar{q} S \left(C_{D_o} + \frac{C_L^2}{\pi e A} \right)$$

$$L = \bar{q} S C_L$$

Thrust variations with airspeed were modeled by assuming constant power, i.e.,

$$T = \frac{T_o V_o}{V}$$

where subscript o refers to initial conditions. Prior to recovery, lift is computed by:

$$C_L = C_{L_o} + C_{L_\alpha} \Delta\alpha$$

$$\Delta\alpha = \Delta\theta - \gamma$$

$$C_{L_o} = \frac{W}{\bar{q}_o S}$$

During the recovery ($t \geq t_1$), the lift is computed by:

$$C_L = \frac{nW}{\bar{q}S}$$

STEADY STATE EQUATIONS

If the pitch perturbation, $\Delta\theta$, is held constant, the airspeed tends to approach a steady state condition. The steady-state airspeed can be found from the above equations by the following steps:

- Set $\dot{V}$ and $\dot{\gamma}$ to 0
- Make small angle approximation for γ

The resulting equations are (subscript s refers to steady state conditions):

$$\gamma_s \doteq \frac{T-D}{W}$$

$$\doteq \frac{T_o V_o}{W V_s} - \frac{\bar{q}_s S}{W}\left[C_{D_o} + \frac{C_{L_s}^2}{\pi e A}\right]$$

$$1 \doteq \frac{L}{W} = \frac{\bar{q}_s S C_{L_s}}{W}$$

$$C_{L_s} = C_{L_o} + C_{L_\alpha}\Delta\alpha_s = C_{L_o} + C_{L_\alpha}(\Delta\theta - \gamma_s)$$

Eliminating C_{L_s} and γ_s from the above 3 equations gives:

$$-\Delta\theta \doteq \frac{1}{C_{L_\alpha}}\left(C_{L_o} - \frac{W}{\bar{q}_s S}\right) - \frac{T_o V_o}{W V_s} + \frac{\bar{q}_s S}{W} C_{D_o} + \frac{W}{\bar{q}_s S}\frac{1}{\pi e A}$$

Substituting the initial conditions

$$C_{L_o} = \frac{W}{\bar{q}_o S}$$

$$T_o = \bar{q}_o S\left(C_{D_o} + \frac{C_{L_o}^2}{\pi e A}\right)$$

gives:

$$-\Delta\theta \doteq \frac{\bar{q}_o S}{W} C_{D_o}\left(\frac{\bar{q}_s}{\bar{q}_o} - \frac{V_o}{V_s}\right) + \frac{W}{\bar{q}_o S}\left[\frac{1}{C_{L_\alpha}}\left(1 - \frac{\bar{q}_o}{\bar{q}_s}\right) + \frac{1}{\pi e A}\left(\frac{\bar{q}_o}{\bar{q}_s} - \frac{V_o}{V_s}\right)\right]$$

Further simplications are hindered by the mixture of equivalent ($\bar{q}_s/\bar{q}_o$) and true (V_s/V_o) airspeeds. This can be eliminated by making either of the following assumptions:

① Thrust is really inversely proportional to equivalent airspeed

② Density variations are negligible

Either assumption produces the result:

$$-\Delta\theta \doteq \frac{\bar{q}_o S}{W} C_{D_o} (\nu^2 - \nu^{-1}) + \frac{W}{\bar{q}_o S} \left[\frac{1}{C_{L_\alpha}} (1 - \nu^{-2}) + \frac{1}{\pi e A} (\nu^{-2} - \nu^{-1}) \right]$$

where ν = ratio of steady state to initial airspeed
(equivalent airspeeds for assumption ①
or true airspeeds for assumption ②)

The above pitch/airspeed relationship is quite linear even for rather large airspeed changes, so a simpler linear approximation is quite adequate. This simplification uses:

$$\nu^k = \left(\frac{V_o + \Delta V}{V_o} \right)^k \doteq 1 + k \frac{\Delta V}{V_o}$$

The final result is therefore:

$$-\Delta\theta \doteq \frac{\Delta V}{V_o} \left[3 C_{D_o} \frac{\bar{q}_o S}{W} + \frac{W}{\bar{q}_o S} \left(\frac{2}{C_{L_\alpha}} - \frac{1}{\pi e A} \right) \right]$$

SPIRAL DIVE EQUATIONS

The purpose of this analysis was to determine the speed increase in a spiral dive. By considering the independent variable to be bank angle rather than time, the analysis can be made without regard to spiral stability considerations. The analysis assumes the aircraft starts in straight, level flight ($\varphi = \gamma = 0$) and bank angle slowly increases. If bank angle increases slowly, acceleration terms can be neglected and the basic lift/drag equations are:

$$L \cos \varphi = W \cos \gamma$$

$$T - D = W \sin \gamma$$

To compute the speed and flight path changes, some assumptions about the longitudinal control and thrust variations must be made. It was assumed that no longitudinal control changes are made, i.e., lift and drag coefficients are constant.

$$L = L_o \nu^2 = W \nu^2$$

$$D = D_o \nu^2 = T_o \nu^2$$

ν = ratio of present to initial equivalent airspeed

Thrust was assumed to vary inversely with equivalent airspeed.

$$T = T_o \nu^{-1}$$

Substituting the above into the basic lift/drag equations gives:

$$\nu^2 \cos \varphi = \cos \gamma$$

$$\frac{T_o}{W} (\nu^{-1} - \nu^2) = \sin \gamma$$

For a given thrust/weight ratio, the above can be solved numerically for the airspeed ratio, ν, and flight path angle as functions of bank angle.

REFERENCES FOR APPENDIX A

A-1. Greer, H. D., J. P. Shivers, M. P. Fink, and C. R. Carter, Wind Tunnel Investigation of Static Longitudinal and Lateral Characteristics of a Full Scale Mockup of a Light Single Engine High Wing Airplane, NASA TN D-7149, May 1973.

A-2. Kohlman, D. L., Flight Test Data for a Cessna Cardinal, NASA CR-2337, Jan. 1974.

A-3. Roskam, J., Methods for Estimating Drag Polars of Subsonic Airplanes, copyright 1971 by the author (LC Cat. Card No. 73-173351).

A-4. Taylor, J. W. R., ed., Jane's All the World's Aircraft, 1973-1974, London, Sampson Low, Marston and Co., Ltd., 1973.

APPENDIX B

ANALYSIS OF LONGITUDINAL CONTROL SYSTEM DYNAMICS

BASELINE CASE

This analysis examines the longitudinal dynamics of a typical general aviation aircraft with a reversible control system. For the frequency range of concern here, variations in airspeed can be neglected. This leaves the classic short period equations plus an elevator equation. The resulting equations of motion, shown in Table B-1, were taken almost directly from Ref. B-1.

To provide a specific example, a cruise of 150 kt IAS at 7000 ft was selected as reasonable for the higher performance single-engine aircraft. Numerical values for an aircraft roughly similar to a Beech Bonanza, Cessna 210, or Mooney M20 were estimated. These values are indicated in Table B-1 under the heading "Baseline Case."

The baseline dynamics consist of 4 poles. Two real roots from an overdamped short period mode and a complex pair, the elevator mode. The elevator mode is clearly at too high a frequency (63.3 rad/sec) to have any significant effects on manual control.

Differences between stick-fixed and stick-free dynamics were considered. The former is equivalent to treating elevator deflection as the input, while the latter is equivalent to treating stick force as the input. The differences are only in the transfer function poles, not the zeros. The stick-fixed characteristic equation is the classic short period one.

$$\Delta_{sp} = s^2 - (M_{\dot{\alpha}} + M_q + Z_w)s - M_\alpha + Z_w M_q \qquad \text{(B-1)}$$

For the baseline case this is a natural frequency of 4.51 rad/sec and a damping ratio of 0.79.

That the numerator zeros are the same for control deflection and control force is easily demonstrated. From the equations of motion we find:

$$\frac{\delta_e}{F_s} = r\ell_s \frac{\Delta_{sp}}{\Delta} \qquad \text{(B-1)}$$

TABLE B-1. LONGITUDINAL DYNAMICS

a. Equations of Motion

$$\begin{bmatrix} s - Z_w & -1 & -Z_{\dot{\delta}_e} \\ -M_{\dot{\alpha}}s - M_\alpha & s - M_q & -M_{\delta_e} \\ [(U_o H'_{\dot{e}} - H_{\dot{\alpha}})s - H_\alpha] & [I''_e s - U_o H'_{\dot{e}} - H_q] & [I'_e s^2 - H_{\dot{\delta}_e} s - H_{\delta_e}] \end{bmatrix} \begin{bmatrix} \alpha \\ q \\ \delta_e \end{bmatrix} = \begin{bmatrix} 0 \\ 0 \\ r\ell_s \end{bmatrix} F_s$$

b. Symbols

F_s Stick force, positive for push

H Hinge moment, positive for tending to trailing edge down

H_e Mass moment of elevator about hinge, positive for tail heavy

H'_e $H_e + rH_s$

H_s Mass moment of stick about its pivot, positive for tending to go forward

H_λ $\partial H/\partial\lambda$ where $\lambda = \alpha, \dot{\alpha}, q, \delta_e$, or $\dot{\delta}_e$

I_e Moment of inertia of elevator about hinge

I'_e $I_e + r^2 I_s$

I''_e $I_e + H_e L_h - rI_s$

I_s Moment of inertia of stick about its pivot

ℓ_s Control stick length

L_h Distance from aircraft c.g. to elevator hinge, positive aft

M_λ Partial derivative of pitch acceleration with respect to λ, where $\lambda = \alpha, \dot{\alpha}, q$, or δ_e

q Pitch rate, positive nose up

r *Control gearing, θ_s/δ_e*

U_o True airspeed

Z_w Partial derivative of vertical acceleration with respect to vertical velocity

$Z_{\dot{\delta}_e}$ $1/U_o$ times partial derivative of vertical acceleration with respect to δ_e

α Angle of attack

δ_e Elevator deflection, positive for trailing edge down

θ_s Stick rotation angle, positive for forward motion

(continued)

TABLE B-1. (Continued)

c. Numerical Values

PARAMETER	UNITS	BASELINE CASE	MODIFIED DYNAMICS
H_e	slug-ft	0.040	0.04
H'_e	slug-ft	0.040	0.144
H_s	slug-ft	0	0.311
H_α	ft-lb/rad	−400	−80
$H_{\dot{\alpha}}$	ft-lb-sec/rad	−21	−4
H_q	ft-lb-sec/rad	−42	−8
H_{δ_e}	ft-lb/rad	−1200	−251
$H_{\dot{\delta}_e}$	ft-lb-sec/rad	−23	−80
I_e	slug-ft^2	0.3	0.3
I'_e	slug-ft^2	0.3	0.3
I''_e	slug-ft^2	0.9	0.9
I_s	slug-ft^2	0	0
ℓ_s	ft	2	2
L_h	ft	15	15
M_α	sec^{-2}	−12.5	−12.5
$M_{\dot{\alpha}}$	sec^{-1}	−1.5	−1.5
M_q	sec^{-1}	−3	−3
M_{δ_e}	sec^{-2}	−35	−35
r	——	0.333	0.333
U_o	ft/sec	281	281
Z_w	sec^{-1}	−2.6	−2.6
$Z_{\dot{\delta}_e}$	sec^{-1}	−0.27	−0.27

d. Transfer Functions

ELEMENT	BASELINE CASE*	MODIFIED DYNAMICS*
Δ	0.3(1.64)(3.71)[.62, 63.3]	0.3(5.33)(264)[.63, 3.48]
$N^q_{F_s}$	−23.1(2.53)	−23.1(2.53)
$N^{n_z}_{F_s}$	−1.57(−15.9)(20.4)	−1.57(−15.9)(20.4)

* Abbreviations: (a) for $s + a$; $[\zeta, \omega]$ for $s^2 + 2\zeta\omega s + \omega^2$

The pitch rate/stick force transfer function can be written as:

$$q/F_s = \frac{q}{\delta_e}\frac{\delta_e}{F_s} \qquad \frac{N^q_{\delta e}}{\Delta_{sp}}\frac{r\ell_s\ \Delta_{cp}}{\Delta}$$

$$= r\ell_s \frac{N^q_{\delta e}}{\Delta}$$

$$= \frac{N^q_{F_s}}{\Delta}$$

Clearly the q/δ_e and q/F_s zeros are identical. This also holds for angle of attack and load factor. Furthermore, the zeros are independent of the elevator characteristics (hinge moment derivatives and inertias).

Since the control system characteristics do not effect transfer function zeros, we only have to worry about possible effects on the poles. In the past, analyses of stick-free dynamics often concentrated on the destabilizing effects on the short period mode. This is not a concern here as FAR Part 23 requires the short period to be heavily damped both stick-free and stick-fixed. The problem thus reduces to determining if the elevator mode poles can be such as to cause pilot control difficulties. Current regulations do not cover that situation.

MODIFIED DYNAMICS

When considering potential locations for the stick-free poles, an important constraint must be observed. This constraint can be derived from the load factor/stick force transfer function. Load factor is given by*:

$$n_z = \frac{U_o}{g}(\dot{\alpha} - q)$$

Therefore:

$$\frac{n_z}{F_s} = \frac{U_o}{g}\left[\frac{sN^{\dot{\alpha}}_{F_s} - N^q_{F_s}}{\Delta}\right]$$

---

* n_z is defined positive down to be consistent with F_s being positive for a push.

The dc value of this transfer function is the steady-state g's per lb. Inverting this to put it in the more common form of stick force per g gives:

$$\left(\frac{F_s}{n_z}\right)_{dc} = \frac{g}{U_o}\left[\frac{\Delta}{sN^{\alpha}_{F_s} - N^{q}_{F_s}}\right]_{s=0}$$

$$= -\frac{g}{U_o}\left(\frac{\Delta}{N^{q}_{F_s}}\right)_{s=0}$$

From Table B-1 it can be seen that:

$$(N^{q}_{F_s})_{s=0} = r\ell_s\,(M_{\alpha}Z^{*}_{\delta_e} - M_{\delta_e}Z_w)$$

$$(\Delta)_{s=0} = I'_e\,P$$

where P = product of the 4 poles

Combining the above gives the constraint:

$$P = \frac{r\ell_s\,(Z_{\alpha}M_{\delta_e} - M_{\alpha}Z_{\delta_e})}{gI'_e}\left(\frac{F_s}{n_z}\right)_{dc}$$

For the baseline case, P = 24,500 $(rad/sec)^4$. Airworthiness and practical considerations prevent a drastic reduction in P and a drastic reduction would be necessary to get the elevator poles from 63 rad/sec to the point where they could be troublesome. The only remaining possibility is to have the elevator mode overdamped with one pole at relatively low frequency and the other very large.

Examination of the equations of motion indicated this could be accomplished only if the hinge moment derivatives, H_{α} and H_{δ} were significantly reduced. This is possible if the elevator were more closely balanced aerodynamically; however, it would be necessary to add a bobweight to maintain a reasonable stick force per g. Therefore the following changes to the baseline case were made.

- H_α, $H_{\dot{\alpha}}$, H_q, and H_{δ_e} were reduced by roughly a factor of 5
- A 5 lb bobweight was added*

One final change to get a lower frequency elevator pole was to increase the hinge moment derivative, $H_{\dot{\delta}_e}$, from −23 to −80 ft-lb-sec/rad. The baseline value included only the aerodynamic damping. Control system friction could substantially increase that value.

The net result of these changes (see Table B-1) was:

- Short period frequency of 3.48 rad/sec with damping ratio of 0.63
- Real elevator mode poles at 5.33 and 264 sec^{-1}
- Force gradient of 10 lb per g

This demonstrates that it is possible to have a low frequency pole due to the control system dynamics.

REFERENCE FOR APPENDIX B

B-1. Greenberg, Harry, and Leonard Sternfield, A Theoretical Investigation of Longitudinal Stability of Airplanes with Free Controls Including Effect of Friction in Control System, NACA ARR No. 4B01, Feb. 1944.

* A 5 lb bobweight is equivalent to a stick mass unbalance of $H_s = 5\ell_s/g = 0.31$ slug-ft.

APPENDIX C

EFFECTS OF MANUAL CONTROL ON DISCRETE AND CONTINUOUS GUST LOADS

JUMBO JET TRANSPORT

A Boeing 747 was selected for analysis as an opposite extreme to the general aviation example. Aircraft data were taken from Ref. C-1. Flight condition number 7 (Mach 0.8 at 20,000 ft) was picked as a reasonable cruise condition. The equations of motion and numerical values are given in Table C-1.

Unsteady aerodynamic effects were approximated by applying Kussner's function to all the gust terms. This resulted in the addition of an unsteady lift transfer function of:

$$\frac{\hat{w}_g}{w_g} = \frac{0.565\omega_a(s + 0.23\omega_a)}{(s + 0.13\omega_a)(s + \omega_a)}$$

where

$$\omega_a = 2U_o/\bar{c}$$

For the discrete gust calculations, the gust shape of FAR Part 23 and 25 was used, i.e.,

$$w_g = \frac{U_{de}}{2}\left(1 - \cos\frac{\pi}{25}\omega_a t\right)$$

The peak load factors were computed using an existing time response program. For continuous gusts, the Dryden gust spectral form was used for computational convenience (an existing computer program could evaluate rms responses for a Dryden form but not a von Karman form).

$$\Phi_{w_g}(\omega) = \sigma^2_{w_g}\frac{L_w}{\pi U_o}\frac{1 + 3(\omega L_w/U_o)^2}{\left[1 + (\omega L_w/U_o)^2\right]^2}$$

where L_w = 1750 ft.

TABLE C-1. DYNAMIC MODEL FOR 747 EXAMPLE

a. Equations of Motion

$$\begin{bmatrix} s(1-Z_{\dot{w}})-Z_w & -U_o s \\ -M_{\dot{w}}s-M_w & s(s-M_q) \end{bmatrix} \begin{bmatrix} w \\ \theta \end{bmatrix} = \begin{bmatrix} Z_{\delta_e} & -Z_{\dot{w}}s-Z_w \\ M_{\delta_e} & \left(\frac{M_q}{U_o}-M_{\dot{w}}\right)s-M_w \end{bmatrix} \begin{bmatrix} \delta_e \\ \hat{w}_g \end{bmatrix}$$

$$n_z = \frac{s}{g}(w - U_o\theta)$$

$$n_{z_p} = n_z - \ell_p s^2\theta$$

b. Numerical Values

U_o	= 830 ft/sec	M_q	= -0.668 sec^{-1}
$Z_{\dot{w}}$	= 0.0144	$M_{\dot{w}}$	= -0.000212 ft^{-1}
Z_w	= -0.624 sec^{-1}	M_w	= -0.00153 ft^{-1}sec^{-1}
Z_{δ_e}	= -32.7 ft/sec^2-rad	M_{δ_e}	= -2.08 sec^{-2}
ℓ_p	= 86 ft	$\bar{c}$	= 27.31 ft

For each control situation, the appropriate n_z/w_g transfer function was computed. For the case of zero attitude change, this is a coupling numerator/numerator ratio:

$$\left(\frac{n_z}{w_g}\right)_{\theta=0} = \frac{N_{w_g}^{n_z\theta}\delta_e}{N_{\delta_e}^{\theta}}$$

The 3 manual control cases are described below.

For the pitch feedback case, an examination of the θ/δ_e transfer function indicated the desire for a pilot lead near the short period frequency. This lead is required to produce a K/s characteristic in the likely crossover region. The pilot model which was used was:

$$Y_{p_\theta} = -K_\theta (s + 1.5) \left(\frac{s - 8}{s + 8}\right)^2$$

The poles and zeros at ±8 rad/sec are to approximate a time delay of 0.5 sec which is the appropriate value when the pilot is generating lead.

The open-loop Bode plot is shown in Fig. C-1. A crossover frequency of 1.7 rad/sec was selected because it provides a 45 deg phase margin and 6 dB gain margin. This is a pilot gain, K_θ, of −5 dB or 0.56 sec. The closed-loop short-period mode has a damping ratio of 0.21 and a natural frequency of 1.42 rad/sec.

For load factor feedback, it is clear that lead equalization is not required as nz_p/δ_e is flat out to the short-period frequency. Because of uncertainties as to an appropriate model for manual control of load factor, two different types were considered. One was no equalization and the other was integral (or lag) equalization. The two pilot models were:

$$Y_{pn} = \begin{cases} K_n \left(\frac{s - 12}{s + 12}\right)^2 \\ \frac{K\int_n}{s} \left(\frac{s - 12}{s + 12}\right)^2 \end{cases}$$

The poles and zeros at ±12 rad/sec are to approximate a time delay of 1/3 sec which is the appropriate value when the pilot is not generating lead.

The open-loop Bode plot for the straight gain feedback is shown in Fig. C-2. A gain, K_n, of −49 dB or 0.00355 rad/g was selected to provide a 6 dB gain margin. This also provides a 53 deg phase margin and a crossover frequency of 1.55 rad/sec. The closed-loop short-period mode has a damping ratio of 0.18 and a natural frequency of 1.80 rad/sec.

The open-loop Bode plot for the integral feedback is shown in Fig. C-3. A gain, $K\int_n$, of −60 dB or 10^{-3} rad/g-sec was selected to provide a 45 deg phase margin. This also provides a 7 dB gain margin and a crossover frequency of 0.62 rad/sec. The closed-loop short-period mode has a damping ratio of 0.21 and a natural frequency of 0.95 rad/sec.

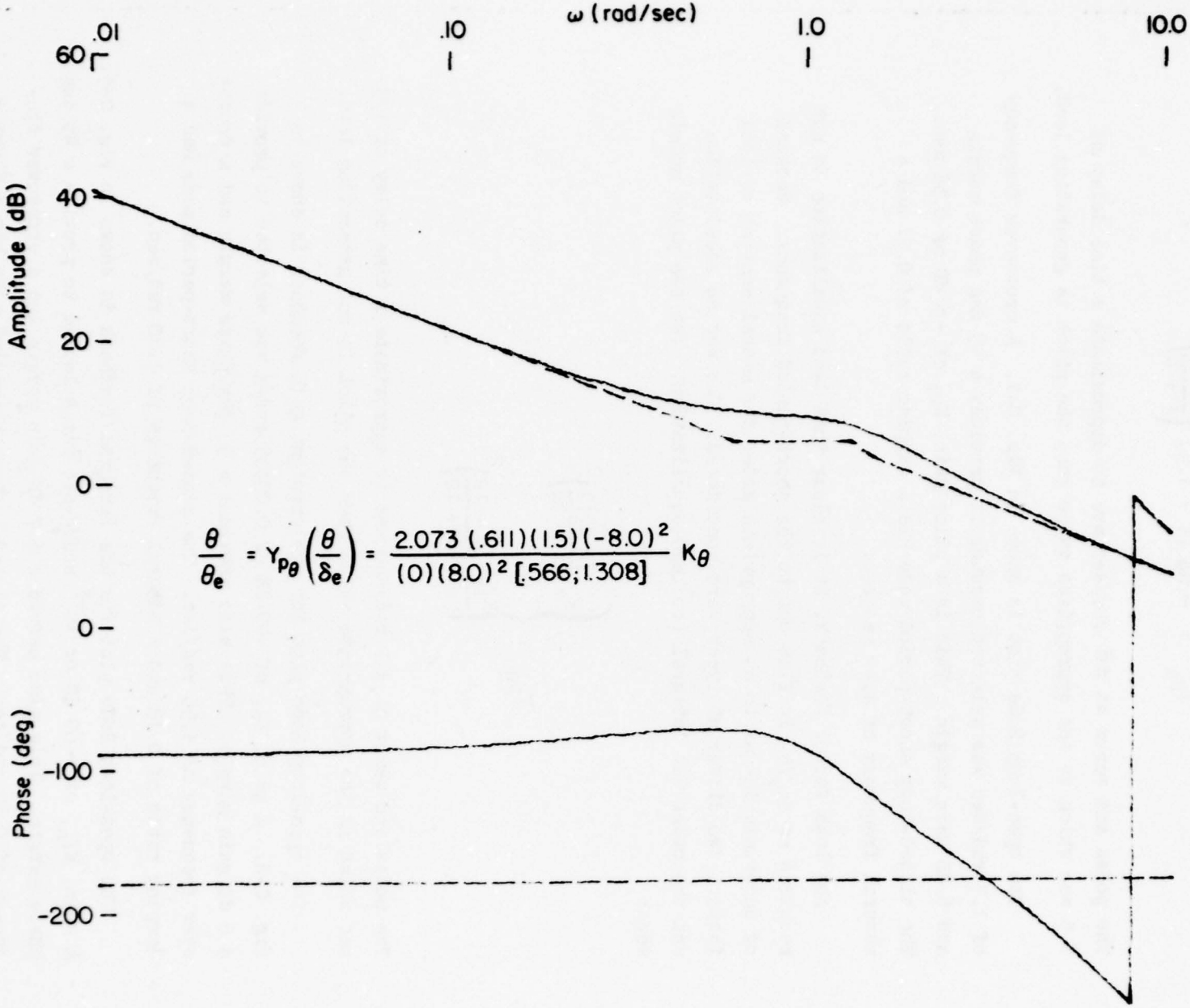

Figure C-1. Pitch Feedback, 747 Example

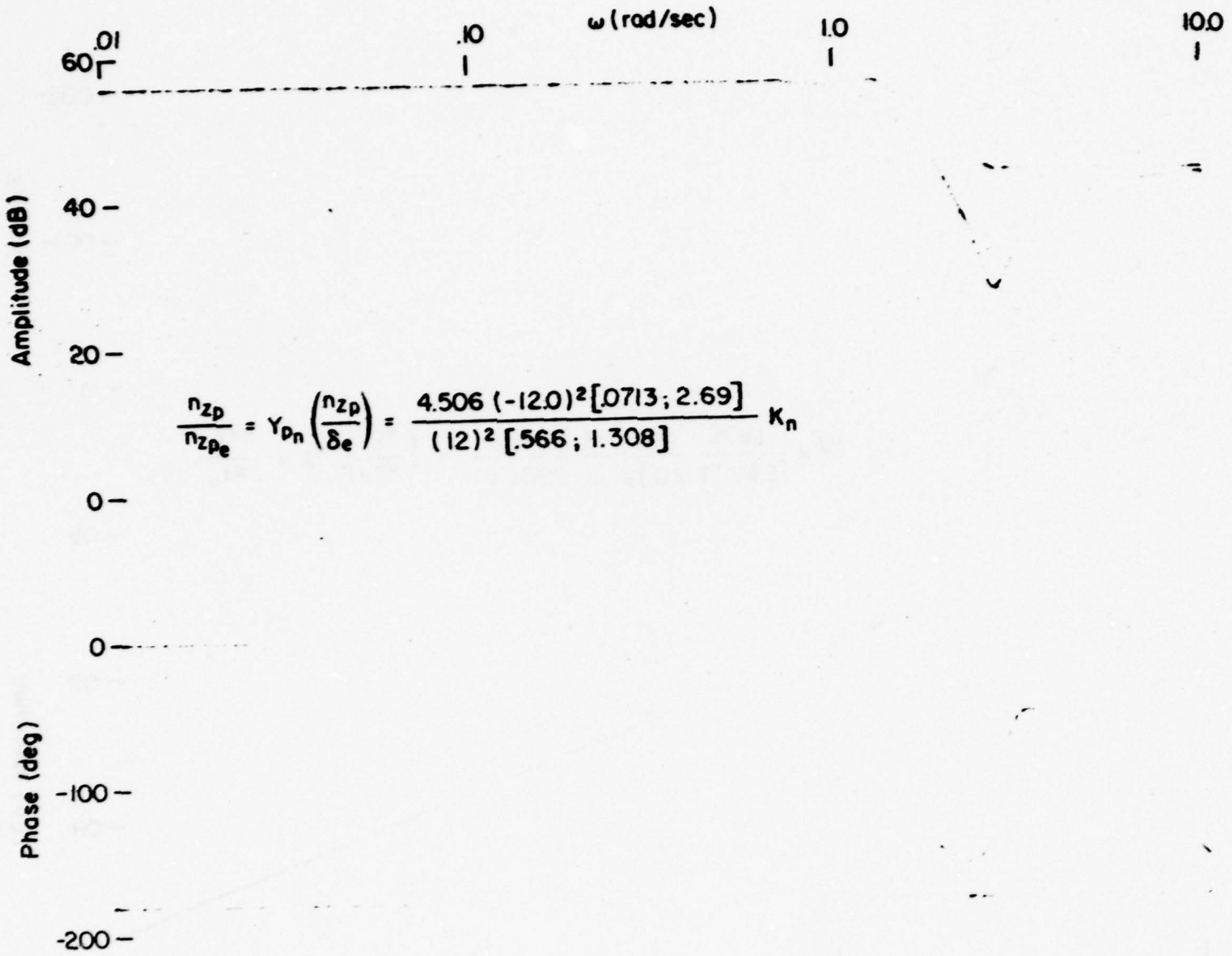

Figure C-2. Load Factor Feedback, 747 Example

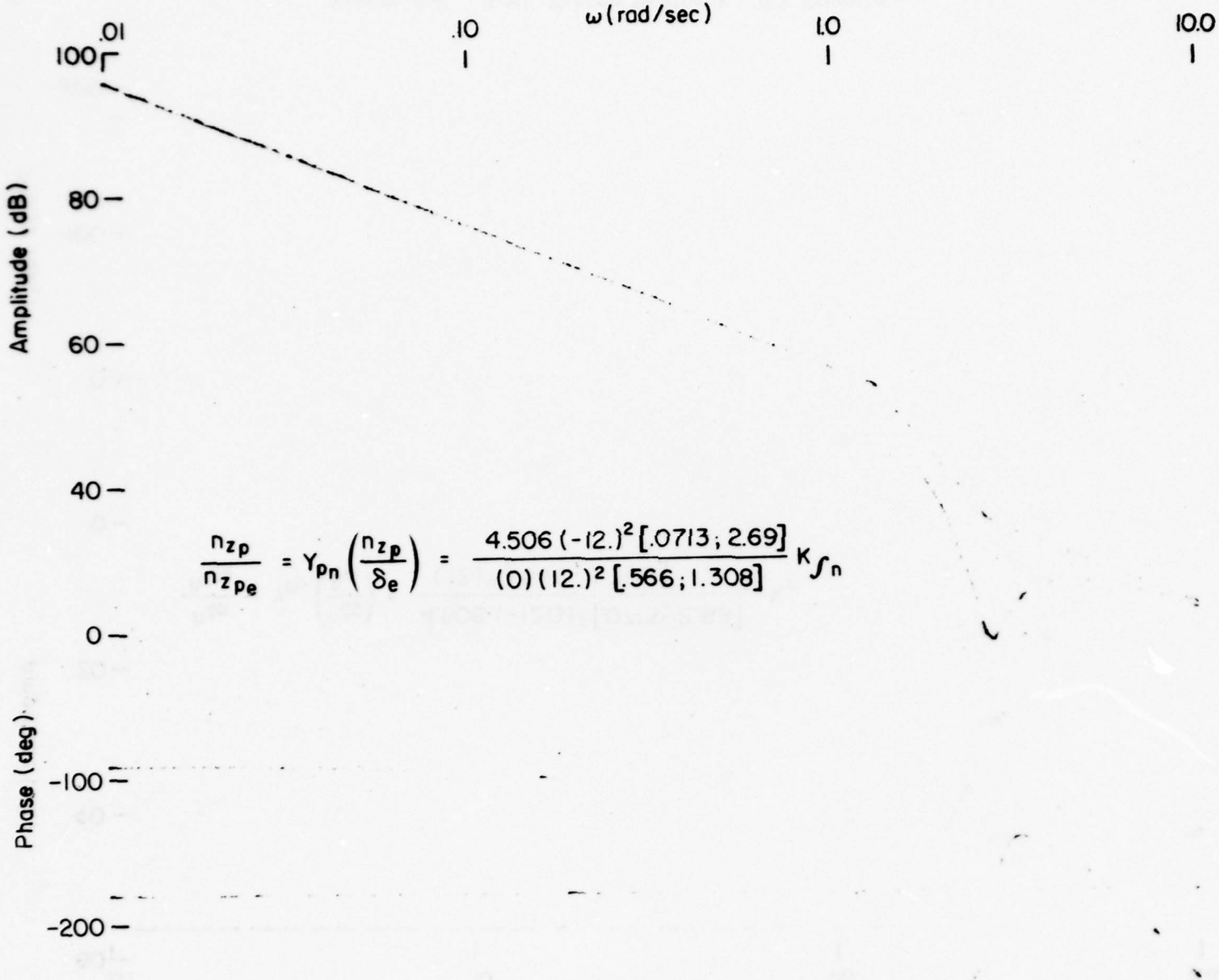

Figure C-3. Integral Load Factor, 747 Example

GENERAL AVIATION AIRCRAFT

This example represents a representative single-engine general aviation airplane. The selected flight condition is 150 kt IAS at 7,000 ft. The aircraft dynamics are identical to the "Baseline Case" of Appendix B.

The procedure for establishing the pilot models was very similar to that described above for the 747 example. For the pitch feedback case, a pilot lead at 3.71 rad/sec was used to cancel the short-period root at that frequency. The complete pilot model was:

$$Y_{p_\theta} = -K_\theta \, (s + 3.71) \left(\frac{s - 8}{s + 8}\right)^2$$

As with the 747, the poles and zeros at ±8 rad/sec are to approximate a time delay of 0.5 sec.

The open-loop Bode plot for this case is shown in Fig. C-4. A gain of 35.4 dB or 59.1 lb-sec/rad was selected to provide a gain margin of 6 dB, a phase margin of 35 deg, and a crossover frequency of 1.5 rad/sec. The closed-loop short-period mode had a damping ratio of 0.32 and a frequency of 1.95 rad/sec.

For load factor feedback, the same pilot model forms as for the 747 were used:

$$Y_{p_n} = \begin{cases} K_n \left(\dfrac{s - 12}{s + 12}\right)^2 \\ \dfrac{K_{\int n}}{s} \left(\dfrac{s - 12}{s + 12}\right)^2 \end{cases}$$

The open-loop Bode for the gain feedback is shown in Fig. C-5. A gain of 28. dB or 25.1 lb/g was selected to provide a gain margin of 5 dB, a phase margin of 60 deg, and a crossover frequency of 2 rad/sec. The closed-loop short-period mode had a damping ratio of 0.21 and a frequency of 3.1 rad/sec.

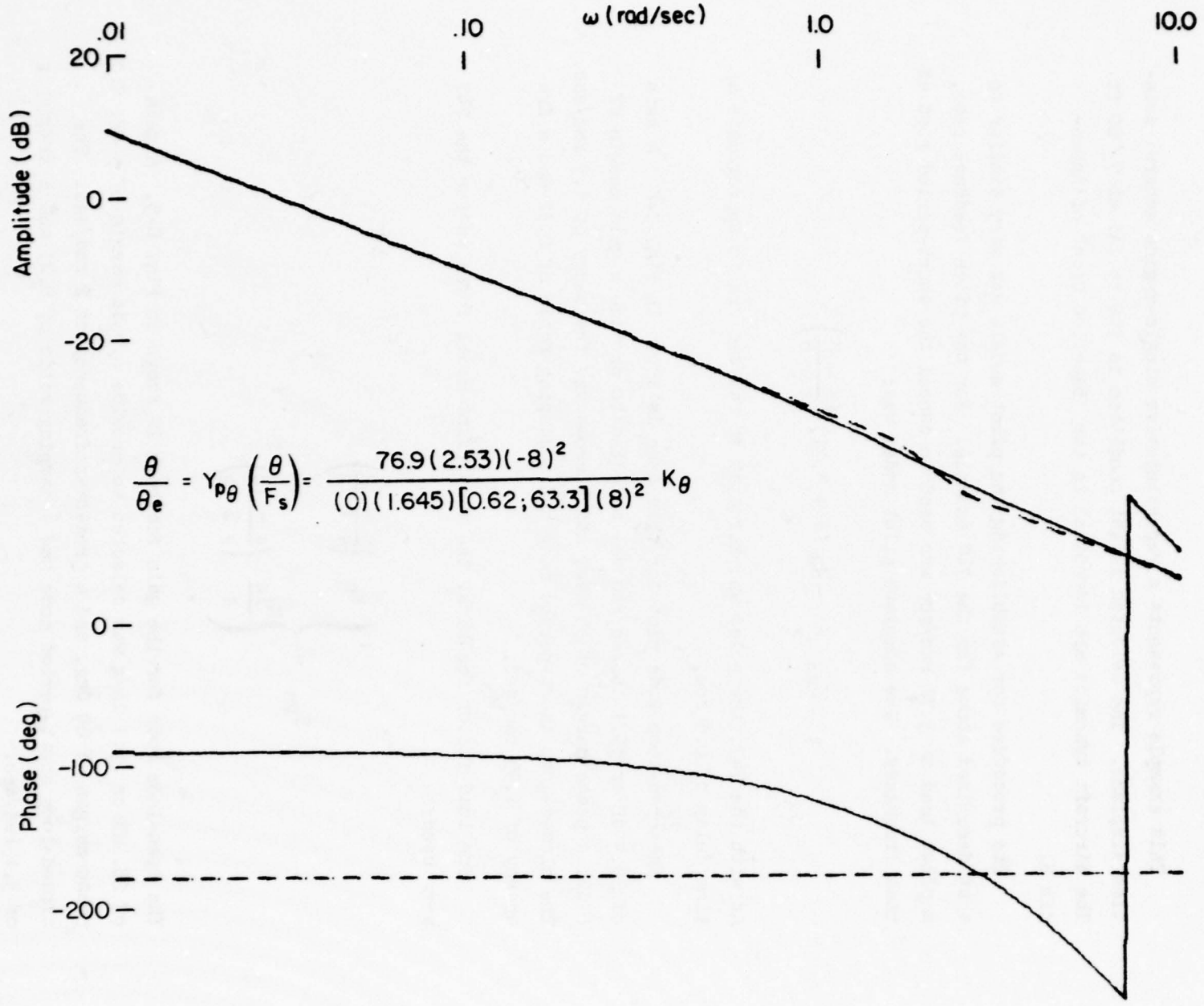

Figure C-4. Pitch Feedback, General Aviation Example

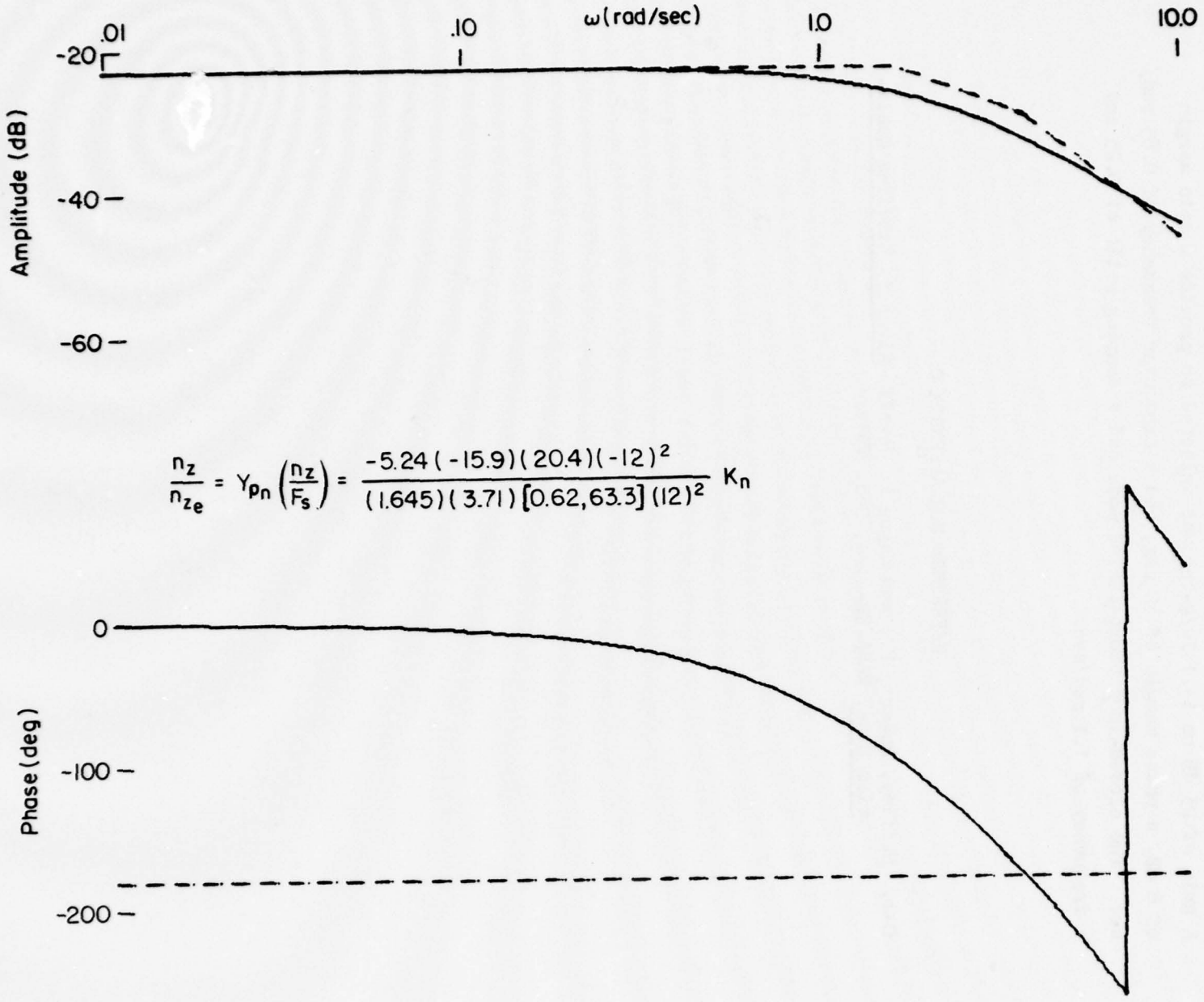

$$\frac{n_z}{n_{z_e}} = Y_{p_n}\left(\frac{n_z}{F_s}\right) = \frac{-5.24(-15.9)(20.4)(-12)^2}{(1.645)(3.71)[0.62,63.3](12)^2} K_n$$

Figure C-5. Load Factor Feedback, General Aviation Example

The open-loop Bode for the integral feedback is shown in Fig. C-6. A gain of 23 dB or 14.1 lb/g-sec was selected to provide a gain margin of 6 dB, a phase margin of 32 deg, and a crossover frequency of 0.85 rad/sec. The closed-loop short-period mode had a damping ratio of 0.25 and a frequency of 1.1 rad/sec.

REFERENCE FOR APPENDIX C

C-1. Heffley, Robert, K., and Wayne F. Jewell, Aircraft Handling Qualities Data, NASA CR-2144, Dec. 1972.

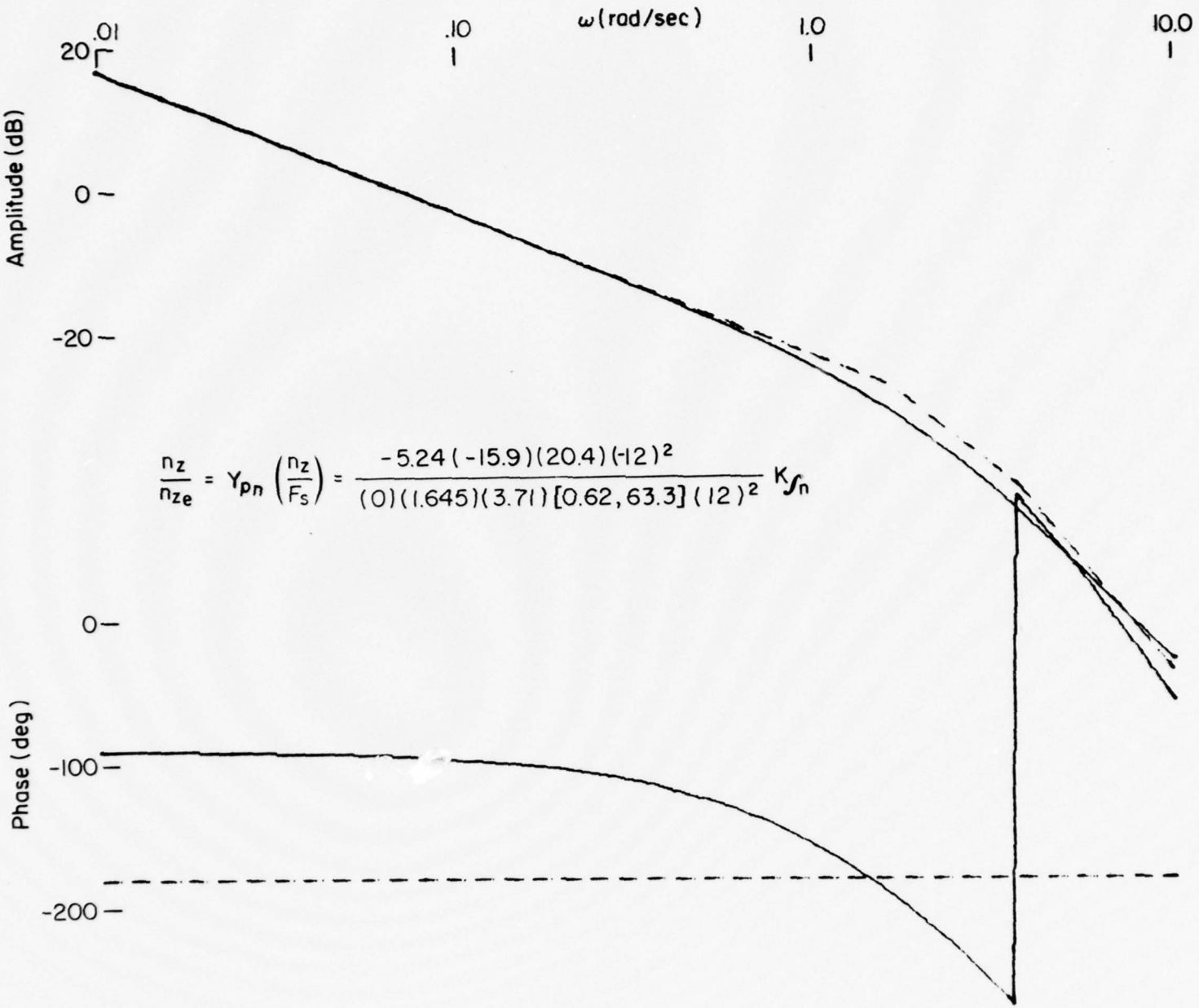

Figure C-6. Integral Load Factor Feedback, General Aviation Example

APPENDIX D

ANALYSIS OF GUST INDUCED TAIL LOADS FOR AIRCRAFT WITH A LIMITED AUTHORITY YAW DAMPER

ANALYSIS MODEL

The model for the tail loads analysis is completely defined by Fig. D-1. The model parameter values were selected to provide a good match to the Dutch roll characteristics of a Boeing 747, as defined in Ref. D-1 for a more complex three degree-of-freedom model.

For simplicity, only the aerodynamic load, F_t, was analyzed. The structural load, F_{t_s}, in this case can be approximated as:

$$F_{t_s} = F_t - m_t a_t$$

where:

m_t = mass of the tail

a_t = inertial lateral acceleration of the tail c.g. ($\doteq$ c.p.).

The acceleration a_t is the sum of the aircraft c.g. lateral acceleration and the relative acceleration of the tail with respect to the aircraft c.g.:

$$a_t = \frac{F_t}{m} - \ell_t \dot{r}$$

Making a direct substitution from the equations of motion for $\dot{r}$ and expressing I_z as mk_z^2, where k_z is the aircraft radius of gyration, yields:

$$F_t - m_t a_t = F_t \left[1 - \frac{m_t}{m}\left(1 + \frac{\ell_t^2}{k_z^2}\right)\right]$$

Thus for this example, F_t is exactly proportional to the structural load; inclusion of inertial load effects would only reduce the load by a small fraction.

Sign Conventions

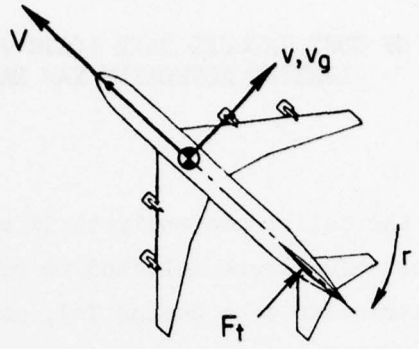

Equations (in Laplace Transform notation)

$$F_t = \frac{F_\beta \beta_t + F_\delta \delta_R}{\tau s + 1} \qquad sr = -\frac{F_t \ell_t}{I_z}$$

$$\beta_t = \beta - \frac{v_g}{V} - \frac{\ell_t r}{V} \qquad \delta_R = K_R r \leq \delta_{R\,limit}$$

$$s\beta = -r + \frac{F_t}{mV} \qquad \Phi_{v_g}(\omega) = \frac{2\omega_g}{\pi} \frac{\sigma_{v_g}^2}{\omega^2 + \omega_g^2}$$

Symbols

F_t = aerodynamic force on tail

F_β, F_δ = derivatives of F_t with respect to sideslip and rudder deflection

I_z = aircraft yaw moment of inertia

K_R = yaw damper gain

ℓ_t = distance from aircraft c.g. to c.p. of tail

m = aircraft mass

r = yaw rate

(continued on following page)

Figure D-1. Definition of Model

s = Laplace transform operator

v = lateral inertial velocity

v_g = lateral gust velocity

V = true airspeed

β = c.g. sideslip angle (v/V)

β_t = tail sideslip angle

δ_R = rudder deflection

$\delta_{R_{limit}}$ = rudder authority limit

σ_{v_g} = root mean square of lateral gust velocity

τ = time constant for aerodynamic lag in force buildup

Φ_{v_g} = power spectral density of v_g

ω = angular frequency

ω_g = break frequency of Φ_{v_g}

Parameter Values

V = 750 ft/sec

m = 20,000 slugs

I_z = 5.2449×10^7 slug-ft^2

ℓ_t = 102.42 ft

F_β = -5.0853×10^5 lb/rad

F_δ = 2.5605×10^5 sec^{-2}

τ = 0.1 sec

K_R = 1.0 sec

$\delta_{R_{limit}}$ = 3.6 deg(nominal)

ω_g = 0.42857 rad/sec

Figure D-1. Concluded

DESCRIBING FUNCTION ANALYSIS

The describing function analysis begins with the determination of a linear gain to approximate the non-linear element. This gain (k_{DF}) is, in general, a function of the characteristics of the input to the non-linearity as well as those of the non-linear element itself. For a random input, k_{DF} can be chosen to minimize the expected value of the mean square error between the non-linearity's output and its linear approximation. Based on the definition and the assumption that both input and output are ergodic random processes, the random input describing function for a simple, isolated non-linearity is derived in Ref. D-2 as:

$$k_{DF} = \frac{\int_{-\infty}^{\infty} x\, f(x)\, p(x)\, dx}{\int_{-\infty}^{\infty} x^2\, p(x)\, dx}$$

where

x	is the input to the non-linear element,
$p(x)$	is its probability density,
$f(x)$	is the output of the non-linear element.

Reference D-2 goes on to evaluate this expression for a simple limiter with unit slope and limits of $\pm a$. The result is

$$k_{DF} = \operatorname{erf}\left(\frac{a}{\sqrt{2}\,\sigma_x}\right) \qquad \text{(D-1)}$$

The describing function analysis of the yaw damper example proceeds from this relationship, based on the assumption that the rudder deflection, as well as all other response variables, are well-represented as normally-distributed random variables, as they would actually be in the linear case. Expressing k_{DF} in terms of the rudder deflection, reflected back to the limiter input, and the authority limit gives

$$k_{DF} = \operatorname{erf}\left(\frac{\delta_{R_{limit}}}{\sqrt{2}\,\frac{\sigma_{\delta_R}}{k_{DF}}}\right)$$

Thus the relationship between authority limit and the describing function gain can then be expressed explicitly, in terms of the system input σ_{v_g}, as:

$$\frac{\sigma_{v_g}}{\delta_{R_{limit}}} = \left(\frac{\sigma_{v_g}}{\sigma_{\delta_R}}\right)_{CL} \quad \frac{k_{DF}}{\sqrt{2}\ \mathrm{erf}^{-1}(k_{DF})}$$

where $(\sigma_{v_g}/\sigma_{\delta_R})_{CL}$ is the rms response ratio for the closed-loop system.

Unfortunately, this expression cannot be solved for k_{DF}, given a known $\delta_{R_{limit}}$, since the closed-loop response ratio depends on k_{DF}. The solution for a given σ_{v_g} and $\delta_{R_{limit}}$ can only be obtained by iterative evaluation for various values of k_{DF}. The first step in each case is to compute the system transfer functions with the yaw damper loop-closed. With the non-linearity replaced by its describing function gain, the model equations can be expressed in matrix form as:

$$\begin{bmatrix} \tau s + 1 & -F_\beta & 0 & 0 & -F_\delta \\ 0 & 1 & -1 & \ell_t/V & 0 \\ -\frac{1}{mV} & 0 & s & 1 & 0 \\ \frac{\ell_t}{I_z} & 0 & 0 & s & 0 \\ 0 & 0 & 0 & -K_R k_{DF} & 1 \end{bmatrix} \begin{bmatrix} F_t \\ \beta_t \\ \beta \\ r \\ \delta_R \end{bmatrix} = \begin{bmatrix} 0 \\ -1/V \\ 0 \\ 0 \\ 0 \end{bmatrix} \left|v_g\right|$$

Resulting literal expressions and corresponding numerical evaluations for key transfer functions are given in Fig. D-2.

From the transfer functions of Fig. D-2 for given k_{DF}, rms gust velocity responses can now be calculated using the standard formula:

$$\sigma_x = \sqrt{\int_0^\infty \left|\frac{x}{v_g}(j\omega)\right|^2 \Phi_{v_g}(\omega)\ d\omega}$$

These responses can, in turn be used to compute other basic parameters, e.g., $\sigma_{v_g}/\delta_{R_{limit}}$, $\sigma_{\dot{F}_t}/\sigma_{F_t}$. Important parameters for the yaw damper analysis are summarized in Table D-1 as a function of k_{DF}.

Yaw Damper Loop Closure

$$k_{DF}K_R \frac{r}{\delta_R} = \frac{(k_{DF}K_R \ell_t F_\delta / I_z)s}{\tau s^3 + s^2 - \left(\frac{F_\beta}{V}\right)\left(\frac{1}{m} + \frac{\ell_t^2}{I_z}\right)s - \frac{F_\beta \ell_t}{I_z}} = \frac{5k_{DF}(0)}{(9.93)\ [0.035,\ 1.]}$$

Closed Loop Gust Response

$$\Delta = s^3 + \frac{1}{\tau}s^2 + \frac{1}{\tau}\left[\frac{F_\delta \ell_t K_R}{I_z} k_{DF} - \frac{F_\beta}{mV} - \frac{F_\beta \ell_t^2}{I_z V}\right]s - \frac{F_\beta \ell_t}{\tau I_z}$$

(numerically determined by closure of damper loop)

$$\frac{F_t}{v_g} = \left(-\frac{F_\beta}{V\tau}\right)\frac{s^2}{\Delta} = 6780.4\ \frac{s^2}{\Delta}$$

$$\frac{\delta_R}{v_g} = \left(\frac{F_\beta \ell_t K_R k_{DF}}{\tau V I_z}\right)\frac{s}{\Delta} = 0.013240\ k_{DF}\ \frac{s}{\Delta}$$

Figure D-2. Key Transfer Functions for Describing Function Analysis

TABLE D-1. RAW DESCRIBING FUNCTION DATA

k_{DF}	$\frac{k_{DF}}{\sqrt{2}\ \mathrm{erf}^{-1} k_{DF}}$	$\sigma_{F_t}/\sigma_{v_g}$	$\sigma_{\dot{F}_t}/\sigma_{F_t}$	$\sigma_{\delta_R}/\sigma_{v_g}$	$\sigma_{\dot{\delta}_R}/\sigma_{\delta_R}$	$\sigma_{v_g}/\delta_{R_{limit}}$
		$\frac{\text{lb-sec}}{\text{ft}}$	$\frac{\text{rad}}{\text{sec}}$	$10^{-3}\ \frac{\text{rad-sec}}{\text{ft}}$	$\frac{1}{\text{sec}}$	$\frac{\text{ft}}{\text{rad-sec}}$
0	.79788	1542.3	1.3476	0	—	∞
.1	.79575	1180.47	1.5486	.22578	1.0210	3524.6
.2	.78940	993.49	1.7254	.37632	1.0310	2097.7
.3	.77858	874.67	1.8850	.49224	1.0409	1581.7
.4	.76277	790.68	2.0313	.58776	1.0507	1297.8
.6	.71292	677.23	2.2945	.74146	1.0701	961.50
.8	.62424	602.37	2.5285	.86396	1.0891	722.55
.9	.54716	573.34	2.6371	.91722	1.0985	596.55
.95	.48470	560.35	2.6896	.94224	1.1032	514.40
.98	.42132	552.98	2.7206	.95680	1.1060	440.35
.99	.38432	550.59	2.7309	.96158	1.1060	399.68
.998	.32330	548.70	2.7390	.96536	1.1077	334.90
1.0	0	548.23	2.7411	.96630	1.1079	0

Three of the parameters in Table D-1 are needed for the definition of the statistical properties of the tail force. $\bar{A}$, or $\sigma_{F_t}/\sigma_{v_g}$, and $\sigma_{v_g}/\delta_{R_{limit}}$ are explicitly listed; N_o, defined as $(1/2\pi)(\dot{\sigma}_{F_t}/\sigma_{F_t})$, completes the threesome. $\bar{A}$ and N_o are plotted vs. $\sigma_{v_g}/\delta_{R_{limit}}$ in Fig. D-3, along with the corresponding describing function gain. Based on the assumed Gaussian properties of F_t, its distribution and exceedance rates are defined as:

$$P(F_t < \bar{F}_t) = \frac{1}{\sqrt{2\pi}\,\bar{A}\,\sigma_{v_g}} \int_{-\infty}^{\bar{F}_t} e^{-(1/2)(x/\bar{A}\sigma_{v_g})^2}\, dx$$

and

$$N(F_t|\sigma_{v_g}) = N_o e^{-(1/2)(F_t/\bar{A}\sigma_{v_g})^2}$$

respectively, with $\bar{A}$ and N_o defined by Fig. D-3 for given values of σ_{v_g} and $\delta_{R_{limit}}$. These conditional statistics are compared with the time domain simulation counterparts in the next section, at selected values of k_{DF}.

Overall mission analysis exceedance rates may now be computed by numerically integrating Eq. V-5 using the conditional exceedance rates defined above. The straightforward computation scheme is shown in Fig. D-4. Table D-2 provides a sample output of the digitally-mechanized calculations. The integration interval used was 0.5 ft/sec.

TIME DOMAIN SIMULATION

The digital time domain simulation used a fixed-interval Runge-Kutta integration scheme to calculate time functions using the equations shown in Fig. D-5. The gust velocity for v_g, a normal distribution, was sampled. The resulting "white noise" was scaled and filtered to match the spectral characteristics of the gust model. The technique is detailed in Fig. D-6.

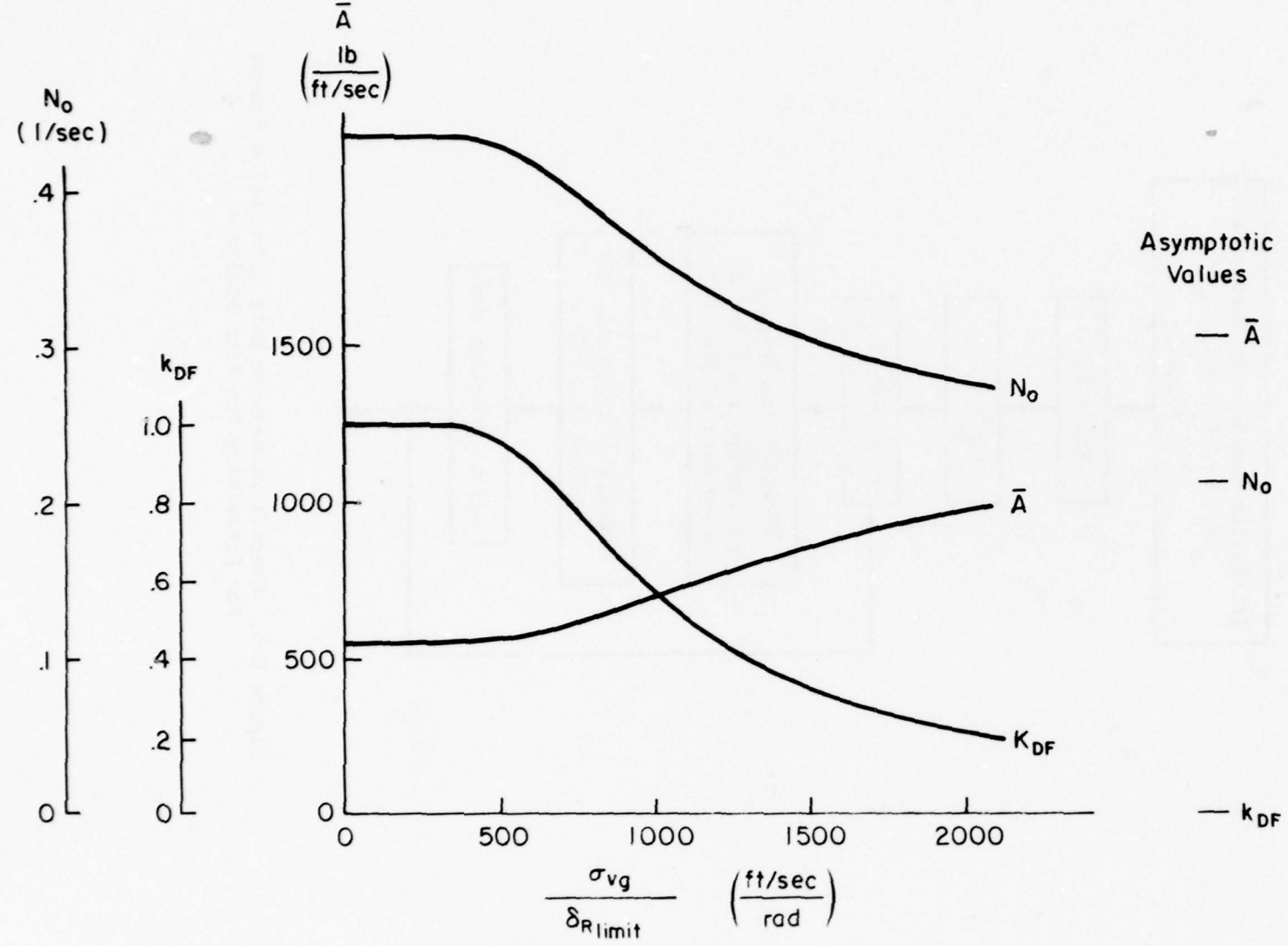

Figure D-3. Variations of Describing Function Analysis Parameters with Gust Velocity.

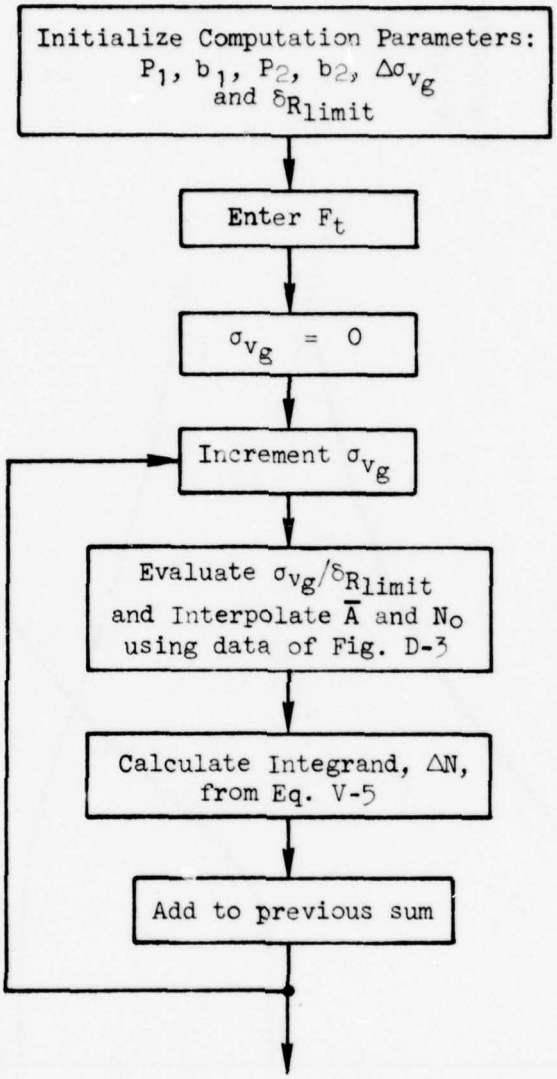

Figure D-4. Overall Exceedance Rate Integration Scheme For Describing Function Analysis

TABLE D-2. SAMPLE CALCULATION OF OVERALL EXCEEDANCE RATE FOR DESCRIBING FUNCTION ANALYSIS

P1, B1, P2, B2: .007,3.,.00011,9.36

RUDDER LIMIT (DRLIM) IN DEGREES: 1.8

INTEGRATION INTERVAL (DS) AND PRINT NO. (NPRT): .5,

F_t = 46,511 lb

σ_{v_g} (ft/sec)	N(1/sec)
0.10000E+01	0.00000E+00
0.20000E+01	0.00000E+00
0.30000E+01	0.00000E+00
0.40000E+01	0.00000E+00
0.50000E+01	0.00000E+00
0.60000E+01	0.00000E+00
0.70000E+01	0.38836E-36
0.80000E+01	0.53086E-29
0.90000E+01	0.31522E-24
0.10000E+02	0.69830E-21
0.11000E+02	0.21685E-18
0.12000E+02	0.19446E-16
0.13000E+02	0.71355E-15
0.14000E+02	0.13428E-13
0.15000E+02	0.15055E-12
0.16000E+02	0.10749E-11
0.17000E+02	0.55839E-11
0.18000E+02	0.22042E-10
0.19000E+02	0.69134E-10
0.20000E+02	0.18362E-09
0.21000E+02	0.41651E-09
0.22000E+02	0.82316E-09
0.23000E+02	0.14531E-08
0.24000E+02	0.23560E-08
0.25000E+02	0.35306E-08
0.26000E+02	0.49321E-08
0.27000E+02	0.64848E-08
0.28000E+02	0.80975E-08
0.29000E+02	0.96811E-08
0.30000E+02	0.11160E-07
0.31000E+02	0.12488E-07
0.32000E+02	0.13638E-07
0.33000E+02	0.14596E-07
0.34000E+02	0.15370E-07
0.35000E+02	0.15975E-07
0.36000E+02	0.16436E-07
0.37000E+02	0.16778E-07
0.38000E+02	0.17025E-07
0.39000E+02	0.17200E-07
0.40000E+02	0.17321E-07
0.41000E+02	0.17404E-07
0.42000E+02	0.17458E-07
0.43000E+02	0.17494E-07
0.44000E+02	0.17517E-07
0.45000E+02	0.17532E-07
0.46000E+02	0.17541E-07
0.47000E+02	0.17546E-07
0.48000E+02	0.17550E-07
0.49000E+02	0.17552E-07
0.50000E+02	0.17553E-07
0.51000E+02	0.17554E-07
0.52000E+02	0.17554E-07
0.53000E+02	0.17554E-07
0.54000E+02	0.17554E-07
0.55000E+02	0.17554E-07
0.56000E+02	0.17554E-07
0.57000E+02	0.17555E-07
0.58000E+02	0.17555E-07
0.59000E+02	0.17555E-07
0.60000E+02	0.17555E-07
0.61000E+02	0.17555E-07
0.62000E+02	0.17555E-07
0.63000E+02	0.17555E-07
0.63500E+02	0.17555E-07

State Equations

$$\dot{F}_t = (1/\tau)\,(F_\beta \beta_t + F_\delta \delta_R - F_t)$$

$$\dot{\beta} = (1/mV)F_t - r$$

$$\dot{r} = -(\ell_t/I_z)F_t$$

Auxiliary Equations

$$\beta_t = \beta - (\ell_t/V)r - (1/V)v_g$$

$$\delta_R = K_R r \leq \delta_{R_{limit}}$$

Figure D-5. Time Domain Simulation Equations

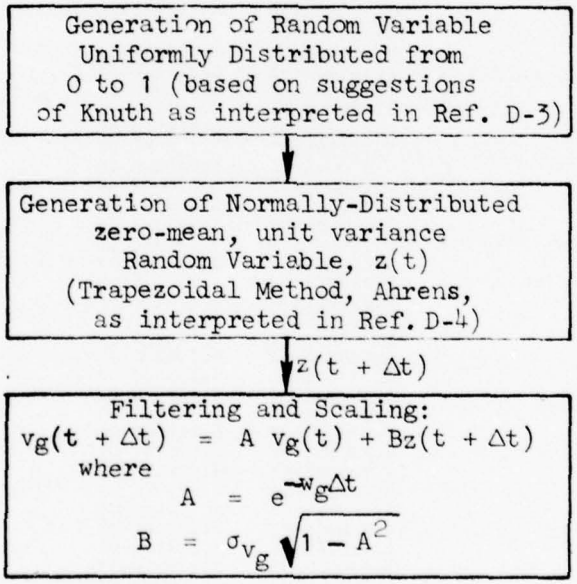

Figure D-6. Gust Velocity Generation Technique for Time Domain Simulation

An integration interval of 0.01 sec was used in the simulation runs. This interval provided sufficient accuracy for the example analysis. The inclusion of high-frequency low-damped structural modes would have required the use of a smaller interval, increasing the costs of the simulation, which are roughly proportional to the inverse of the integration interval.

The yaw damper with no authority limit ($k_{DF} = 1$) was run first to validate the simulation. Cumulative tail force statistics were output every five minutes as a check on simulation operations and also as an indication of the degree to which the results represented their asymptotic values. Probability distribution and exceedance rates for several tail force levels are plotted versus run time in Fig. D-7. Comparison with the linear analysis results shown for reference in Fig. D-7 indicates satisfactory progress toward the predicted values. The degree of accuracy decreases with increasing tail load, i.e., with the lower frequency of occurrence, as expected.

Overall (30 minutes) statistics are compared with the theoretical results in Figs. D-8 and D-9. Figure D-8 shows that the tail load is indeed normally distributed. The data match the theoretical curve extremely well. Likewise, Fig. D-9 shows a very good match of the exceedance rates at least to rates as low as 0.003/sec with:

- accuracy to within 20 percent and generally better than 10 percent
- close agreement between $\pm F_t$ exceedances.

Below 0.003/sec the number of exceedances is too small to provide an accurate estimate of the rates.

With the simulation validated, thirty minute runs were then made at rudder authority limits corresponding to describing function gains of 0.8, 0.6 and 0.2. The resulting statistics are compared with the corresponding describing function predictions in Figs. D-10 through D-15.

For convenience the simulation runs were made for $\sigma_{V_g} = 1$ ft/sec but the results can be scaled for other gust levels. For a fixed value of the describing function gain, k_{DF}, the tail load is proportional to the gust level, i.e.,

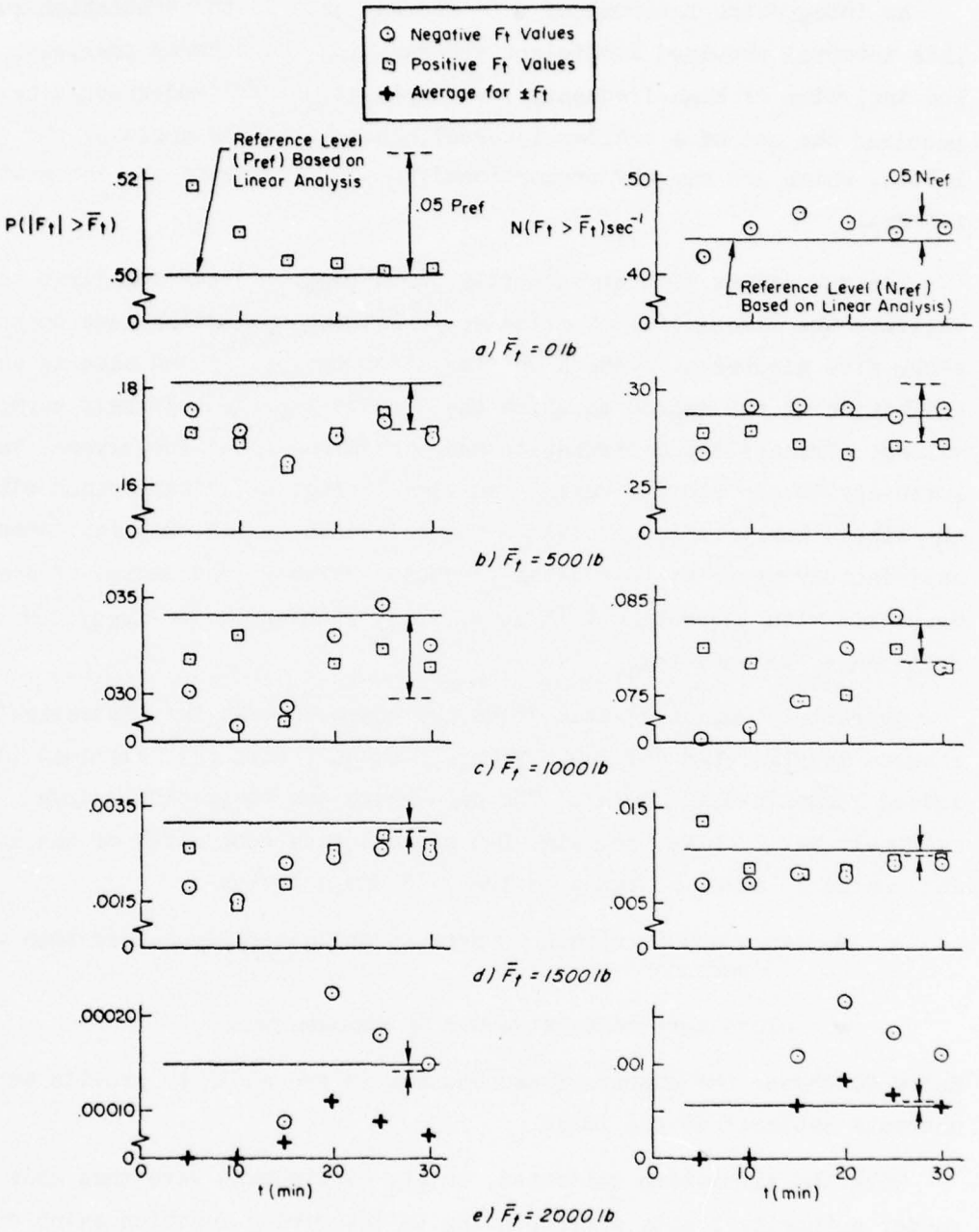

Figure D-7. Time Variation of Selected Cumulative Tail-Force Statistics

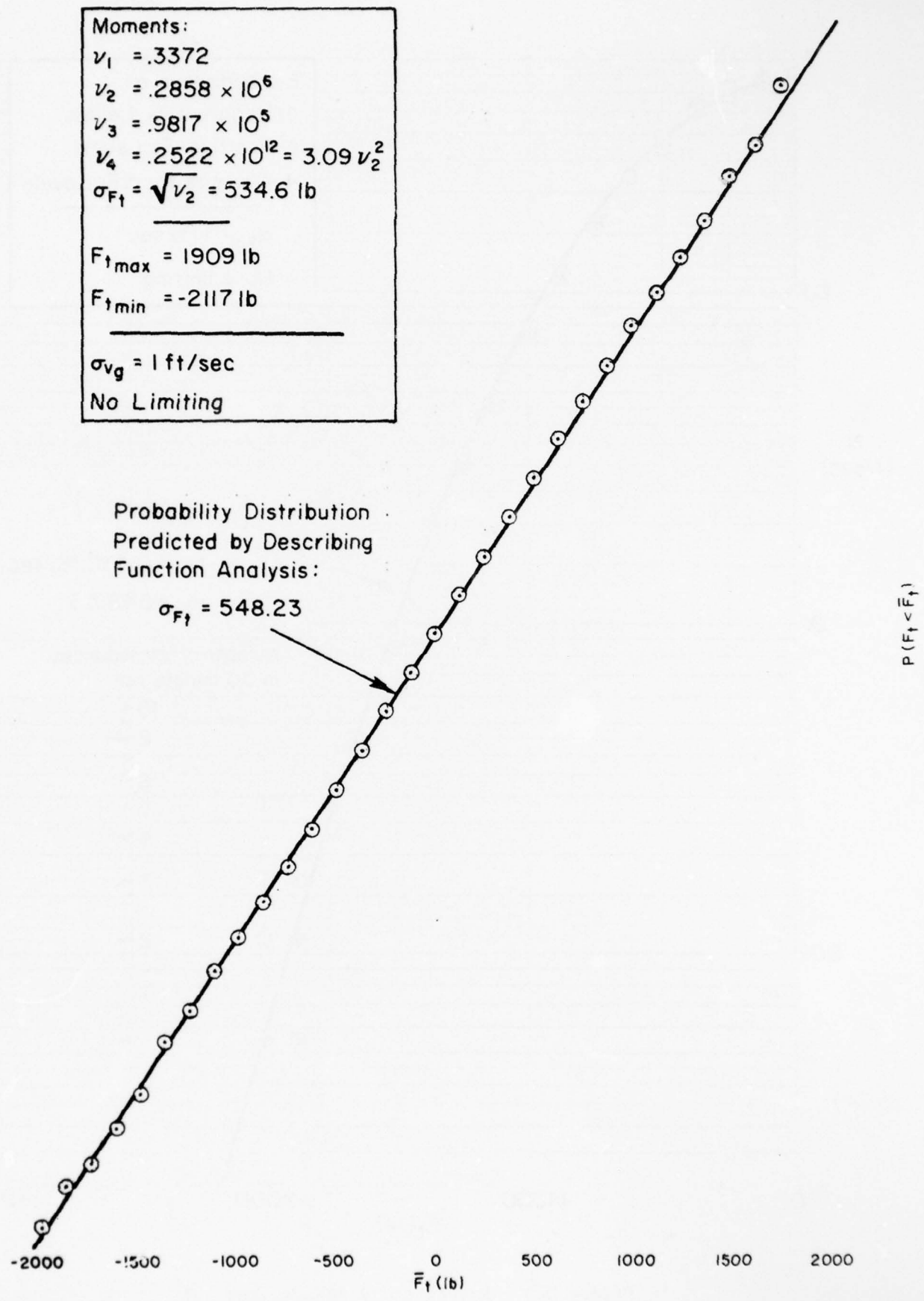

Figure D-8. Probability Distribution for k_{DF} = 1.

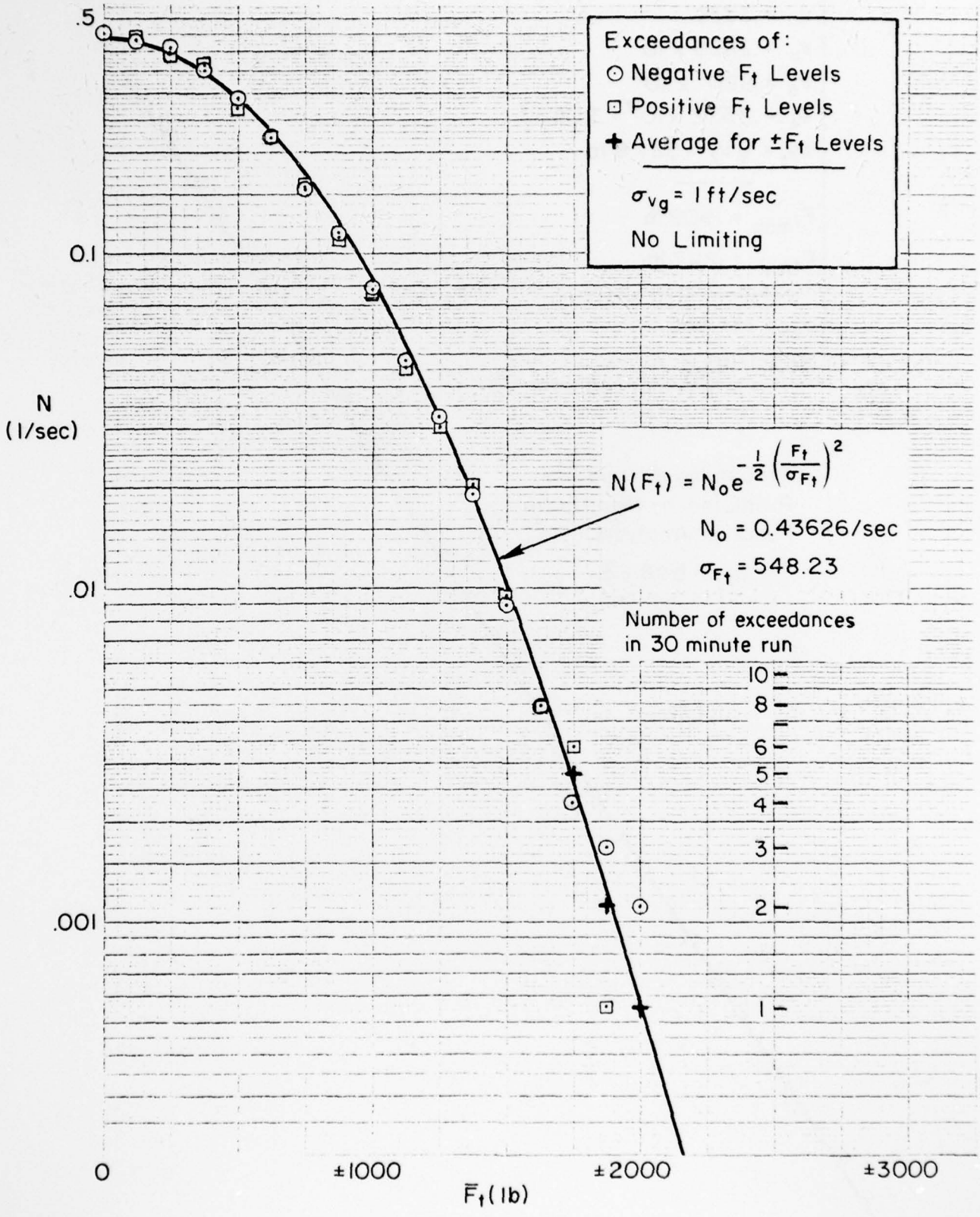

Figure D-9. Exceedance Rates for $k_{DF} = 1$

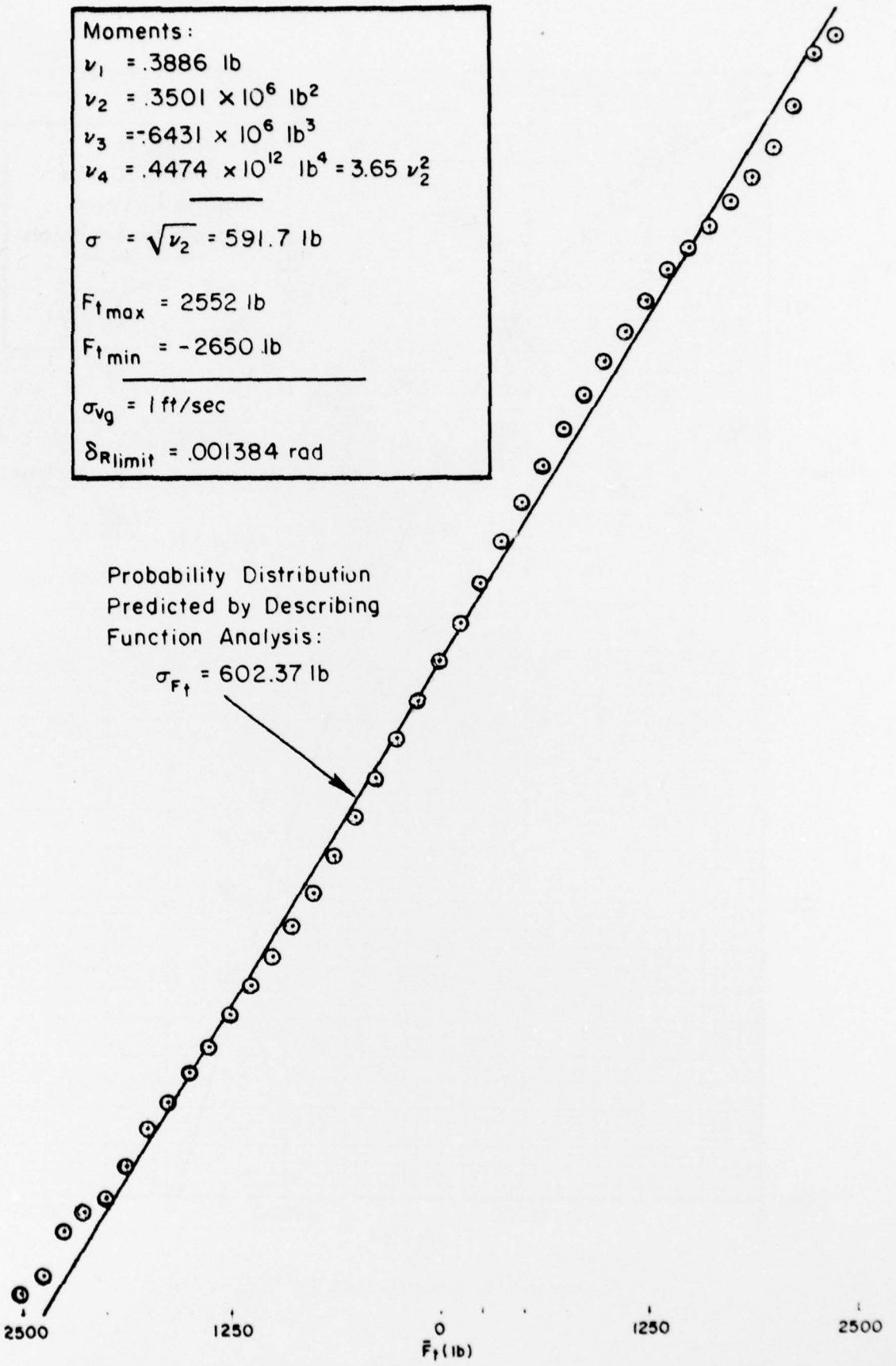

Figure D-10. Probability Distribution for k_{DF} = 0.8

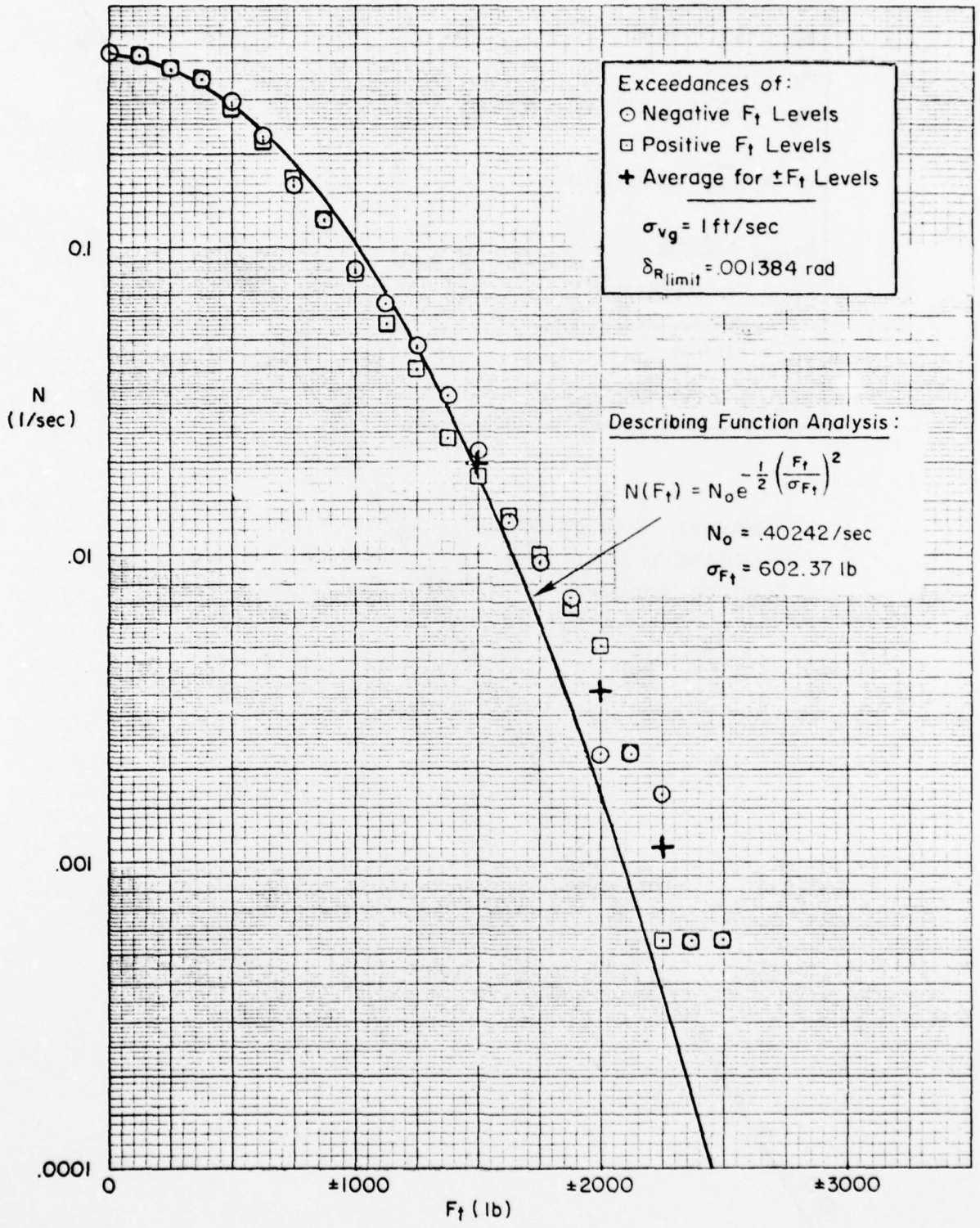

Figure D-11. Exceedances for $k_{DF} = 0.8$

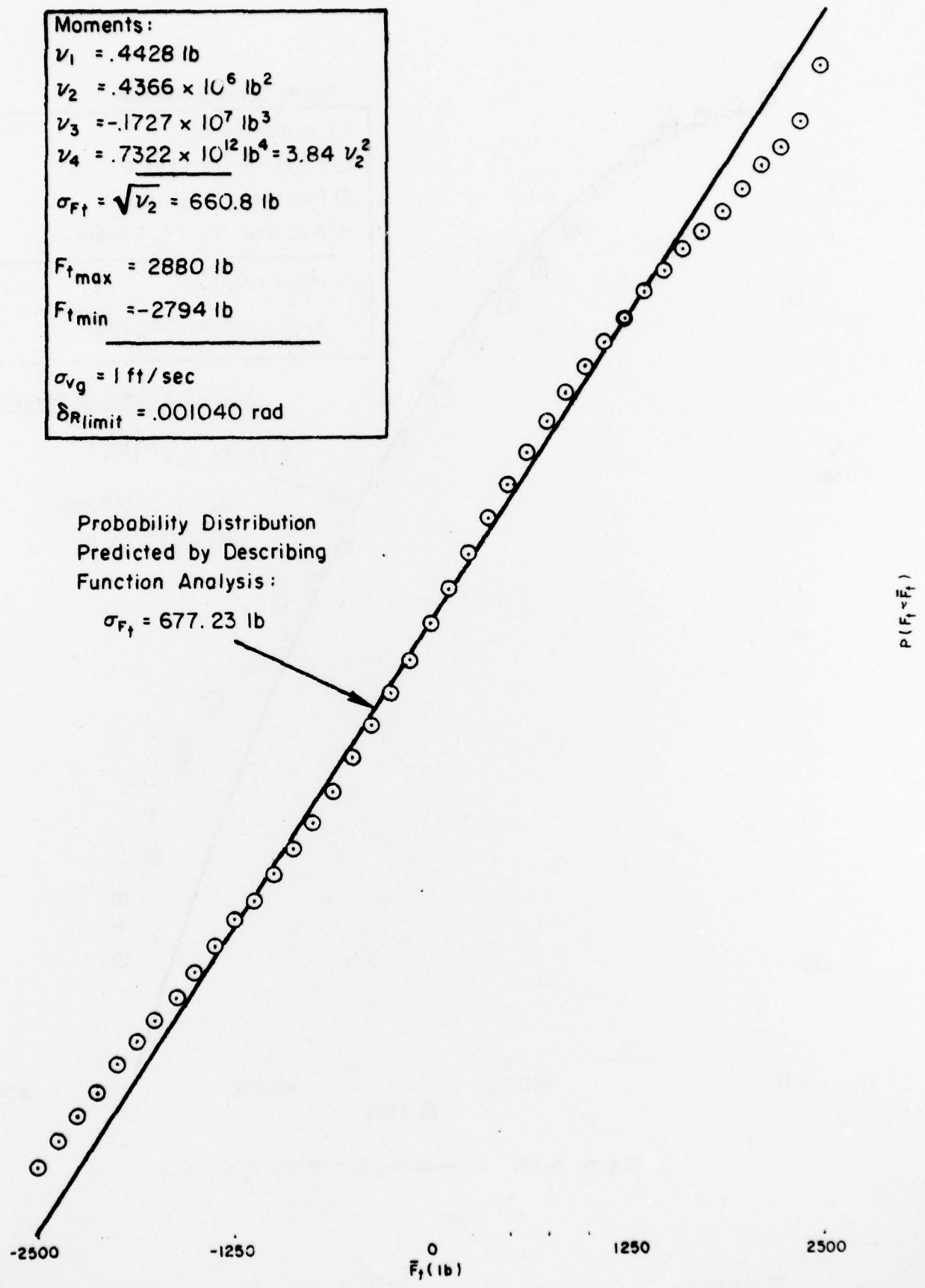

Figure D-12. Probability Distribution for k_{DF} = 0.6

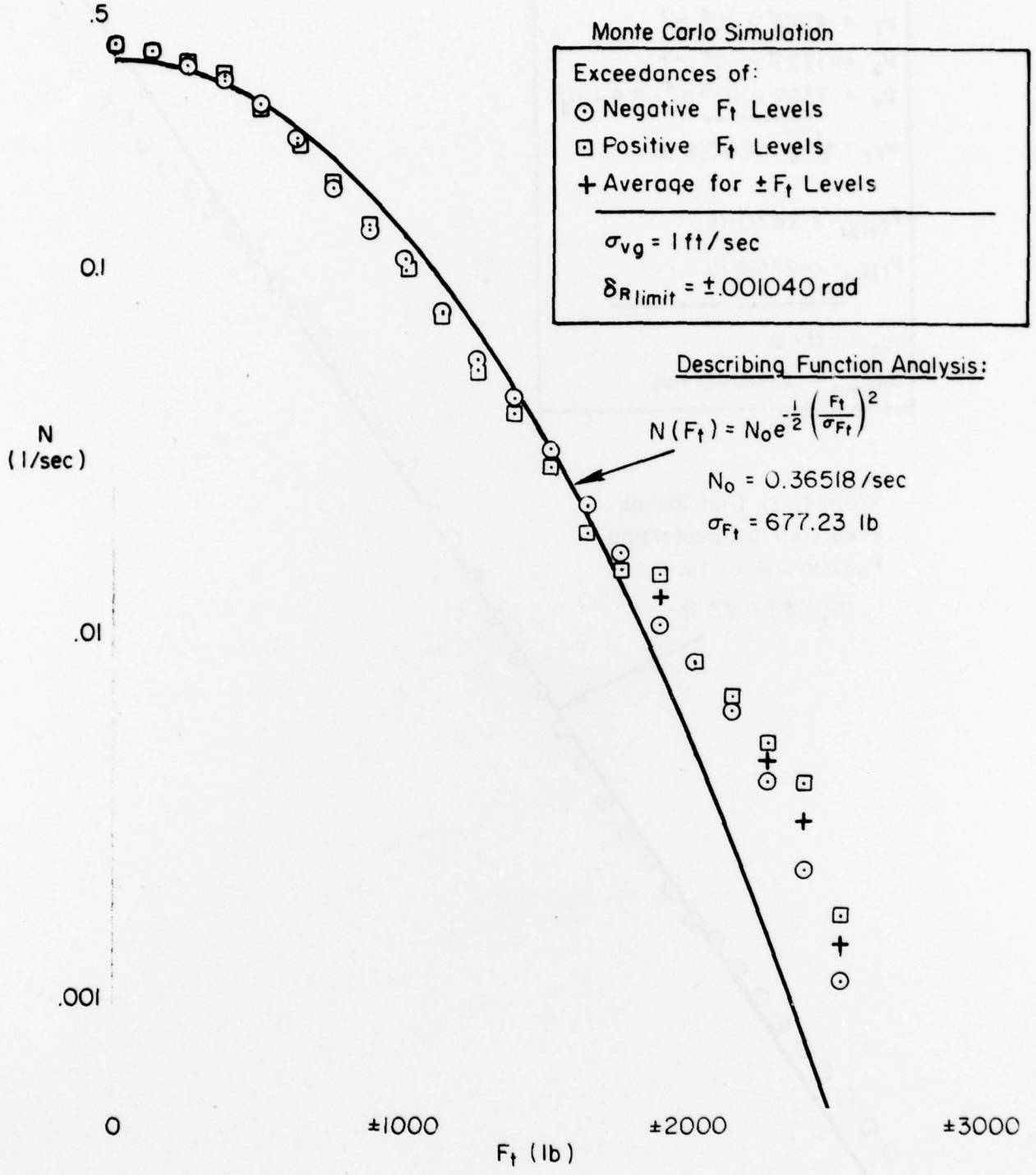

Figure D-13. Exceedance Rates for $k_{DF} = 0.6$

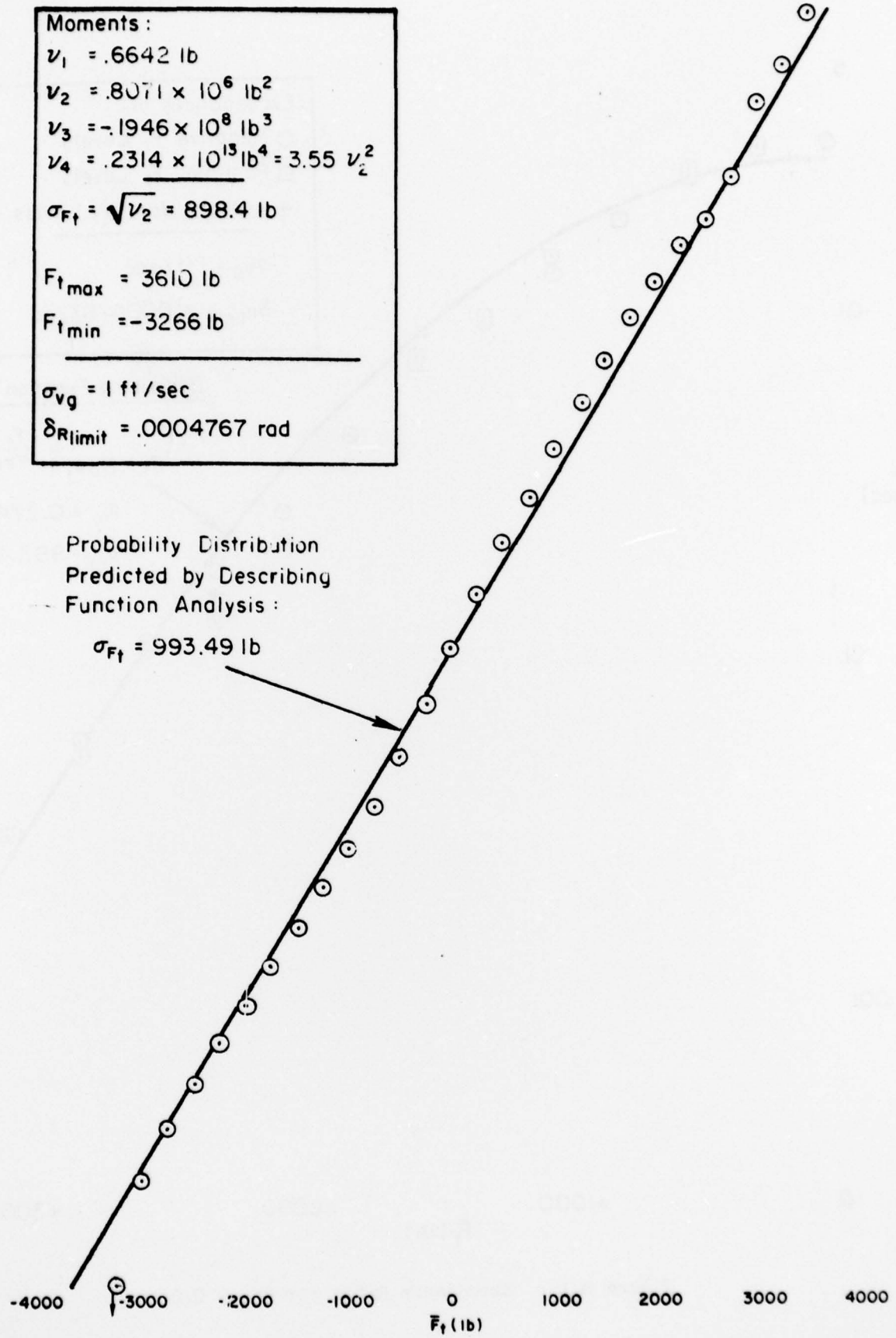

Figure D-14. Probability Distribution for k_{DF} = 0.2.

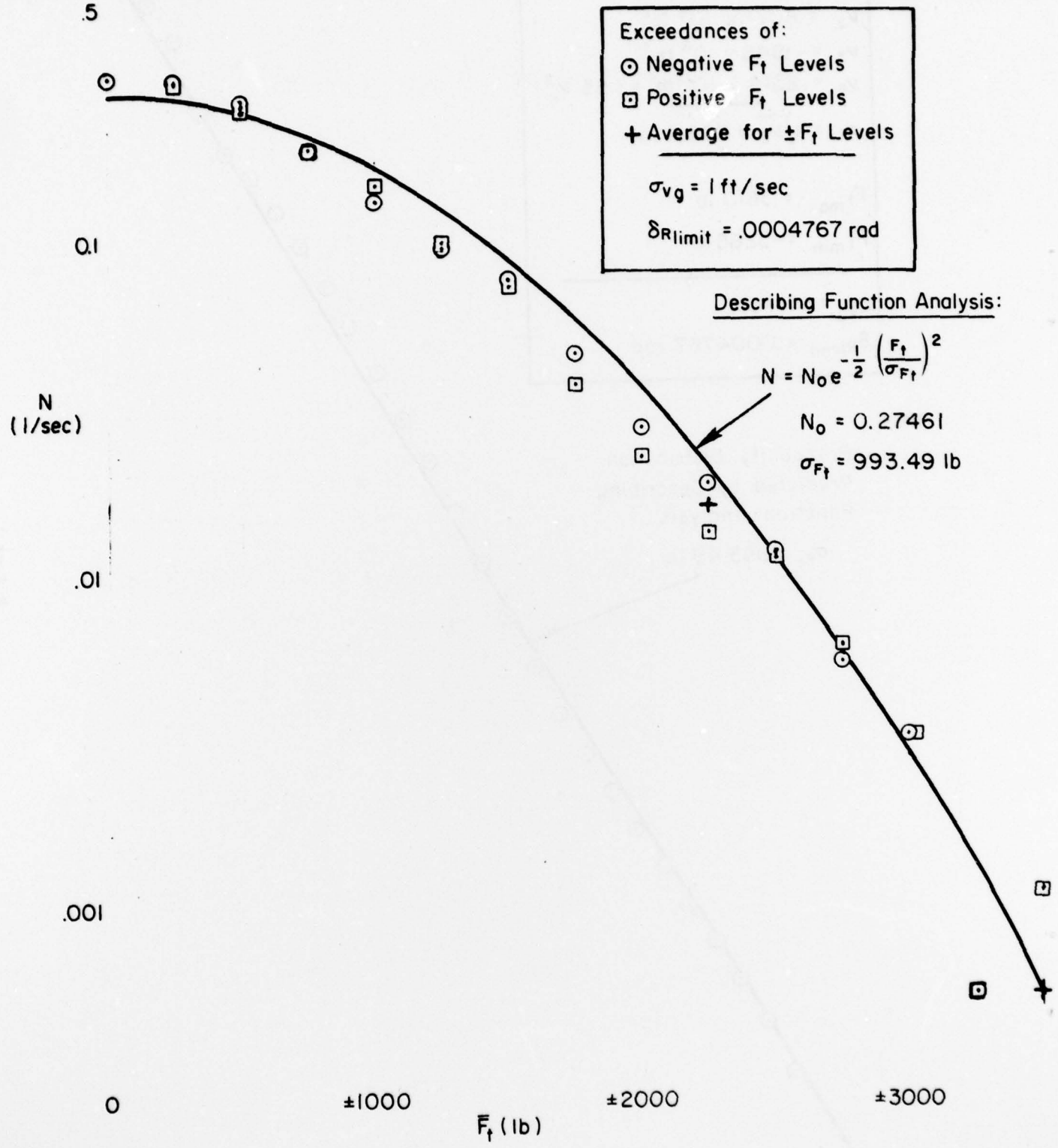

Figure D-15. Exceedance Rates for k_{DF} = 0.2

$$\sigma_{F_t} = \sigma_{v_g} f(k_{DF}).$$

Since k_{DF} is a function of $\delta_{R_{limit}}/\sigma_{v_g}$, the scaling equation can be written as:

$$\frac{\sigma_{F_t}}{\sigma_{v_g}} = f\left(\frac{\delta_{R_{limit}}}{\sigma_{v_g}}\right)$$

Thus Fig. D-10 and D-11 apply for all combinations of $\delta_{R_{limit}}/\sigma_{v_g} = 0.001384$ rad-sec/ft if the abscissas are relabeled as F_t/σ_{v_g} (lb-sec/ft).

This scaling was used in the calculation of the overall exceedance rates. Equation V-5 was numerically integrated just as in the describing function analysis. In this case, however, the conditional exceedance rates $N(F_t|\sigma_{v_g})$ were interpolated directly from the time domain simulation data. The computation scheme is shown in Fig. D-16.

The calculation is somewhat more involved than that for the describing function analysis. This is due not just to the double interpolation requirement, but also to the limited data on which it is based. The data shortage is, of course, a practical problem which must be traded-off against the costs of running the simulation. In this case, conditional exceedance rate data had been generated only for three values of $\sigma_{v_g}/\delta_{R_{limit}}$, with a fourth set provided by the linear analysis for the no-limiting case. The simulation data were also limited in accuracy by the 30 minute run length as noted earlier.

To obtain acceptable accuracy on the overall result, two parameter transformations were used to make the data more linear. Cross plots of the data showed it was more linear with k_{DF} than with $\sigma_{v_g}/\delta_{R_{limit}}$. Since the transformation of $\sigma_{v_g}/\delta_{R_{limit}}$ to k_{DF} could be quite precisely defined from a series of inexpensive describing function calculations, k_{DF} was selected as the interpolation parameter. The other transformation was to interpolate the logarithm of $N(F_t|\sigma_{v_g})$ rather than $N(F_t|\sigma_{v_g})$. The previous data plots show that a logarithmic interpolation should be much more accurate as $N(F_t|\sigma_{v_g})$ varies over several orders of magnitude.

Table D-3 shows a sample computer output for the overall exceedance rate computation based on simulation results.

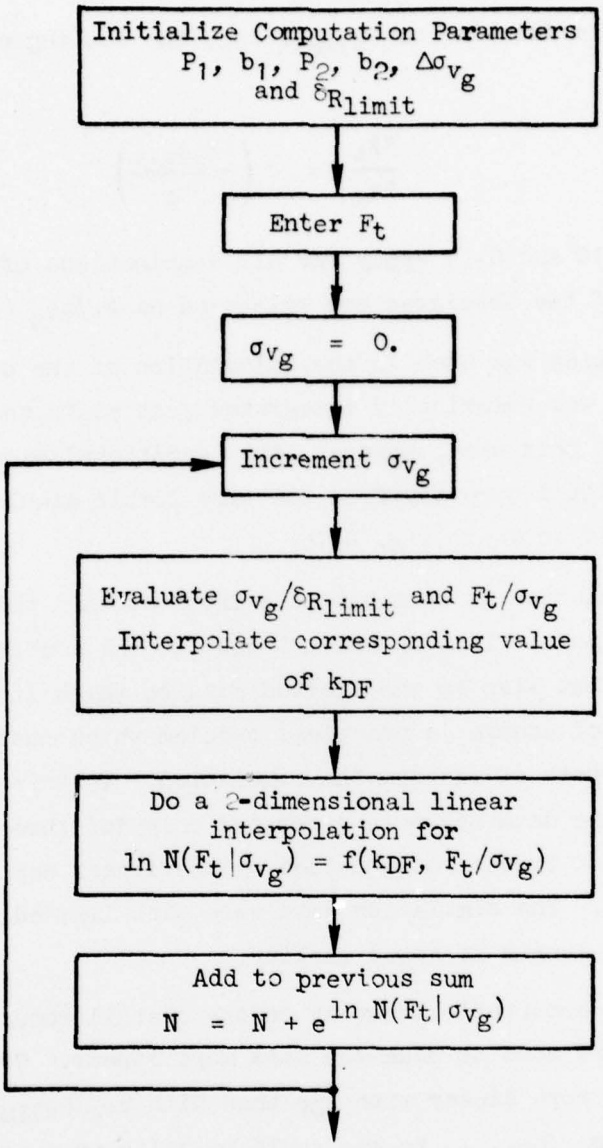

Figure D-16. Overall Exceedance Rate Computation Scheme for Time Domain Analysis

TABLE D-3. SAMPLE CALCULATION OF OVERALL EXCEEDANCE RATE FROM TIME DOMAIN SIMULATION RESULTS

P1, B1, P2, B2: .007,3.,.00011,9.36

RUDDER LIMIT (DRLIM) IN DEGREES: 1.8

INTEGRATION INTERVAL (DS) AND PRINT NO. (NPRT): .5

F_t = 46,511 lb

$\sigma_{\dot{y}_g}$ (ft/sec)	κ_{DF}	ΔN(1/sec)	N(1/sec)
0.10000E+01	0.99981E+00	0.00000E+00	0.00000E+00
0.20000E+01	0.99962E+00	0.00000E+00	0.00000E+00
0.30000E+01	0.99943E+00	0.00000E+00	0.00000E+00
0.40000E+01	0.99924E+00	0.00000E+00	0.00000E+00
0.50000E+01	0.99905E+00	0.00000E+00	0.00000E+00
0.60000E+01	0.99886E+00	0.00000E+00	0.00000E+00
0.70000E+01	0.99867E+00	0.47733E-36	0.47733E-36
0.80000E+01	0.99848E+00	0.62302E-29	0.62343E-29
0.90000E+01	0.99829E+00	0.35539E-24	0.35789E-24
0.10000E+02	0.99810E+00	0.75009E-21	0.77289E-21
0.11000E+02	0.99612E+00	0.23511E-18	0.25114E-18
0.12000E+02	0.99219E+00	0.21434E-16	0.24272E-16
0.13000E+02	0.98653E+00	0.78552E-15	0.94913E-15
0.14000E+02	0.97784E+00	0.14647E-13	0.19251E-13
0.15000E+02	0.96495E+00	0.16276E-12	0.23458E-12
0.16000E+02	0.95207E+00	0.10806E-11	0.17586E-11
0.17000E+02	0.93372E+00	0.53851E-11	0.96441E-11
0.18000E+02	0.91434E+00	0.19701E-10	0.40024E-10
0.19000E+02	0.89343E+00	0.57190E-10	0.13134E-09
0.20000E+02	0.86818E+00	0.14378E-09	0.36795E-09
0.21000E+02	0.84294E+00	0.30638E-09	0.88805E-09
0.22000E+02	0.81770E+00	0.56493E-09	0.18784E-08
0.23000E+02	0.79204E+00	0.78549E-09	0.33525E-08
0.24000E+02	0.76539E+00	0.98976E-09	0.52210E-08
0.25000E+02	0.73874E+00	0.11408E-08	0.74525E-08
0.26000E+02	0.71209E+00	0.10885E-08	0.96609E-08
0.27000E+02	0.68544E+00	0.99862E-09	0.11707E-07
0.28000E+02	0.65880E+00	0.88893E-09	0.13541E-07
0.29000E+02	0.63215E+00	0.78720E-09	0.15159E-07
0.30000E+02	0.60550E+00	0.70167E-09	0.16607E-07
0.31000E+02	0.58498E+00	0.60364E-09	0.17864E-07
0.32000E+02	0.56605E+00	0.49591E-09	0.18909E-07
0.33000E+02	0.54712E+00	0.39706E-09	0.19751E-07
0.34000E+02	0.52819E+00	0.30914E-09	0.20412E-07
0.35000E+02	0.50926E+00	0.23160E-09	0.20912E-07
0.36000E+02	0.49033E+00	0.17027E-09	0.21281E-07
0.37000E+02	0.47140E+00	0.12290E-09	0.21549E-07
0.38000E+02	0.45247E+00	0.88313E-10	0.21742E-07
0.39000E+02	0.43354E+00	0.62491E-10	0.21879E-07
0.40000E+02	0.41461E+00	0.43411E-10	0.21974E-07
0.41000E+02	0.39744E+00	0.29562E-10	0.22040E-07
0.42000E+02	0.38623E+00	0.19621E-10	0.22084E-07
0.43000E+02	0.37501E+00	0.12809E-10	0.22112E-07
0.44000E+02	0.36380E+00	0.82386E-11	0.22131E-07
0.45000E+02	0.35259E+00	0.52214E-11	0.22143E-07
0.46000E+02	0.34138E+00	0.32616E-11	0.22150E-07
0.47000E+02	0.33017E+00	0.20031E-11	0.22155E-07
0.48000E+02	0.31895E+00	0.12101E-11	0.22157E-07
0.49000E+02	0.30774E+00	0.72124E-12	0.22159E-07
0.50000E+02	0.29809E+00	0.42376E-12	0.22160E-07
0.51000E+02	0.29192E+00	0.24520E-12	0.22161E-07
0.52000E+02	0.28575E+00	0.14008E-12	0.22161E-07
0.53000E+02	0.27958E+00	0.79013E-13	0.22161E-07
0.54000E+02	0.27342E+00	0.44030E-13	0.22161E-07
0.55000E+02	0.26725E+00	0.24229E-13	0.22161E-07
0.56000E+02	0.26108E+00	0.13166E-13	0.22161E-07
0.57000E+02	0.25491E+00	0.70650E-14	0.22161E-07
0.58000E+02	0.24874E+00	0.37442E-14	0.22161E-07
0.59000E+02	0.24257E+00	0.19598E-14	0.22161E-07
0.60000E+02	0.23640E+00	0.10132E-14	0.22161E-07
0.61000E+02	0.23023E+00	0.51737E-15	0.22161E-07
0.62000E+02	0.22407E+00	0.26096E-15	0.22161E-07
0.63000E+02	0.21790E+00	0.13006E-15	0.22161E-07
0.63500E+02	0.21481E+00	0.91395E-16	0.22161E-07

REFERENCES FOR APPENDIX D

D-1. Heffley, Robert K., and Wayne F. Jewell, Aircraft Handling Qualities Data, NASA CR-2144, Dec. 1972.

D-2. Graham, Dunstan, and Duane McRuer, Analysis of Nonlinear Control Systems, New York, Dover, 1971.

D-3. Forsythe, George E., Michael A. Malcolm, and Cleve B. Moler, Computer Methods for Mathematical Computations, Englewood, NJ, Prentice-Hall, Inc., 1977.

D-4. Ahrens, J. H., "Computer Methods for Sampling from the Exponential and Normal Distributions," Communications of the ACM, Vol. 15, No. 10, Oct. 1972.

APPENDIX E

SAMPLE V-n DIAGRAMS

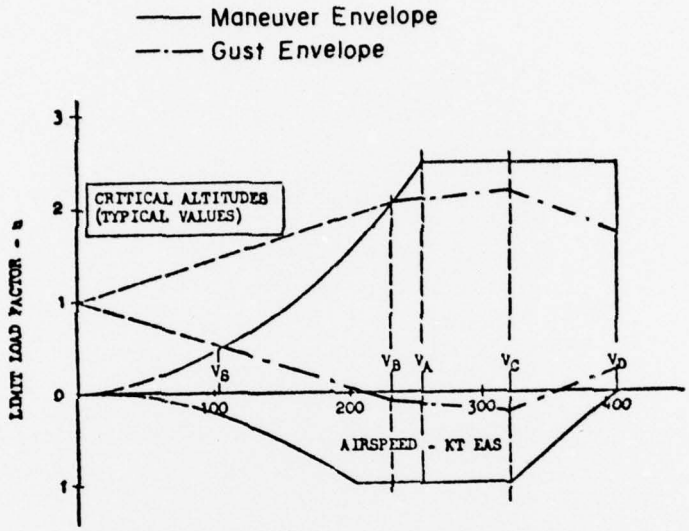

Figure E-1. First Generation Jet Transport

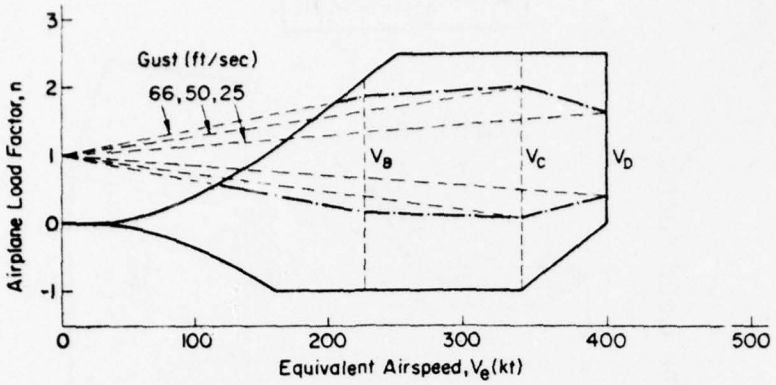

a) Maximum Weight at Sea Level

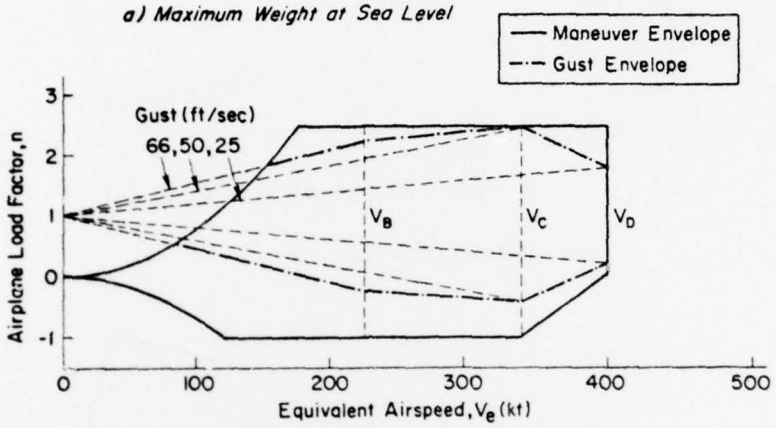

b) Typical Landing Weight at Sea Level

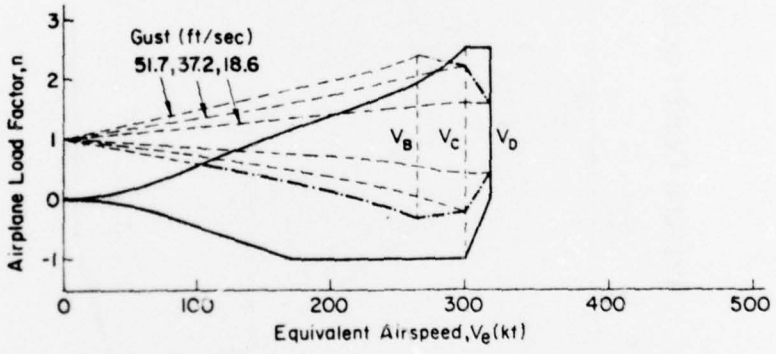

c) Typical Weight at 35300 ft

Figure E-2. Another First Generation Jet Transport

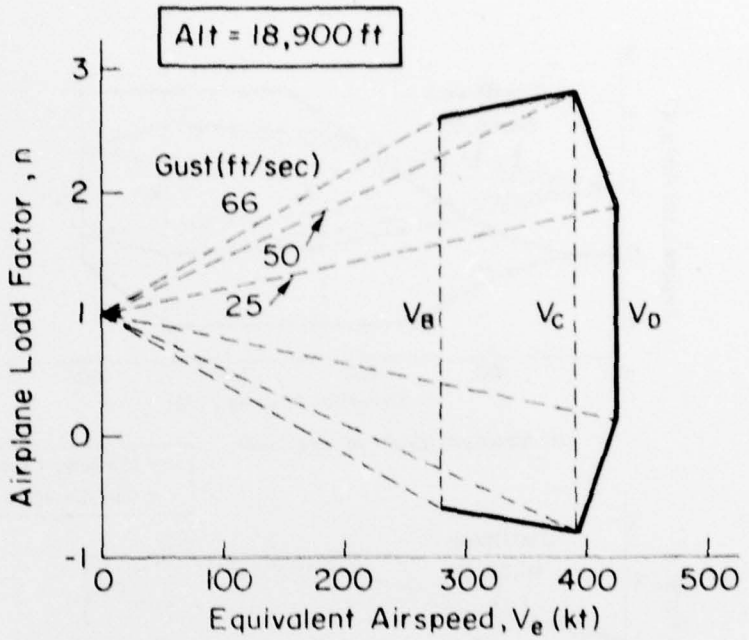

a) Maximum Weight

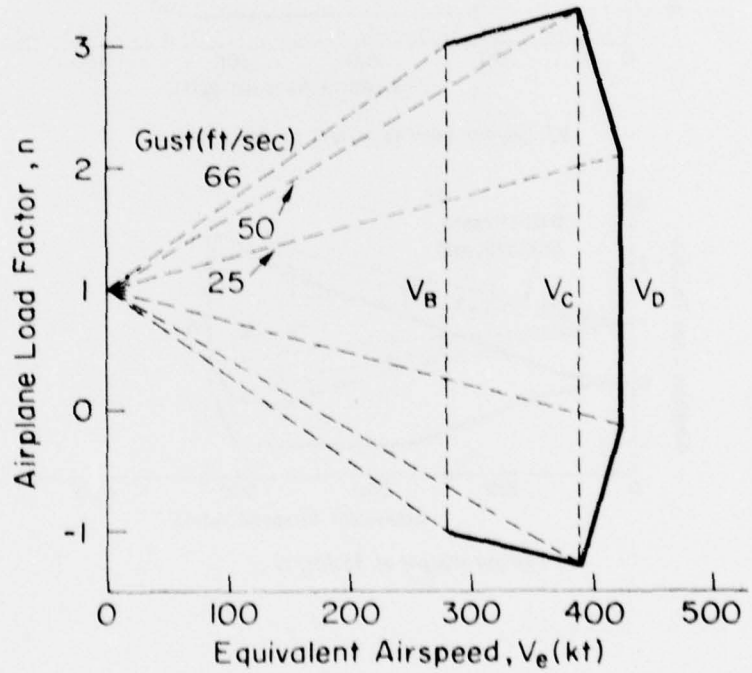

b) Typical Weight

Figure E-3. Second Generation Jet Transport